CR-132780

(NASA-CR-132780) TETHERED BODY PROBLEMS AND RELATIVE MOTION ORBIT DETERMINATION Final Report (Analytical Mechanics Associates, Inc.) ~~316~~ 317 p HC $18.00 CSCL 22A G3/30

N73-31723

Unclas 08461

Final Report

TETHERED BODY PROBLEMS AND RELATIVE MOTION ORBIT DETERMINATION

PART I

J.B. Eades, Jr.
Henry Wolf

Contract NAS5-21453
Report No. 72-35
August 1972

ANALYTICAL MECHANICS ASSOCIATES, INC.
10210 GREENBELT ROAD
SEABROOK, MARYLAND 20801

FOREWORD

This report was prepared under NASA Contract NAS5-21453. The work was conducted under the direction of E. R. Lancaster, Trajectory Analysis and Geodynamics Division, Goddard Space Flight Center.

The Analytical Mechanics Associates, Inc. program was conducted under the direction of Dr. J. B. Eades, Jr.

TABLE OF CONTENTS

LIST OF FIGURES

List of Figures (cont)

List of Figures (cont)

List of Figures (cont)

List of Figures (cont)

MAJOR SYMBOLS*

a	Coefficient (see eq. (B.21)); semi-major axis length.
A_j, B_j	Constants.
ARG	Argument.
$\mathcal{C}$, $\mathcal{C}_i$	Constant.
c	Damping constant (see Appendix B).
$\bar{e}_j$	Unit vector ($j \equiv x, y, z; r, \varphi, z; \ell, n, z$).
Det_i	Determinant value.
E_i	Specific total energy.
F	Force
$\tilde{F}_g$	Dimensionless specific force parameter, in gee's $\left(\equiv \frac{F/m_2}{g_o}\right)$.
$\bar{g}$	Gravitational vector ($\lvert\bar{g}\rvert \equiv \mu/r^2$).
h_i	Specific moment of momentum.
H	Unit operator (see Appendix B), altitude.
H.O.T.	≡ higher order term.
i	Complex number ($\equiv \sqrt{-1}$).
k	Spring constant (see Appendix B).
K_j	Constant ($j = \theta, \tau$; see section II).
ℓ, L	Tether length.
m_i	Mass (particle).
M	Mass parameter ($\equiv \Sigma m_i$).
$\tilde{m}$	Reduced mass parameter $\left(\equiv \frac{m_1 m_2}{M}\right)$.

*Symbols for Appendix A and Section V are found in those parts of the report rather than here.

$\bar{n}_i$	Unit normal vector (see eq. (H.23)).
N_j	Dimensionless parameter (j = v, ℓ, f; see section III).
$\bar{r}_i$, r_i	Radius vector, distance.
R_j	Dimensionless ratio (j = t, sw; see section III).
s	Root (value) from characteristic equation (see eq. (B.20b)).
sgn (~)	≡ sign of (~).
T	Tension force.
T_s	Tether force (section III).
T_j	Period (j = n, d).
t	Time.
$\bar{V}_i$, V_i	Velocity vector, speed.
$\bar{v}_i$	Relative velocity vector.
x, y, z	Cartesian coordinates (local valued).
α_i	Position angle (for $\bar{F}_i$, Appendix E).
β	Position angle (see eq. (B.21c)).
γ_i	Elevation angle (see eq. (D.39)).
δ_i	Slope parameter (see eq. (III.18)).
Δ_i	$\equiv r_i/r_g$, r/r_1 (see eq. (B.6)).
ϵ_i	Eccentricity of orbit.
θ	Position angle, tether (measured from $\bar{e}_r$).
λ	Dimensionless tether length ($\equiv \ell/r_1$, ℓ/r_g).
μ	Primary mass particle (parameter).

ξ, η, ζ	Dimensionless cartesian coordinates (see Appendix H).
σ	Dimensionless length ($\equiv \varkappa/\ell_o$).
$\tilde{\sigma}$	Value of σ measured from σ_{st}.
τ	Dimensionless specific force parameter $\left(\equiv \frac{F/\tilde{m}}{r_1\dot{\varphi}_1^2}\right)$; see also eq. (H.6).
φ, $\dot{\varphi}$	True anomaly, orbit rotational rate.
$\varkappa$	Tether stretch.
$\bar{\omega}_j$; ω_j	Rotational vector; frequency (see Appendix B).
Ω	Frequency ratio $\left(\equiv \sqrt{\frac{k/\tilde{m}}{3\dot{\varphi}^2}}\right)$.

Subscripts

a	Apocenter (Appendix C).
a, b	Index values (section III).
c	Critical value; constant; circular orbit value.
d	Damping.
e	Equivalent value (Appendix D).
f	Final values.
g	Refers to c.g.
i, j	Indices.
m	Extremal.
n	Natural; normal.
o	Initial (natural), reference value.
p	Pericenter (Appendix C).

r	Relative value (Appendix H).
s	Spring.
st	Static parameter.
T	Transfer path parameter.
σ	Pertaining to σ-motion coordinate.
1, 2	Refers to mass particles.

Superscripts

i	Index.
$(\dot{})$	Time derivative.
$()'$	Derivative wrt φ; index.

TETHERED BODY PROBLEMS AND RELATIVE MOTION ORBIT DETERMINATION

by

J. B. Eades, Jr. *
H. Wolf**

SUMMARY

For this investigation selected problems dealing with orbiting tethered body systems have been studied. In addition, a relative motion orbit determination program was developed. Results from these tasks are described and discussed in this report.

First, the expected tethered body motions were examined, analytically, to ascertain what influence would be played by the physical parameters of the tether, the gravity gradient and orbit eccentricity. After separating the motion modes these influences were determined; and, subsequently, the effects of oscillations and/or rotations, on tether force, were described.

This information is expected to serve as the basic guidelines for design and understanding of these systems.

Second, a study was undertaken, by examining tether motions, to see what type of "control" actions would be needed to accurately place a mass particle at a prescribed position relative to a main vehicle. In conjunction with this part of the analysis a set of universal parameters were developed; these are used to determine the operating parameters for prescribed extensible tether operations. (Several modes of the extension maneuver were examined, here).

Next, following the above, other applications for tethers were studied. Principally these were concerned with the producing of low-level "gee forces" by means of stabilized tether configurations; and, the initiation of free "transfer" trajectories from tether supported vehicle relative positions.

*Senior Analyst, AMA, Inc.
**Senior Scientist, AMA, Inc.

The orbit determination method, which has been developed for this work, was built around a particular set of relative motion equations utilizing a Kalman filtering technique. The analysis is complete; a working computer program could be formulated, as a next step.

INTRODUCTION

To those readers having a knowledge of maritime terminalogy, names like "heaving" and "messenger" lines, "distance" and "high" lines, and a number of other such nautical terms, form a familiar nomenclature. The idea that the uses which these names imply might be carried over into astronautics may come as somewhat a surprise. Yet, it is not too far-fetched to envision situations and conditions where the same sort of operations may be adapted to spacecraft and related vehicles. For example, the transfer of cargo, men and materiel, by some system akin to a "high line", is both realistic and natural in concept. In fact, schemes close to this idea have already been suggested in the popular literature.

The one factor to which all of these schemes relate, here, is the use of a light weight, flexible line in the execution of some specific task. This is, then, the concept which can be carried over, and put to use, in the performance of similar tasks for space operations. To date, some small use has been made of tethers - as an application of light weight, flexible connectors - in space ventures. However, there are many more uses to which flexible lines can be put other than those which have been demonstrated in the past.

In part, the current work, as reported here, has been directed to the study of systems involving tethers; and, to possible applications for these flexible connectors. For some of the problems investigated, the tasks are aimed at specific situations while for others the concepts are more general. As a means of providing information, and for orientation purposes, a brief outline of the work discussed in this report is presented in the following paragraphs.

Descriptions of the various tasks undertaken in the course of this investigation are given in the four main sections of the report. In section II the emphasis was on ascertaining what influence the physical properties of the tethered system had on its motion. Coupled with this was the influence of gravity

gradient and orbit eccentricity, these have been considered separately and together.

Through this approach the several influencing factors could be identified and their effect on the system's motion could be evaluated. Many of these consequences, which were noted, have been reported previously in the literature. The interested reader might wish to peruse references [5], [13] and [4], in particular. For additional information on these types of systems, it is recommended that references [6], [7], [8] and [14] be consulted. From these the reader will gather more than is needed for a basic understanding of tethered body system's behavior. These references are concerned with studies which are directed to more varied situations than those supposed in this investigation.

In this section of the report the basic motions, for this system, and the influencing factors, are identified and described. In addition to the above an examination of in-plane oscillatory (and rotational) motions has been conducted. From this the motion types were separated and the subsequence levels of tether force were described, in a manner somewhat analogous to that discussed in reference [3].

It was determined that the effect of orbit eccentricity could not generalize in the same fashion as the other influencing factors. Consequently, the manner in which this affected the tethered body motions had to be examined on a case-by-case basis. For this purpose use was made of the program which was developed by the contractor, and is described in reference [12].

Section III of the report describes the work which was carried out on extensible tether systems. Here both analytical and numerical studies were undertaken. In part these were done to determine what forces should be applied through the tether, per se, to accomodate a given motion for a suspended mass particle. This indirect approach was undertaken since the governing equations of motion were not amenable to a direct analytic solution. However,

in conjunction with this work it was discovered that one closed form solution type could be obtained, for an "extensible" tether system. (This case is documented in the section).

The numerical studies, noted above, were undertaken to obtain more explicit information on the handling and control of tethered mass systems. Recently some work on this aspect of the tethered bodies problem has been reported, see reference [16]. The primary undertaking, for the present work, was directed towards ascertaining how one might maintain control over the tethered system during its reel-out and reel-in operations. In this regard it was found that proper "control" could be maintained by selecting the correct "launch conditions", and holding a proper level of line tension throughout the maneuver.

For this phase of the investigation three modes of operation were examined. For each of these the conditions required for a successful handling of the system were determined, as were the "limits" imposed on each operational type. In addition to describing the "control" aspects of these problems, it was found that the operating characteristics for each system could be represented in a "universal parameter" format. The advantage of such a representation is that all solutions of a similar type are described by the same universal parameters. Hence, all solutions of a given family are known once a single solution has been acquired. (A similar approach to this concept was noted in reference [17]; however, there, a discrepancy in notation was apparently made. This led to an erronous representation, in the universal format, for the describing parameters). It is demonstrated, herein, that these systems can be manipulated so that tethered masses can be directed to almost any position (in-plane) relative to the spacecraft. These positions may be close (within a few meters) or far (hundreds of meters) from the main vehicle; of course, the positions, per se, must be within the dynamical limits attainably by the system. The advantage of such an operating scheme is most obvious -- here is a

maneuvering capability which will allow tethers to be used for an almost unlimited number of applications: Rescue, retrieval, cargo handling, other transport and transfer operations, to mention but a few. Not only is system versatility in evidence, but here is a scheme which can be employed over and over again at an almost negligible weight penalty. It is likely that some of the past reluctance to the use of tethers has been due to not having this understanding of "control" for these systems. Certainly it would be worthwhile to consider tethers seriously, for operational purposes, in future space ventures.

In section IV, herein, some special applications for tethers have been described, also. Specifically, the use of this system as a means of developing various levels of "gee" force has been examined. There one will find what length of line is needed to acquire a given force, for a prescribed orbit altitude. The range of "gee" which could be achieved by this means, gives rise to a large range of applications. It would seem that here is the means to maintain a steady force, at almost any level (within physical, practical limits), for as long as desired. This suggests uses for all sorts of experiments, for manufacturing and for direct spacecraft housekeeping (etc.) chores.

Allied with this phase of the investigation is another application for this system. That is, using the tether to establish a positional state, (say) below the spacecraft, where one could initiate a free "transfer maneuver" for the mass particle suspended from the line. Of course, variations of this basic concept also come to mind; and, in the report, several of these are examined, described and discussed. For reference purposes comparisons between these various transfer modes are made so that the reader may determine the relative merits of each. Here again is the evidence of a reusable system which would "cost" very little to operate as a space application. Of course, this idea could be incorporated with some other uses for tethers, making the whole concept more attractive than before.

Section V is devoted to the discussion of an orbit determination formulation which has been developed in conjunction with this investigation. This scheme differs from most other such methods in that it has been built around a set of relative motion state equations. Hence, this is a "relative motion" orbit determination scheme -- one referred to a moving "base point" rather than a "fixed" origin. Even though the work presented herein shows only the mathematical developments, the work is sufficiently complete to allow for the building of a computer program, implementing this method. (Development of an o.d. program has been partially completed, insofar as the mathematics is concerned. It is being developed as an Encke scheme).

With regard to tethered bodies problems, which have been the basis for most of this report, it is envisioned that this relative motion o.d. scheme could be adapted to some of these other situations. For example, the method could be employed to monitoring tether operations, and to "warn" at the onset of undesirable motions being developed. One possibility would be to monitor the tether force, and the motion of the suspended body, using this knowledge to predict subsequent events and to sound warnings as necessary. Whether or not this is a best concept to pursue has not been ascertained; such a task was not proposed for the present study.

The foregoing paragraphs have outlined the various tasks undertaken here. However, before leaving this section of the report, it seems advisable to say a few words which are more explicit regarding the report's makeup.

As noted above the several sections of this document are given to describing the work undertaken in this investigation. There the descriptions and discussions, along with sample cases, are presented. For all practical purposes no mathematical developments are presented in the main body of the report. This does not imply that the supporting mathematics is not to be found (here). The several appendices, included as the latter pages of this document, are devoted to these mathematical evaluations. They are referred to, as needed, in the descriptive

materials - thus, the reader can easily find the appropriate formulation if he so desires. The reason for constructing the report in this manner was to unincumber the descriptive material by keeping the mathematical developments separate from it. In this regard, it was felt that the reader would be better able to peruse the descriptive comments if the analytical statements were not immediately in evidence.

It should be mentioned, also, that one of the purposes for which this material is intended, is that it serve as a guide for the design and understanding of tethered body systems. It is for this reason that the first section (II) of the report has been included; and, for that matter the reason for some of the applications in the latter sections. Hopefully, these purposes are met, in addition to the reporting of other findings which have come to light as a consequence of this investigation.

TETHERED BODY SYSTEMS, WITH ELASTIC TETHERS

II.1 General.

The concept of two or more bodies joined by tethers, and used in space operations, is certainly not a new idea. Historically, the first astronaut's "space walk", or EVA* operation, was accomplished with the aid of a tether - primarily as a safety line. Subsequently, during the GEMINI series of flights, a tethered body experiment was conducted. There, the parent spacecraft and the spent AGENA stage were maneuvered together as a tether connected body system.

In this latter experiment the line length and properties were more akin to an elastic tether than was the system used during the earliest (and subsequent) EVA operations. From a speculative point of view it is likely that tethers will see expanded usage in future space applications, and for a variety of tasks.

In connection with this possibility the following paragraphs will discuss certain concepts and mechanical properties of these systems; and, some of the attendant consequences to operational situations. It should be remembered throughout this part of the report that the tether is considered, essentially, as an elastic member, not as an extensible one. The study of extensible tethers will be deferred until later in this documentation.

II.2 Equations Describing Tether Motions.

The differential equations describing the action of two tethered bodies, subject to gravitational attraction and the elastic forces of the tether, per se, are set down in Appendix B, in several forms. The most general expression is that given by eq. (B.2a); while the corresponding scalar (in-plane) expressions are noted as eqs. (B.9).

In these various equations ℓ is the tether length while θ is the orientation angle, for the line, relative to a local vertical, directed through the c.g. of the

*EVA is the acronym for Extra Vehicular Activities.

system.

It is immediately apparent that these general expressions are not amenable to analytical solution; and, that subsequent approximations are necessary if a form, which is convenient for mathematical manipulation, is obtained. Several such approximations are developed in section B.6 of the appendix. One of the more revealing formats is that shown as eqs. (B.13). There a simplification of the earlier noted equations is presented; one for small displacements, written in terms of the normalized stretch length ($\sigma \equiv \varkappa/\ell_o$). These particular expressions are:

$$\ddot{\sigma} + \frac{c}{\tilde{m}}\dot{\sigma} + \left[\frac{k}{\tilde{m}} - \left(\dot{\varphi}^2 + 2\frac{\mu}{r_g^3}\right)\right]\sigma \cong 2\dot{\varphi}\,\dot{\theta} + \left(\dot{\varphi}^2 + 2\frac{\mu}{r_g^3}\right),$$

and

$$\ddot{\theta} + 3\frac{\mu}{r_g^3}\theta \cong -(2\dot{\varphi}\dot{\sigma} + \ddot{\varphi}). \tag{II.1}$$

These equations are approximations for in-plane* motions; they include the necessary elastic properties (c, k), the gravitational influence (μ), and the effect of the orbit (through $\dot{\varphi}$, $\ddot{\varphi}$). The expressions are not independent, even through the small displacement approximations have been invoked. Here coupling is present through the Coriolis terms (a consequence of selecting a moving reference frame in which to describe the motions).

Interestingly, one can see that the θ-equation shows an influence of orbital eccentricity (through the $\ddot{\varphi}$ quantity). As a matter of reference this quantity may be described, for Keplerian motion, by

$$\ddot{\varphi} = -\frac{2V_c^2}{r^2}\,\epsilon \sin\varphi. \tag{II.2}$$

Here V_c, r, φ are "local" orbit values; however, ϵ is the path eccentricity; (V_c is the local circular orbit speed defined by $V_c^2 = \mu/r$).

*See figures in Appendix B for a graphical representation of this system.

A study of eqs. (II.1) indicates that they are in the same form as noted by eqs. (B.20a), Appendix B. This would suggest, for instance, that the "σ-frequency of motion" can be identified as:

$$\omega_\sigma^2 \equiv \frac{k}{\tilde{m}} - \left(\dot{\varphi}^2 + 2\,\frac{\mu}{r_g^3}\right), \tag{II.3a}$$

wherein

$$\omega_\ell^2 \equiv \frac{k}{\tilde{m}} \quad \begin{array}{l}\text{(the "natural frequency" of the}\\ \text{spring-mass system)*.}\end{array} \tag{II.3b}$$

In addition, the "θ-frequency of motion" may be described as:

$$\omega_\theta^2 \equiv 3\,\frac{\mu}{r_g^3}\ . \tag{II.3c}$$

Looking for the moment at ω_σ, one sees that this frequency is <u>less</u> <u>than</u> the natural frequency, ω_ℓ, by the amount indicated. There the two parameters noted are locally influenced. That is, they are affected through the orbit ($\dot{\varphi}$), and by the gravity gradient effect, $2\,\frac{\mu}{r_g^3}$ (see section B.8, Appendix B, for a discussion). It is somewhat unusual to find that these same two influences appear as "driving functions" in the equation for σ.

The remaining "forcing function", $2\dot{\varphi}\dot{\theta}$, for that expression, is the coupling term mentioned above.

The differential equation for θ (in eq. (II.1)) is the lesser affected of the two. It does not have a damping term, per se; it is not influenced (obviously) by the tether's elasticity except, in an implicit fashion, through the coupling (Coriolis) term. Yet it does have the afore noted effect from eccentricity through $\ddot{\varphi}$.

II.2.1 <u>Circular Orbit Approximation.</u>

When the concept of a circular reference (c.g.) orbit is impressed onto

*The parameter $\tilde{m}$ is the "reduced mass" of the tethered mass system.

eqs. (II.1) the results are found to be:

$$\ddot{\sigma} + \frac{c}{\tilde{m}} + \left[\frac{k}{\tilde{m}} - 3\dot{\varphi}^2\right]\sigma \cong 2\dot{\varphi}\,\dot{\theta} + 3\dot{\varphi}^2,$$

and

$$\ddot{\theta} + 3\dot{\varphi}^2\theta \cong -2\dot{\varphi}\dot{\sigma}. \tag{II.4}$$

It is evident that here, also, the in-plane coordinates cannot be described, analytically, in a closed form solution - the coupling terms do not allow this. However, it is not necessary to acquire such solutions in order to gather information about the motion of the system (see Appendix E, for more descriptive developments).

Considering the left side of eqs. (II.4) to be the "driving functions"; then the form-of-the-motion can be ascertained from the homogeneous equations. The "forcing functions", of course, have an influence provided through coupling ($\dot{\theta}$, $\dot{\sigma}$); and, from the orbital altitude (through $\dot{\varphi}$). Even though these latter effects are not readily described, analytically, the nature of them can be gathered from prior knowledge of similar solutions, from numerical results, or from a reasonable approximation (having some a priori knowledge of the motions to be simulated). Rather than to pursue this aspect of the problem, at this time, we shall pass on to a more general perusal of this situation.

From eqs. (II.4) it can be shown that the apparent (σ, θ) motions will not be, necessarily, displayed symmetrically. As a matter of fact (see section B.9b, Appendix B) there is a static state for these variants, namely:

$$\sigma_{st} = \frac{1}{\Omega^2 - 1}, \qquad \theta_{st} = 0, \tag{II.5}$$

wherein

$$\Omega^2 \equiv \frac{k/\tilde{m}}{3\dot{\varphi}^2} \equiv \frac{\omega_\ell^2}{\omega_\theta^2}, \qquad (\omega_\theta^2 = 3\dot{\varphi}^2 \text{ for circular orbits}).$$

The value of θ_{st} is obvious; i.e., the system should seek a zeroth position (this, of course, can be construed as a $\theta = \pi$ position, also). What is somewhat unforeseen here is the σ_{st} level. Regardless of this it should be recognized that σ_{st} represents a stretch, produced by the combined gravity gradient-orbit influence, and counteracted by the "spring" effect of the tether. Now, it is apparent that if the system is to have σ-oscillations, it will be necessary that $\Omega > 1.0$ (hence $\omega_\ell^2 > \omega_\theta^2$, as a lower limit on k).

As a consequence of σ_{st}, a new variable ($\tilde{\sigma}$) is defined - this is the displacement measured from σ_{st}. Corresponding to this definition the homogeneous differential equations are (see eqs. (B.18), Appendix B) now

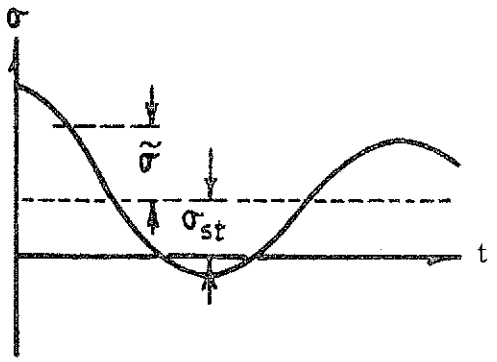

Fig. II.1. Description of $\tilde{\sigma}$ on graph of $\sigma = \sigma(t)$.

$$\ddot{\tilde{\sigma}} + \frac{c}{\tilde{m}}\dot{\tilde{\sigma}} + 3\dot{\varphi}^2(\Omega^2 - 1)\tilde{\sigma} \cong 0,$$

and

$$\ddot{\theta} + 3\dot{\varphi}^2\theta \cong 0. \qquad \text{(II.6)}$$

(Note that the coupling terms have been neglected here).

The basic motions (in $\tilde{\sigma}$, θ), for this system, are oscillations; one (for $\tilde{\sigma}$) is a damped sinusoid, while the other is not damped. (Actually, the damping in θ was noted, earlier, to be of second order - involving both $\dot{\sigma}$, $\dot{\theta}$ - this quantity was deleted in the "reduction - to-first-order" of terms).

II.2.2 Characteristics of the In-Plane Motion.

When the two motion types, depicted by eqs. (II.6), are examined independently it is found that they are generally patterned after the quantities described in section B.9, Appendix B.

For identification purposes the following quantities are noted:

(a) the natural σ- and θ-frequencies are,

$$\omega_\theta^2 \equiv 3\dot{\varphi}^2,$$

and

$$\omega_\sigma^2 \equiv 3\dot{\varphi}^2 (\Omega^2 - 1) = \omega_\ell^2 - \omega_\theta^2. \tag{II.7a}$$

Incidentally, the "natural frequency" for the circular orbit will be defined herein as: $\omega_o \equiv \dot{\varphi}$ (a constant for the motion).

(b) For the damped σ-oscillations the characteristics of the motion are described by the root pair:

$$s_{1,2} = \omega_\sigma \left[-\frac{c}{c_c} \pm i \sqrt{1 - \left(\frac{c}{c_c}\right)^2} \right], \tag{II.7b}$$

wherein, the critical damping coefficient,

$$c_c \equiv 2\tilde{m}\omega_\sigma = 2\tilde{m}\dot{\varphi} \sqrt{3(\Omega^2 - 1)}, \tag{II.7c}$$

with Ω described in eq. (II.5). This form for the s_j presupposed that $c/c_c < 1.0$; if this is not so (overdamping being present), then the motion is described in terms of real exponential functions.

Also, in agreement with the description of a damped frequency (see eq. B.20d, Appendix B), it is apparent that this quantity may be expressed here by,

$$\omega_{\sigma_d} = \omega_\sigma \sqrt{1 - \left(\frac{c}{c_c}\right)^2}, \tag{II.7d}$$

where ω_σ is defined above.

(c) Representing the characteristic roots (II.7b) as

$$s_j = (a \pm i\, \omega_{\sigma_d})_j, \quad (j = 1,2), \quad i \equiv \sqrt{-1}; \tag{II.7e}$$

(see section B.9, Appendix B), it is evident that eq. (II.7e) can be graphed as the unit circle,

$$\frac{s_j}{\omega_\sigma} = \left(\frac{a}{\omega_\sigma} \pm i \frac{\omega_{\sigma_d}}{\omega_\sigma} \right)_j , \qquad (j = 1, 2)$$

shown below. The shaded region, as noted in the appendix, represents a zone for divergent σ-motion (herein $c < 0$, and the system is fed energy through this "excitation"). The region where $a < 0$ is that one which describes "damped motions".

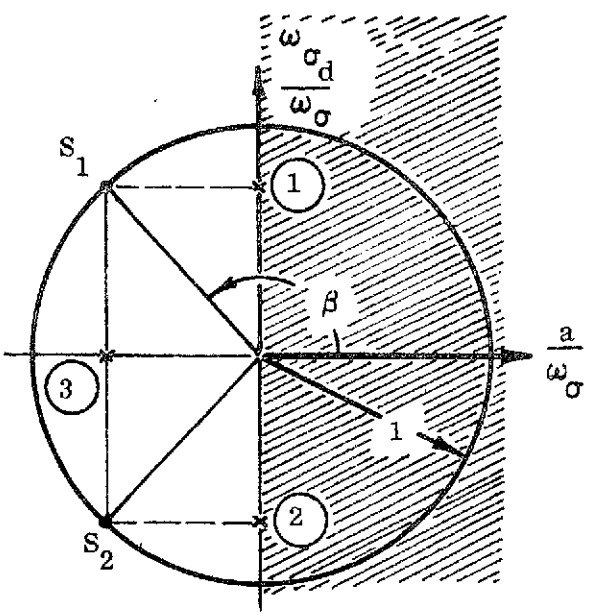

Fig. II.2(a). Argand Diagram of Characteristic Roots $s_{1,2}$ ($\equiv a + i\omega$), for a Damped Oscillation.

Note that here a representative root pair has been depicted. The points (1) and (2) describe "$i\omega_{\sigma_d}$" from the characteristics; while point (3) describes the reciprocal of the time constant for the motion.

The angle β, shown on the sketch, can be used to represent the damping ratio for the system, since

$$\tan \beta_j = \left(\frac{\omega_{\sigma_d}}{a} \right)_j = \pm \left[\frac{1 - \left(\frac{c}{c_c} \right)^2}{-\frac{c}{c_c}} \right], \qquad (II.8)$$

(for $j = 1, 2$).

Note that $|\beta| > \frac{\pi}{2}$ is a necessary condition for damped sinusoids to occur, as a trace of the σ-displacement in time.

If the sketch above is altered, so that the radius of the figure becomes ω_σ, then the effect of varying the parameters (k, c) for the system can be

simply illustrated. That is, on this modified figure, the points (1) and (2) denote $\pm i\,\omega_{\sigma_d}$, while point (3) is a location described by $-\frac{c}{c_c}\,\omega_\sigma$. It should be recognized that as $|\mathcal{I}(s)|$ ($\equiv \omega_{\sigma_d}$) is increased, in value, the period of the motion is decreased (see eq. (B.22a), Appendix B); conversely, as $|\mathcal{R}(s)|$ is increased the "stability" of the system is enhanced (or, the time constant, is decreased).

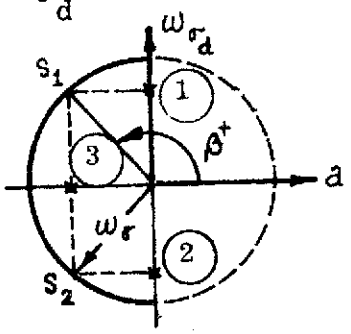

Fig. II.2(b). Characteristic Roots.

(d) The following diagrams will aid to clarify these comments.

First, two root pairs, $(s_j)_1$ and $(s_j)_2$, are assumed. These have a common value of frequency (ω_{σ_d}), but differing time constants ($1/a_\sigma$). As a consequence of these differences the envelopes, enclosing the motion's amplitudes, are not identical throughout. Necessarily, the root pair $(\sim)_2$ has the more confining exponential (decay) - hence the smaller time constant. Since the (assumed) frequencies are identical then the two motion types have a same periodicity for the oscillations.

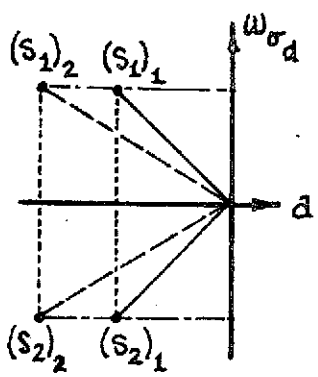

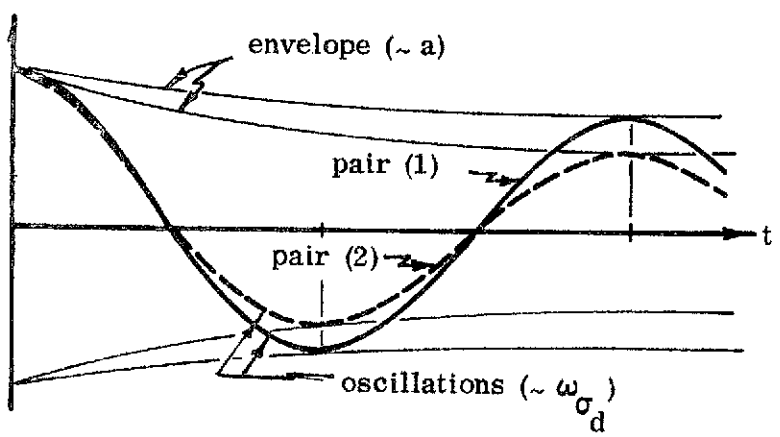

Fig. II.2(c). Motions for two Roots with a Same Frequency but Different Time Constants. Pair $(\sim)_2$ is the more Stable Case; both Pairs have a Same Period of Motion.

Contrary to the example above, the two root pairs, $(s_j)_3$ and $(s_j)_4$ have a same a_σ-value but different frequencies. Typical motion traces for these root types are depicted on the accompanying sketch (Fig. II.2d). There it is evident that the amplitude envelopes are identical for both traces, but that the oscillations have their individual periods, as indicated.

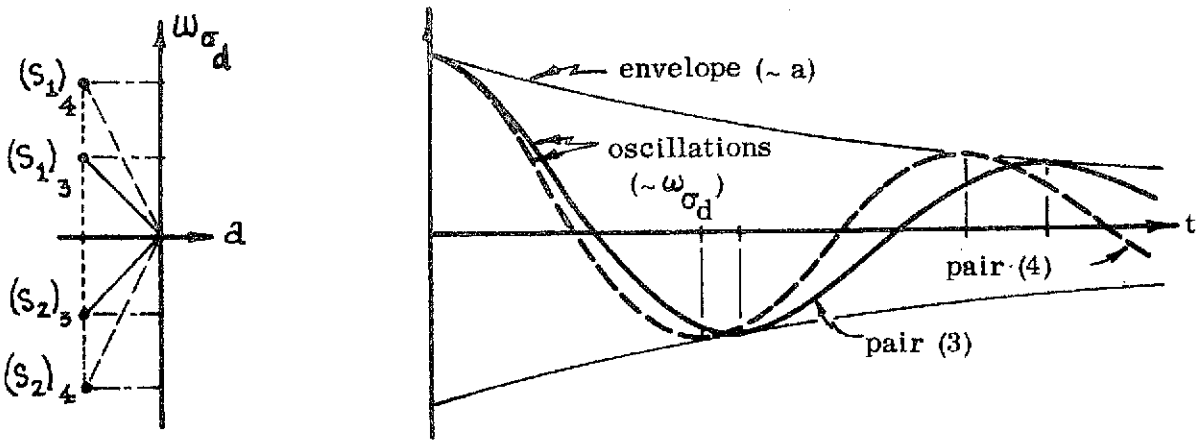

Fig. II.2(d). Motion for Root Pairs with a same "a" Value. Pair $(\sim)_3$ has the Larger Period; both Pairs have same Stability Trend.

(e) The characteristics for the θ-motion are considerably simpler than those in the case just described. In this instance (see eqs. (II.6)) the roots are:

$$s_{1,2} = \pm i \sqrt{3}\ \dot{\varphi}\ , \qquad \text{(II.9)}$$

signifying a pure oscillatory mode with a frequency which is $\sqrt{3}$ times that of the orbit ($\omega_o \equiv \dot{\varphi}$). (Note that when this root type is described on a phase diagram (ω, a) the points corresponding to eqs. (II.9a) are located where the circle cuts the vertical axis - i.e., where a = 0!). Here the frequency is related to the gravity gradient effect of the orbit rather than any mechanical property of the system.

(f) The full characteristics for the (σ, θ) motions are those to be obtained from the approximate governing equations (see eqs. (II.4)), reduced for motion

occurring about σ_{st}.

For conciseness, and simplicity in notation, let the independent variable (t) be replaced by an equivalent quantity - namely φ ($\equiv \dot{\varphi}\, t$)*. For these specializations eqs. (II.4) reduce to the following set:

$$\tilde{\sigma}'' + \frac{c}{\tilde{m}\omega_o}\,\tilde{\sigma}' + 3\,(\Omega^2-1)\,\tilde{\sigma} \cong 2\theta' \,,$$

and

$$\theta'' + 3\theta \cong -\,2\tilde{\sigma}' \,; \qquad \text{(II.10a)}$$

wherein $\omega_o \equiv \dot{\varphi}$, and $(\sim)'$ refers to differentiation with respect to φ.

The characteristic equations (in s), for this system of expressions (obtained by assuming a solution of the form, K exp (sφ), for each of the variables) are found to be:

$$\left[s^2 + \frac{c}{\tilde{m}\omega_o}\,s + 3\,(\Omega^2-1)\right]\tilde{\sigma} - (2s)\,\theta \cong 0,$$

and

$$\left[s^2+3\right]\theta + (2s)\,\tilde{\sigma} \cong 0. \qquad \text{(II.10b)}$$

The characteristic determinant for this set of algebraic equations is readily noted to be:

$$\text{Det}_c = s^4 + \frac{c}{\tilde{m}\omega_o}\,s^3 + (3\Omega^2+4)\,s^2 + 3\,\frac{c}{\tilde{m}\omega_o}\,s + 9\,(\Omega^2-1)\,. \qquad \text{(II.10c)}$$

Recalling that the roots here ($\text{Det}_c = 0$) describe the characteristic eigenvalues for the equation set (II.10b), then the solution to the above quartic determines the fundamental frequencies for the problem at hand. Obviously these values are explicitly dependent on the physical parameters which describe a particular tethered bodies problem.

*The $\dot{\varphi}$ value used here is that corresponding to the motion on the circular orbit.

It is easily seen that for the limiting state conditions ($\Omega^2 = 1$), see eqs. (II.5), and without damping in the system, the motion is divergent (as expected). Likewise, it can be argued that the absence of damping ($c = 0$) would lead to a situation which cannot necessarily guarantee a "stable" mode of motion - at best the system's motion could be classed as quasi-stable. As a matter of fact, it can be demonstrated that a stable mode of motion does not occur unless there <u>is</u> some damping in the system. It is not so much a question of "how-much damping" as it is the fact that there <u>is</u> damping present. Of course, it is also presupposed (here) that the "design" of the tether is such that the static state (σ_{st}, θ_{st}) is satisfied for any problem under consideration.

These statements, regarding the stability of in-plane motions, are based on the idea that the roots of the characteristic determinant will have negative real parts, ideally. It is essential not to have any roots with positive real parts since such quantities lead to the divergent motions which ultimately drive the system unstable. A systematic investigation * of the equations used here will indicate that the system, moving from its static state, will at least exhibit <u>asymptotic</u> stability.

A brief summary of the requirements for stability of a linear autonomous system (the Routh-Hurwitz Criterion for asymptotic stability) are set down below:

Suppose the characteristic equation from the determinate, eq. (II.10c), is expressed symbolically by:

$$a_o s^4 + a_1 s^3 + a_2 s^2 + a_3 s + a_4 = 0. \qquad \text{(II.10d)}$$

The conditions which will guarantee that <u>all</u> roots here have negative real parts are that the following determinants, formed from the constant coefficients, will be positive valued. That is, all of the determinants,

*See Art. 6.3 Stability of Linear Autonomous Systems. Routh-Hurwitz Criterion, in <u>Methods of Analytical Dynamics</u>, by L. Meirovitch, McGraw-Hill, 1970.

$$\text{Det}_1 \equiv a_1, \quad \text{Det}_2 = a_1 a_2 - a_o a_3 ,$$

$$\text{Det}_3 = a_1 \text{Det}_2 - a_4 a_1, \quad \text{Det}_4 = a_4 \text{Det}_3, \tag{II.10e}$$

must be positive valued when the system parameters are known*. For reference purposes these determinants, for the current case, are:

$$\text{Det}_1 = \frac{c}{\tilde{m}\omega_o} , \qquad \text{Det}_2 = \frac{c}{\tilde{m}\omega_o}(3\Omega^2+1),$$

$$\text{Det}_3 = 12\left(\frac{c}{\tilde{m}\omega_o}\right)^2, \text{ and,} \qquad \text{Det}_4 = 9(\Omega^2-1)\,\text{Det}_3. \tag{II.10f}$$

Necessarily the numbers obtained from these determinants are for the present problem. For other cases, examples, etc., the reader should consult reference [9].

Another consequence of equations (II.10a) is the modal amplitude ratio for these motions. What is inferred by this quotient is a description of the relative amplitudes of the motion for each eigenvalue from the characteristic equation.

Based on the premise that the motions are not unstable, the amplitude ratio may be written down immediately, and most simply, from the second of equations (II.10b). Thus,

$$\frac{\tilde{\sigma}}{\theta} = -\frac{s^2+3}{2s} , \tag{II.10g}$$

wherein s represents any of the characteristic roots from equation (II.10c). A more illuminating representation of this is acquired by assuming that the general solution format is expressed as

$$\tilde{\sigma}(t) \equiv \sum_1^4 A_j \exp(s_j t), \tag{II.10h}$$

and

*An assumption here is that eq. (II.10a) was written with $a_o > 0$.

$$\theta(t) \equiv \sum_{1}^{4} B_j \exp(s_j t); \qquad (j = 1, \ldots, 4), \tag{II.10h cont.}$$

for the present system.

Making substitutions into eqs. (II.10g) it follows that (after manipulation),

$$\frac{A_j}{B_j} = \frac{s_j^2 + 3}{-2s_j} \equiv \frac{1}{\mathcal{C}_j}, \qquad (j = 1, \ldots, 4). \tag{II.10i}$$

This determines each B_j ($\equiv \mathcal{C}_i A_j$) with the $\mathcal{C}_j$ described as shown. For an initial value problem it is evident that the A_j (or B_j) are acquired from the description of the initial state pertinent to the case being considered. For a more detailed discussion, see reference [15].

II.3 Summary.

For more immediate reference purposes the various descriptions presented and discussed in the foregoing paragraphs are summarized below. It is expected that in this manner the reader will be better able to quickly locate the various situations discussed, and to compare results in a more comprehensive manner.

The various case situations, for the in-plane motions (ℓ, θ), are described in terms of the governing differential equations, and as typical solution expressions, where applicable. The pertinent parameters for these solution types are noted; also, these are correlated to one another, generally, and as applicable.

For the small displacement approximations the usual coordinates (ℓ, θ) are replaced by the relative displacements (σ, θ; and/or $\tilde{\sigma}$, θ). This has been done for convenience, conciseness and mathematical simplicity of representation. It should be recalled that here, $\ell \equiv \ell_o + \varkappa$; $\sigma \equiv \varkappa/\ell_o$; $\tilde{\sigma} = \sigma - \sigma_{st}$, with σ_{st} referring to the static state value for σ (see section II.2.1).

Summary (Linear Elasticity)

II.3.1 General Differential Equations. (see section B.5, Appendix B); in-plane motion, two tethered bodies.

(tether motion) $$\ddot{\ell} - \ell(\dot{\theta}+\dot{\varphi}_g)^2 = -\frac{\mu}{r_g^3}\left[r_g\cos\theta\left(\Delta_2^{-3}-\Delta_1^{-3}\right)+\ell_1\Delta_1^{-3}+\ell_2\Delta_2^{-3}\right]-\ell\left[\frac{k}{\tilde{m}}\left(1-\frac{\ell_o}{\ell}\right)+\frac{c}{\tilde{m}}\frac{\dot{\ell}}{\ell}\right];$$

(θ-motion) $$2\dot{\ell}(\dot{\theta}+\dot{\varphi}_g)+\ell(\ddot{\theta}+\ddot{\varphi}_g) = \frac{\mu}{r_g^3}\left[r_g\sin\theta\left(\Delta_2^{-3}-\Delta_1^{-3}\right)\right],$$

wherein $\Delta_i \equiv \left[1+2(-1)^i(\ell_i/r_g)\cos\theta+(\ell_i/r_g)^2\right]^{\frac{1}{2}}$, $\tilde{m}\equiv m_1 m_2/\sum_1^2 m_i$ (see Appendix B for other definitions).

II.3.2 Approximations. ($\sigma \equiv \varkappa/\ell_o$, $\ell = \ell_o + \varkappa = \ell_o(1+\sigma)$; $\ell_o \equiv$ unstretched length, $\varkappa \equiv$ stretch).

(stretched tether motion) $$\ddot{\sigma}+\frac{c}{\tilde{m}}\dot{\sigma}+\left[\frac{k}{\tilde{m}}-(\dot{\theta}+\dot{\varphi})^2-\frac{\mu}{2r_g^3}(1+3\cos 2\theta)\right]\sigma \cong \frac{\mu}{2r_g^3}(1+3\cos 2\theta)+(\dot{\theta}+\dot{\varphi})^2;$$

(θ-motion) $$\ddot{\theta}+\frac{2\dot{\sigma}}{1+\sigma}\dot{\theta}+\frac{3\mu}{2r_g^3}\sin 2\theta \cong -\left(\ddot{\varphi}+\frac{2\dot{\sigma}}{1+\sigma}\dot{\varphi}\right),$$

or

$$\frac{d}{dt}\left[(1+\sigma)^2(\dot{\theta}+\dot{\varphi})\right] \cong -(1+\sigma)^2\frac{3\mu}{2r_g^3}\sin 2\theta;\ (\sim)_g \text{ refers to c.g. values*.}$$

*$(\sim)_g$ has been dropped from $\dot{\varphi}$, for convenience; the subscript is inferred.

II.3.3 Small Displacement Approximations (Linear Theory).

1. General Descriptions:

$$\ddot{\sigma} + \frac{c}{\tilde{m}}\dot{\sigma}\left[\frac{k}{\tilde{m}} - \left(\dot{\varphi}^2 + 2\frac{\mu}{r_g^3}\right)\right]\sigma - 2\dot{\varphi}\,\dot{\theta} \cong \left(\dot{\varphi}^2 + 2\frac{\mu}{r_g^3}\right),$$

$$\ddot{\theta} + 3\frac{\mu}{r_g^3}\theta + 2\dot{\varphi}\dot{\sigma} \cong -\ddot{\varphi}; \quad \text{where } r_g,\ \dot{\varphi},\ \ddot{\varphi}, \text{ etc. are for c.g.}$$

2. Special Case Description: (c.g. on circular orbit; $\frac{\mu}{r_g^3} = \dot{\varphi}^2$)

$$\ddot{\sigma} + \frac{c}{\tilde{m}}\dot{\sigma} + \omega_\sigma^2\,\sigma \cong 2\omega_o\dot{\theta} + 3\omega_o^2, \qquad \ddot{\theta} + \omega_\theta^2\,\dot{\theta} \cong -2\omega_o\dot{\sigma};$$

wherein

$$\omega_\theta^2 \equiv 3\omega_o^2,\ \omega_o \equiv \dot{\varphi};\ \omega_\sigma^2 \equiv \omega_\ell^2 - 3\omega_o^2,\ \omega_\ell^2 \equiv \frac{k}{\tilde{m}},\ \tilde{m} \equiv m_1 m_2 / \sum_1^2 m_i .$$

3. Static State:

$$\sigma_{st} \equiv (\Omega^2 - 1)^{-1},\ \Omega^2 \equiv \omega_\ell^2/\omega_\theta^2;\ \theta_{st} = 0 \quad (\sigma_{st},\ \theta_{st} \text{ are constants for the linear approximations}).$$

4. Motion Relative to the Static State: ($\tilde{\sigma} \equiv \sigma - \sigma_{st};\ \tilde{\theta} \equiv \theta - \theta_{st} = \theta$)

$$\ddot{\tilde{\sigma}} + \frac{c}{\tilde{m}}\dot{\tilde{\sigma}} + 3\omega_o^2(\Omega^2 - 1)\,\tilde{\sigma} = \frac{2}{\sqrt{3}}\omega_\theta\,\dot{\theta}, \qquad \ddot{\theta} + \omega_\theta^2 = -2\omega_o\dot{\tilde{\sigma}}.$$

II.3.4 Small Displacement Approximations. Restricted Cases.

1. Independent Motions: (a). θ-only: $\ddot{\theta} + 3\omega_\theta \theta = 0$.

Typical Solution (SHM): $\theta(t) = \theta_o \cos(\sqrt{3}\,\dot{\varphi}t) + \frac{\dot{\theta}_o}{\omega_o} \sin(\sqrt{3}\,\dot{\varphi}t)$; $\omega_\theta = \sqrt{3}\,\dot{\varphi}$, $(\sim)_o$ = init. value.

Period of Motion: $T_\theta = \frac{2\pi}{\omega_\theta} = \frac{2\pi}{\sqrt{3}\dot{\varphi}} = \frac{T_{orb}}{\sqrt{3}}$; $T_{orb} = \frac{2\pi}{\dot{\varphi}}$ (Modified Schuler Period).

(b). $\tilde{\sigma}$ - only (undamped): $\ddot{\tilde{\sigma}} + 3\omega_o^2 (\Omega^2 - 1)\,\tilde{\sigma} = 0$.

Typical Solution (SHM): $\tilde{\sigma}(t) = \tilde{\sigma}_o \cos\left(\sqrt{3(\Omega^2-1)}\,\dot{\varphi}t\right) + \frac{\dot{\tilde{\sigma}}_o \sin\left(\sqrt{3(\Omega^2-1)}\,\dot{\varphi}t\right)}{\sqrt{3(\Omega^2-1)}\,\dot{\varphi}}$.

Period of Motion: $T_{\tilde{\sigma}} = \frac{2\pi}{\sqrt{3(\Omega^2-1)}\dot{\varphi}} = \frac{T_{orb}}{\sqrt{3(\Omega^2-1)}}$; or, $T_{\tilde{\sigma}} = \frac{T_\theta}{\sqrt{\Omega^2-1}}$; $\Omega^2 \equiv \frac{k/\tilde{m}}{\omega_\theta^2}$.

(c). $\tilde{\sigma}$-only (damped): $\ddot{\tilde{\sigma}} + \frac{c}{\tilde{m}}\dot{\tilde{\sigma}} + 3\omega_o^2 (\Omega^2-1)\,\tilde{\sigma} = 0$; oscillations occur when:

$3\omega_o^2 (\Omega^2-1) > \left(\frac{c}{\tilde{m}\omega_o}\right)^2$. Critical damping constant: $\frac{c_c}{\tilde{m}} \equiv 2\omega_o \sqrt{3(\Omega^2-1)}$;

damped frequency: $\omega_{\tilde{\sigma}_d} \equiv \omega_{\tilde{\sigma}} \sqrt{1 - \left(\frac{c}{c_c}\right)^2}$, $\omega_{\tilde{\sigma}} \equiv \sqrt{3(\Omega^2-1)}\;\omega_o$,

II.3.4 Small Displacement Approximations (cont)

Characteristics: $$s_{1,2} = -\frac{c}{c_c}\omega_{\tilde{\sigma}} \pm i\sqrt{1-\left(\frac{c}{c_c}\right)^2}\,\omega_{\tilde{\sigma}}\,;\ \text{or,}\ \ s_{1,2} \equiv a_{\tilde{\sigma}} \pm i\,\omega_{\tilde{\sigma}_d}\ .$$

Typical Solution: $$\tilde{\sigma}(t) = \exp\,(a_{\tilde{\sigma}}t)\left[\tilde{\sigma}_o \cos\,(\omega_{\tilde{\sigma}_d}t) + \frac{\dot{\tilde{\sigma}}_o - a_{\tilde{\sigma}}\tilde{\sigma}_o}{\omega_{\tilde{\sigma}_d}} \sin\,(\omega_{\tilde{\sigma}_d}t)\right].$$

Period of Motion: $$T_{\tilde{\sigma}_d} = \frac{2\pi}{\omega_{\tilde{\sigma}_d}} = \frac{T_{\tilde{\sigma}}}{\sqrt{1-\left(\frac{c}{c_c}\right)^2}} = \frac{T_{orb}}{\sqrt{3(\Omega^2-1)\left[1-(c/c_c)^2\right]}}.$$

Time Constant for Motion (Time required for a reference displacement ($\tilde{\sigma}_{ref}$) to reduce to $\tilde{\sigma}_{ref}/e$):

$$t_c = \frac{1}{|a_{\tilde{\sigma}}|} = \frac{\sqrt{1-\left(\frac{c}{c_c}\right)^2}}{\omega_{\tilde{\sigma}_d}} = \frac{T_{\tilde{\sigma}_d}}{T_{orb}}\ .$$

2. Interdependent Motions (with Coupling).

$$\tilde{\sigma}'' + \frac{c}{\tilde{m}\omega_o}\tilde{\sigma}' + 3(\Omega^2-1)\tilde{\sigma} = 2\theta';\ \text{where, e.g.,}\ \tilde{\sigma}' \equiv \frac{\dot{\tilde{\sigma}}}{\dot{\varphi}},\ \text{etc.};$$

$$\theta'' + 3\theta = -2\tilde{\sigma}'.$$

II.3.4 Small Displacement Approximations (cont)

Characteristic eqn: $$\mathrm{Det}_c = s^4 + \frac{c}{\tilde{m}\omega_o} s^3 + (3\Omega^2+4)\, s^2 + 3\,\frac{c}{\tilde{m}\omega_o}\, s + 9\,(\Omega^2-1) = 0.$$

(Solutions to this quartic describe the characteristic roots (eigenvalues, $s_j \equiv (a \pm i\,\omega_d)_j$ for system).

Modal (Amplitude) Ratio: $$\left(\frac{\tilde{\sigma}}{\theta}\right)_j \equiv -\frac{s_j^2 + 3}{2s_j} = \frac{1}{\not{C}_j}$$ (for each eigenvalue).

Solution Type (format): $$\tilde{\sigma}(t) = \sum_1^4 A_j \exp(s_j \omega_o t); \quad \theta(t) = \sum_1^4 B_j \exp(s_j \omega_o t),$$

wherein; $$B_j \equiv A_j \not{C}_j \text{ (see above).}$$

II.4 The Swinging Tethered System.

The studies conducted in the foregoing paragraphs have been addressed to describing particular, but somewhat general, in-plane tethered body motions. In this section the θ-motion, alone, is examined to define the pendulous behavior of this dynamical system.

For the study of this motion consider (again) a circular reference orbit ($\dot{\varphi}$ = constant); thus, the appropriate governing equation is (see eqs. (B.11), Appendix B):

$$\ell\ddot{\theta} + 2\dot{\ell}\,(\dot{\theta}+\dot{\varphi}) + \frac{3}{2}\,\ell\dot{\varphi}^2 \sin 2\theta \cong 0. \tag{II.11}$$

(Note Fig. II.3, below, for a description of coordinates, etc.).

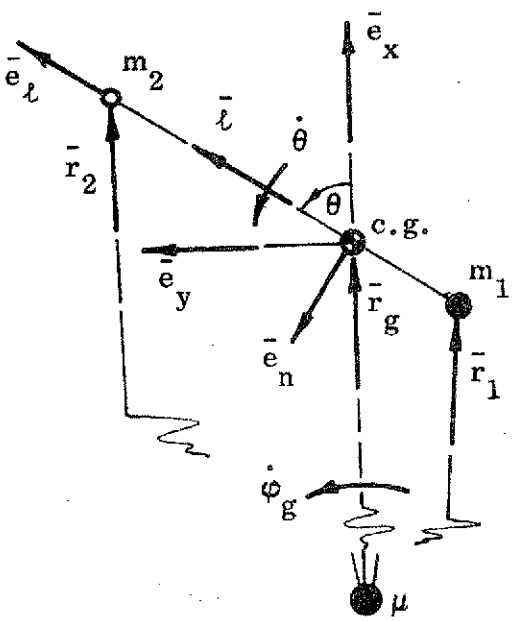

Fig. II.3. Sketch Depicting a "Swinging" Tether System.

Assuming that the tether stretch is small, then $\ell \cong$ constant, and the expression above reduces to

$$\ddot{\theta} + \frac{3}{2}\dot{\varphi}^2 \sin 2\theta \cong 0.$$

To solve this equation, multiply it through with $\dot{\theta}$; then it may be recast as;

$$\frac{d}{dt}\left(\frac{\dot{\theta}^2}{2} - \frac{3}{4}\dot{\varphi}^2 \cos 2\theta\right) = 0;$$

from which it is inferred that,

$$\dot{\theta}^2 - \frac{3}{2}\dot{\varphi}^2 \cos 2\theta = \mathcal{C}_1, \tag{II.12}$$

where $\mathcal{C}_1$ is a constant.

If eq. (II.12) is examined as an explicit state-valued problem, then the constant can be evaluated for (say) the condition:

$$\dot{\theta} \to 0 \quad \text{as} \quad \theta \to \theta_m:$$

(this infers an oscillatory motion). Here θ_m refers to the extremal in this variable; hence eq. (II.12) could be rewritten as;

$$\left(\frac{\dot{\theta}}{\dot{\varphi}}\right)^2 = \frac{3}{2}(\cos 2\theta - \cos 2\theta_m), \tag{II.13a}$$

with $(\theta, \dot{\theta})$ describing the "state" at some given "point" during the motion.

Equally useful as a general form is eq. (II.12) written as:

$$\left(\frac{\dot{\theta}}{\dot{\varphi}}\right)^2 = \frac{3}{2}\left[\frac{2\mathcal{C}_1}{3\dot{\varphi}^2} + \cos 2\theta\right], \tag{II.13b}$$

wherein, the state $(\theta, \dot{\theta})$ must be consistently described.

To acquire some insight into the representations drawn from this result, consider the following situations:

(1) For oscillatory motions:

Since $\dot{\theta}^2 \geq 0$; and, here, $|\cos 2\theta| \leq 1.0$, then it is apparent that for,

$$-1 \leq \cos 2\theta \leq 1,$$

$$\frac{3\dot{\varphi}^2}{2} \geq \mathcal{C}_1 \geq -\frac{3\dot{\varphi}^2}{2}. \tag{II.14}$$

This expresses the range of values $\mathcal{C}_1$ may take on the SHM*.

(2) For a rotating system:

In view of the conditions set down above, it is evident that for this case,

$$\mathcal{C}_1 > \frac{3\dot{\varphi}^2}{2}.$$

This should provide for $\dot{\theta}^2 > 0$, for all times, generally. Thus, the system is in a continuous rotational state of motion.

*SMH is an acronym for simple harmonic motion.

With this information at hand, it is intersting to graph eq. (II.13b) - as a means of representing the behavior of $\dot{\theta} = \dot{\theta}(\theta)$.

Figures II.4 are plots of $(\dot{\theta}/\dot{\varphi})^2$, and $\dot{\theta}/\dot{\varphi}$, as functions of θ, for the angle range $0 \leq \theta \leq \pi$. This restricted range in θ has been used since the symmetry of equation (II.13b) describes the repetition in graphing over a full (2π) range. The cyclic nature of these functions is indicative of the obvious symmetry which must exist.

Looking at Fig. II.4a, one sees the several curves plotted for selected values of $\mathcal{C}_1/\dot{\varphi}^2$. The reasoning behind the selection of these numbers, in particular, will become evident subsequently.

Recognizing that $\dot{\theta}^2 \geq 0$ for any "real" case, then the shaded region (for $\dot{\theta}^2 < 0$) has no physical significance to the tether problem. Also, from the graph, it is apparent that for values of $\mathcal{C}_1/\dot{\varphi}^2 < \frac{3}{2}$, the motion is constrained to a specific range of θ. Also, note that if $\mathcal{C}_1/\dot{\varphi}^2 = -\frac{3}{2}$, then there are no real motions apparent. At best, then, the system will remain static at the positions $(0, \pi)$.

When $(\mathcal{C}_1/\dot{\varphi}^2)$ is increased to $-\frac{5}{4}$ there are θ-regions in which oscillations may occur. In particular, for this level for $\mathcal{C}_1/\dot{\varphi}^2$, the motions are constrained to;

$$-16.78^\circ \leq \theta \leq +16.78^\circ, \text{ and } 163.22^\circ \leq \theta \leq 196.78^\circ.$$

An overall view of this figure indicates that oscillations may be predicted for assigned values of $\mathcal{C}_1/\dot{\varphi}^2$ satisfying the inequality

$$-\frac{3}{2} \leq \frac{\mathcal{C}_1}{\dot{\varphi}^2} \leq +\frac{3}{2}.$$

For $\mathcal{C}_1/\dot{\varphi}^2 > +\frac{3}{2}$ the motions are rotations. It should be pointed out that for $\mathcal{C}_1/\dot{\varphi}^2 = \frac{3}{2}$ the motion remains constrained (in one or the other of the $\theta = \pi$ regions) since $\dot{\theta}$ vanishes at $\theta = \pi/2$ (and $-\pi/2$).

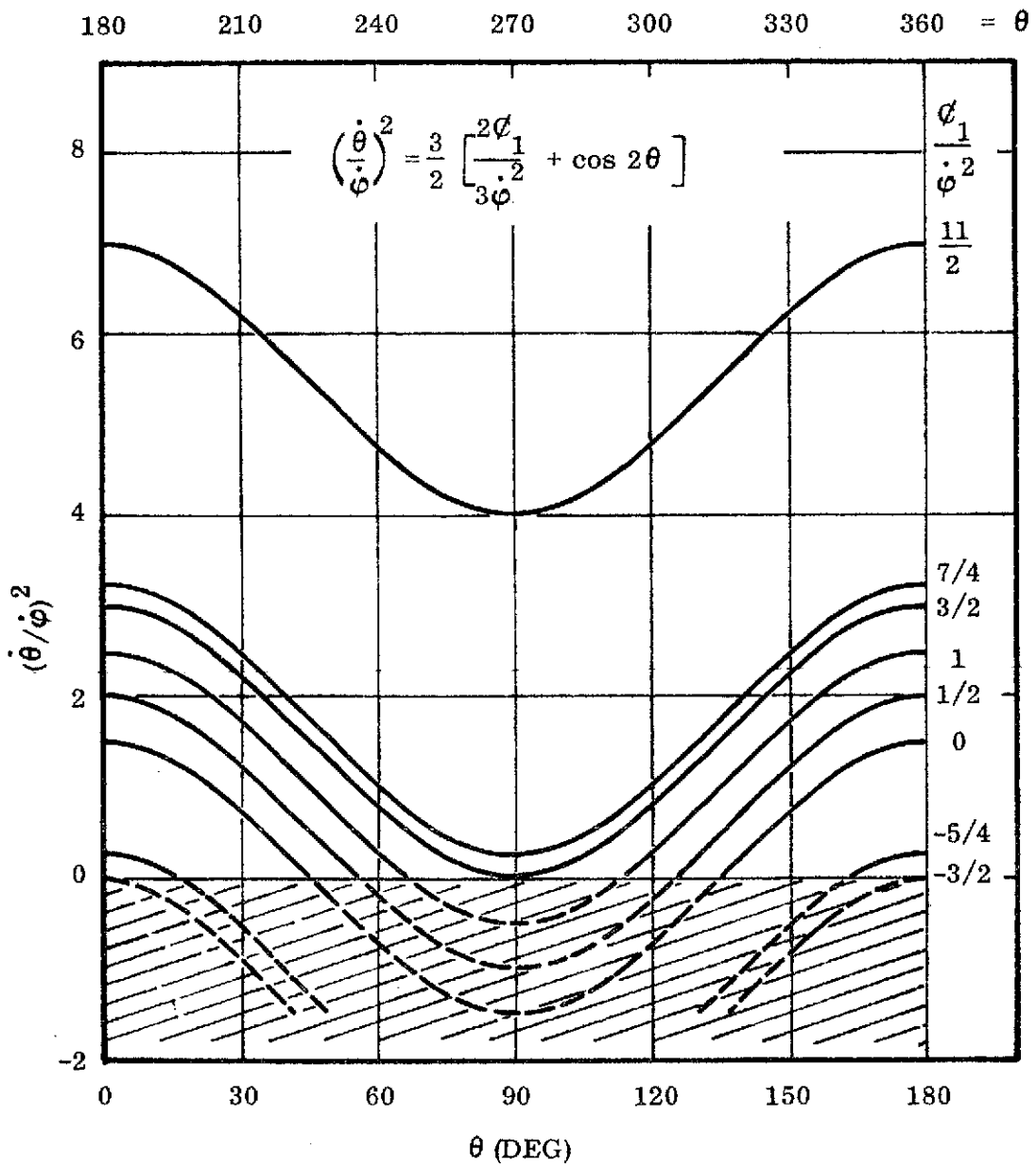

Fig. II.4(a). Pendulous Motion ($\dot\theta$), in Terms of θ, for Selected Values of the Constant, $\mathcal{C}_1$.

As an aid to understanding Fig. II.4a, the tabulation below describes the constraint boundaries, for the oscillations. (This is for $\mathcal{C}_1/\dot{\varphi}^2 < \frac{3}{2}$, as seen on the plot).

$\mathcal{C}_1/\dot{\varphi}^2$	Bounds on θ (I, IV)*	Bounds on θ (II, III)*
$+\frac{3}{2}$	$-90^\circ \le \theta \le +90^\circ$	$90^\circ \le \theta \le 270^\circ$
$+1$	$-65.905 \le \theta \le +65.905^\circ$	$114.095^\circ \le \theta \le 245.905^\circ$
$+\frac{1}{2}$	$-54.736^\circ \le \theta \le +54.736^\circ$	$125.264^\circ \le \theta \le 234.736^\circ$
0	$-45.0^\circ \le \theta \le +45.0^\circ$	$135.0^\circ \le \theta \le 225.0^\circ$
$-\frac{5}{4}$	$-16.78^\circ \le \theta \le +16.78^\circ$	$163.22^\circ \le \theta \le 196.78^\circ$
$-\frac{3}{2}$	$\theta = 0$ (static state)	$\theta = \pi$ (static state).

The more interesting graph here is that shown on Fig. II.4b; here one finds the angular speed ratio, $\dot{\theta}/\dot{\varphi}$, plotted as a function of θ. This figure is simply a revision of the former one, but one which shows both the $\pm\,\dot{\theta}$ range (and the θ constraints) for the prescribed values of $\mathcal{C}_1/\dot{\varphi}^2$.

It is immediately apparent that $\dot{\theta}$ is limited, in magnitude, for each level of $\mathcal{C}_1/\dot{\varphi}^2$ assumed. Likewise the possible range in θ, for which oscillations may occur, is graphically evidenced here. Once again, the static state situation, existing for $\mathcal{C}_1/\dot{\varphi}^2 = -\frac{3}{2}$, is noted by the $\dot{\theta} = 0$ value(s) at the $\theta = 0, \pi$ positions.

For the range $-\frac{3}{2} < \mathcal{C}_1/\dot{\varphi}^2 < +\frac{3}{2}$ oscillations are predicted; however, when $\mathcal{C}_1/\dot{\varphi}^2 > \frac{3}{2}$, the system is rotational (as noted earlier).

The curves drawn here, depicting the oscillatory modes, are not complete insofar as the region(s) of acceptable θ-values are concerned. It should be recalled that (from symmetry) there is a corresponding trace - below $\theta = 0$, and above $\theta = \pi$ - into which these constrained motions continue**. Also, recognizing

* Denotes quadrants.

** This is described, and accounted for, on the figure by means of the dual θ-scales.

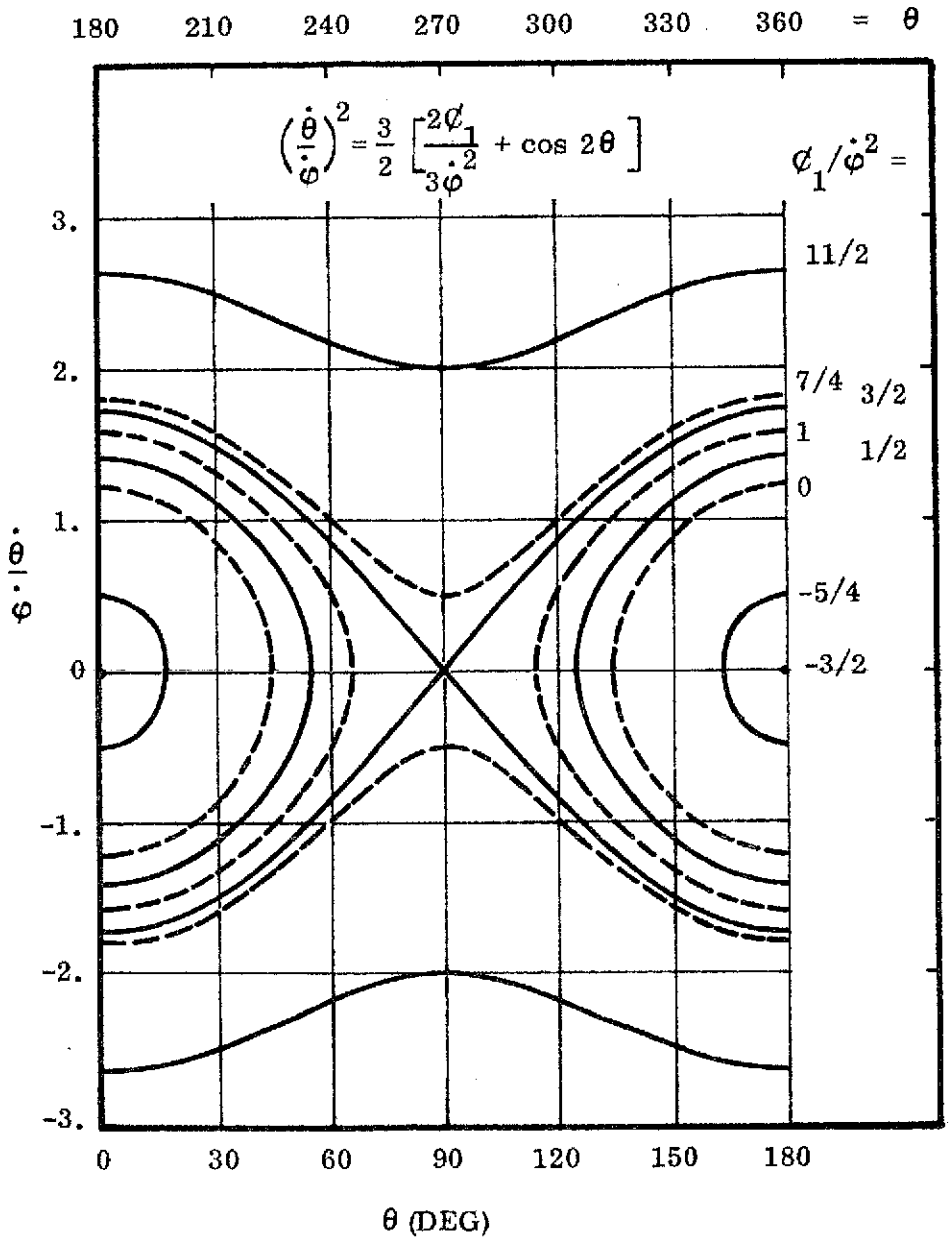

Fig. II.4(b). The Pendulous Motion, Showing $\pm\dot{\theta}$ Values, as a Function of θ, for Selected Values of $\mathcal{C}_1$.

that any oscillation will have both $\pm\,\theta$ values, then each curve (of this type) depicts the $\dot{\theta}$, θ relationship which must exist for a "non-rotating" tethered body problem.

Those curves, for $\mathcal{C}_1/\dot{\varphi}^2 > \frac{3}{2}$, which do not reach the $\dot{\theta} = 0$ line describe rotating tethered systems. Since these modes are unconstrained in θ, these particular curves are mainly indicative of the variations in $\dot{\theta}$ which <u>may</u> occur for a given (selected) system.

Allied with these various motions is the force system which is developed and counteracted by the tether, provided the system retains its constrained length. Following along with the conditions and results noted immediately above, the investigation described in the next few paragraphs will be concerned with these tether forces. Not only will the force magnitudes be determined, but the consequences of the ($\dot{\theta}$, θ) state will be indicated.

II.5 Tether Forces.

So far, here, the problem investigated has dealt with various mechanical actions for the tethered bodies problem. In particular,information on the displacements of the system has been gathered. Throughout these studies it was presumed that the member joining the masses was itself massless - thus it has not been affected by external forces - also, it is incapable of sustaining compressions. In this regard the study has not been complicated by having to consider traveling waves, etc. along the tether.

Even with all of the simplifications presumed so far, it would be useful to have some idea of the force magnitudes which the tether must support. Likewise it would be interesting to learn how these forces may be affected by particular motions for the system. In the paragraphs which follow, this topic will be pursued and examined.

In defining the force levels which must be supported by the tether, it is assumed that this task depends directly on that one conducted in the previous section. That is, the forces will be dependent on the θ-oscillations and rotations for the system.

Knowing that the swinging motions are not symmetrically disposed, with and against the orbital motion, then it follows that the force magnitudes would be affected accordingly.

The describing equation, to be used in determining the supporting force(s) from the tether, is eqs. (B.11), Appendix B. For compatibility with the discussion on the θ-motions it is assumed that the tether length is essentially constant.

Here eq. (B.11): i.e.,

$$\ddot{\ell} - \ell\,(\dot{\theta}+\dot{\varphi})^2 \cong \frac{\mu\ell}{2r_g^3}\,(1+3\cos 2\theta) - \frac{k}{\tilde{m}}\,(\ell-\ell_o) - \frac{c}{\tilde{m}}\,\dot{\ell}\,,$$

is specialized as noted above, and simplified for a circular reference orbit (r_g = constant); it becomes,

$$\frac{T_s}{\tilde{m}} \equiv \ell\,(\dot{\theta}+\dot{\varphi})^2 + \frac{\ell\dot{\varphi}^2}{2}\,(1+3\cos 2\theta), \qquad \text{(II.15)}$$

wherein T_s is the supporting (tensile) force developed in the tether. This force, obviously, can become or replace the elastic spring force assumed earlier.

Since the conditions, here, must be compatible with those used to study the θ-motion (above); then those results may be impressed onto this evaluation. Consequently, eq. (II.13b) is used here, subjected to the constraints and conditions described in section II.4.

Rearranging eq. (II.15) and drawing on eq. (II.13b) for the description of $\dot{\theta}/\dot{\varphi}$, then it is found that the <u>specific</u> force equation is:

$$\frac{T_s}{\tilde{m}\ell\dot{\varphi}^2} = \frac{3}{2}\left\{\left(1 + \frac{2\mathcal{C}_1}{3\dot{\varphi}^2}\right) + 2\left[\cos 2\theta \pm \sqrt{\frac{2}{3}\left(\cos 2\theta \frac{2\mathcal{C}_1}{3\dot{\varphi}^2}\right)}\right]\right\}. \qquad \text{(II.16)}$$

Note that this is a dimensionless format; and, that the ± sign on the radical refers (directly) to the ± $\dot{\theta}$ rotations (oscillations) for the system.

The correspondence between the supporting tension and the $\dot{\theta}$-motion is apparent here. Particular solutions relate to the particular values of $\mathcal{C}_1/\dot{\varphi}^2$ used in describing the $\dot{\theta}$ regimes. The task now is to define the force variations and to determine the extremes and the zeros for the forces.

II.5.1 Extremals for the Specific Tensile Force.

An evaluation of the extremals can be carried out by classical theory. In this regard it is convenient to examine eq. (II.16) in terms of the variant, (2θ). Thus the conditions for extremals may be obtained from

$$\frac{d}{d(2\theta)}\left[\frac{2T_s}{3\tilde{m}\ell\dot{\varphi}^2}\right] = 0.$$

After differentiation and simplification it is found that the conditions obtained for extremals are:

(a) $\sin 2\theta = 0,$

and

(b) $\cos 2\theta = \frac{1}{6} - \frac{2}{3}\left(\frac{\mathcal{C}_1}{\dot{\varphi}^2}\right).$ (II.17a)

The first condition obviously indicates extremals are to be found at $\theta = \pm \frac{n\pi}{2}$, $(n = 0, 1, 2.....)$. The second condition should be somewhat more revealing since it is tied to the "levels" of $\dot{\theta}/\dot{\varphi}$ which the system experiences - and, correspondingly, to the regions of θ where these occur.

One condition to be placed on the extremals for this study is in conjunction with the recognition that $-1 \leq \cos 2\theta \leq +1$. For this condition it follows, directly, that

$$-\frac{5}{4} \leq \frac{\mathcal{C}_1}{\dot{\varphi}^2} \leq \frac{7}{4}; \tag{II.17b}$$

but without regard to sgn $\dot{\theta}$.

A look at Figs. II.4 indicates that for this range of $\mathcal{C}_1/\dot{\varphi}^2$ the tether system will exhibit oscillations, for the most part; but it may have some rotational modes for a part of the range. In particular, oscillations are expected for,

$$-\frac{5}{4} \leq \frac{\mathcal{C}_1}{\dot{\varphi}^2} \leq \frac{3}{2}; \tag{II.17c}$$

and rotations are apparent when,

$$\frac{3}{2} < \frac{\mathcal{C}_1}{\dot{\varphi}^2} \leq \frac{7}{4}. \tag{II.17d}$$

It is evident, now, that some of the extremals for the tension parameter $\left(\frac{T_s}{\tilde{m}\ell\dot{\varphi}^2}\right)$ occur at other than $\theta = \frac{n\pi}{2}$, for oscillatory motions. To ascertain whether or not these positions correspond to maxima or minima, one could examine for this, via the second* derivative, and check the sufficiency conditions there.

For reference purposes several values of $\mathcal{C}_1/\dot{\varphi}^2$ are examined to define these extremals, and to indicate the location(s) for each. Generally the numbers used here are those indicated on Fig. II.4.

*It should be recalled that second derivatives may not be sufficient, within themselves, and higher derivatives may be needed. See standard texts for a more complete discussion.

EXTREMALS FOR THE TETHER TENSION

$\mathcal{C}_1/\dot{\varphi}^2$	Extremal type for $\left(T_s/\tilde{m}\ell\dot{\varphi}^2\right)$	Location of extremal[(a)] ($\pm\theta$)	Value of $T_s/\tilde{m}\ell\dot{\varphi}^2$ at the extremal[(c)]
$\frac{7}{4}$ (b)	min	270^o, 90^o	$-\frac{3}{4}$; $+\frac{5}{4}$ (d)
$\frac{3}{2}$	min	253.22^o, 73.22^o	$-\frac{1}{2}$
1	min	240^o, 60^o	0
$\frac{1}{2}$	min	229.797^o, 49.797^o	$+\frac{1}{2}$
0	min	220.203^o, 40.203^o	+1
$-\frac{5}{4}$	min	360^o, 180^o	$+\frac{9}{4}$

(a) $\cos 2\theta = \frac{1}{6} - \frac{2}{3}\left(\frac{\mathcal{C}_1}{\dot{\varphi}^2}\right)$. (b) Rotating System. (c) Values are for $\dot{\theta} < 0$.
(d) Value at $\dot{\theta} > 0$.

The extremals listed here appear to be minima, generally. Evidentally these conditions occur as such since the maxima are described by the first condition for the extremal. It will be noted, subsequently, when representative plots are presented, that these various conditions do occur as predicted.

There is, yet, one other condition for the specific tension which should be examined and commented upon. This is a determination of the "zeros" in the tensile force. In the next subsection this topic is explored.

II.5.2 Zeros for the Tensile Force.

From a physical point of view it is likely that this condition will be most evident for a system in rotation, and in oscillation, with $\dot{\theta} < 0$. What would be happening in this case is that the pendulous action, and/or rotation, would be "against" the orbital motion. This would tend to reduce the centrifugal force acting on the "suspended" mass of the tether system.

To examine this situation return to eq. (II.16), let $T_s = 0$, separate and solve the resulting quadratic. Of course, the condition of $\dot{\theta} < 0$ infers a negative radical in this equation. Having carried out the mathematical operations and simplified the result, one finds that the θ-position, for $T_s = 0$, is described by:

$$\theta = \frac{1}{2}\cos^{-1}\left\{\frac{1}{2}\left[\frac{2}{3}\left(\frac{\mathcal{C}_1}{\dot{\varphi}^2}\right)+\frac{1}{3}\right] \pm \frac{1}{3}\sqrt{2\left[\left(\frac{\mathcal{C}_1}{\dot{\varphi}^2}\right)-1\right]}\right\}. \qquad \text{(II.18)}$$

For this expression it is apparent that $\left(\frac{\mathcal{C}_1}{\dot{\varphi}^2} \geq 1\right)$. There does not appear to be any upper limit on this quantity. However, it is recognized (see Fig. II.4) that $\frac{\mathcal{C}_1}{\dot{\varphi}^2} = 1$ indicates the upper limit for oscillatory motions. Values in excess of this level would represent a rotating tethered mass system.

One added piece of information on this problem can be gleaned from eq. (II.18). This answers the question regarding any other limiting value, for $\mathcal{C}_1/\dot{\varphi}^2$, at which $T_s = 0$.

Without becoming involved in the mathematics of this relationship, it is easily demonstrated that $\mathcal{C}_1 = \frac{11}{2}\dot{\varphi}^2$ describes this limit. Apparently for $\mathcal{C}_1 > \frac{11}{2}\dot{\varphi}^2$ the $(-\dot{\theta})$ rotating system acquires sufficient energy to keep the tether taut throughout each cycle. In this regard, then, the sought for limit on $\mathcal{C}_1$ has been determined. Consequently, the reader now should have a firm understanding of these rotating (or oscillating) fixed length, in-plane tethered body motions.

For the purpose of illustrating these varied conditions, and some others, several plots will be presented, next. These describe the variations of T_s with $\dot{\theta}$, for both the oscillating and rotating systems. Also, they lead to descriptions of other factors influencing the problem.

II.5.3 Representation of Tether Tension.

Figures II.5 are graphs showing variations of the dimensionless, specific tension ($T_s/\tilde{m}\ell\dot{\varphi}^2$) with θ, using $\mathcal{C}_1/\dot{\varphi}^2$ as a plotting parameter. (To correlate the tensions with the turning rates, $\dot{\theta}$, the reader should consult Figs. II.4).

Generally speaking, Fig. II.5a* depicts the variations for oscillatory motions, while Fig. II.5b is more representative of the rotating systems.

On this first graph (II.5a), the curve for $\mathcal{C}_1 = \frac{11}{2}\dot{\varphi}^2$ does not define an oscillation; however, it does represent a limiting situation (the boundary value described in section II.5.2).

It should be brought out, rather strongly, that these plots are for only a region of the total θ-range which does exist. In particular, only one quadrant of the overall situation is described on these graphs. From the symmetry of the governing equations ($T_s/\tilde{m}\ell\dot{\varphi}^2$, $\dot{\theta}/\dot{\varphi}$, $\dot{\theta}^2/\dot{\varphi}^2$) it is recognized that the figures "repeat" over the full $\theta(2\pi)$ range. Specifically, these plots are reflected in the $\theta = 0$ axis, and in the $\theta = \frac{\pi}{2}$ axis. This accounts for the two angle scales shown on the figures. Also, since the system assumed here cannot accept compressive forces, the curve segments for $T_s < 0$ are always shown as broken lines.

To describe a particular behavior of T_s with θ, over a given cycle of motion, consider (as an example) the curve for $\mathcal{C}_1 = \dot{\varphi}^2$, Fig. II.5a. Beginning with the uppermost ordinate, and presuming that this corresponds to $\theta = \pi$, then the θ-motion is traced out and down along that curve. What is implied is that as θ increases (beyond π) the tension is decreasing! Here the motion is given by $\dot{\theta} > 0$. The largest value of θ which can be reached by this system (with $\mathcal{C}_1 = \dot{\varphi}^2$) is $\theta \equiv \pi + 65.905^\circ$. At this point $\dot{\theta} = 0$ (see Fig. II.4a and/or II.4b) and there the tension is $T_s = \frac{1}{2}\tilde{m}\ell\dot{\varphi}^2$.

*A curve similar to this one is found in reference [3]. The analysis has been expanded here.

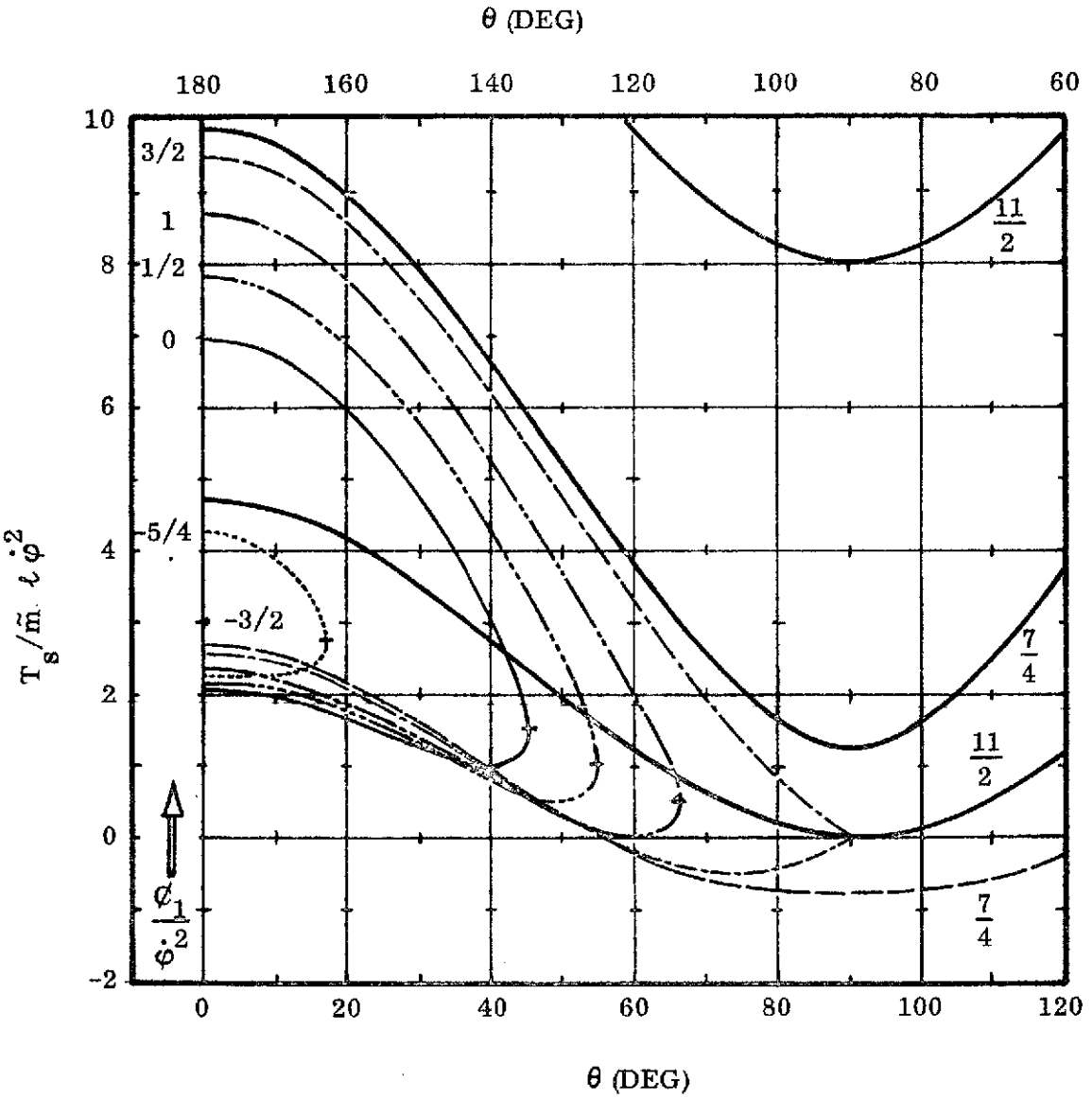

Fig. II.5(a). Variations in Tether Tension (T_s) due to Assigned Values of $\pm\,\dot{\theta}$. Note Values of $\phi_1/\dot{\varphi}^2$ designated on Curves. Each Curve, for Oscillatory Motions, has a tic noting Location where $\dot{\theta}$ Changes Sign.

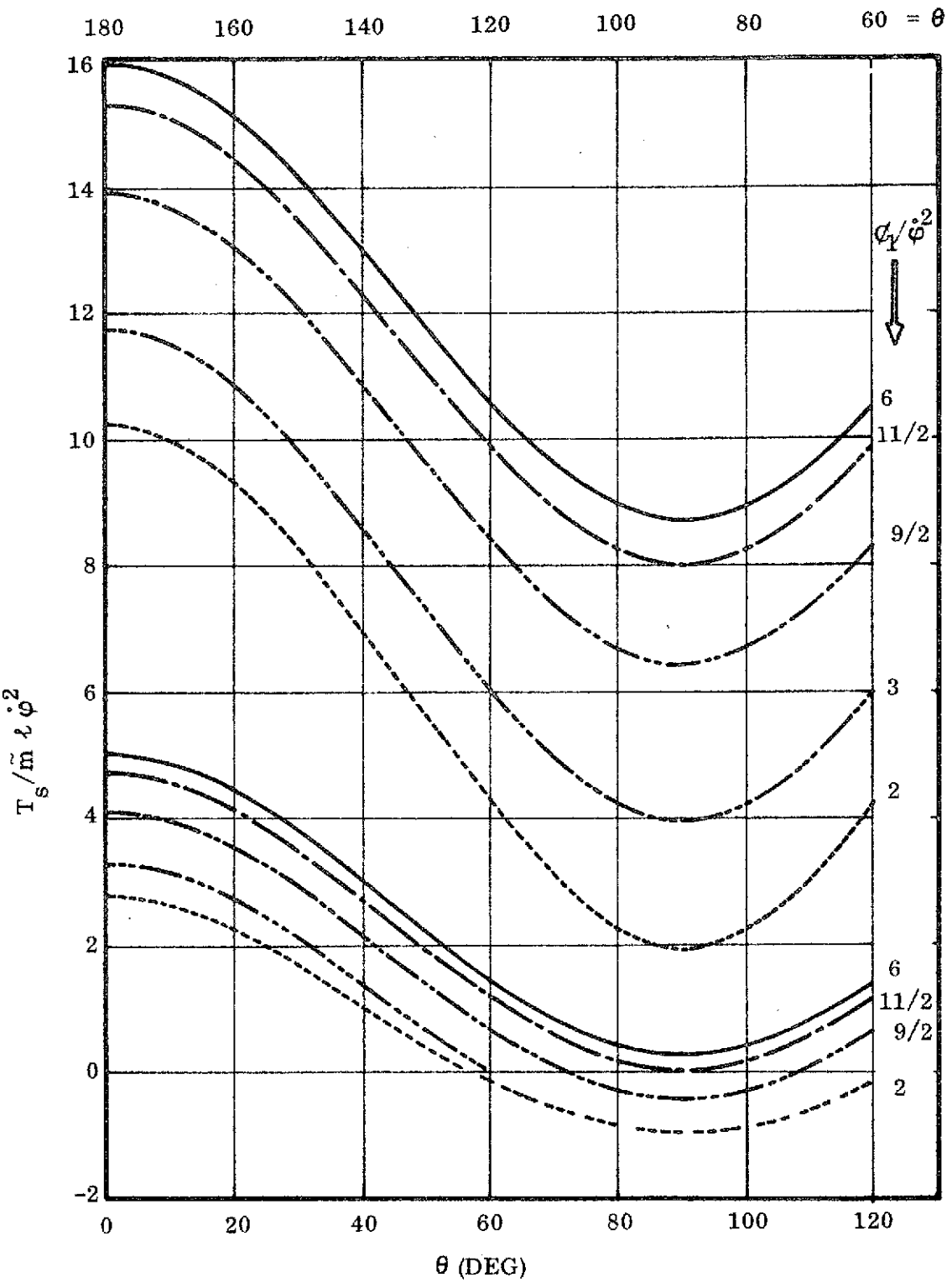

Fig. II.5(b). Variations in Tether Tension (T_s), for Values of $\phi_1/\dot{\varphi}^2$ Describing θ-Rotations (primarily).

The oscillation continues, but with $\dot{\theta} < 0$ now. As the motion continues T_s diminishes, reaching its lowest level, $T_s = 0$, at $\theta = \frac{4\pi}{3}$ (an extremum). Beyond this point the tension is increasing, $\dot{\theta} < 0$, and the system is tending (back) toward $\theta = \pi$. When the oscillation reaches $\theta = \pi$, the tension reaches a local maximum ($T_s = 2.3377\ \tilde{m}\ell\dot{\varphi}^2$).

With the motion continuing into the $-\theta$ region, the trajectory is a mirrored image of the trace shown on Fig. II.5a. Thus, with $\dot{\theta} < 0$, still, the tension is decreasing toward $T_s = 0$ (the local minimum). The tension vanishes (again) at $\theta = \pi - \frac{\pi}{3}$, then rises to $T_s = 0.5\ \tilde{m}\ell\dot{\varphi}^2$, at $\theta = \pi - 65.905^{\circ}$, where $\dot{\theta}$ passes through zero and becomes positive. Continuing, the tensile force is increasing and the system is moving toward $\theta = \pi$, along a trace which is the reflection of that shown on the figure. Finally, at $\theta = \pi$, the system has returned to the starting point, having completed one full excursion in this oscillation. At $\theta = \pi$ the tension reaches its maximum value of $T_s = 8.6623\ \tilde{m}\ell\dot{\varphi}^2$.

In the description just completed it was mentioned that during the oscillations $\dot{\theta}$ changed sign twice. (At these points the tension is, necessarily, continuous with $T_s\ (-\dot{\theta}) = T_s\ (+\dot{\theta})$). The magnitude of the specific force, and the (θ) location, at this condition should be of interest.

For computational purposes, expressions describing these quantities are set down below; also, a tabulation, for selected values of $\mathcal{C}_1/\dot{\varphi}^2$, is included here:

(1) Location (θ) for the condition, $T_s\ (-\dot{\theta}) = T_s\ (+\dot{\theta})$:

$$\theta = \frac{1}{2}\left[\cos^{-1}\left(-\frac{2}{3}\,\frac{\mathcal{C}_1}{\dot{\varphi}^2}\right)\right]. \tag{II.19}$$

(2) Value of T_s at this position:

$$\frac{T_s}{\tilde{m}\ell\dot{\varphi}^2} = \frac{3}{2}\left[1 - \frac{2}{3}\,\frac{\mathcal{C}_1}{\dot{\varphi}^2}\right]. \tag{II.20}$$

SELECTED TABULATIONS FOR EQS. (II.19), (II.20).
(θ-OSCILLATORY MODE)

$\mathcal{C}_1/\dot{\varphi}^2$	Eq. (II.19)*	Eq. (II.20)
$\frac{3}{2}$	90°, 270°	0
1	65.905°, 245.905°	$\frac{1}{2}$
$\frac{1}{2}$	54.73°, 234.73°	1
0	45°, 225°	$\frac{3}{2}$
$-\frac{5}{4}$	16.78°, 196.78°	$\frac{11}{4}$

* $\pm\,\theta$ values are inferred.

The "single point" on the graph, at $\theta = \pi$ (and/or 0), where $T_s = 3\tilde{m}\ell\dot{\varphi}^2$, corresponds to $\mathcal{C}_1 = -\frac{3}{2}\dot{\varphi}^2$, as shown on Fig. II.4. These conditions describe a gravity gradient, stabilized system.

The trace, on Fig. II.5a, for $\mathcal{C}_1 = \frac{3}{2}\dot{\varphi}^2$, is the upper bound on the oscillatory modes of motion. Here the oscillations are confined to a range of $\Delta\theta = \pm\frac{\pi}{2}$ about the vertical. Note that so long as $\dot{\theta} < 0$, the "tension" becomes a compressive force and the tether would go slack. For such a situation the motion could not be predicted by the present analysis; another method would be needed; e.g., the study of two bodies in free, relative motion.

From the analysis conducted here the largest value of $\mathcal{C}_1$ which should be used, to guarantee a continuous tether tension, would be $\mathcal{C}_1 = \dot{\varphi}^2$. Of course, it is readily seen that the system operating at $\mathcal{C}_1 = \frac{3}{2}\dot{\varphi}^2$ would <u>regain</u> its tension once the tethered mass moved back <u>toward</u> the vertical.

The remaining limit condition depicted on Fig. II.5a is that corresponding to the curve $\mathcal{C}_1 = \frac{11}{2}\dot{\varphi}^2$ (and $\dot{\theta} < 0$). A trace of the tension for this situation

also suggests a vanishing T_s; but $T_s = 0$ only at $\theta = \pm 90^o$. This is a momentary condition, and is a lower limit on the rotating systems (see, also Fig. II.5b). (From Fig. II.5b, one can easily ascertain that so long as $\mathcal{C}_1 > \frac{11}{2}\dot{\varphi}^2$ the rotating systems retain their tension regardless of sgn $\dot{\theta}$).

There is no need to discuss Fig. II.5b to any large extent. It is self explanatory to a distinctive degree, and is not nearly as complicated as is Fig. II.5a. The symmetry of the traces, noted earlier, is also apparent here; i.e., the curves are to be reflected into the $\theta = 0$ and π axes. The remaining additional information to be gathered is concerned with realizing that the tensions decrease as one moves away from the vertical. Also, the $+\dot{\theta}$-rotations have continuous tension, while the tethers with $-\dot{\theta}$-rotations may be conditionally tensioned.

This completes the examination of the tensile force developed in fixed length tethers, during their in-plane motions. It has been shown that there can be large variations in this force during the motions. Also, the systems have been found to have some conditional characteristics (for $T_s > 0$); this could easily become a factor of concern in an operational application using tethers. Certainly, the findings here do point to the need of exercising some care in the use of these systems, if one is to be assured of retaining their mechanical integrity.

Prior to leaving this part of the analysis, in the report, it would be well to discuss one more factor which influences tethered mass systems. This is the effect of orbital eccentricity on the motions and reactions of the system, as a whole. Unfortunately this factor was not too successfully simulated, analytically, consequently the source of information on this was a numerical study. A discussion on some of these findings is included below.

II.6 Eccentricity, A Disturbing Influence.

The influence felt by a tether system having an eccentric base orbit, rather than a circular one, was mentioned in the discussion of eq. (II.1). A

simple description of the effect was illustrated in eq. (II.2) where the acceleration ($\ddot{\varphi}$) was related to the familiar orbital quantities, for a Keplerian trajectory. It is surmised that such a condition will affect the tethered body problem much like the influence from a small disturbing force. Consequently, the response to an eccentric path should be akin to that expected from a force system having a periodic variation to it. This variation might be explained in terms of the changing altitude for the base trajectory.

In the analytical studies, which were undertaken during the investigation, the eccentricity effect was not simulated well enough to warrent including it here. In that simulation, expansion techniques were used to simplify the governing differential equations. It was found that when solutions were obtained, they were most conveniently expressed in terms of Mathieu functions (see ref. [10]). Instead of simplifying the analysis these functions add a complication due to the inherent stability considerations which must be included. Of course, this could be cared for, in a given case, by adjusting the problem's physical parameters. Since the aim (here) was to provide easily followed guidelines, for the design of tethers and tethered systems, it was felt that the complexity arising from the use of Mathieu functions did not fit this concept. Hence, the approach was not continued. Instead, the quantitative (and qualitative) effects of eccentricity have been considered by means of numerical studies.

II.6.1 Illustrating Eccentricity Effects.

An example problem has been investigated, numerically, as the means of demonstrating the effects of eccentricity and damping on a tethered body system. This example problem was designed to have separate in-plane and cross-plane motions. However, only the in-plane motion is shown here, graphically. The damping was varied, as will be seen, and the base orbit was changed so that the effect of eccentricity could be included. Since both problems were initiated at a same altitude, the cases used to illustrate eccentricity are not for equi-

energy paths. Even though this difference is present it does not negate the effects which are to be demonstrated.

(The In-Plane Case). The circular orbit is at an altitude of 0.025 earth radii, and has a period of 5260 sec. In this first representation the initial state is set so that the tethered body moves, initially, along the orbit radius. Due to the tether's elasticity, and the dynamics of the problem, the "extension" becomes coupled with the swinging motion and the geometry which develops is that shown on Fig. II.6a*. (Note: the damping for this case is some small percent of the critical. The ordinates of this figure define tether length (ℓ) versus x-displacement. This x-displacement is in the direction of motion, normal to the radius vector for the reference orbit).

A brief description of the motion follows: The suspended mass (m_2) begins its action at a tether length of 35.052 m. (115.0 ft); ℓ_o = 30.48 m (100 ft). Leaving the initial point the tether stretches ($\dot{\ell} > 0$) and m_2 moves forward (in the direction of motion, $\dot{x} > 0$). This continues until the tether attains a maximum extension; then it begins to contract, swinging forward and reaching its maximum x-displacement. Following this, the motion is due to a contraction and a backward movement ($\dot{\ell}$, $\dot{x} < 0$); this continues until $\dot{\ell} = 0$; thence the motion occurs with $\dot{\ell} > 0$, $\dot{x} < 0$ until the maximum extension (at $x \cong 0$) is reached. The full extension, as shown on the figure, is roughly 1.7 meters; also,the x-displacement, for this first excursion, was about 1.34 meters. Subsequent motion continues, and is repeated for the following cycles, but at a diminished scale.

From the numerical data obtained here it was estimated that the θ-period was $T_\theta \cong 3440$ sec. Comparing this to the calculated T_θ value, ($\equiv 3066$ sec), from the linear theory expression ($T_{orb}/\sqrt{3}$, see section II.3.4), it is noted that agreement is within 10%. In addition, the measured and calculated T_σ values have approximately this level of agreement.

*These numerical studies were carried out using the program developed and described in references [11] and [12].

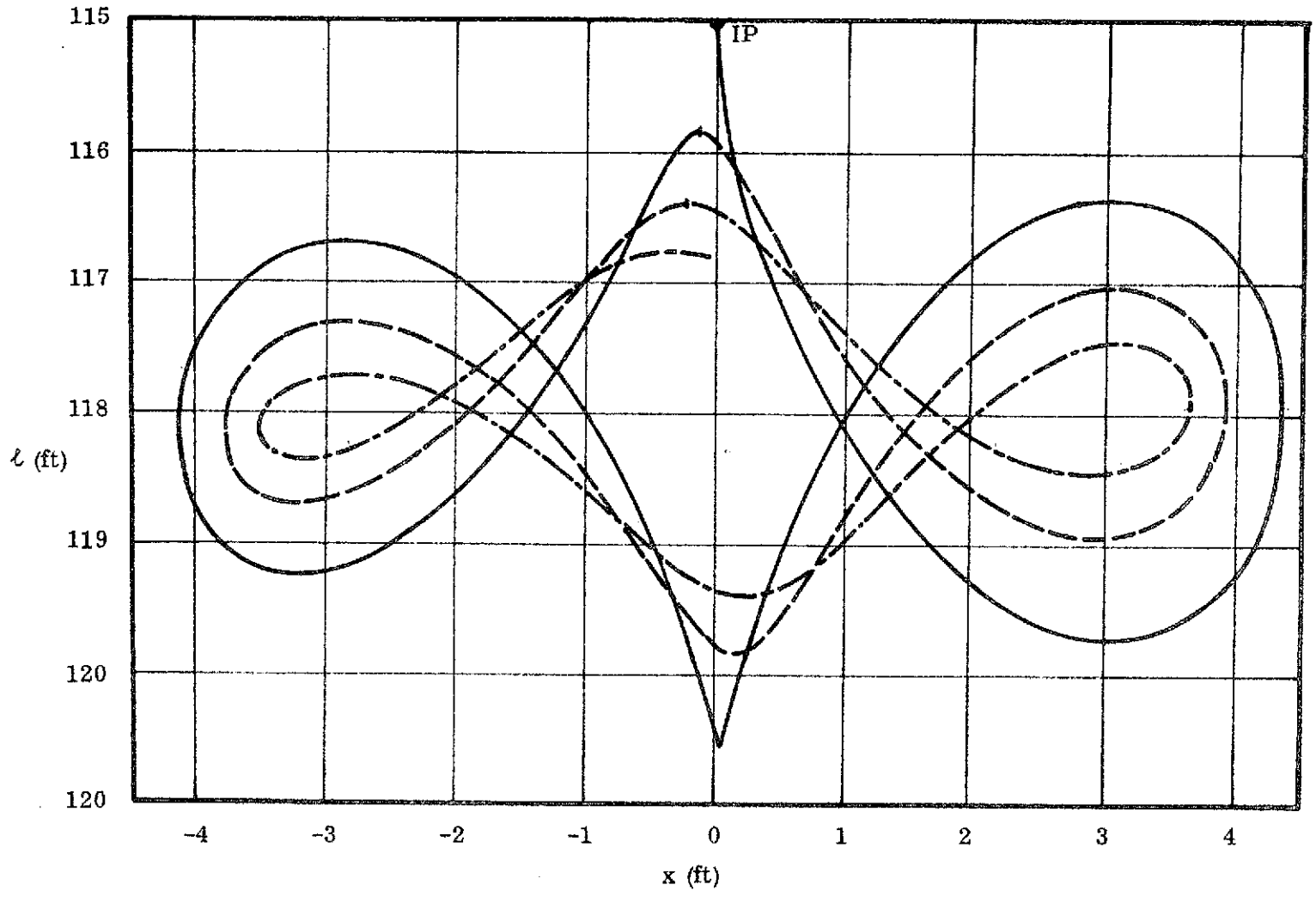

Fig. II.6(a). Trace of an In-Plane Tethered Body Motion for an Elastic Tether with $c/c_c \cong 0.03$. Unstretched Length (ℓ_o) is 100 ft; Initial Stretch ($\Delta\ell$) is 15 ft. IP Signifies the Initial Position. Note that each Cycle (ℓ) is Graphed differently; the Amplitude (for x) $\cong 2^o$.

Next, consider Fig. II.6b which shows a similar trace for this motion, but where the tether is presumed to be critically damped. Here, a distinct difference in the motions is apparent; certainly the cyclic nature of ℓ is supressed and the x-displacement is reduced. It would appear, from this figure, that the system is moving toward a gravity-gradient stabilized position (x = 0) with the tether extended to approximately 35.97 m (118 ft). This would represent a static extension of 5.846 m (18 ft) beyond the unstretched length (ℓ_o).

The next two figures (II.6c, II.6d) are included to show the influence of: (1), eccentricity; and (2), eccentricity and damping. The initial state for these figures is the same as that for the two previous graphs.

Here, motion starts at pericenter on a trajectory whose eccentricity is 0.1. Figure II.6c should be compared with Fig. II.6b, to see the influence of eccentricity, since both cases are "critically damped". It is interesting to see that the motions begin alike, but rapidly diverge in their geometry. Now, the suspended particle begins to move at $\dot{\ell} > 0$ but abruptly it changes direction, begins to contract ($\dot{\ell} < 0$) and moves counter to the orbit's motion ($\dot{x} < 0$). (The subsequent apo - and peri-center positions are indicated on the figure). It is felt that this total motion is stable, though this is not fully evident from the traces shown. There is not a sufficient number of cycles plotted for one to get a clear indication of the ultimate trends.

Fig. II.6d is the same as II.6c except that the damping has been altered. (Note that one curve is for an overdamped motion (10 time critical), while the other is for an underdamper case). What is most significant here is that the degree of damping does appear to be of real consequence. The highly overdamped case shows only small excursions while the true converse is seen for the underdamped motion.

From the limited information provided here, it is evident that damping and eccentricity can be joined to produce significant effects on some tethered

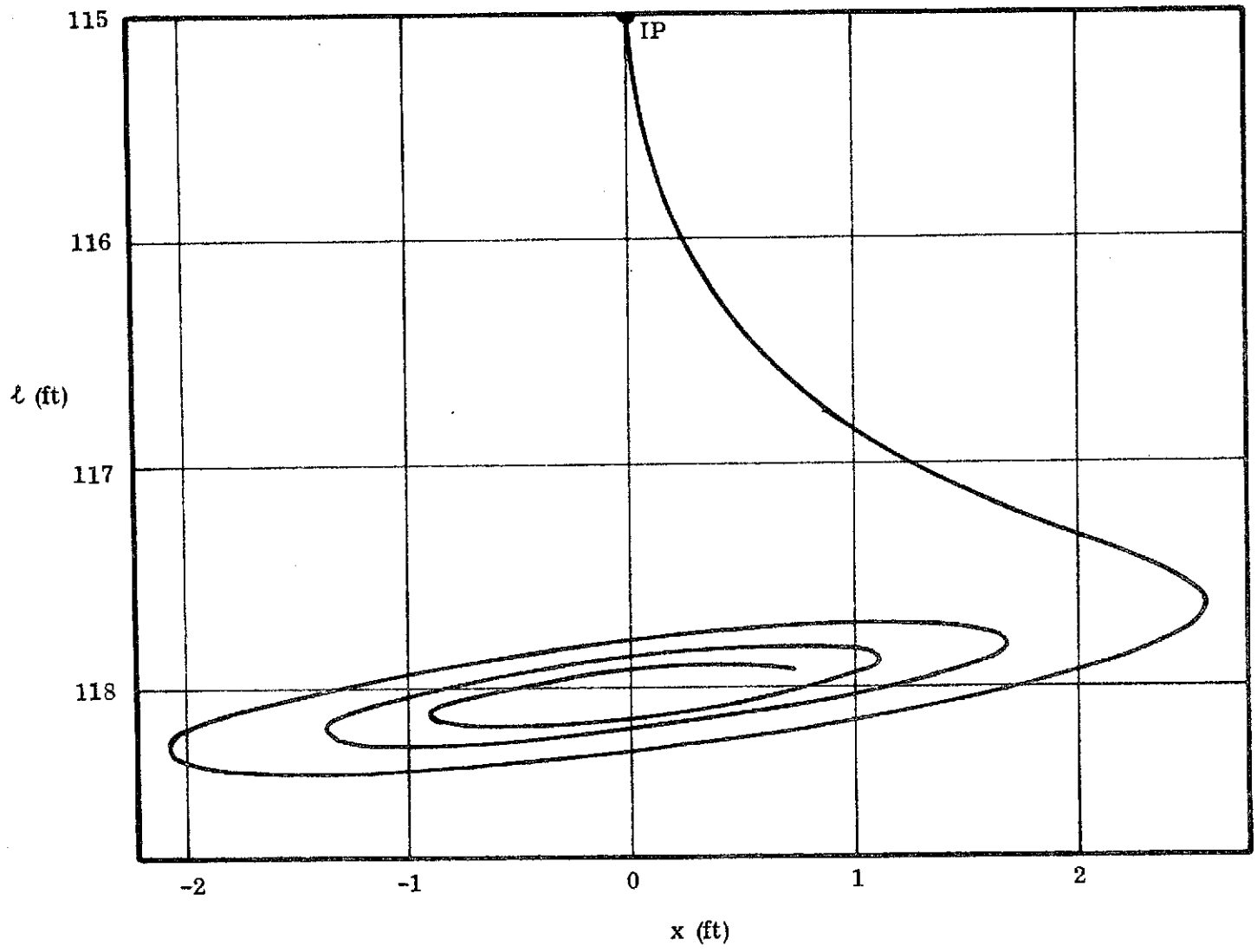

Fig. II.6(b). Trace of an In-Plane Motion for $c/c_c \cong 1.0$. Here the Reference Orbit is Circular; IP denotes the Initial Position. Note Motion Tending to $\ell \cong 118.1$ ft, and $x \cong 0.0$.

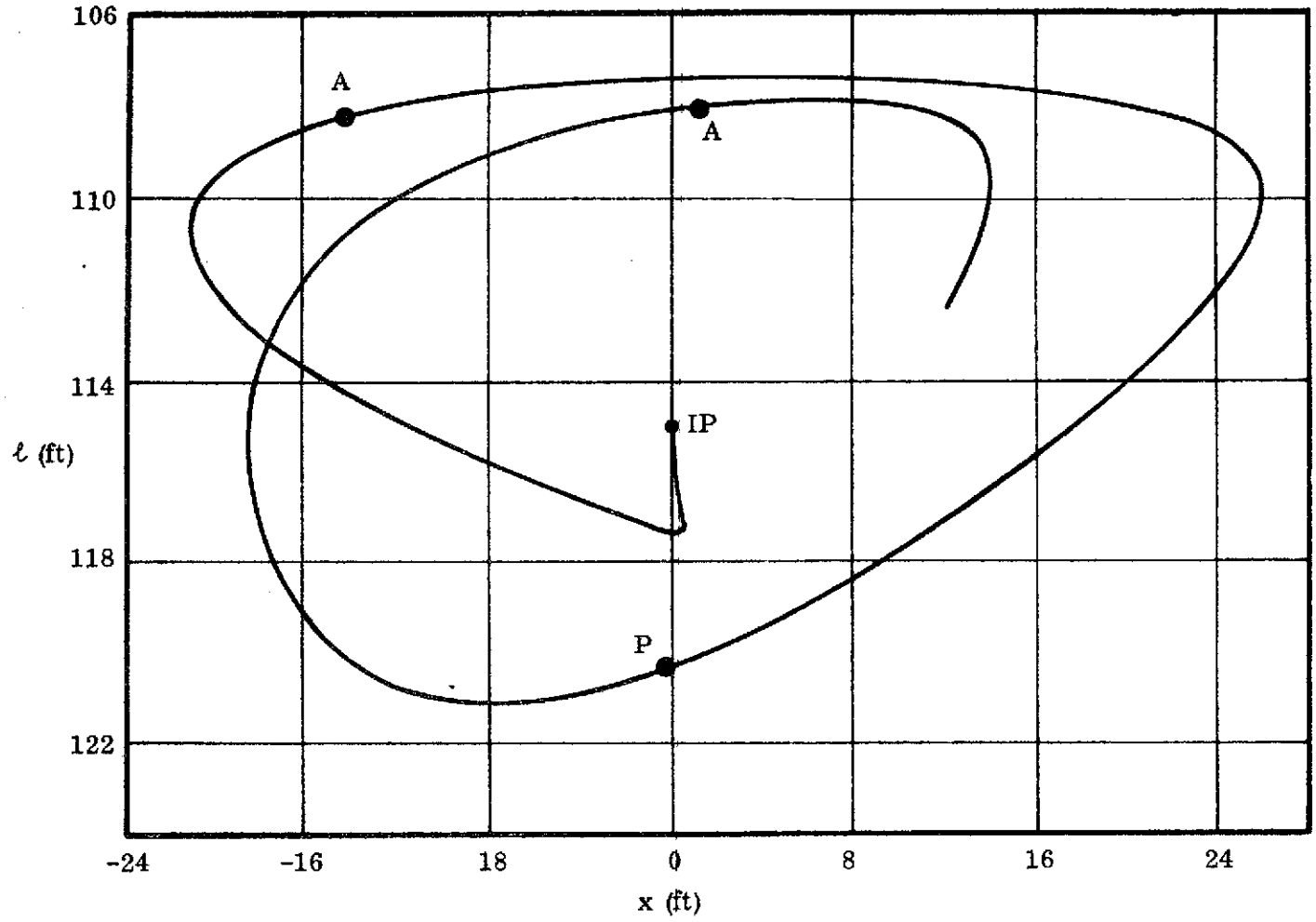

Fig. II.6(c). Trace of an In-Plane Motion, Illustrating Effect of Eccentricity and Damping. The Reference Orbit Eccentricity (ϵ) is 0.1; the Tether is Elastic with $c/c_c \cong 1.0$. IP Denotes the Initial Position (a Pericenter); A, P Correspond to Subsequent apo-and peri-centers, for the Reference Orbit.

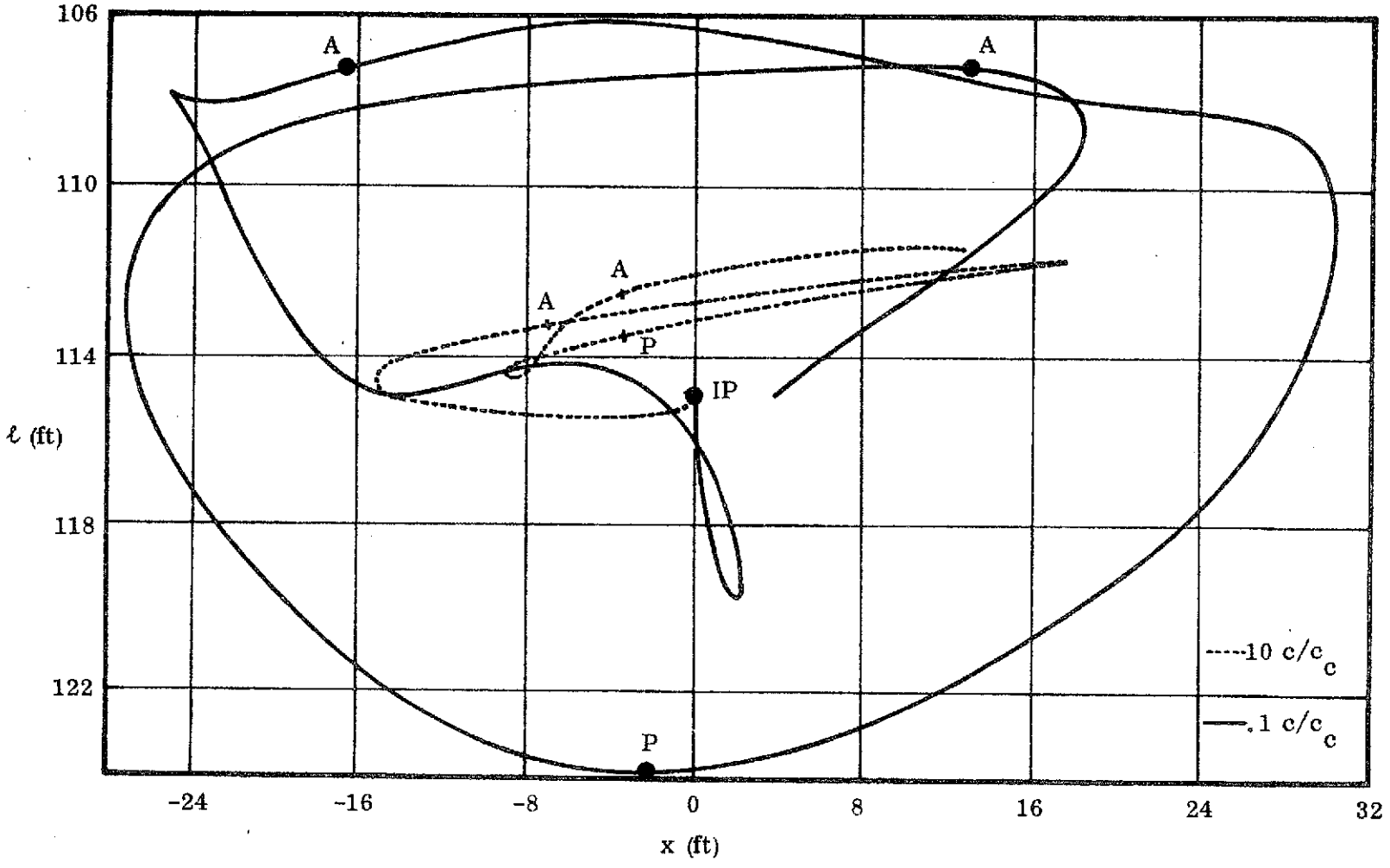

Fig. II.6(d). Trace of Under-and Over-Damped In-Plane Motions for an Eccentric ($\epsilon = 0.1$) Reference Orbit. IP Denotes the Initial Position (a pericenter); A, P Correspond to Subsequent apo-and peri-centers, on the Reference Orbit.

body motions.

Also, from the limited results obtained using other initial states (set to produce other motion types), it has been found that the measured values and the calculated ones (from linear theory) agree to an acceptable level. For instance, the case of a cross-plane motion was examined (numerically) and found to have a period of motion close to that of the θ-motion. It can be surmised that, in general, the pendulous motions (for highly damped tethers) are not significantly affected by other than gravity gradient effects (for circular, base orbits). Here, as elsewhere, eccentricity caused a marked change in the geometry of the traces.

For a clearer understanding of the agreements and disagreements found in these numerical studies, some numbers (measured and calculated) are given below, for the several cases examined. All orbits begin at 1.025 earth radii. The circular ones have $\dot{\varphi} = 1.19452\ (10^{-3})$ rad/sec., and $T_{orb} = 5260$ sec.

The tether spring effect was set by $k/\tilde{m} \equiv 360 \left(\frac{\text{rad}}{\text{hr}}\right)^2$; the damping was varied, as needed and desired.

Three distinct motions types were attempted in the simulations. These were: (a) σ (tether) motions; (b) θ (swinging) motions, and (c) z (cross-plane) motions. Necessarily some coupling existed; this will be noted below. In the simulations overdamping was employed as a means of suppressing the tether extensions from the other motions.

From the inputs in the simulations:

$$\omega_\ell^2 \equiv \frac{k}{\tilde{m}} = 360\ (\text{rad/hr})^2,$$

$$\omega_\theta^2 \equiv 3\dot{\varphi}^2 = 55.46\ (\text{rad/hr})^2 \text{ (circular orbits)},$$

and

$$\Omega^2 = (\omega_\ell/\omega_\theta)^2 \cong 6.49.$$

Static Extension for the Tether (circular case).

$$\frac{\ell_{st}}{\ell_o} = \frac{\Omega^2}{\Omega^2 - 1} = 1.18212 \text{ (see section II.3.3(3))}.$$

Calculated Periods of Motion (see sect. II.3.4).

$$T_\theta = \frac{T_{orb}}{\sqrt{3}} = \frac{5260}{\sqrt{3}} \cong 3036. \text{ sec.}$$

$$T_{\tilde{\sigma}} = \frac{T_{orb}}{\sqrt{3(\Omega^2 - 1}} = \frac{5260}{\sqrt{3(5.49)}} \cong 1296. \text{ sec.}$$

Measured Periods of Motion.

(a) $T_\sigma \cong 1180$ sec. (with $c < c_c$),

(b) $T_\theta \cong 3122$ sec. (with $c \geq c_c$),

(c) $T_z \cong 2760$ sec. (with $c \geq c_c$). (Also T_θ (coupled) $\cong 2760$ sec., here).

This tabulation completes the discussion for this part of the investigation. In the following segments of this report the tasks to be described and discussed are related to special applications for tethered masses; and, to the control and handling of these systems.

EXTENSIBLE TETHERS

III.1 General.

In the foregoing section of this report a discussion on elastic tethers, their properties and behavior was presented. There the connected bodies were assumed to have a described "orientation", in their tether-connected configuration, with the subsequent motions which developed being the topic of interest.

For the next part of the report, efforts will be of acquiring a given tethered-body configuration. Here the aim will be (first) to develop analytic methods which define those conditions necessary to accomplish the desired tasks. Second, and in conjunction with this work, results from numerical studies will be presented. These will show how one may predict the characteristics of a system, and thereby describe methods for controlling the extensible tether connected bodies moving in orbit.

This kind of information is obviously of interest to systems designers and operations planners. Especially so when one recognizes the number of possible applications in which tethers may play a relevant role in connection with future space ventures.

Generally, this section of the report is separated into two primary sub-sections. The first will describe certain "analytical experiments" which provide information on tether operations. In the latter sub-section results from numerical studies will be presented. These are the consequence of various simulations which were conducted to determine how the tethered body systems behave, and how they might be made to perform in a desired manner.

III.2 Proposed Analytical Experiments.

The mathematical expressions developed in Appendices E and F will be used to conduct certain analytical experiments. These are preliminary studies concerned with the gathering of information relevant to the use of extensible

tethers. The proposed experiments are undertaken prior to performing more exact studies of the problem by numerical analysis.

In part, the objective here will be to acquire analytic representations for specific quantities which relate to the problem of tethered bodies moving in orbit. The particular kind of information being sought is a consequence of the fact that the governing differential equations cannot be solved in closed form. Hence the influence of, and means to acquire, the specifics for these systems are not immediately available.

III.2.1 Tension Laws.

In the study of extensible tether-body motions the tensions laws, and the inherent influence which they play, are of immediate interest. Even though one cannot solve for the resulting motions, per se, analytically, when using a prescribed tension law, the converse situation has merit and should be worth pursuing. A plan of attack would be to devise an analytical representation for the body motions (ℓ, θ); and, subsequently,to determine the tension law which results. In effect, this would be an indirect approach to the problem.

For this particular experiment a set of general equations could be those given as eqs. (E.20), Appendix E. However, a more useful and concise system is found as eqs. (E.25) in that appendix. (Note that the coordinates there have been specialized to the non-dimensional pair (σ, θ); these are defined just prior to the mathematical expressions). Making use of some parameters defined from these equations, one can obtain a "time history" of the dimensionless force components,

$$\tau_m \cos \alpha_2 \ , \quad \tau_m \sin \alpha_2 \ .$$

Necessarily they evolve as a result of the motions assigned for study. From these data the magnitude and direction of the "required force law" can be ascertained; i.e.,

$$\tau_m \equiv \sqrt{(\tau_m \cos \alpha_2)^2 + (\tau_m \sin \alpha_2)^2} \quad , \tag{III.1a}$$

and

$$\alpha_2 = \tan^{-1}\left(\frac{\tau_m \sin \alpha_2}{\tau_m \cos \alpha_2}\right). \tag{III.1b}*$$

Necessarily, in an experiment such as this, the analytical representation of the motion (σ, θ) must be cast into a form which meets all desired end conditions. For this reason it is advantageous to have a prior knowledge of the probable behavior of these systems and their motions.

Even without a clear, a priori, understanding of the tethered bodies problem it is still possible to conduct a meaningful experiment, as proposed. For instance, a motion could be described; subsequently a force law would be developed; and, the results could be analyzed to determine whether or not the force system is feasible and/or realistic. From this type of an investigation one could gain an insight into the mechanization of tethered systems, and begin to understand the interplay between the several factors which are involved.

To illustrate several features of this suggested experiment one should, first, view equations (E.25), but cast in a form which will define the "force components"; e.g., write

$$\begin{aligned} \tau_m \sin \alpha_2 &= \sigma\theta'' + 2\sigma'(1+\theta) + \frac{3}{2}\sigma \sin 2\theta, \\ \tau_m \alpha_2 &= \sigma'' - \sigma(2+\theta')\theta' - \frac{3}{2}\sigma(1+\cos 2\theta), \end{aligned} \tag{III.2}$$

wherein;

$$\tau_m \equiv \frac{F_2/\tilde{m}}{\ell_m \dot{\varphi}_g^2}\ ;\ \sigma \equiv \frac{\ell}{\ell_m} = \frac{\lambda}{\lambda_m}\ ;\ \sigma' \equiv \frac{\ell'}{\ell_m} = \frac{1}{\dot{\varphi}_g}\frac{\dot{\ell}}{\ell_m} = \frac{\lambda'}{\lambda_m}\ ;$$

with $\lambda_m \equiv \dfrac{\ell_m}{r_g}$; ($\ell_m \equiv$ maximum tether length), $(\sim)_g \equiv$ c.g. value.

From the standpoint of the analytical formulations which follow, the

*See Appendix E for sketches defining these quantities; also see Fig. III.1.

motion coordinates must fit the general range of values:

$$\sigma_o \leq \sigma \leq 1.0, \quad (\sigma_o \geq 0),$$

and

$$\theta_o \leq \theta \leq \theta_f, \quad (\theta_o, \ \theta_f \ (\equiv \text{terminal values})).$$

Since the angle (α_2) describes an orientation for the line of action of τ_m, relative to the direction $\bar{e}_\ell$ (the unit vector directed from one particle to another), it is reasonable to expect that this quantity should undergo changes not to exceed $\pm \pi/2$. If it is outside of this range then the resultant tether force would be directed not toward the mass it was holding, but away from it.

III.2.2 Example Situations.

For the specification of a simulated tether motion the most convenient analytical representation would be one assumed in the form of elementary functions. These could include linear relations; trigonometrics; exponentials; and, combinations of these.

In the interest of illustrating this approach to the extensible tether problem, two examples are described below. For these two cases the assumed motions (σ, θ) are defined, analytically, and parameters depicting the behavior of the system are determined. In presenting the data acquired, some selected results will be plotted. Those graphs will be examined and discussed to aid in providing an insight into each of the case studies.

III.2.2 Example 1.

For this example a "reel-out" tether system is assumed. That is, from the main body (m_1) a particle (m_2) is "ejected" with some initial payout rate. During the ensuing motion the tether is unwound to its assigned final length (ℓ_m, or $\sigma = 1$).

In this example the tether is assumed to have a fixed pay-out rate (i.e., σ' = constant), as well as an assigned θ-range. The initial and terminal states for this case are described by:

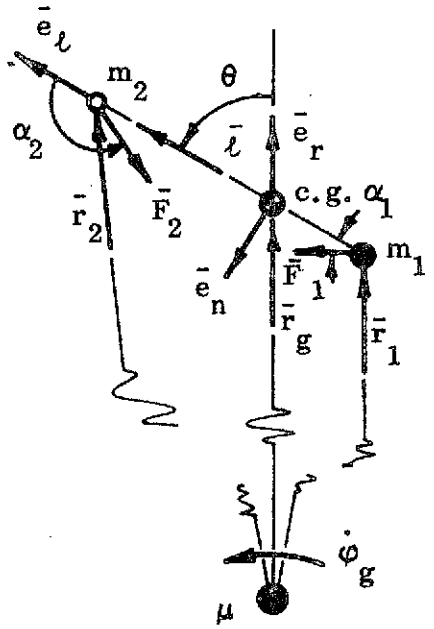

Fig. III.1. Sketch of a Tether System.

at $t = 0$ $(k\varphi = 0)$*:

$$\theta_o = \pi, \qquad \theta'_o = 0$$

$$\sigma_o = 10^{-5}, \qquad \sigma'_o \equiv \text{const};$$

at $t = t_f$ $(k\varphi \equiv \pi)$:

$$\theta_f = \pi, \qquad \theta'_f = 0$$

$$\sigma_f = 1.0, \qquad \sigma'_f \equiv \text{const.}$$

(Note that time (t) and position angle (φ) may be used, alternately, to describe the independent variable. The inclusion of "k" with "φ" will be justified and discussed below).

In simulating the in-plane motions (σ, θ), the following analytical expressions are used:

$$\sigma' \equiv \text{constant},$$

and

$$\theta \equiv \tilde{\theta} + \Delta\theta \cos(2k\varphi), \tag{III.3a}$$

with

$$\tilde{\theta} \equiv \frac{7\pi}{8}, \quad \Delta\theta \equiv \frac{\pi}{8}.$$

Here $\tilde{\theta}$ and $\Delta\theta$ are constants for the particular case at hand.

As a consequence of the above relations it follows that;

*The $(\sim)_g$ has been dropped from φ for conciseness in notation. It is understood that the reference value(s) are referred to the main particle.

$$\sigma = \sigma_o + \sigma' \varphi \equiv \sigma_o + \frac{\sigma_o' \, (2k\varphi)}{2k} \quad ,$$

and

$$\theta' = -\, 2k\Delta\theta \sin\,(2k\varphi), \tag{III.3b}$$

where σ_o is an initial value, etc.

Here, k is chosen so that θ_o' acquires its correct (assigned) value; also, σ_o' is defined so that σ acquires the specified value of $\sigma_f \equiv 1.0$!

Having selected these various coordinate representations (directly, or indirectly), a solution for the parameter τ_m and α_2 follows. As a point of interest, three separate cases have been studied for this example; and, selected data from these are presented on Figs. III.2, III.3, below.

On Fig. III.2, one finds a graphic description of the assumed motions (σ, θ). These are plotted against fractional parts (0 to 1.0) of the argument ($2k\varphi$). The graph is presented in this form since it leads to a universal representation for this particular problem (i.e., all cases are described by the same curves).

It is evident, here,that σ is linear in φ (hence $2k\varphi$), and that θ is symmetric about the midpoint of the argument quantity. In particular, for this case θ varies from 180^o to 135^o, and back to 180^o. (See Fig. III.1 for a sketch of the problem's geometry).

On Figs. III.3a, III.3b, the specific tension parameter (τ_m), and the action angle α_2, are depicted for the three cases selected. Incidentally, these cases are identified by σ' values of: (1) 0.20264, (2) 0.40528, and (3) 0.81056; and, each lead to transfer angles, φ_1, of: (1) 282.74^o, (2) 141.37^o, and (3) 70.868^o, respectively.

The case (2) situation, from above, represents $\dot{\theta} = \dot{\varphi}$, while cases (1) and (3) describe $\dot{\theta} \equiv 0.5\dot{\varphi}$ and $\dot{\theta} = 2.0\dot{\varphi}$, respectively. According to the graphs this smallest $\dot{\theta}$ rate would come closest to describing a realistic tethered system,

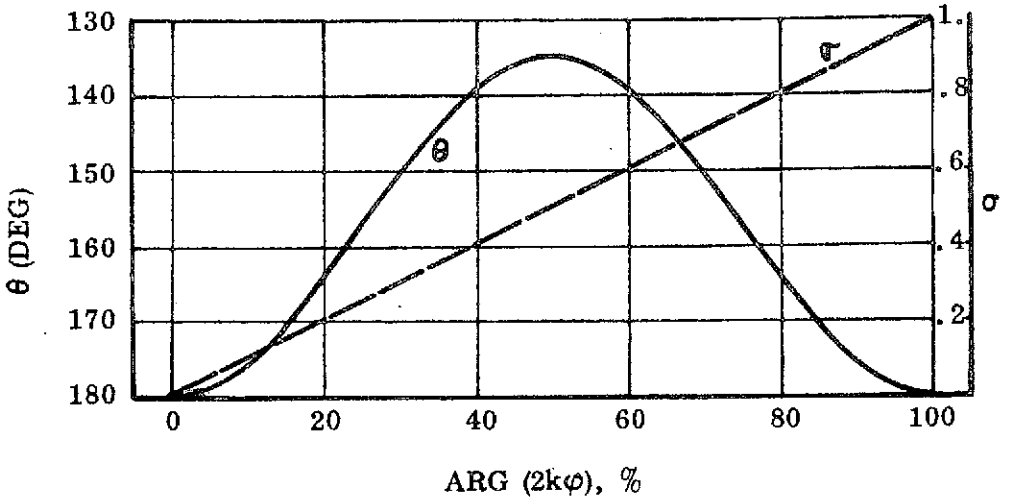

Fig. III.2. Trace of σ, θ Coordinates During Tether Extension; Example 1, a Reel-Out Case.

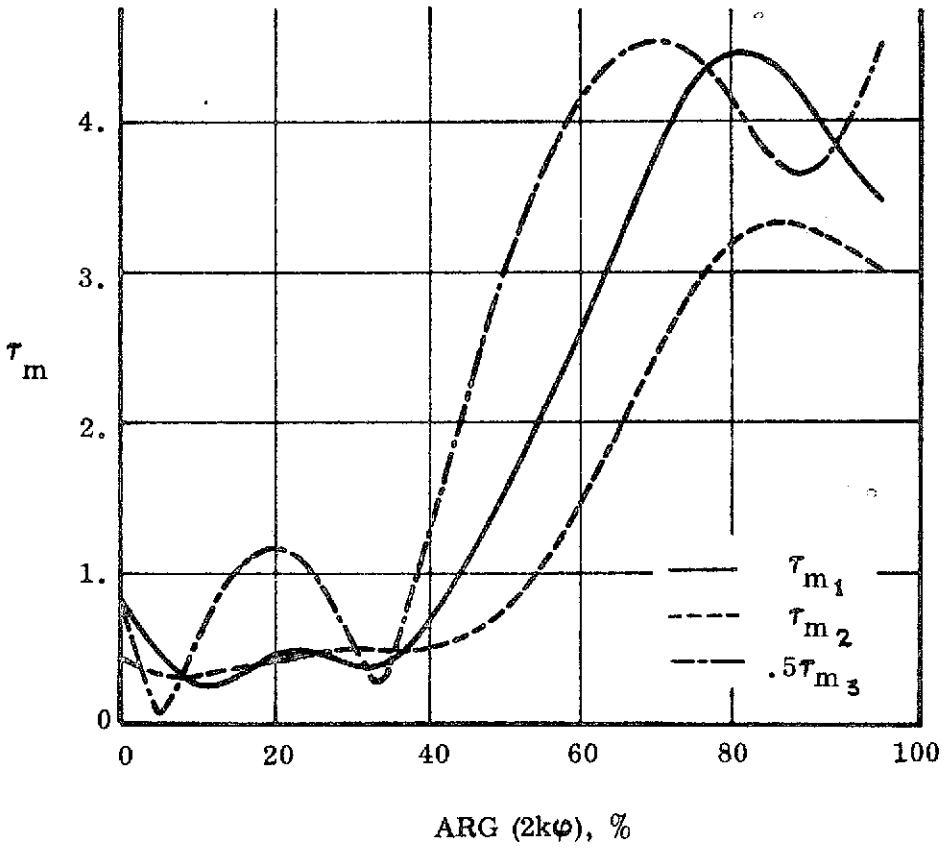

Fig. III.3(a). History of the Specific Tension Parameter, for Assigned $\dot{\theta}$ Rates; Example 1.

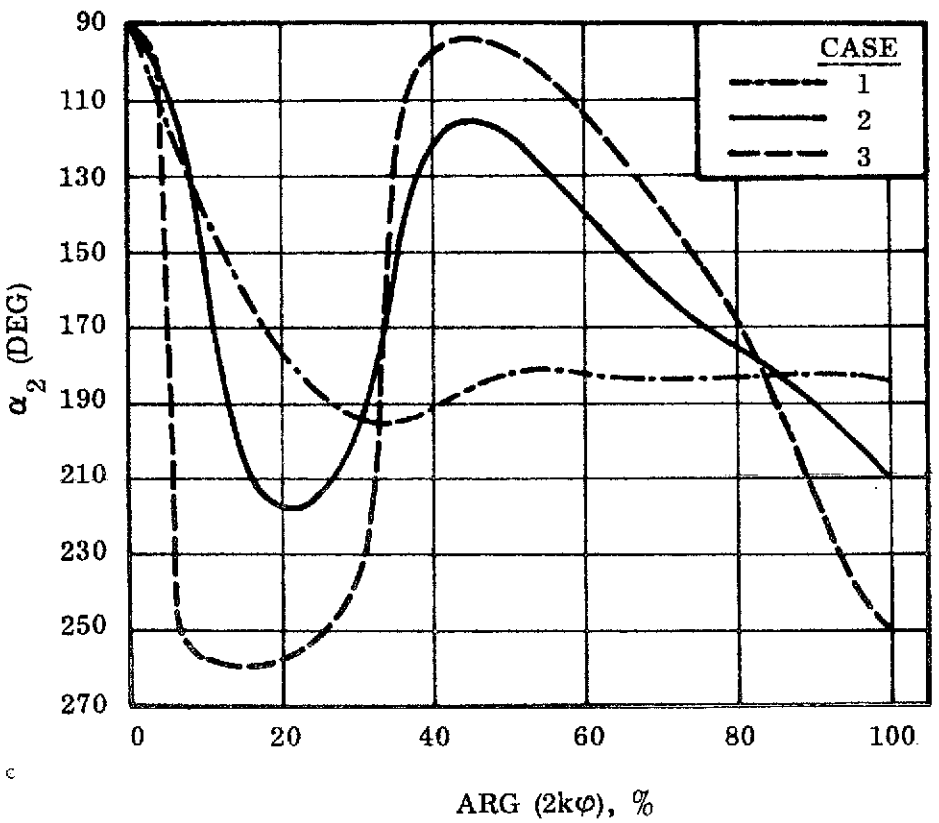

Fig. III.3(b). Variations in α_2, During Extension, due to the Assigned Motions (σ, θ); Example 1.

as would be desired for these simulations. There, the action angle (α_2) moves toward π, rather rapidly, and remains close to that value from then on. Also, it is seen that the tension varies most uniformly, and most simply, for this case. Evidentally these conditions suggest an easiest control problem, if the mechanization of this system would be undertaken.

Counter to this simplest situation, the case of $\dot{\theta} \equiv 2\dot{\varphi}$ represents a most complicated one - there the tension varies in a far more complex manner; and the action angle undergoes wide excursions. It might be surmised, from the limited data available here, that the constant tether payout mode behaves most conveniently (from a controls point of view) when the rotation rate ($\dot{\theta}$) is smallest. A study of the graphs could indicate that this operational scheme may not be the best* to select.

III.2.2 Example 2.

The second example is formulated to describe a "reel-in" tether system. The primary difference between this case and the previous one, is the obvious operational change. A more subtle difference occurs in the nature of the expressions used to describe the desired in-plane motions (σ, θ).

The two primary descriptive state equations are chosen to be:

$$\sigma = (1+\sigma_f) - \sin(\sigma_o' \varphi),$$

$$\theta = \theta_f + \Delta\theta\,[1 - \sin(\sigma_o' \varphi)]\,; \qquad \text{(III.4a)}$$

where, in particular, the following constants are applied:

$$\theta_f \equiv \pi,\ \Delta\theta \equiv \frac{\pi}{4},\ \text{and}\ \sigma_f \equiv 10^{-5}.$$

Note that here the angle argument, for the trigonometric functions, is modified by σ_o'. The reason for this will be noted subsequently.

*Best and ease of mechanization are synonomous terms, here!

As a consequence of the above expressions it follows that:

$$\sigma' = \sigma'_o \cos(\sigma'_o \varphi); \text{ with } \sigma'_o > 0;$$

and

$$\theta' = -\sigma'_o \Delta\theta \cos(\sigma'_o \varphi). \tag{III.4b}$$

For these analytical definitions, $0 \leq \sigma'_o \varphi \leq \pi/2$, necessarily. It should be evident, also, that the reason for selecting this particular argument for the trigonometric functions - i.e., $(\sigma'_o \varphi)$ - is to be assured that the derivative (σ') would have a proper physical representation and dimension. In addition, it is apparent, now, that σ'_o will be chosen so that there will be a desired level of rotation (θ') for the system.

Based on the stated conditions above, and other data selected to represent this system, the curves presented on Fig. III.4, III.5, describe the behavior of this simulated physical situation.

In discussing the geometric properties of this example it should be noted, first, that Fig. III.4 shows the displacement's time history. Here both σ and θ diminish, with σ decreasing due to the reeling-in action, while θ decreases from its largest amplitude toward its terminal value, $\theta = \pi$. As before, the state variables are plotted as a percentage of the argument $(\sigma'_o \varphi)$.

The data shown on Fig. III.5 are analogous to those of Fig. III.3. The tension parameter (τ) and the action angle (α) are presented for three cases: (1) $|\dot{\theta}| = 0.5\dot{\varphi}$; (2) $|\dot{\theta}| = \dot{\varphi}$; and, (3) $|\dot{\theta}| = 2\dot{\varphi}$. Each of these corresponds to a transfer angle, for m_1, of 141.37^o, 70.686^o, and 35.34^o, respectively.

It is interesting to note, again, the rather marked change in the system's behavior due to the increase in rotational rate $(\dot{\theta})$. So long as the rotation stays below a level of $O[\dot{\varphi}]$ the tether response has a lesser variance. For the case of $\dot{\theta} \equiv \dot{\varphi}$ (and greater) the tension drops to a minimum but rises again as the terminal state is approached. Also, the line of action for these cases appears markedly different from that seen for the slower rotation.

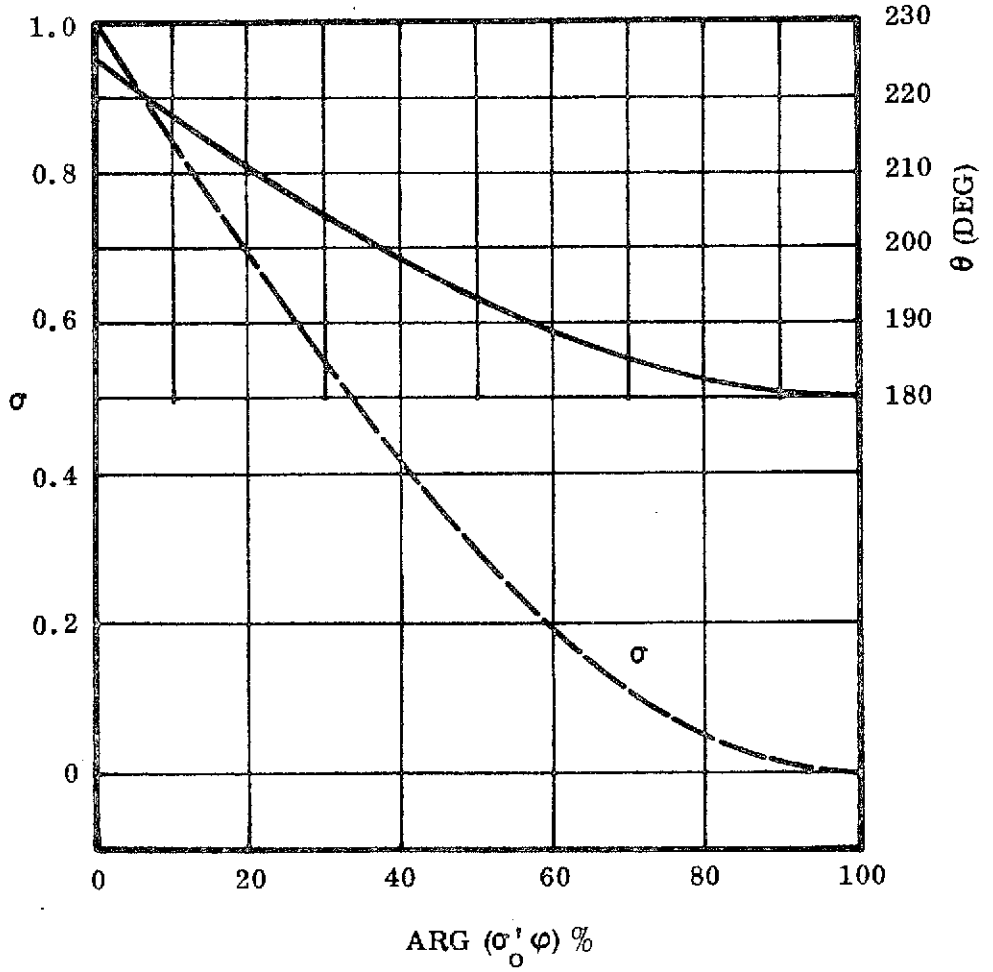

Fig. III.4. Trace of Coordinates (σ, θ), During a Reel-In Operation; Example 2.

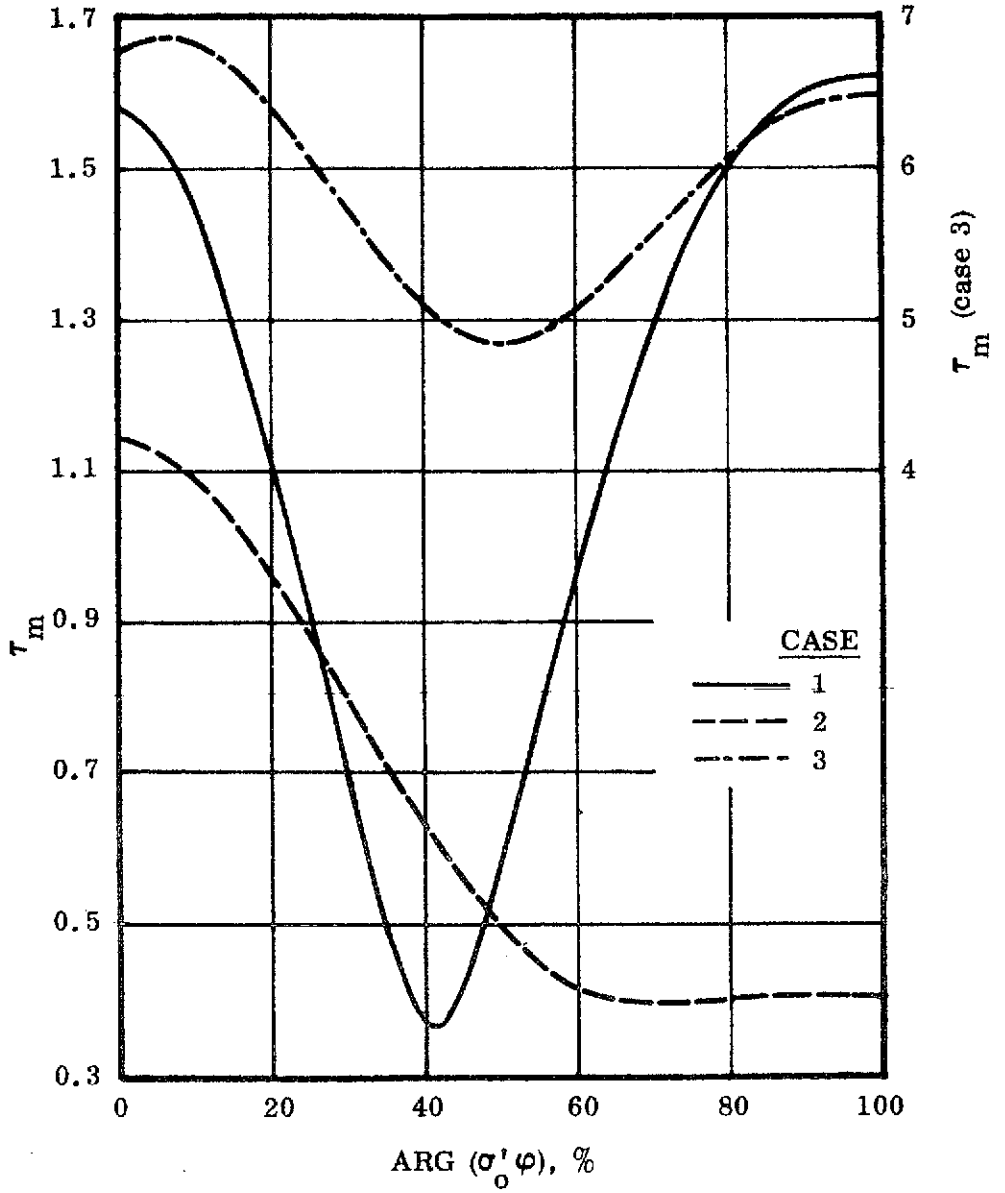

Fig. III.5(a). Specific Tension Parameter Variations, during Reel-In, for Assigned $\dot{\theta}$ Rates; Example 2.

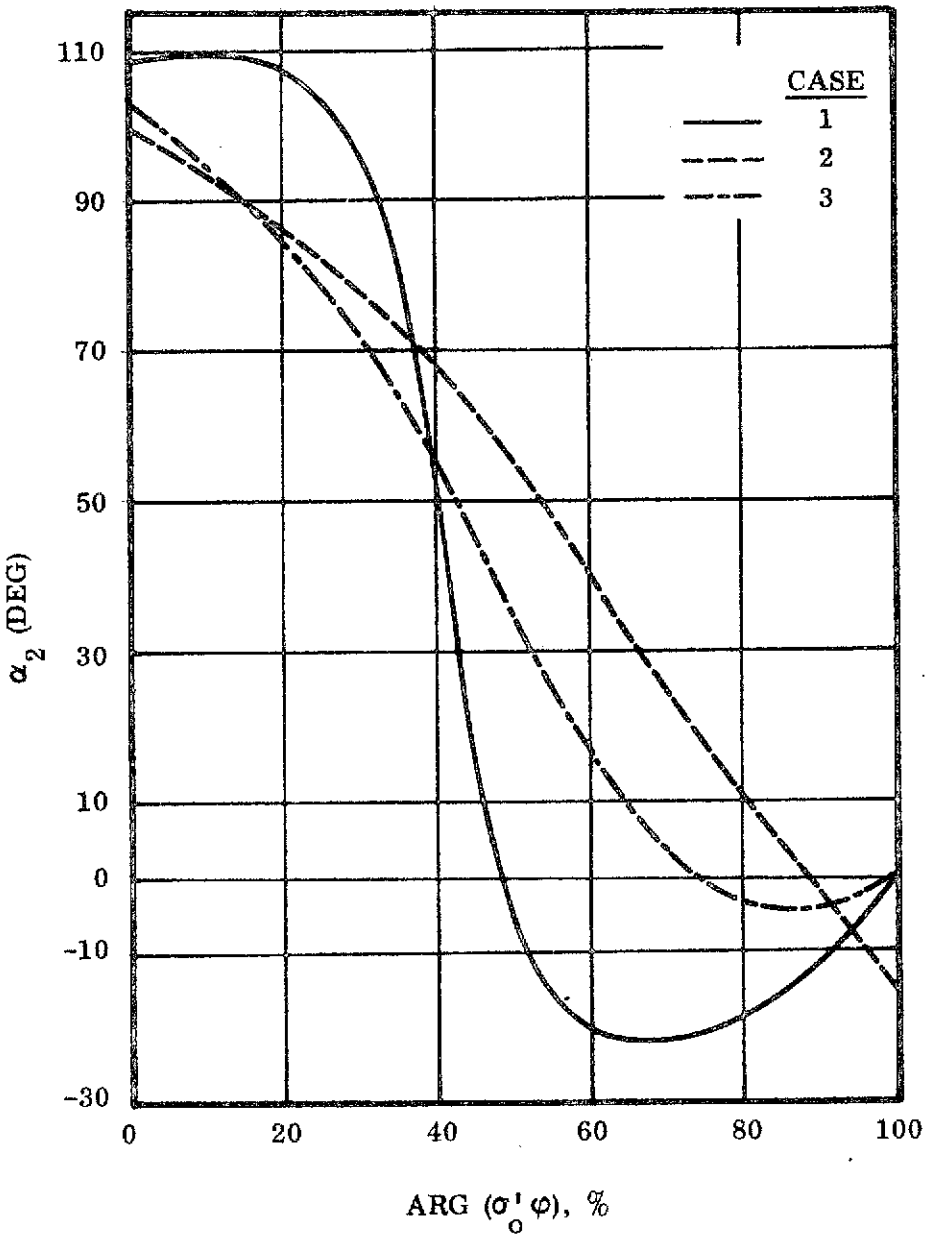

Fig. III.5(b). Variations in α_2, During Reel-In, for the Assumed Motion (σ, θ); Example 2.

All in all, it would appear that this simulation could not be reasonably classed as a passive tethered body configuration. Mainly, the gyrations which would have to be imposed (physically) on the tether are not feasible. Undoubtly the required response, through τ, would be indicative of some mechanical system capable of being manipulated to meet the reaction requirements of the system, and its state.

The two examples, above, were chosen somewhat at random to illustrate the indirect approach which could be employed in obtaining a solution to this problem type. The limited data which have been acquired points to the fact that there are numerous difficulties to be overcome if one is to obtain satisfactory and reasonable results, here.

This comment, however, does not in any way rule out the ideas employed here; there is much to be learned from this approach - unfortunately, most of what could be gleaned from a systematic investigation cannot be described from so few sample cases. A more exhaustive study would be needed if one wished to develop definite conclusions about tethered body systems.

The next example is rather unique in that it does afford a direct, analytic solution for a tethered body problem. Also, it will serve as a direct link to some of the numerical investigations which were carried out and are to be described later as a part of this work.

III.2.2 Example 3.

The previous examples were undertaken to determine "tension laws" based on assumed motion types. This next example is presented to extend the knowledge gained from the previous simulations, and to overcome some of the physical inconsistencies which did appear there.

Before formulating the example there are some pertinent questions which should be answered regarding this extensible tether problem, in particular.

A first question is: What conditions allow (or make) the action angle (α_2) to be equal to π? For an answer to this question return to eqs. (III.2), noting that one condition may be expressed by:

$$\theta'' = -\left[2\,\frac{\sigma'}{\sigma}\,(1+\theta) + \frac{3}{2}\sin 2\theta\right], \text{ (provided } \sigma \neq 0). \tag{III.5}$$

It is immediately apparent that unless (σ, θ) are restricted, θ'' is not constrained. However, on the supposition that the operational constraint,

$$\frac{\pi}{2} \leq \theta \leq \frac{3\pi}{2}$$

is imposed, then it follows that $\theta'' \gtrless 0$ in agreement with the sign and magnitude of quantities appearing in the equation above.

Suppose that in addition to this condition it is required that θ remains constant during a tether operation. As a consequence of this the example can be described by the reduced set of governing equations:

$$\tau_m = -\sigma'' + \frac{3}{2}\,\sigma\,(1+\cos 2\theta),$$

and

$$\sigma' = -\frac{3}{4}\,\sigma \sin 2\theta\ (\equiv K_\theta \sigma). \tag{III.6}$$

From these expressions one can obtain an immediate first integral (for σ); namely,

$$\sigma = \sigma_o \exp\,(K_\theta \varphi). \tag{III.7}$$

Here σ_o is that value of σ ($\equiv \ell/\ell_m$) described at $\varphi = 0$! It is apparent now that the extensibility of the tether is exponentially defined, for the conditions stated.

In order to develop an appropriate tension law ($\tau_m(\varphi)$), substitutions are made into the appropriate expression above. That is, from

$$\tau_m = \frac{3}{2}\,\sigma\,(1+\cos 2\theta) - \sigma'',$$

after substitution and manipulation, one finds:

$$\tau_m = \left[\frac{3}{2}(1+\cos 2\theta) - K_\theta^2\right]\sigma. \qquad \text{(III. 8)}$$

This last equation is seen to yield a tension law which is linear in the extension, σ. (If the constant of proportionality, here, is denoted as

$$K_\tau \equiv \frac{3}{2}(1+\cos 2\theta) - K_\theta^2, \text{ then } \tau_m \equiv K_\tau \sigma).$$

Of course, it is also seen that the extension rate (σ') is, itself, linear in σ - its constant of proportionality being K_θ.

(a). Time Required for Extensible Tether Operations.

The time to complete a prescribed tether extension (or retraction) is easily obtained from (say) the displacement relation $\sigma \equiv \sigma(\varphi)$.

For this evaluation, recall that

$$\varphi \equiv \dot{\varphi} t;$$

thus, it can be shown that the time to reach a given tether length, ℓ, is:

$$t = \frac{1}{K_\theta \dot{\varphi}_g} \ell n\left(\frac{\sigma}{\sigma_o}\right) = \frac{1}{K_\theta \dot{\varphi}_g} \ell n\left(\frac{\ell}{\ell_o}\right), \qquad \text{(III. 9)}$$

wherein ℓ_o is the "initial length" (tether extension) at $\varphi = 0$, the "beginning position" for the operation. It should be pointed out that this time equation is not restricted to just extensions of the tether alone. In this regard, since time is construed to be a monotonically increasing quantity, the constant K_θ will have to change sign (along with the logarithm function) to account for the system operating with an extension or contraction of the connecting tether line.

(b). Motion Constraints.

Looking at the speed expression (σ') it is evident that when $\sigma > 0$ (an

extensible system) it will be necessary for $\sin 2\theta < 0$. This suggests a restricted range of operation, in θ (here); thus, for extensions:

$$\frac{\pi}{2} < \theta < \pi, \text{ (say).}$$

Conversely, for a contracting (or reel-in) system ($\sigma' < 0$) it will be necessary that $\sin 2\theta > 0$; consequently, θ is constrained to a range of values:

$$\pi < \theta < \frac{3\pi}{2} .$$

Necessarily, the schemes just described are recognized to be operating as "earth pointing" devices; hence they will have motions only in the 2nd and 3rd (θ) quadrants. For systems pointing away from earth the operating ranges for θ are equally well defined, occurring in the 4th and 1st quadrants.

(c). A Numerical Example.

To illustrate a calculations procedure, and to provide some insight into this problem, an example is studied, in detail, below:

For this case let the system be for an extensible tether ($\sigma' > 0$); one which begins with a line length (ℓ_o) of 10 ft. (3.048m); also, let the final length (ℓ_m) be 10010 ft. (3051.054m). This assignment of lengths is made so that $\sigma \neq 0$ for any computation, and to provide a $\Delta\ell \equiv 10^4$ ft.

The base (reference) orbit is assumed to have a constant angular rate ($\dot{\varphi}_g$) of 10^{-3} rad/sec. For this example suppose the tether position angle is set at $\theta = 150^o$, a fixed value. Thus, the input information is:

$$\ell_o = 10.0 \text{ ft. } (3.048\text{m}),\ \ell_m = 10010 \text{ ft. } (3051.054\text{m}) \equiv \ell_f,$$

$$\theta = 150^o,\ \dot{\varphi}_g = 10^{-3} \text{ rad/sec.} \qquad \text{(III.10)}$$

For the system, then

$$K_\theta \equiv -\frac{3}{4}\sin 2\theta = -\frac{3}{4}\left(\frac{\sqrt{3}}{2}\right) = 0.64952. \tag{III.11}$$

(1). The time needed to complete the extension, from ℓ_o to ℓ_m, is:

$$t_m = \frac{1}{K_\theta \dot{\varphi}_g}\, \ell n\left(\frac{\sigma_m}{\sigma_o}\right) = \frac{1}{K_\theta \dot{\varphi}_g}\, \ell n\left(\frac{\ell_m}{\ell_o}\right). \tag{III.12}$$

But, $\ell n\left(\frac{\ell_m}{\ell_o}\right) = \ell n\left(\frac{3051.0541}{3.048}\right) = 6.90876$; consequently,

$$t_m = 10.6367\ (10^3)\ \text{sec};$$

or, the extension occurs during a main body transfer of

$$\varphi \equiv \dot{\varphi} t = 10.6367\ \text{rad.} = 1.6929\ \text{orbits.}$$

(2) Next, the tension law for this tether action is obtained as:

$$\tau_m \equiv \frac{F_2/\tilde{m}}{\ell_m \dot{\varphi}^2} = \left[\frac{3}{2}(1+\cos 2\theta) - K_\theta^2\right]\sigma$$

$$= \left[\frac{3}{2}\left(\frac{3}{2}\right) - \left(\frac{3}{4}\,\frac{\sqrt{3}}{2}\right)^2\right]\sigma = \frac{9(13)}{64}\,\sigma\,. \tag{III.13}$$

To define the specific tether force $(F_2/\tilde{m})$, one uses the definition for τ_m, which leads directly to:

$$\frac{F_2}{\tilde{m}} = \tau_m\,(\ell_m \dot{\varphi}_g^{\,2}) \equiv \frac{9(13)}{64}\,\sigma\,(\ell_m \dot{\varphi}_g^{\,2}),$$

or

$$\frac{F_2}{\tilde{m}} = \left(\frac{9(13)}{64}\,10^{-6}\right)\ell, \quad (\text{since } \sigma \equiv \frac{\ell}{\ell_m}\,). \tag{III.14}$$

(Note that the specific force is linearly related to the tether length, ℓ; hence, the specific force range expected here must satisfy the inequality:

$$\left(\frac{F_2}{\tilde{m}}\right)_o \leq \frac{F_2}{\tilde{m}} \leq \left(\frac{F_2}{\tilde{m}}\right)_f, \text{ (since } \ell_o \leq \ell \leq \ell_f).$$

Corresponding to these expressions, the particular end values are:

$$\left(\frac{F_2}{\tilde{m}}\right)_o = \left(\frac{9(13)}{64}\ 10^{-6}\right) 10.0 \qquad = (1.828)\ 10^{-5}\ f/s^2,$$
$$(\text{or, } (5.572)\ 10^{-6}\ m/s^2);$$

and

$$\left(\frac{F_2}{\tilde{m}}\right)_f = \left(\frac{9(13)}{64}\ 10^{-6}\right) 10010.0 \qquad = (1.83)\ 10^{-2}\ f/s^2$$
$$(\text{or, } (5.58)\ 10^{-3}\ m/s^2).$$

(3). To calculate the "pay-out rates", $(\dot{\ell})$, and in particular the values at the beginning and end of the extension, one may proceed as follows:

Since $\sigma' \equiv K_\theta \sigma$; then from the definition of σ';

$$\frac{d(\ell/\ell_m)}{d\varphi} = \frac{1}{\ell_m}\left(\frac{\dot{\ell}}{\dot{\varphi}_g}\right),$$

it is found that,

$$\dot{\ell} = (K_\theta \dot{\varphi}_g)\ \ell, \tag{III.15}$$

as a generalization. Consequently, for the present problem the end values are:

$$\dot{\ell}_o = \left(\frac{3}{4}\ \frac{\sqrt{3}}{2} * 10^{-3}\right) 10.0 = (+\ 0.6495)\ 10^{-1}\ f/s,$$
$$(\text{or, } (+1.9797\ 10^{-3}\ m/s);$$

and

$$\dot{\ell}_f = 0.6495\ (10010.0) \qquad = 6.5017\ f/s,$$
$$(\text{or, } 1.982\ m/s).$$

(For the purpose of "joining" these end values recall that the speed $(\dot{\ell})$ has a linear variation with tether length, ℓ).

These calculations, and generalizations, are the results of an "exact" analytical solution for this particular tethered bodies problem. It should be apparent that the converse situation, that of reeling-in a tether, is determined from a similar procedure. The one consideration which must be given to the reel-in case is that for the action angle (θ). This is (again) a constant value, but is in a range between π and $3\pi/2$, for "earth- or planet-pointing" systems. This statement does not indicate that these tethered systems cannot function in directions pointing away from the primary mass; obviously this is not a constraint for the class of tethered body operations just described.

In order to provide additional information on this problem the parameters from a general analysis have been determined. These cover the entire operating range: ($\pi/2 \leq \theta \leq \pi$) for reel-out tethers, and ($\pi \leq \theta \leq 3\pi/2$) for reel-in systems. By this description the total θ-region is "mapped" and particular quantities are described for the problem. On the graphs, presented below, one will find information on the time required to complete the operation; the initial and terminal specific tether force(s); and the initial and final tether rates ($\dot{\ell}$); all as functions of the orientation angle (θ).

(d). Discussion.

The information presented on Figs. (III.6, III.7, III.8) is particular to the example problem described in the foregoing paragraphs. For that study the calculations were based on specified tether conditions (ℓ, θ, etc.) and a definite orbit ($\dot{\varphi}$). Here, the present conditions are the same as those in the example; however these graphs cover an entire operating range, in θ, for an extendible tethered body system.

Fig. (III.6a) defines the required initial extension rate ($\dot{\ell}_o$) for this operation, as a function of θ, for $\pi/2 < \theta < \pi$. It is quite obvious from the figure that the rate is largest at $\theta = 3\pi/4$, and tends toward zero as $\theta \rightarrow \pi/2$ and π. From an inspection of the equations describing this problem one will note that the system cannot function at $\theta = n\pi/2$, (n = 0, 1...).

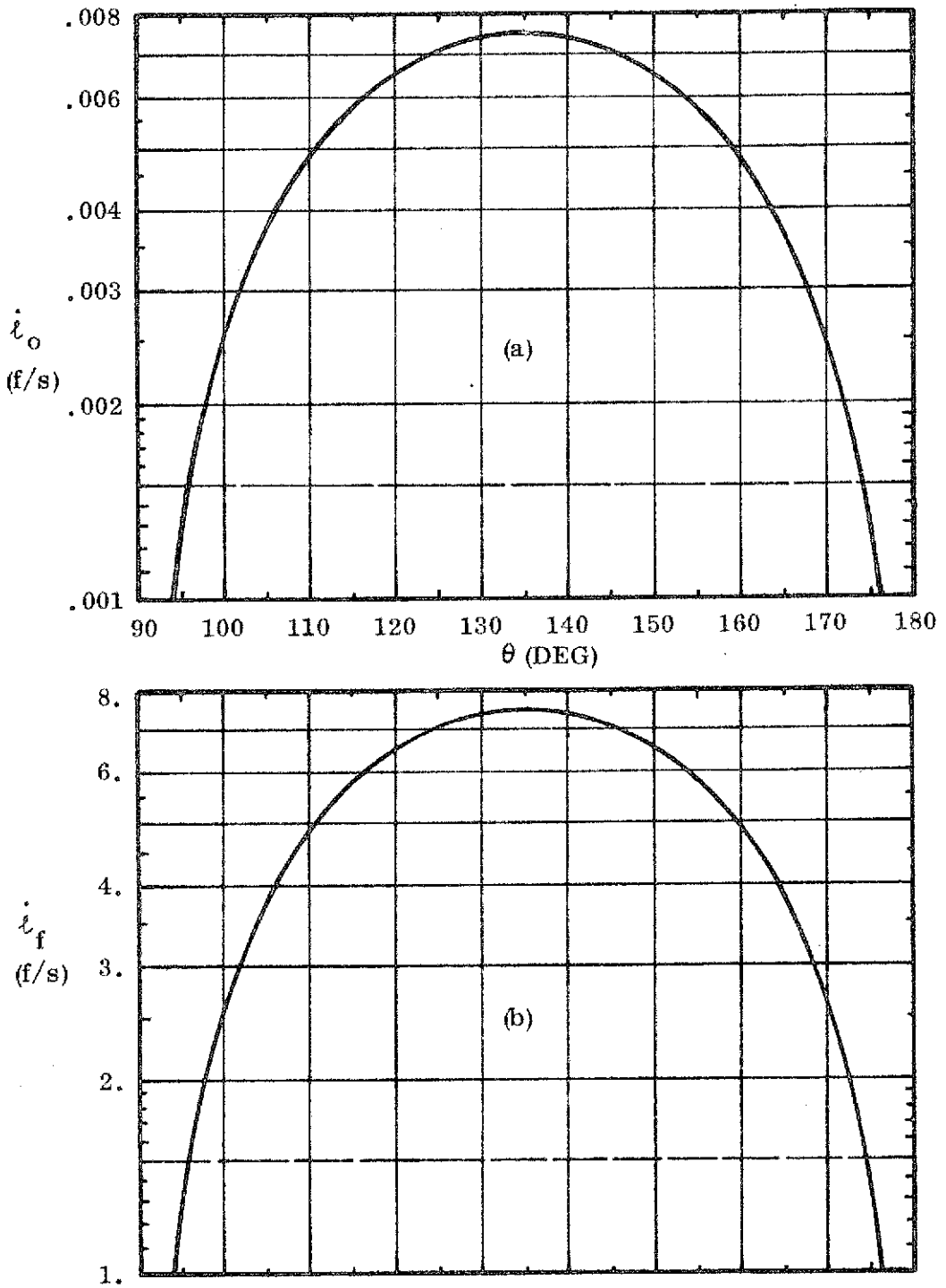

Fig. III.6(a,b). Initial and Final Extension Rates ($\dot{\ell}_o$, $\dot{\ell}_f$) for Constant θ, Variable Tension Examples. For this Case: $\ell_o \equiv 10$ ft, and $\dot{\varphi} \equiv 10^{-3}$ rad/sec.

Fig. (III.6b) depicts the terminal extension rate ($\dot{\ell}_f$) for this operation over the same θ-range. The noted similarity of this curve with the former one is expected (see eq. (III.15)). Also, due to symmetry of the parameter K_θ ($\equiv -\frac{3}{4}\sin 2\theta$) one should expect that the extensible tether system would operate in the angle range, $3\pi/2 \leq \theta \leq 2\pi$. In this regard the information shown on Figs. (III.6) would be equally applicable to both ranges indicated. The reader is reminded that the extension rate ($\dot{\ell}$) is linearly dependent on length (ℓ), hence the speed at any intermediate extension, between ℓ_o and ℓ_f, can be immediately determined.

To illustrate the influence of θ on the specific force acting in the connecting line, the quantity $(F/\tilde{m})_o$ has been plotted on Fig. (III.7). Here the level of force needed to initiate the extension (at $\ell = \ell_o$) for this example case is found. On Fig. (III.7) the θ-angle is varied as indicated. (Since the variation in force extends over three orders of magnitude, for the plot, this is represented by interrupted curves (as plotted) with a notation for the proper exponent attached to each arc. Because of symmetry (see eq. (III.13)) this curve is reflected into the $\theta = \pi$ line for the figure. The final tension level is not described graphically, here, however the construction for it would have a marked geometric similarity to what is seen on Fig. (III.7)).

Fig. (III.8) is a plot of the time required for the tether's extension to be completed; this also appears as a function of the angle (θ). One can see that the required time is least when $\theta = 3\pi/4$; however it grows without limit as $\theta \to n\pi/2$. From functional symmetry, and the problem's physical considerations, it is apparent that the time curve would be applicable to both extensions and contractions; hence it would be a repeated geometry for each θ-quadrant (identically)*.

One of the more interesting facts drawn from a study of these figures is that there can be large variations in the parameters which are needed to make

*It should be remembered that eqs. (E.25), Appendix E, were written after the quantity $\Delta (\equiv r/r_1)$ was reduced by linearization. This reduction removes the slight difference, in predictions, caused by gravity gradient, in the fully developed expressions.

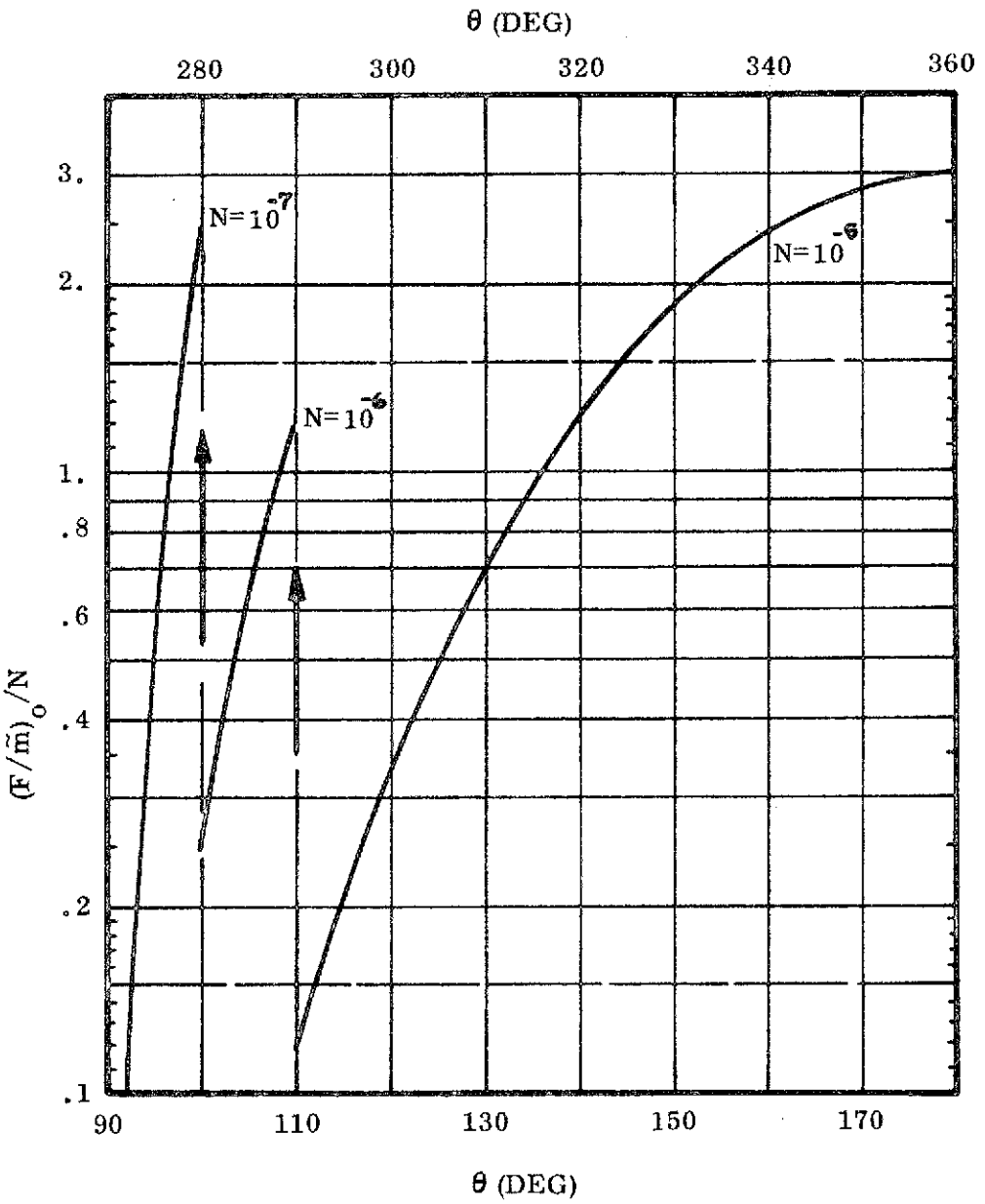

Fig. III.7. Required Initial Specific Tension, for Constant θ-Variable Tension Tether Extension Operations. The Reel-Out Case is Illustrated; Operating Conditions are noted on Fig. III.6.

Note (for example) that at $\theta \cong 96.5^{o}$, $(F/m)_o \cong .4(10^{-6})$ ft/sec^2.

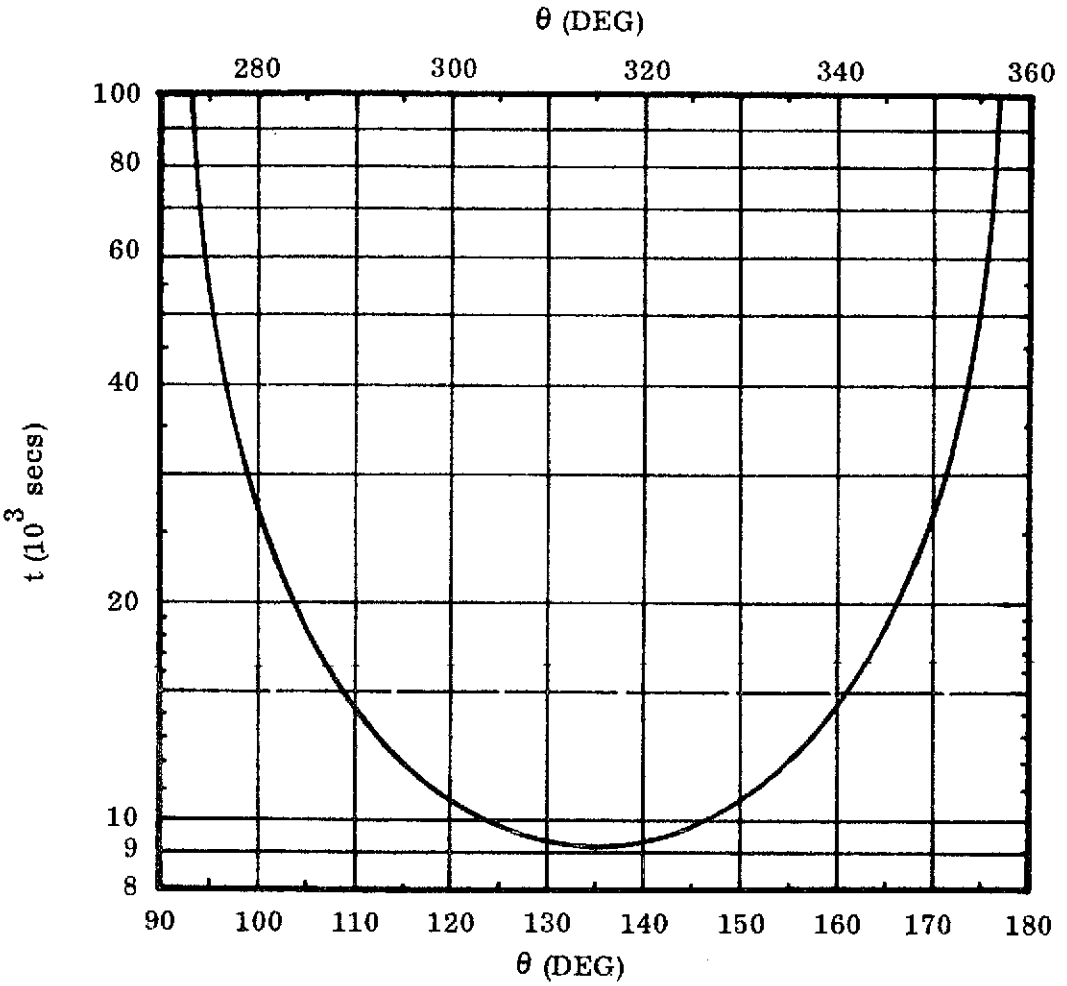

Fig. III.8. Time Needed to Complete Constant θ-Variable Tension Tether Extensions. Operating Conditions are noted on Fig. III.6.

the system work; and for small changes in the angle (θ). This is, necessarily, the situation which exists near the $\theta = n\pi/2$ operating angles. Contrary to this the system is best behaved near to the $k\pi/4$ points. There the specific tensions are largest but the time required is least. Even though the required and developed extension rates are (also) largest, there, the sensitivity of the scheme is best at these latter angles. From a mechanization point of view it would behoove the engineering designer to work in a vicinity near to these ($k\pi/4$) positions.

Another interesting aspect of this problem, and particularly its formulation, is that the major parameters can be grouped and arranged in a universal representation. That is, one can describe the overall operational characteristics for these systems in terms of the constants, K_θ and K_τ. According to the formulae developed in this study the dimensionless quantities τ_m, σ', $t\dot{\varphi}$, and σ can be related by these defined constants. That is, one can form the ratios noted below:

$$\frac{\tau_m}{\sigma} = K_\tau, \quad \frac{\sigma'}{\sigma} = K_\theta, \quad \text{and} \quad \frac{t\dot{\varphi}}{\dot{\ell}_n (\ell/\ell_o)} = \frac{1}{K_\theta} \quad ; \tag{III.16}$$

where, as before,

$$K_\theta \equiv -\frac{3}{4} \sin 2\theta,$$

and

$$K_\tau \equiv \frac{3}{2} (1 + \cos 2\theta) - K_\theta^2 .$$

Making use of these relationships, after having decided on the principal character of a tethered system, it is possible to determine the system's general behavior immediately. For instance, picking an orbital altitude (i.e., having selected $\dot{\varphi}$), deciding on a tether length (ℓ_m) and an operating angle (θ), then the system's operational requirements are defined. Here, after calculating K_θ and K_τ, the required tension law, time of the extension, initial and final payout rates ($\dot{\ell}$) are all ascertained by simple calculations*.

*The one remaining drawback to this procedure is concerned with the lack of knowledge regarding error levels, associated with these analytical results, as compared to the numerical (more exact) counterparts. This will be shown, later, not to be a critical factor for this study.

There is no need to introduce an example of this procedure, here, since it would merely repeat that one conducted above (in the example problem).

III.2.3 Remarks.

The above case studies represent an analytical approach to the extensible tether problem. The more general schemes, as indicated above, are those associated with the determination of tension laws based on preassigned variations for the state parameters. From a more extensive investigation of this type one could gather considerable information on the "cause and effect" of a system's operating characteristics, and the subsequent influence of these. While the investigator may not be able to simulate a probable tethered body state accurately, he certainly can learn much about the system's behavior through this type of an analytical experiment.

The last example case studied could be of immediate use to the designer since it gives information which is directly useful for prediction purposes. However, these data are limited in applicability due to the very nature of the constraints placed on the motion. What would be most desirable would be to find a scheme which provides general information for a wide range of operational conditions. Unfortunately the general problem is too well coupled, and nonlinear in character, for such a methodology to exist.

What would normally be the next logical step to undertake, in a general information gathering sequence, would be a systematic study for a large variety of conditions (initial and operational). In the next subsection a beginning of this sort is made; however, it will be shown that it is not necessary to conduct a very large number of numerical studies simply to obtain this needed information. Instead, a method is described which allows one to generalize the results so that typical values can be applied to an entire family of like problem situations.

III. 3 Numerical Studies for Extensible Tethers.

The previous paragraphs, on extensible tethers, were concerned with analytical evaluations for the conditions necessary to maintaining a prescribed state of motion. Also, there, a special class of tethered body operations were examined, analytically, with the result that the system's requirements were determined in a general formula format. All in all those examples which have been studied were useful in providing general information; but, they lacked an ability to produce "exact" results for operational purposes. Mainly the difficulties which were encountered, there, are associated with the inability to solve the general, direct problem in closed form. The main obstacle contributing to this restriction can be traced to the analytically unyielding form of the governing equations.

For the acquisition of "exact" information regarding the control, manipulation and handling of tethered systems a computer program was designed. This program was used to evaluate a variety of extensible tethered body problems; but, to do so without the added complexity of an operationally sophisticated formulation.

The mathematical developments for this program are found in Appendices E and F. The more general aspects of the formulations are found in Appendix E, while the work described in Appendix F is addressed more to the specifics associated with the present problems. Finally, in Appendices G and I one will find the equations used in the program; and its description. For compatibility with other computer formulations, employed herein, the computational equations were referred to a moving cartesian frame; one attached to the main orbiting particle (m_1).

Internally the program's calculations were carried out in a non-dimensional format; but the output was converted to dimensional form before it was written as a displayed item.

III.3.1 Assumptions.

In the formulation of the program it was assumed that the two tether connected mass particles were moving (generally) under the influence of a single attracting mass particle (μ). For convenience the particles were presumed to be sized so that $m_1 \gg m_2$; and, subsequently, m_1 was assumed to move on a circular orbit about μ. The connecting tether was considered to be a massless member, without elasticity but capable of transmitting some level of tension throughout the entire "time" duration of the problem. Since the program was not designed to solve the problem of two freely orbiting particles, then it was necessary that the tether be kept taut at all times.

In keeping with the idea that $m_1 \gg m_2$, that m_2 is the "suspended" mass, and that the tether is massless, there has been no accounting made of the mass "paid-out" during the "extension" of the tether; i.e., $m_1 \cong$ constant.

II.3.2 Program Description.

The computer program, TETHER*, has been designed to solve the extensible tethered body problem; i.e., to describe the motion of the "suspended" particle as it moves on its own spatial path. Actually, the problem which is solved is one of relative motion wherein the mass particle (m_2) is influenced by gravity (gravity gradient) and by the constraint afforded through the tether. Under the assumptions used in the program the only force allowed in the tether is a tension which must act solely along the line vector "connecting" the two bodies. In this regard the connecting line serves as an idealized tether, but it does provide the desired constraint which, in turn, so effectively influences the subsequent body motions.

Since the program was designed with the idea of simulating a variety of operational modes, it accepts a variety of "end conditions" and other instructions essential to its mechanization. In its most basic mode of operation the program

*See Appendix I for a brief description of TETHER, and its operations.

will describe a "time history" of the suspended body's state, for whatever inputs the investigator has assigned. Thus, the state is determined from a set of initial conditions (for the suspended mass) and from the influence of tether tension and the gravitational attraction of the primary mass (μ)*. These general studies are useful in ascertaining the influence of initial values, etc.; however, when determining the control and handling qualities, of tethers, the program had to be more specific, in design, to meet these requirements.

III.3.3 Control and Handling Qualities for Tethers.

The qualities referred to here are those concerned with the manipulation of tethered systems to meet and/or maintain the requirements designed into the TETHER program. In addition they are expected to satisfy the specified end conditions for each of the selected modes of operation.

In explanation of this design philosophy, it was felt that for whatever reason tethers might be employed, one overriding requirement would be that of control. Here control is considered as that ability to predict, maintain and adjust the system so that it can be manipulated in a desired manner. For all of these defined conditions it was felt that a most desirable quality would be simplicity in operation coupled with a "means" to control the system.

Recognizing that tethers are likely to be used as cargo handling and transfer devices; as safety and retrieval mechanisms, for men and material moving on adjacent orbits; and for other concepts having to do with positioning and moving of orbiting particles; the investigation has been channeled in the directions indicated below.

For all of these operational modes there is the need to be able to maneuver particles in a manner which does not lead to catastrophic consequences. Thus, an understanding of how to "reel-in" and "reel-out" tethers, in a controlled manner, is essential. In order to reach adjacent orbiting particles, using tethers, it is

*See Appendix F (and E) for a sketch of the problem geometry.

necessary to know the correct "launch conditions", and control functions, if success is to be achieved.

For some operations it may be necessary to constrain the motion of (say) a retrieved particle; consequently, the manipulation of the tether, here, is of prime importance. And, finally, under any operational scheme one must know the limits of the system - when and where it can be made to function - if a successful maneuver is to be achieved. These were the main considerations under which this phase of the investigation was conducted.

In order to determine how control of an extensible tether system could be acquired, the basic computer program was modified to describe, as output, those conditions needed to achieve a desired "goal" during an operation. In particular, if a prescribed terminal state was to be reached the investigator would need to know how to start the operation, and what to do to maintain it. Necessarily, before undertaking any maneuver, it is essential to know whether or not the defined end conditions are a feasible consequence for the system and its operation. As an illustration of how these aims might be met, the investigation described in the following paragraphs was conducted.

III.3.4 Extensible Tether Operation Modes.

The operational concepts, next set forth, are indicative of how one can acquire the knowledge needed for the proper manipulation of a tethered system. The schemes which are studied here were those aimed at satisfying the requirement types noted above. In principal this investigation leads to a determination of those conditions which would assure that the tethers acquire desired end conditions with the stated constraints imposed on them. By systematically varying the initial values, the computer program is able to describe limits for the system, and to define other conditions and constraints which are particular to these problems.

For the first part of this effort the tether was chosen to operate at a fixed level of tension. It was manipulated so that it could reach its prescribed final state (tether length (ℓ), angular position (θ) and angle rate ($\dot{\theta}$)), while undergoing moderate motions. For the system to operate in this prescribed manner, it was decided that a simplest approach would be one where the program iteratively scanned the initial values and (finally) determined those which produced the desired results.

In order to mechanize this approach the computer program has an iterator built into it. This was used to scan the initial values and select that set which led to the prescribed end conditions. In particular, the iterator was to provide proper magnitudes for the extension rate ($\dot{\ell}$) and specific tension ($F/\tilde{m}$); other initial values are given as inputs. In the determination of system limits, these followed naturally as a by-product of the iterative scheme itself. E.g., in the scanning process, when the system failed, completely, a limit was determined. (Other limits followed in a like manner).

For the first applications of this method the tether was not restricted as to how its intermediate state could vary. One exception to this was that during the tether's extension (or contraction) it could not exceed its physical limit on length prior to attaining the preset terminal state. That is, for a system designed as a reel-out operation, it was not allowed to exceed the final length, or to reel-in completely (as a dynamically induced phenomenon), prior to reaching the defined final state. One other restriction placed on all of these tethered systems was that they are constrained to oscillatory motions (at most); they are not allowed to become rotational,about the main orbiting body, at any time.

As a consequence of the above restrictions any tether operation is said to "fail" if:

(1) It could not attain the desired end conditions.

(2) It exceeded the prescribed limits, of the operation, prior to reaching the terminal state.

(3) The system became rotational rather than remaining oscillatory.

If, for any reason, the system "failed" then those initial conditions were deemed not to be acceptable values; consequently, such a set would be outside of the bounds for the system.

The operational scheme described above will be designated as "Mode A", the "Reel-Out, Reel-In System".

As a second approach to the control of tethered body operations, the system was modified so that there was a restraint placed on how the line would be allowed to extend. The condition which was to be overcome by this restriction was that of having the tether alternately reel-out and reel-in during a given operation. It was reasoned that possibly the time or the force required for a desired extension could be altered if this "yo-yoing" effect for the tether could be eliminated. In the mechanization of this operational mode the computer program was modified so that when, or if, the tether attempted to change its "extension-rate" ($\dot{\ell}$ changed sign) the line would become fixed in length. During this fixed length condition the tether could only have a pendulous (swinging) mode of motion; this would persist until the tether could revert to a combined extension - swinging motion. When the system reverted to this latter state, it would continue to extend until the terminal conditions were reached.

In order to describe this "locking" of the tether, when the $\dot{\ell}$-term attempts to change sign, the system is visualized as having a "snubber" installed on it. The purpose of the snubber is to (figuratively) lock the "spool" on which the tether is wound, much like the latching of a window-shade, so that it could not reel-in the line. If the supported mass (m_2) is subsequently acted on by forces which tend to reel-out more tether, then the snubber is released and a "paying-out" of the line is resumed.

Obviously this intermediate, fixed length pendulous mode-of-motion is provided for by the snubber. Without this locking device the system would behave as it did in the previous description (Mode A).

This second operational scheme is said to "fail" if it encounters any of the same constraining conditions noted in the discussion of the simpler reel-out, reel-in system.

In this mode the tether also works against a fixed tension level, except when the "snubber" is activated. (During the time when the tether length is fixed, the line tension is below its preset operational level. Once this level is regained, the snubber is released and the original reel-out operation is continued).

This latter mode for the tethered system is handled internal to the computer program in much the same way as the Mode A system. That is, the iterator is employed to determine those values of initial rate ($\dot{\ell}$) and tension (τ) which produce the desired terminal conditions. Incidentally, the terminal conditions here are conceptually the same as those for the previous operation.

The method just described, for maneuvering a tethered mass, will be designated as "Mode B", the "Snubber-Augmented System". A sketch depicting its geometry will be shown subsequently.

There is a third extensible tether operation which has been examined using the computer program. This method differs from the others in that, here, the line tension is not preset to a fixed value, but has a variable magnitude. Also, the method does not rely on the iterator to determine a proper initial state and tether tension. Rather, these quantities are defined by an auxiliary calculation (see Appendix F). From these calculations the tension law is predetermined, for a described set of initial state quantities. All of this information is subsequently incorporated into the computer program as input. The program, per se, is exercised to obtain a time history of the motion, and to assure that the desired terminal state is acquired.

It should be pointed out that this scheme is conceptually the same as that described in section III.2.2. The two are different in that here the governing equations have not been "reduced" whereas those used for the analytic solution were modified to yield a tractable set of mathematical expressions.

For continuity in notation and nomenclature the method just described will be designated as "Mode C", the "Variable-Tension System". A sketch, to aid in describing this concept, is included with later discussions.

The word descriptions, above, are adequate for a general understanding of these operational modes. However, to acquire precise information, and more explicit definitions, each of the mode types will be examined in some detail below. There, sample results will be displayed and discussed. This will allow the reader to better understand and appreciate what was obtained from this phase of the investigation.

III.3.5 Discussion.

In these paragraphs the reader will find remarks addressed to describing various example cases making use of the operational modes noted above. There will be several graphs presented; these are included to illustrate the variety of conditions examined and other particulars of these operations.

Generally, each of the "Modes" will be examined separately, but with some cross referencing indicated. For each of the sample cases pertinent state information, and other data, will be mentioned so that one can compare cases and become acquainted with the general behavior of each concept.

It should be mentioned that for each of the cases studied there will be some data which are consistent throughout. Specifically, the final tether length (ℓ_f), to be attained has been set at 10,000 feet (3048.061m). Also, the circular orbit for the main body (m_1) is to be at an altitude corresponding to a turning rate ($\dot{\varphi}$) of 10^{-3} rad/sec. (These numbers were selected for use, here, by

virture of their convenience in plotting results,and for data reductions to be described later).

For consistency and conciseness of notation each graph will be identified by its operational Mode Type (A, B, or C); and, by a parenthetic notational remark. The "remark" will be used to indicate the tether's position angle at the "beginning" and "end" of an operation. For example: $(150/180) \equiv (\theta_o/\theta_f)$, indicates a tether orientation of 150^o, at $t = 0$, and one of 180^o, at $t = t_f$. (See Fig. F.1, or III.1, for the proper geometry).

Each graph will be presented as a polar plot depicting the coordinates (ℓ, θ) for the various cases. The scale numbers shown on these graphs will describe length (ℓ), in 10^3 feet, and position angle (θ), in degrees.

(a). Mode A; Reel-Out, Reel-In System.

This operational mode has been verbally described, earlier. The sketch, below, is included to clarify this scheme and the state conditions encountered during a given "extension"*. On the sketch m_1 is the main particle; m_2 plays the role of the suspended mass, connected to m_1 by the tether.

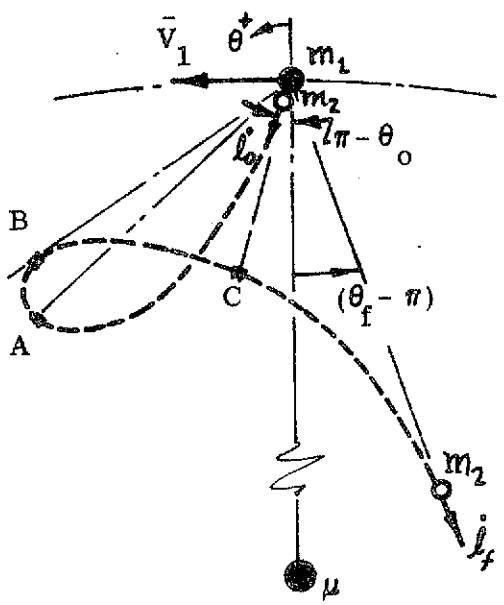

Fig. III.9. Sketch Depicting a Mode A, Constant Tension Extension.

The initial state $(\ell_o, \theta_o; \dot{\ell}_o, \dot{\theta}_o)$ and the terminal values $(\ell_f, \theta_f; \dot{\theta}_f = 0)$ are set conditions; $\dot{\ell}_f$ is a parameter described by the program's output.

Refer to the sketch, Fig. III.9: From the beginning point $(\sim)_o$, to "A", the system pays-out line $(\dot{\ell} > 0)$; from "A" to "C" the tether is being reeled-in $(\dot{\ell} < 0)$; but, from there to the terminus, $\dot{\ell} > 0$. At

*The use of "extension" throughout these discussions should not be taken too literally. The ideas, which are noted, generally apply to "contractions" as well as "extensions".

point "B", $\dot{\theta} = 0$ (and changes sign); also, at the terminus $\dot{\theta} = 0$ (this is a constraint imposed on the operation). Mainly, the terminal constraints have been selected so that only minimal transients will need to be applied if the system is brought to rest, there!

(1) Example Cases. The first case described is the simplest mode of operation for an extensible tether system. See Fig. III.10.

On the graph, the curve at left describes an extendible system; the one at right portrays a contracting tether. These two examples are identified as the "Lowering-" and "Raising-System", respectively.

This overall operation is designated as a: Mode A, constant tension system (180/180). The initial (I.C.) and terminal (T.C.) conditions for these two operations are noted below:

For the Lowering System:

I.C.: $\ell_o = 0$, $\theta_o = 180^o$, $\dot{\ell}_o = 14.9$ f/s (4.54 m/s),

T.C.: $\ell_f = 10^4$ ft, $\theta_f = 180^o$, $\dot{\ell}_f = 10.7$ f/s (3.26 m/s), $\dot{\theta}_f = 0$,

t (time, ℓ_o to ℓ_f) = 2322 sec.,

$F/\tilde{m}$ (specific tension) = 0.0204 f/s^2 (0.0062 m/s^2).

For the Raising System:

I.C.: $\ell_o = 10^4$ ft, $\theta_o = 180^o$, $\dot{\ell}_o = -10.7$ f/s (-3.26 m/s), $\dot{\theta}_o = 0$,

T.C.: $\ell_o = 0$, $\theta_f = 180^o$, $\dot{\ell}_f = -7.8$ f/s (-2.38 m/s),

t (time, ℓ_o to ℓ_f) = 2322 sec.,

$F/\tilde{m}$ (specific tension) = 0.0204 f/s^2 (0.0062 m/s^2).

From the graph it is evident that the "lowering" of m_2 occurs in the 2nd θ-quadrant, while the "raising" is confined to the 3rd quadrant*. The symmetry

*These quadrants are for an earth-pointing system.

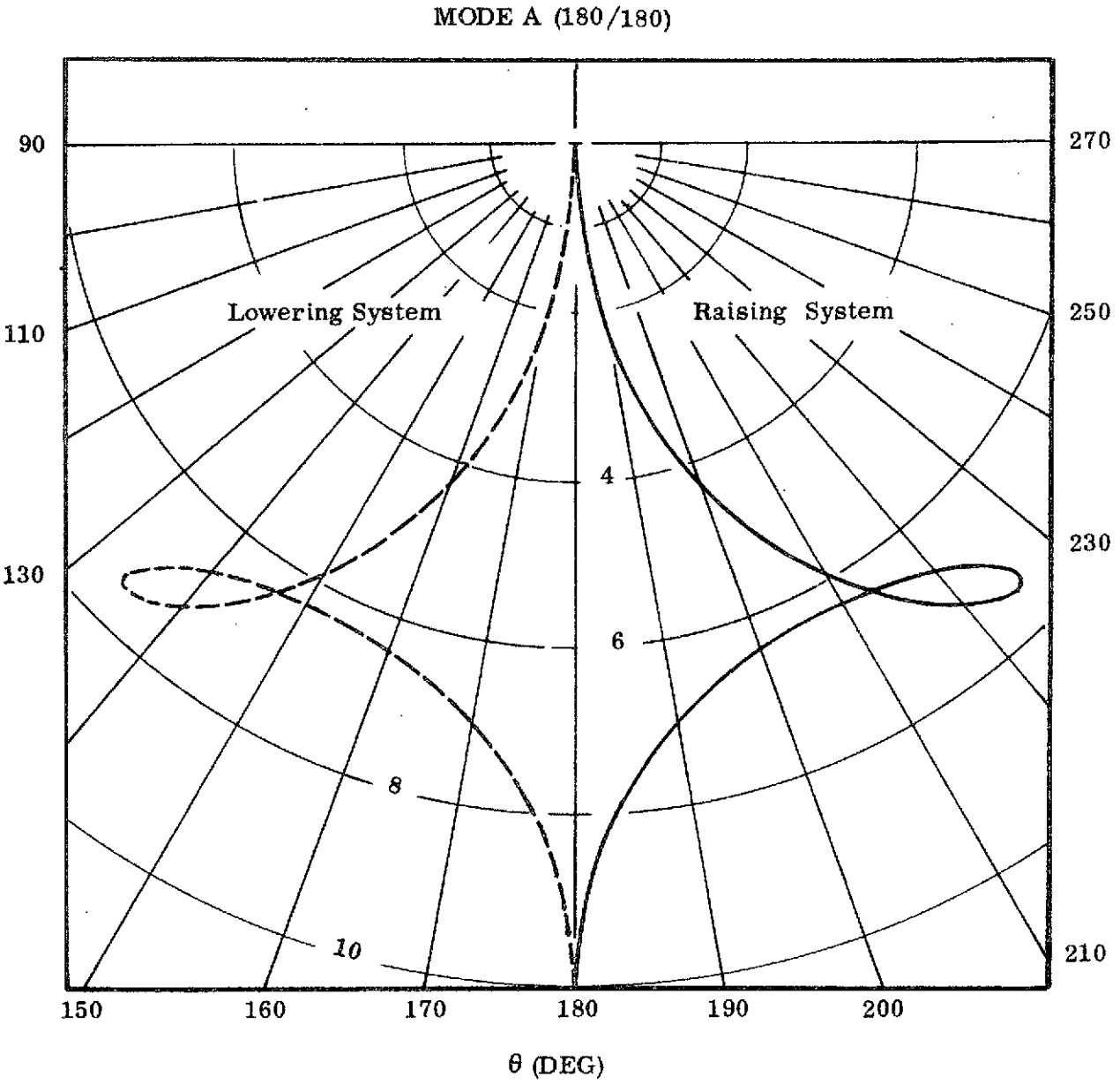

Fig. III.10. History of ℓ, θ for a Mode A (180/180) Operation. Dashed Curve Traces Displacements During Extension; Solid Line Depicts a Reel-In Maneuver. Here the Maximum Tether Length is set at 10^4 Feet.

which is apparent here is typical to this case only. It should be noted that during the lowering of m_2 the motion occurs initially in a direction with the motion of m_1, while for the raising it is initially against the orbiting motion. It can be seen that for both of these cases the θ-amplitude, during the operation, is $\Delta\theta \cong \pi/4$.

For the lowering case, the "reel-back" which occurs is not large. The tether undergoes an approximate 1000 ft. contraction; this is dynamically induced by the system. "Loops" in the motion traces (reversals in the general trends) are typical to these unconstrained modes.

(2). The second case to be described (Fig. III.11) represents a limit situation for the Mode A (xxx/180) cases. This is the smallest θ_o value acceptable to the operation. As seen from the plot, the system is initiated at $\theta_o = 150^o$; it terminates at 180^o, and has a roll-back of approximately 4000 ft. (1219 m).

For this system the operational conditions are:

I.C.: $\ell_o = 0$, $\theta_o = 150^o$, $\dot{\ell}_o = 17.4$ f/s (5.3 m/s),

T.C.: $\ell_f = 10^4$ ft, $\theta_f = 180^o$, $\dot{\ell}_f = 15.5$ f/s (4.72 m/s), $\dot{\theta}_f = 0$,

t (time, ℓ_o to ℓ_f) = 2279 sec.,

$F/\tilde{m}$ (specific tension) = 0.01813 f/s^2 (0.0055 m/s^2).

It is interesting to compare this case with those above; and, in particular, to note that the time needed here is shorter than that for the former. Also, this case has a larger "roll-up" loop than the previous ones. In part,the shorter time requirement is offset by the increased initial (and terminal) payout rates.

(3). The third Mode A simulation to be discussed is a (270/180) case. (See Fig. III.12). From the trace plot the supported mass is seen to exhibit a large θ-excursion; also it undergoes a rather extensive "roll-up" of the tether during its reversed ($\dot{\ell} < 0$) motion.

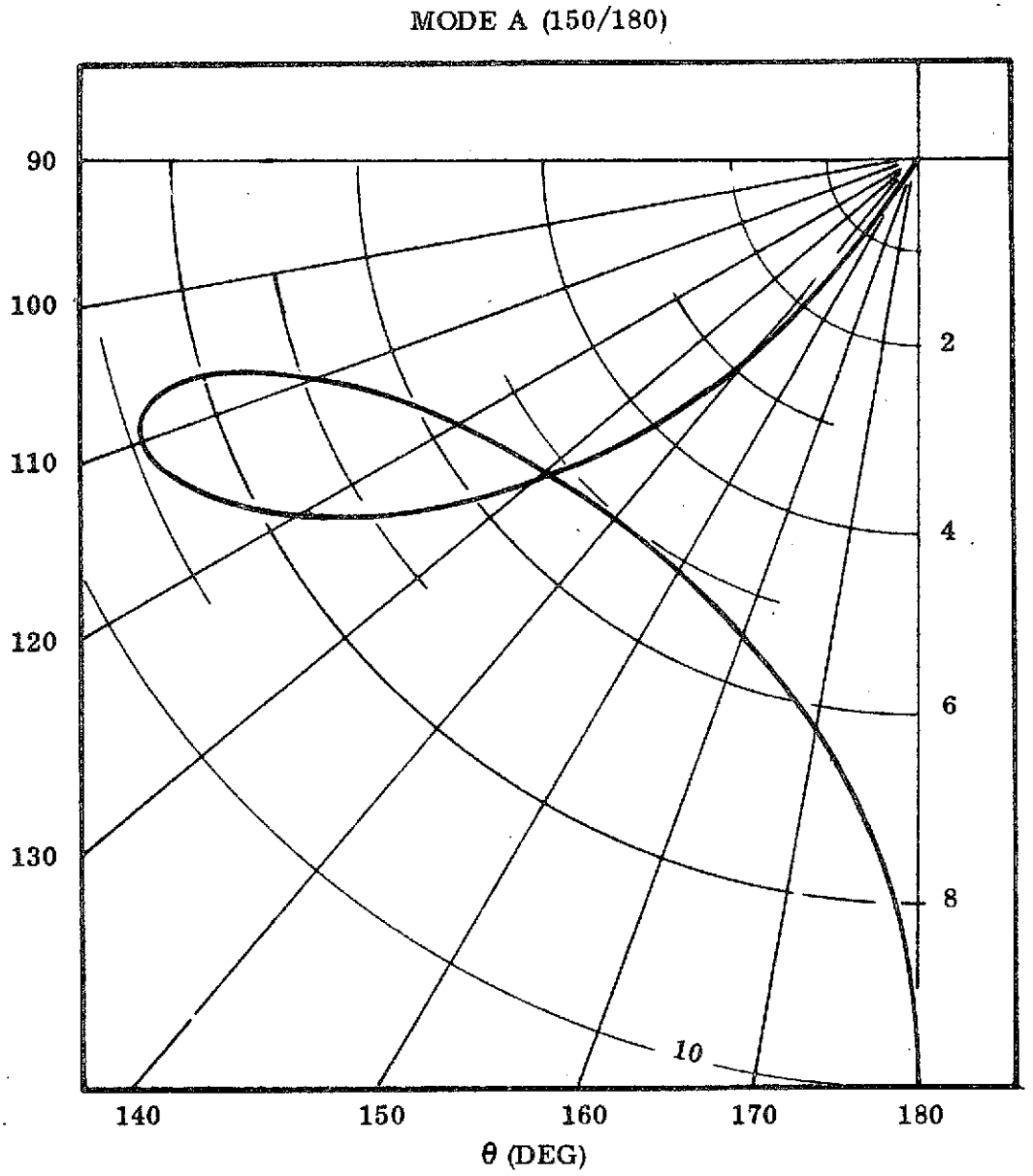

Fig. III.11. A Limit Case for Mode A Operation. This Limit is due to θ_o.

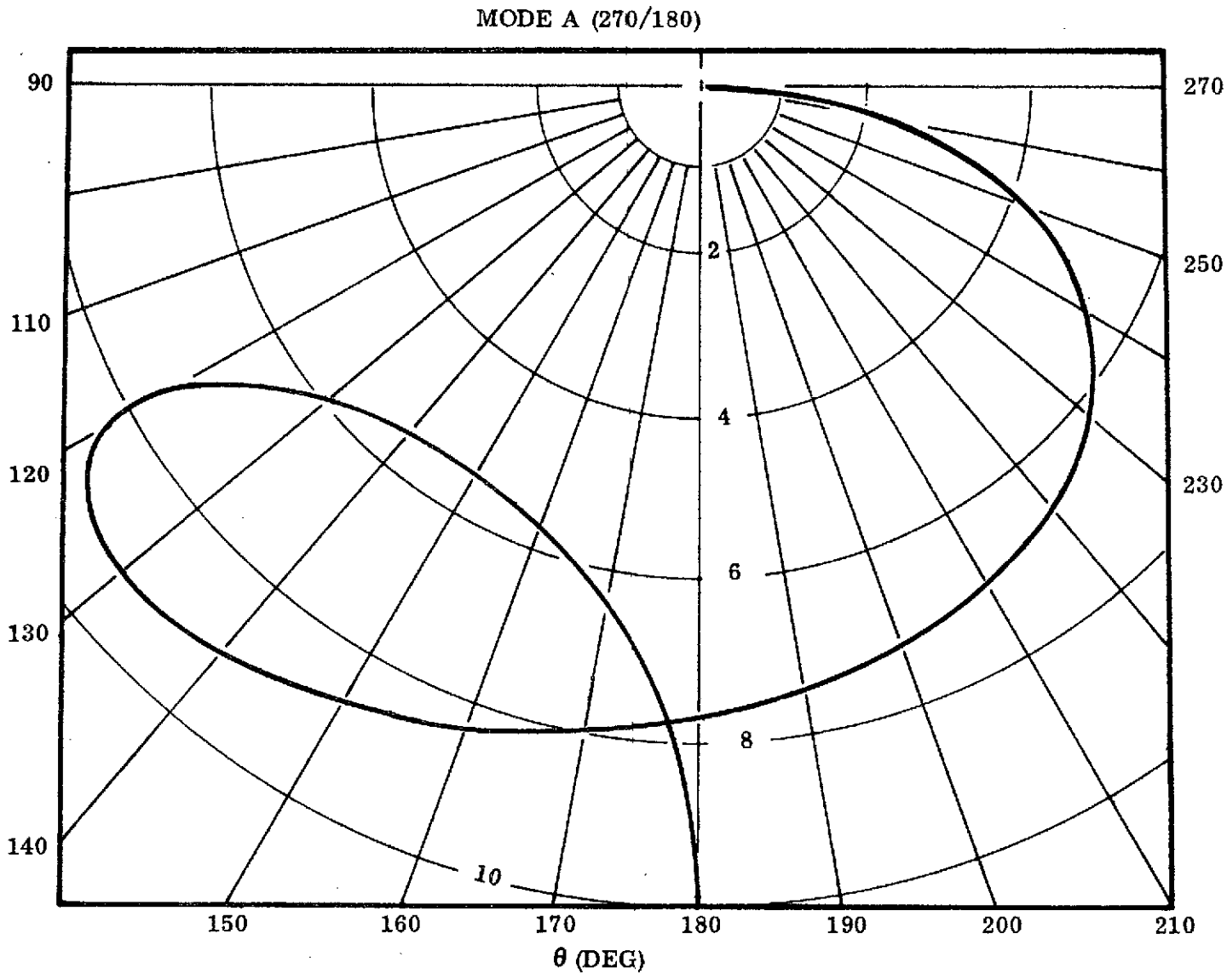

Fig. III.12. Example of a Mode A Constant Tension Tether Extension.

This case is interesting in that it is indicative of the extended range which can be accomodated by these controlled tether operations. Apparently, then, one is able to reach a position "below" ($\theta = 180^{o}$) a spacecraft, with a particle (m_2), using a large range of "aiming" angles. Also, it can do this without having a large variation in initial pay-out rates ($\dot{\ell}_o$).

The operational parameters for this mode are:

I.C.: $\ell_o = 0$, $\theta_o = 270^{o}$, $\dot{\ell}_o = 15.2$ f/s (4.63 m/s),

T.C.: $\ell_f = 10^4$ ft, $\theta_f = 180^{o}$, $\dot{\ell}_f = 14.9$ f/s (4.54 m/s), $\dot{\theta}_f = 0$,

t (time, ℓ_o to ℓ_f) = 3282 sec.,

$F/\tilde{m}$ (specific tension) = 0.01545 f/s^2 (0.00471 m/s^2).

(4). On Fig. III.13 another limit case for the Mode A (constant tension) trajectories is seen. This is the (155/205.9) case, where the terminal angle, at $\theta_f = 205.9^{o}$, is the limit value.

From the trace geometry it is apparent that when one attempts to reach a larger θ_f position, the tether length exceeds 10^4 feet before reaching its terminal state; and, by definition, such an operation would "fail". According to the figure there is a large roll-up in the tether length (approximately 5000 ft. of line are rewound) before the system recovers and returns to its extending itself.

The operating characteristics for this maneuver are:

I.C.: $\ell_o = 0$, $\theta_o = 155^{o}$, $\dot{\ell}_o = 24.83$ f/s (7.57 m/s),

T.C.: $\ell_f = 10^4$ ft, $\theta_f = 205.9^{o}$, $\dot{\ell}_f = 13.42$ f/s (4.09 m/s), $\dot{\theta}_f = 0$,

t (time, ℓ_o to ℓ_f) = 1966 sec.,

$F/\tilde{m}$ (specific tension) = 0.0339 f/s^2 (0.01033 m/s^2).

Next, a sampling of the Mode B (constant tension; snubber) operations will be made. As with the case studies above, both general and special situations will

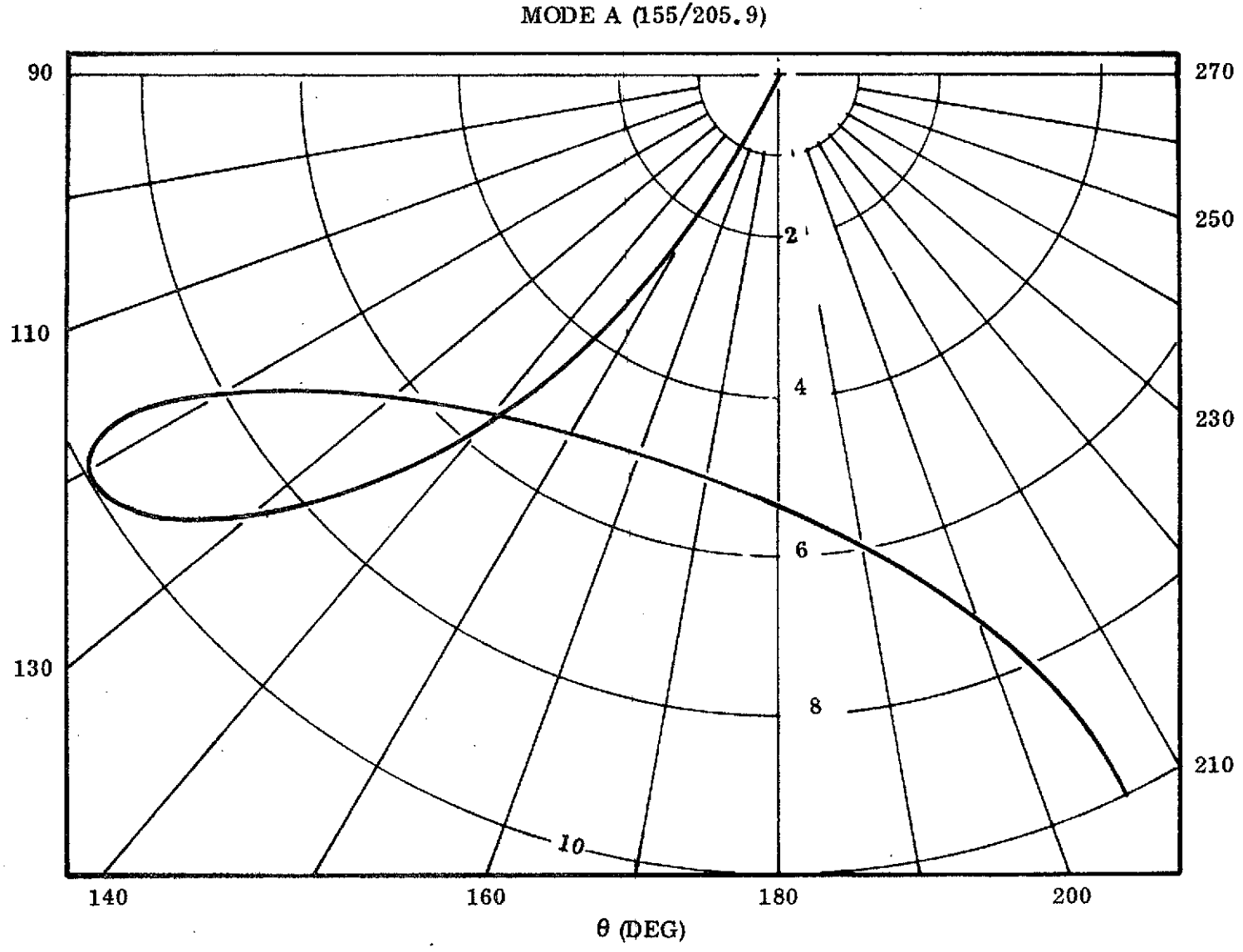

Fig. III.13. A Limiting Situation for Constant Tension Operations. Limit due to Intermediate Tether Extension.

be described, verbally and graphically, and briefly discussed. Where corresponding terminal states are to be achieved, a direct comparison between modes - for operating characteristic - will be made.

Prior to actually examining cases, a description of this mode's motion is presented. (See Fig. III.14).

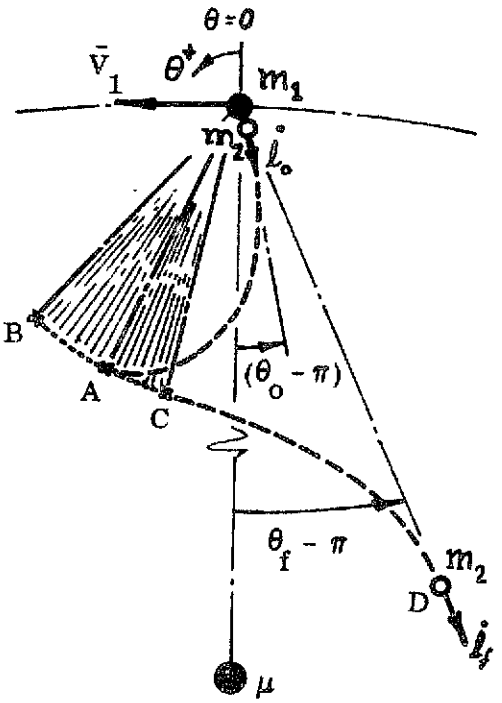

Fig. III.14. Sketch Depicting Mode B Tether Extensions.

A desired motion for the Mode B system begins at θ_o, $\dot{\ell}_o$, $\ell_o = 0$. Leaving m_1, the mass (m_2) moves to point "A" working against the fixed line tension. At "A" the snubber is engaged and the motion becomes a fixed-length oscillation. At "B" the particle reaches its amplitude position ($\dot{\theta} = 0$), the swing reverses, and the pendulous motion persists until point "C" is reached. There the snubber is disengaged, and the system reverts to its original motion - paying out line and swinging toward its terminal location. At "D" the desired terminus is reached ($\ell = \ell_f$, $\theta = \theta_f$, $\dot{\theta}_f = 0$); the final payout rate ($\dot{\ell}_f$) is again a consequence of the dynamics, etc. of the problem. A true null state could be attained at "D" by means of a transient; one to reduce the state residuals to zero.

The above description is general in context, not necessarily a composite description for all cases to be expected. In the examples which follow a number of situations will be described to illustrate various aspects of this operational mode.

(5). As a first example, Fig. III.15, this case is designated as a Mode B (180/180) case. Here, the system commences much like the Mode A (180/180) example except that when the tether reaches $\theta \cong 140^{o}$, the snubber is engaged and the particle commences its pendulous motion, with $\ell = 6581$ ft. (2006 m). The oscillation reaches a largest amplitude at $\theta \cong 137^{o}$, it swings back to $\theta \cong 147^{o}$, where the snubber is released and the particle descends to its 10^{4} ft. terminal length.

The operating characteristics for this mode are:

I.C.: $\ell_{o} = 0$, $\theta_{o} = 180^{o}$, $\dot{\ell}_{o} = 16.4$ f/s (5.0 m/s),

T.C.: $\ell_{f} = 10^{4}$ ft, $\theta_{f} = 180^{o}$, $\dot{\ell}_{f} = 7.42$ f/s (2.26 m/s), $\dot{\theta}_{f} = 0$,

t (time, ℓ_{o} to ℓ_{f}) = 2536 sec.,

$F/\tilde{m}$ (specific tension) = 0.0257 f/s^{2} (0.0078 m/s^{2}),

t_{s} (time <u>in</u> pendulous motion) = 760 sec.

By comparison with the Mode A (180/180) problem, this one takes a longer time to reach its final state; and, too, it requires a larger specific tension (slightly more than 25% increase) to make it work. Physically, the motions are comparable (in state) except for the obvious differences which occur when the snubber is <u>and</u> isn't operating. There is nothing of substance here to suggest why one mode type should be recommended over the other.

(6). On Fig. III.16 the Mode B type is designated as a (155/180) case; this can be correlated to the situation described on Fig. III.11. Much like that comparison maneuver, this one is also a limit situation. Here the limit is linked to the initial angle ($\theta = 155^{o}$). That is, the system does not acquire the desired end conditions for $\theta_{o} < 155^{o}$.

For this mode the tether reaches a length, $\ell = 6009$ ft. (1831.5 m), before the snubber is engaged, at $\theta \cong 120^{o}$. During the fixed length oscillation the

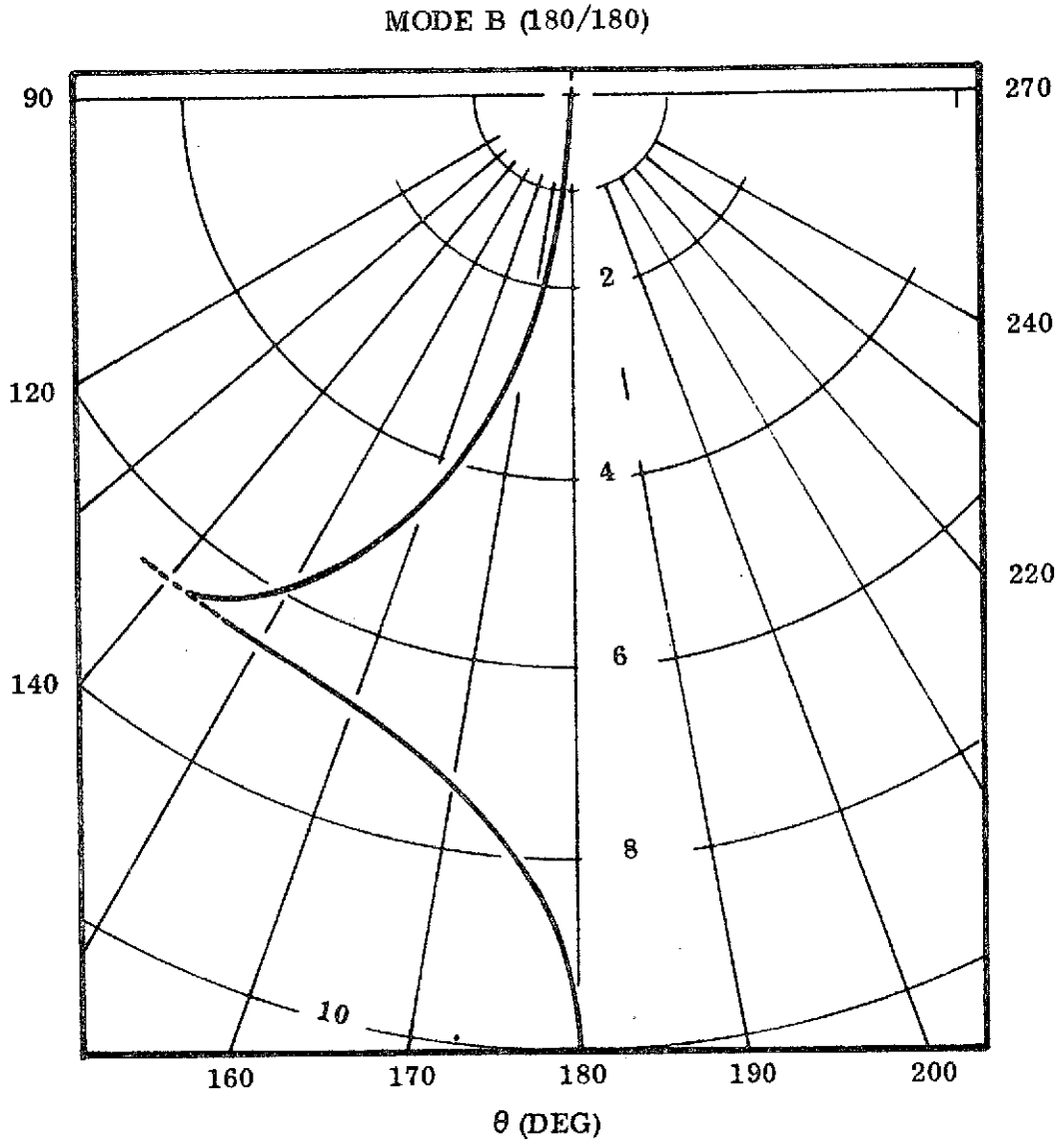

Fig. III.15. Motion Trace for the Mode B (180/180), Constant Tension (with Snubber) Tether Extension. Dashed arc Depicts a Constant Length, Pendulous Action. All Cases are for a Tether Length of 10^4 Feet.

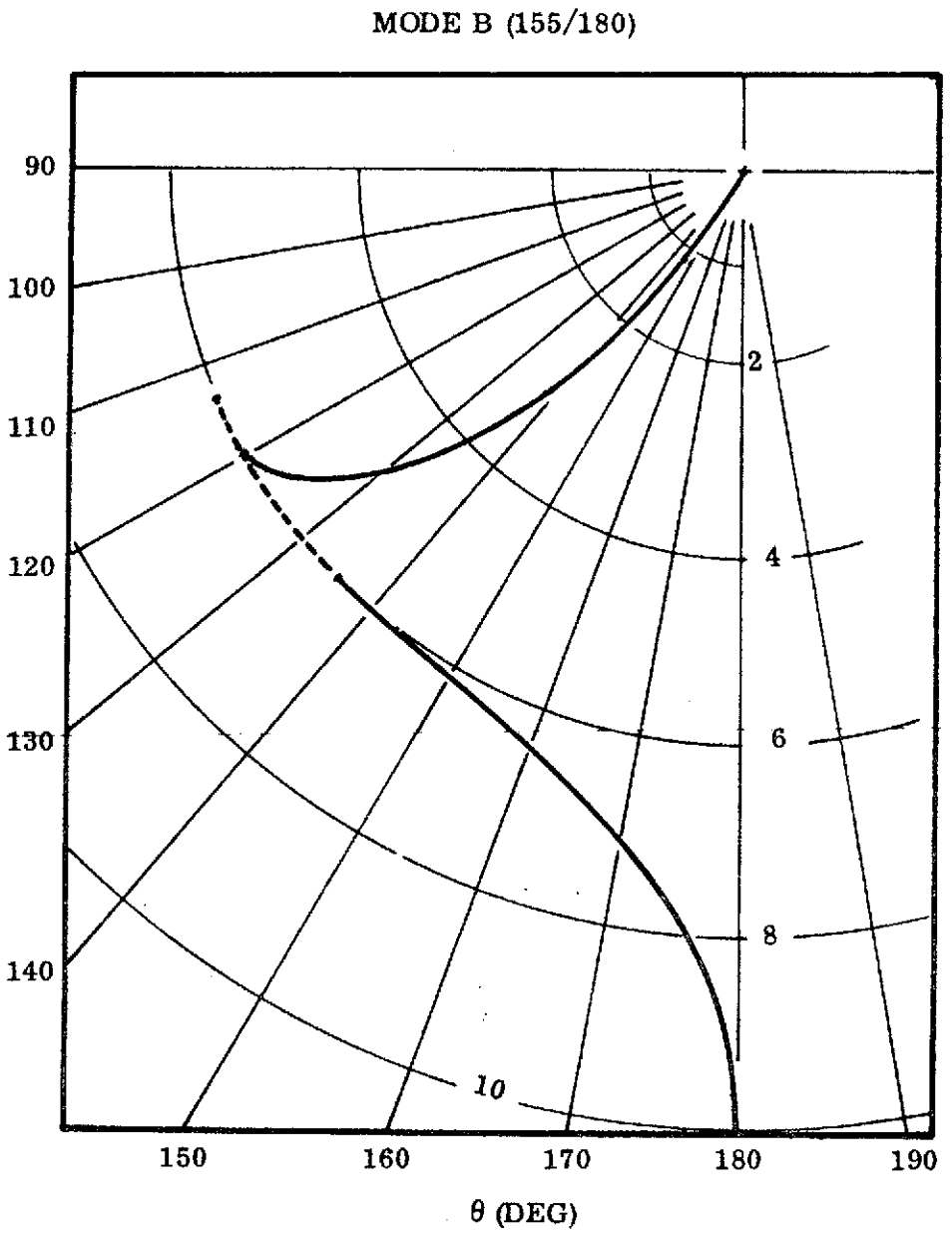

Fig. III.16. A Limiting Case for Mode B Operations. Limit due to θ_o.

maximum amplitude is reached at $\theta \cong 114^{o}$; the back swing returns m_2 to $\theta \cong 135.4^{o}$ where the snubber is released and the tether unwinds to its maximum length. For this operation the system's characteristics are described as:

I.C.: $\ell_o = 0$, $\theta_o = 155^{o}$, $\dot{\ell}_o = 17.45$ f/s (5.32 m/s),

T.C.: $\ell_f = 10^4$ ft, $\theta_f = 180^{o}$, $\dot{\ell}_f = 7.9$ f/s (2.41 m/s), $\dot{\theta}_f = 0$,

t (time, ℓ_o to ℓ_f) = 2672 sec.,

$F/\tilde{m}$ (specific tension) = 0.027 f/s^2 (0.00823 m/s^2),

t_s (time of pendulous motion) $\cong$ 1037 sec.

Comparing characteristics between the two limit cases (noted above) it is evident that this mode takes a longer time to complete; and it requires an approximate 50% increment in specific force for its operation. The amplitude displacement here is smaller than for the previous case, but not markedly so. It does seem that now there could be a reason for selecting one mode type over another, but only if the systems were rather critical in regard to load carrying capabilities.

One advantage exhibited by this present system is its relatively small terminal extension rate ($\dot{\ell}_f$). Such a condition would necessitate a smaller energy expenditure to overcome terminal transients, and bring the final state to rest.

(7). The system described on Fig. III.17, Mode B (210/195.75), represents another limiting situation. This time the limit is in θ_f; now the tether cannot reach an angle $\theta > 195.75^{o}$, from the given θ_o.

The characteristics for this case are:

I.C.: $\ell_o = 0$, $\theta_o = 210^{o}$, $\dot{\ell}_o = 22.76$ f/s (6.94 m/s),

T.C.: $\ell_f = 10^4$ ft, $\theta_f = 195.75^{o}$, $\dot{\ell}_f = 0.19$ f/s (0.058 m/s), $\dot{\theta}_f = 0$,

t (time, ℓ_o to ℓ_f) = 3190 sec.,

$F/\tilde{m}$ (specific tension) = 0.0398 f/s^2 (0.0121 m/s^2),

t_s (time of pendulous motion) $\cong$ 1340 sec.

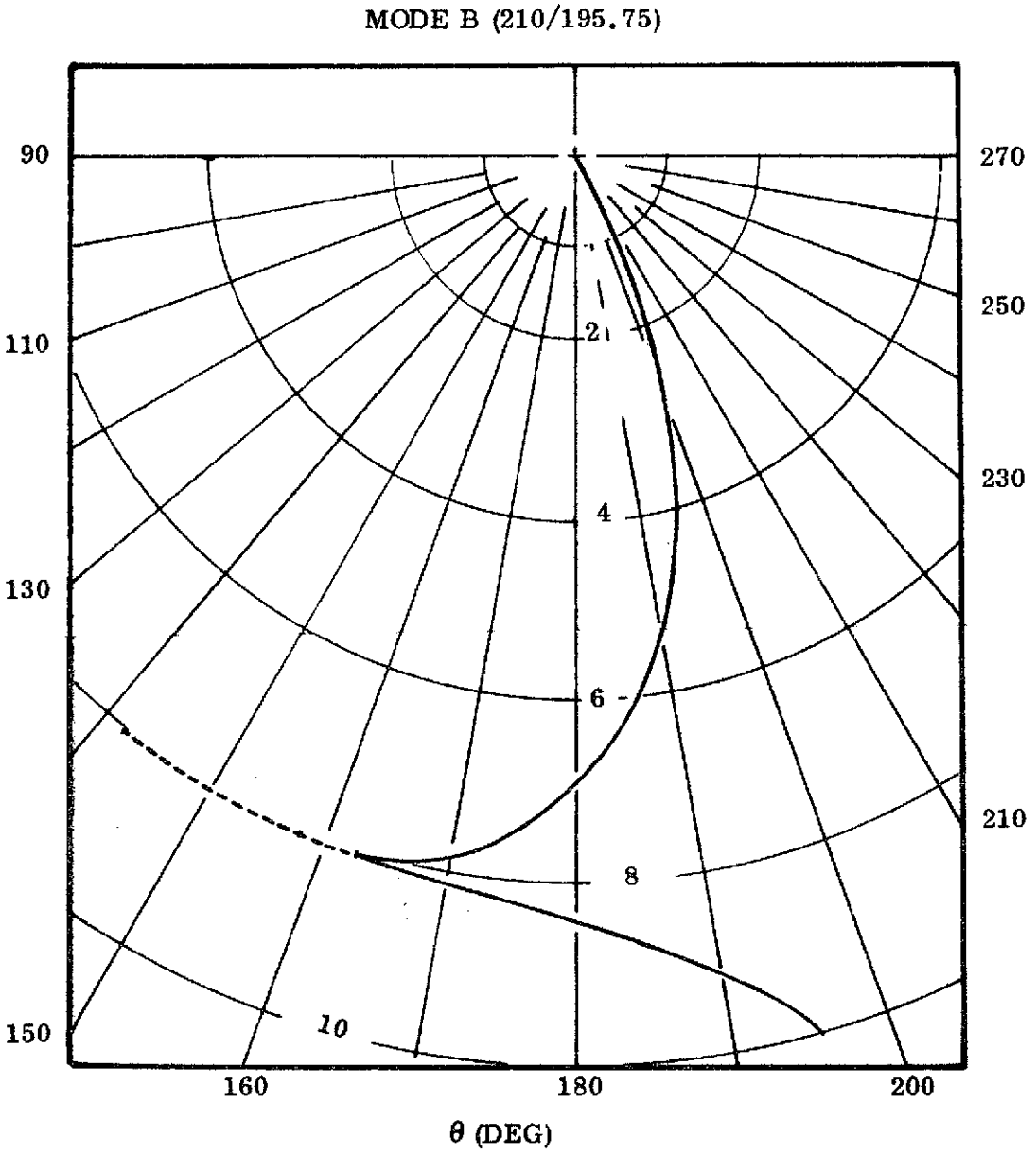

Fig. III.17. A Limiting Case for Mode B Operations. Limit due to θ_f.

From the polar diagram it is noted that the suspended mass reaches a length of 8002 ft. (2439 m) before the snubber engages. This occurs at $\theta \cong 162.5^{o}$. Then the system swings to its amplitude position, $\theta \cong 142^{o}$; from there it swings back to $\theta \cong 157.75^{o}$ where it is returned to the "pay-out" condition. This operation is unusual in that at its terminal state it would require only a very small transient to null it completely. (Incidentally, the tension level here is only about 15% more than that for the limit case, Mode A (155/205.9)).

(8). A rather interesting situation is depicted on Fig. III.18; Mode B (210/160.5), which is a near limiting simulation. What one surmises from an inspection of this graph is that the pendulous action appears to be non-existant. As a matter of fact, that is almost the case; and, for all $\theta < 160.5^{o}$ (approx.) the fixed-length oscillation disappears completely. Consequently, all operational situations whose designations fit into the range, (210/160.5) to (210/127), are free from the Mode B distinction. This means that there will be no distinction between the Mode A and Mode B operations within the classification range noted above.

For this near limit case the system's characteristics are:

I.C.: $\ell_o = 0$, $\theta_o = 210^{o}$, $\dot{\ell}_o = 9.0$ f/s (2.74 m/s),

T.C.: $\ell_f = 10^4$ ft, $\theta_f = 160.5^{o}$, $\dot{\ell}_f = 10.57$ f/s (3.22 m/s), $\dot{\theta}_f = 0$,

t (time, ℓ_o to ℓ_f) = 2718 sec.,

$F/\tilde{m}$ (specific tension) = 0.0118 f/s^2 (0.0036 m/s^2),

t_s (time of pendulous motion) = 42 sec.

For this example the tether reaches a length of 5931 feet (1808 m) before the snubber is activated. During the "first motion phase" m_2 moves from $\theta_o = 210^{o}$ to $\theta = 138.5^{o}$ (its "smallest" θ value), in a time lapse $\Delta t = 1664$ sec. From there to $\theta \cong 138.75^{o}$, the system is in its fixed length oscillation; however,

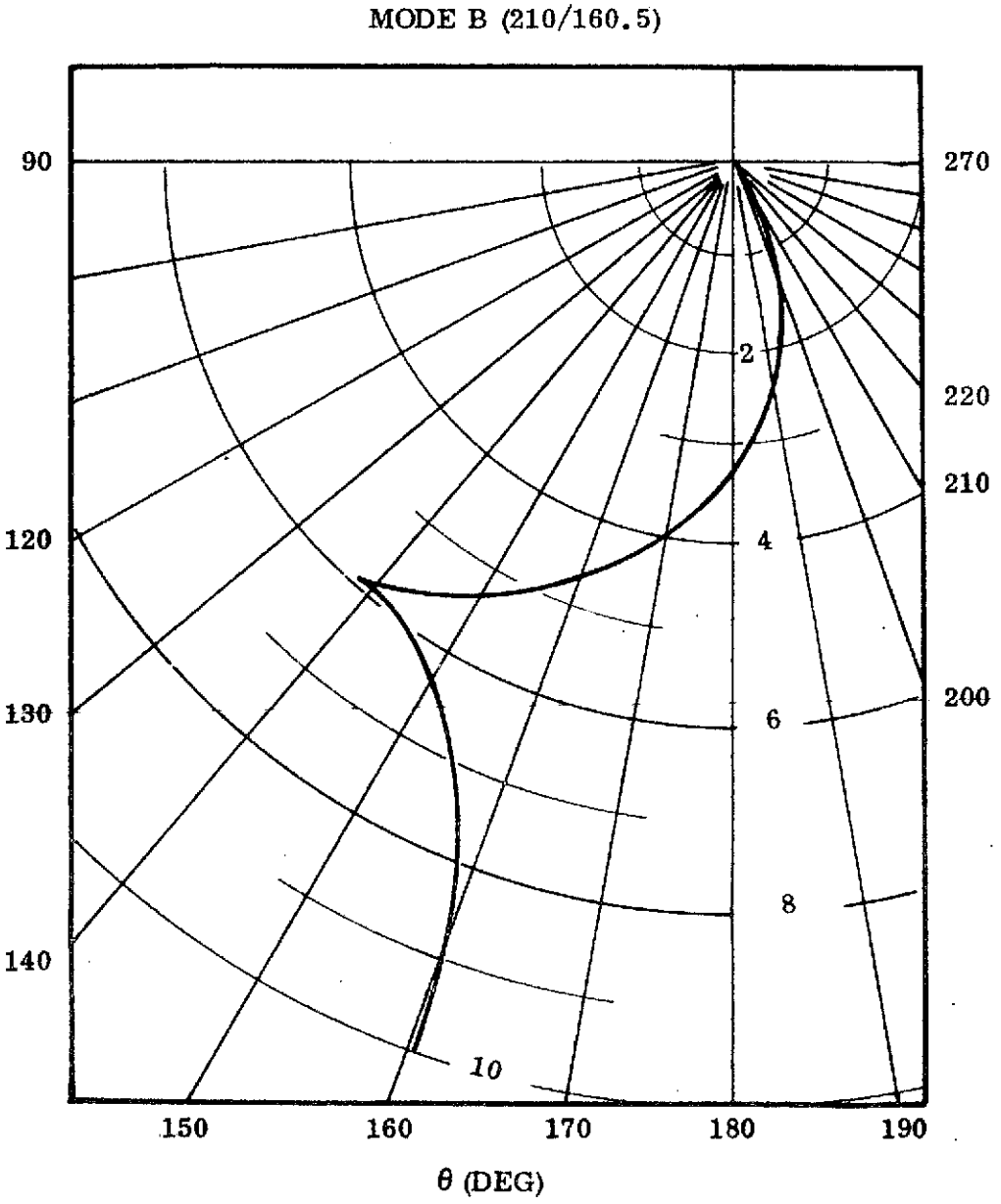

Fig. III.18. A Mode B Constant Tension (with Snubber) Operation. Note that Pendulous Action is almost Non-Existant. For $\theta_f \leq 160^o$ Mode A and Mode B Operations are identical, at $\theta_o = 210^o$.

after that, and to the end of the operation, the system reverts to its "pay-out" condition.

(9). The last example to be described, now, can be simply classed as a Constant Tension mode (either Mode A or Mode B). This duality of classification is used since the system, operating as a Mode B type, would not exhibit the fixed length oscillation. (See Fig. III.19 for a polar plot geometry). This case has been designated as a (225/135) simulation.

This rather peculiar motion trace is accompanied by a plot of $\dot{\ell}$, versus θ, for the example. The numeric scale for $\dot{\ell}$ is the same as that for ℓ; however, the scale values which refer to $\dot{\ell}$ are in f/s directly, while those for ℓ are in 10^3 ft.

For identification, the characteristics for this operation are noted below:

I.C.: $\ell_o = 0$, $\theta_o = 225^o$, $\dot{\ell}_o = 3.82$ f/s (1.164 m/s),

T.C.: $\ell_f = 10^4$ ft, $\theta_f = 135^o$, $\dot{\ell}_f = 9.03$ f/s (2.75 m/s), $\dot{\theta}_f = 0$,

t (time, ℓ_o to ℓ_f) = 3125 sec.,

$F/\tilde{m}$ (specific tension) = 0.00415 f/s^2 (0.00126 m/s^2).

On the figure the dashed line shows $\dot{\ell}$ to diminish initially (to almost 2 f/s, at $\theta \cong 130^o$) from its value at θ_o. Beyond this intermediate position, to the terminus, the pay-out rate increases almost linearly with θ. The $\dot{\ell}$ rate (here) is incrementing at an approximate value of 1.4 f/s per deg.

As an operational description the supported mass is descending, from the $\theta \cong 130^o$ position, in an almost radial direction and at a continually increasing rate. It is rather unusual to note, in comparison with the majority of cases shown, that this system has increased its pay-out speed, instead of decreasing it, at the terminus compared to the initial state value.

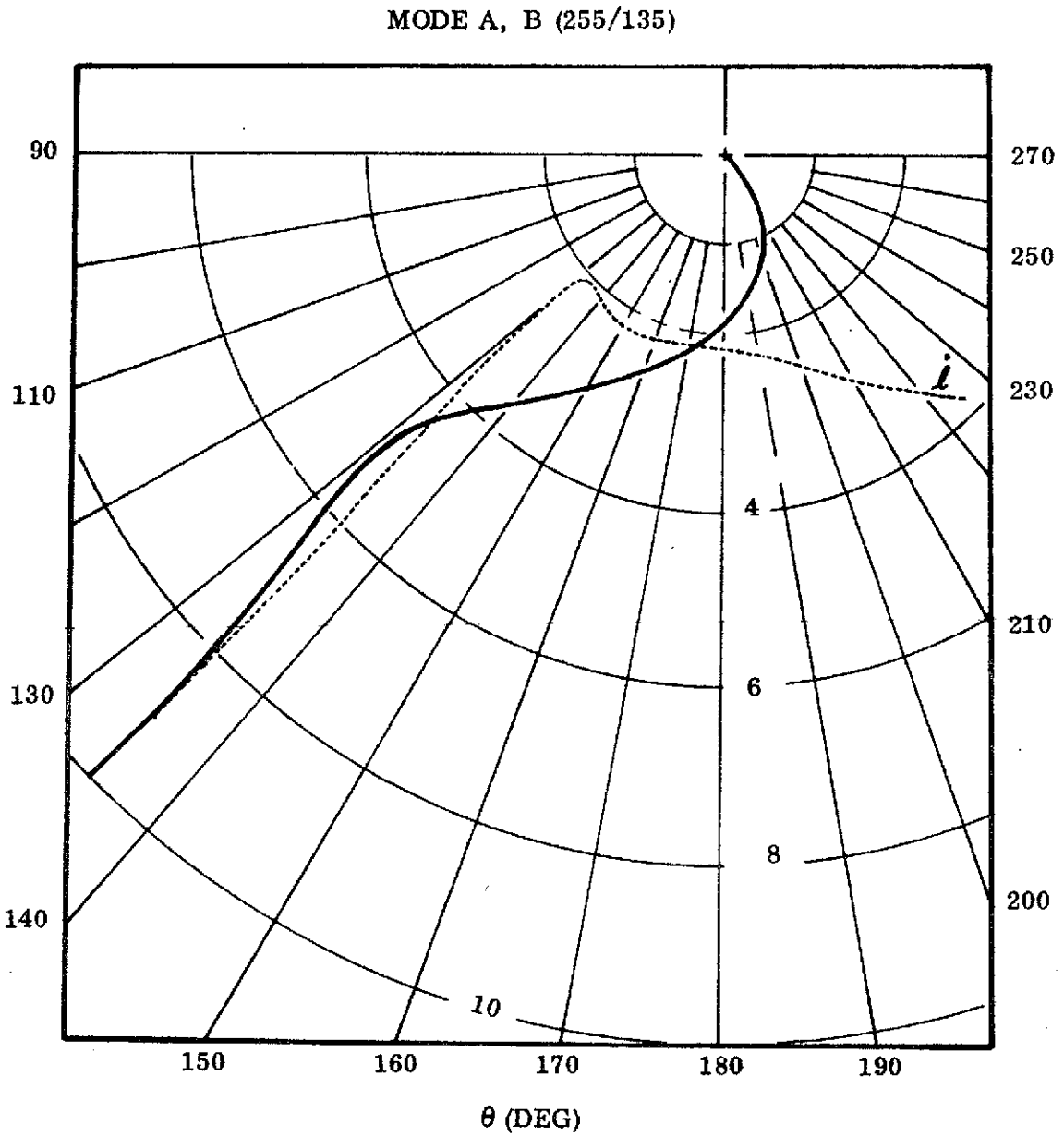

Fig. III.19. A Constant Tension Tether Extension Operation Without Distinction Between Mode A or Mode B Types. Note that both ℓ and $\dot{\ell}$ Traces are Included.

The fact that the tension level is low does, in part, explain the increase in time needed for this maneuver. It is somewhat odd to see the initial behavior for this operation, as compared to the latter half operating characteristics. In relation to the more "usual" case, shown here, this one represents a rather unexpected situation.

III.3.6 Transfer From an Extensible Tether System.

During the development of the computer program, TETHER, it was suggested that some indication of the "transfer" capability for these systems be included in with the various other calculations. In order to describe such a maneuver the program should determine what pericentric radius and speed could be attained, by the suspended particle (m_2), if the tether would be "cut" at any time during its extension. In this regard the motion state, during pay-out, would play the role of "initial values" for the transfer.

The philosophy behind this addition to the calculation output was that the extensible system might be used as a means of re-entering "packages" from an orbiting spacecraft. With the tether serving as the means of acquiring some "lower-than-orbit" altitude, then re-entry might be made to occur (at pericenter) by (say) the added influence of atmospheric drag which would occur there.

To illustrate this capability of the program, Fig. III.20 has been prepared from an example situation. The problem which it describes begins at a circular orbit (r_1) of 4267 statute miles (3706 n.m., or 6867 km). The tethered particle is ejected from the spacecraft (m_1) and allowed to extend to a final tether length of 23.03 st. mi. (20.0 n.m., or 37.06 km) against a constant tension. The initial "direction" for this tether operation is $\theta = 155^{\circ}$; the terminal value is $\theta = 205^{\circ}$; hence this is a Mode A (155/205) operation.

On the graph there are two curves shown; one is a trace for r_2 (the tethered body planetocentric radius) and the other is for r_p (the peri-radius); both are

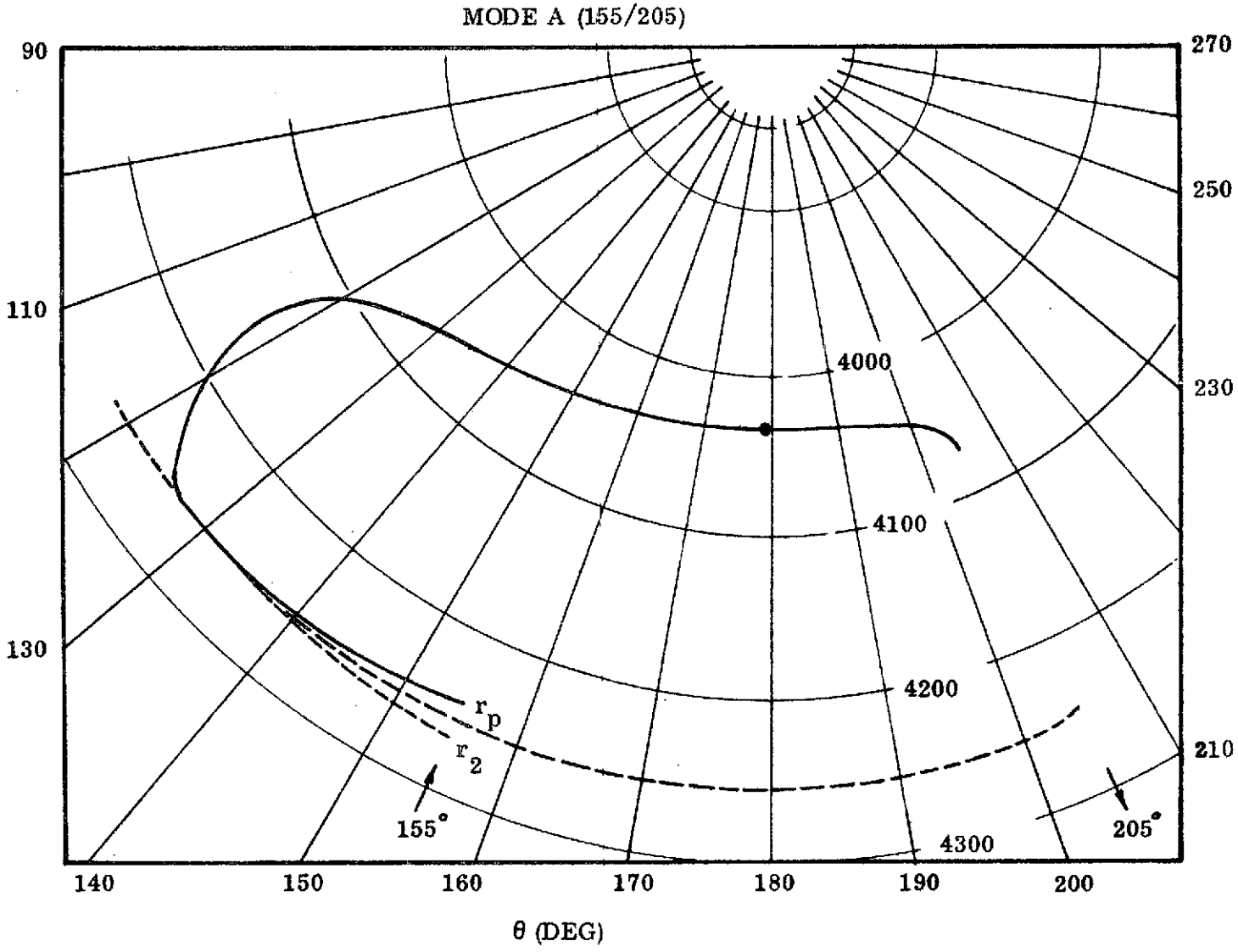

Fig. III.20. Description of Transfers-to-Pericenter Accomodated by Tether Extension Operations. Note: A Lowest Pericenter can be reached from $\theta = 179^{\circ}$, with $\ell \cong 23$ mi. Displacement Scale is in Statute miles.

noted as functions of θ. From the plot it can be seen that the r_2 trace begins at 4267.0 st. mi. ($= r_1$). It descends to roughly 4250 n.m. (at the θ_{min} position $\cong 114^\circ$). From there it swings back toward the $\theta = 205^\circ$ point where the tether has extended to its full length of 23.03 st.mi.

The solid line traced on the figure describes the peri-radius which could be attained from any position (ℓ, θ) during the extension. For instance, if the particle (m_2) would be released from m_1, at its initial state, it could reach a peri-radius of 4240.0 st. mi. However, as the tethered body swings toward $\theta \cong 114^\circ$, the peri-radius rises (to the r_2 orbit altitude, itself). Just before reaching the θ_{min} position the attainable peri-radius begins to decrease, markedly. As the system swings back toward the θ_f position, the peri-radius continues to decrease, but more slowly.

From the computer output it is found that the lowest peri-radius which could be achieved by the tethered particle corresponds to a "release" from the $\theta \cong 179^\circ$ position. From there m_2 would acquire a pericenter whose altitude would be approximately 72 st. mi. (62.5 n.m., or 116.0 km). Beyond this θ position the attainable peri-radius increases, slightly.

For reference, the characteristics of this operation are:

I.C.: $\ell_o = 0$, $\theta_o = 155^\circ$, $\dot{\ell}_o = 331.$ f/s (100.9 m/s),

T.C.: $\ell_f = 23.03$ s.m., $\theta_f = 205^\circ$, $\dot{\ell}_f = 181$ f/s (55.17 m/s), $\dot{\theta}_f = 0$,

$F/\tilde{m} = 0.4995$ lb_f/slug of suspended mass.

The length of tether used here may seem rather large; and, as a consequence, would be of some concern regarding its own weight. To quell any doubts which might arise, it has been conservatively estimated that the "weight penalty" for this tether is most modest. Actually this particular operation would require a tether weight of only 1 pound (or kg) for each 15 pounds (or kg) of transported mass. This is certainly a most modest requirement.

The most obvious advantage of this system is that it is reusable! That is, the tether could be rewound and used over and over again for this same purpose, or for other purposes! Unlike a reaction system (where mass is expelled and lost) this operational device could have an almost limitless lifetime.

It should be evident that this last example is only one of the many possibilities for which tethers could be used in "space operations". Other system applications are to be indicated in the next section; also the imaginative reader can easily visualize many other applications through his mind's eye.

III.3.7 Remarks.

It has been demonstrated that the manipulation and control of tethered systems is both feasible and possible. The next and most impressive step will be that of making use of these ideas in real and practical situations. This task, however, will be left to the systems designer and operations planner.

There does remain the one other mode of operation to be discussed. This one was mentioned earlier when it was described with the analytical developments at the front of this section. In the paragraphs below a more rigorous evaluation of this system -- the variable tension, fixed-θ operation -- will be undertaken.

III.3.8 Variable Tension, Extensible Tether Systems.

The extensible tether method, which is described and discussed in the following paragraphs, will be designated as a "Mode C" operation.

The idea, for this situation, is to produce and maintain an extensible tether mode which can be carried out at a fixed θ angle. It has been demonstrated that such a maneuver is likely to exist since the analytical work described in section III.2.2 did allow a closed form solution to the problem described there. That study was for an in-plane operation (as is this one), but one which utilized equations with some small reductions in the order of magnitude of some terms.

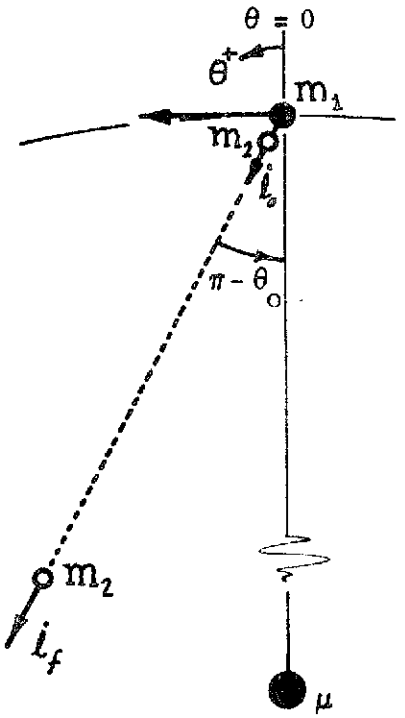

Fig. III.21. Sketch Describing Mode C Extensions.

Here the full Keplerian type equations are manipulated (in the program, TETHER).

As indicated on the sketch, Fig. III.21, this extensible tether simulation is initiated, in its' motion, at (ℓ_o, $\dot{\ell}_o$, θ_o) with $\dot{\theta}_o = 0$. An initial tension $[(F/\tilde{m})_o]$ is to be applied; however, to maintain the the tethered body motion, at the fixed angle, the tension law requires F/m to increase (with ℓ). Correspondingly, $\dot{\ell}$ must increase simultaneously. Theoretically, the extension can be made to continue to any desired ℓ_f, by properly adjusting the pull-back force (tension) in the tether.

In order to determine what "tension law" is needed here, a set of equations were developed (see section F.9, Appendix F). The particular expression defining this tension law is (from eq. (F.21)):

$$\tau = (1 - \Delta^{-3})(\lambda + \cos\theta)\left[1 - \frac{3\sin^2\theta}{4\Delta^5}\right]; \qquad \text{(III.17)*}$$

wherein

$$\tau \equiv \frac{F/\tilde{m}}{r_1\,\dot{\varphi}^2}\,,\quad \lambda \equiv \frac{\ell}{r_1}\,,\quad \Delta \equiv [1 + 2\lambda\cos\theta + \lambda^2]^{1/2}.$$

An evaluation for the specific tension, as a function of λ, should be carried out as an a priori mathematical exercise. Once the "law" is determined, the data could be fitted by (say) a polynomial expression; and, that used as an input to the program. This polynomial must describe the required tension law over the entire

*To complete the set equations used for this problem, the expression for λ', given as eq. (F.19), Appendix F, should be taken into account.

extension range. (From the limited number of case studies made, using the program TETHER, it was found that a reasonable polynomial fit could be obtained using a three term expansion. This would require no more than λ^2-terms in the series. The example cases to follow will demonstrate the particulars of this methodology).

III.3.9 Examples: Fixed θ, Extensible Tethers.

Two sample cases describing Mode C operations are presented in the following discussions. In these the tether system is used to lower a mass (m_2) from an orbiting vehicle which is assumed to be moving along a circular path (r_1).

For the most part the procedure used to establish inputs for these simulations is that outlined above; however, it will be shown that, at least in some instances, the analytical results (section III.2.2) would suffice for this purpose.

For conciseness only two cases, for different orientations (θ), are reported here. Of these, the first will illustrate that the program TETHER could be used to define input quantities which subsequently produce tether operations closely approximating those desired for the problem.

(1). In this simulation the tether operation is classified as, Mode C (150/150).

For this case one input to the computer program will be defined from eq. (III.17); this leads to a tension law (τ) which is needed for the full operation. Other conditions* for this maneuver are selected as follows:

$$\ell_o \equiv 10 \text{ ft. } (3.048 \text{ m}),$$

$$\ell_f \equiv 10010 \text{ ft. } (3051.054 \text{ m}),$$

$$\theta \equiv 150^o \text{ (constant)},$$

and

$$\dot{\varphi} \equiv 10^{-3} \text{ rad/sec.}$$

*The input quantity, $\dot{\ell}_o$, is determined from eq. (F.19), Appendix F.

Subsequently, it was found that an appropriate "tension law" could be formulated as:

$$F/\tilde{m} \equiv (F/\tilde{m})_o + \delta_1 (\ell - \ell_o) + \delta_2 (\ell - \ell_o)^2; \qquad \text{(III.18)*}$$

with

$$(F/m)_o \equiv (0.1828)10^{-4},$$

$$\delta_1 \equiv (0.1828)10^{-5},$$

and

$$\delta_2 \equiv (-0.38)10^{-13}.$$

The output from the computer program yields a time history of the extension (ℓ), and its rate ($\dot{\ell}$), in addition to the other information discussed previously (see, also, Appendix I). Since ℓ and $\dot{\ell}$ are of principal interest here, these quantities are plotted on Fig. III.22 below. In order to account for the full range of values obtained for this example they are plotted on logarithmic scales, as noted. From an inspection of the figure it is apparent that the operation can be simulated as desired; and that the variants do behave as suggested earlier.

Probably it is more evident here than it was in the section on the analytical formulation, that $\dot{\ell}$ has the wide variations which it does. As a matter of fact $\dot{\ell}$ predicts a very slow paying-out of the line during the early stages of the maneuver. Note that, here, it takes roughly 3500 secs. for the line to attain its first 100 ft. (30.48 m) extension. Contrary to this, near the end of the maneuver the line is extending at a more rapid rate. Consequently, it may be desirable to place some length constraints on the system in order not to have the tether unwind too rapidly at some terminal-state conditions.

As a means of comparison the characteristics of this system are listed (below) with companion values from the analytical solution. It should be noted that the mathematical analysis appears able to provide reliable characteristics for this operation, also.

*The program TETHER is designed to accept a polynomial expansion for the tension law. The input parameters needed are the quantities: $(F/\tilde{m})_o$, δ_1 and δ_2.

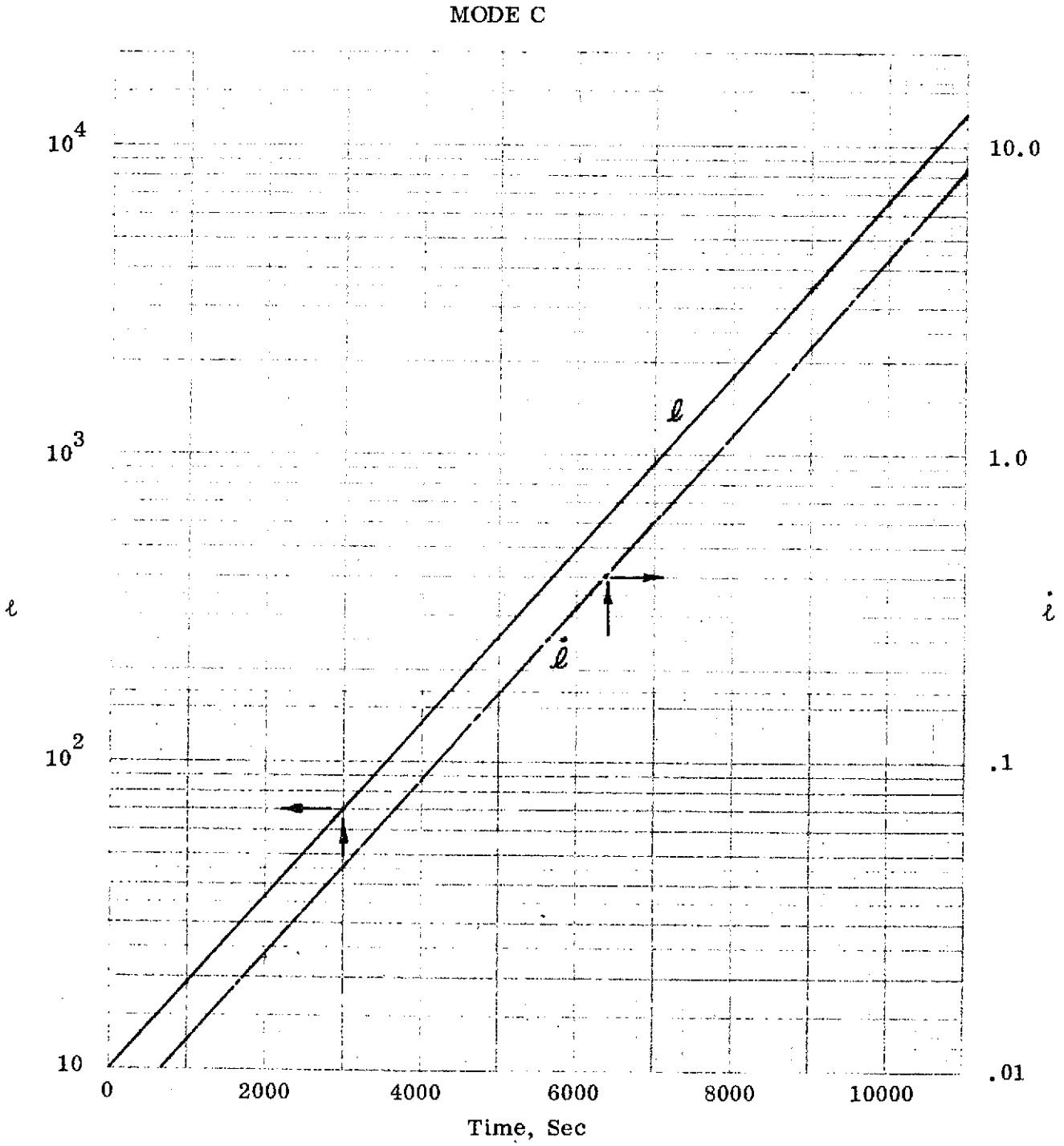

Fig. III.22. A Mode C Variable Tension Tether Extension Operation. Shown is a History of ℓ, $\dot{\ell}$ during an Extension, for a Tether Length of 10^4 feet, with $\theta = 150^\delta$.

Quantity	Numerical Results	Analytical Values
$\dot{\ell}_o$, (f/s)	0.0065	$(0.6495)10^{-2}$
$\dot{\ell}_f$	6.5058	6.5017
t, (sec)	10635.	10637.
$(F/\tilde{m})_o$, (f/s^2)	$(0.1828)10^{-4}$	$(1.82813)10^{-5}$.

(2). The second example is classed as, Mode C (135/135). Here, as in the previous case, the conditions imposed on tether extension, etc. are:

$$\ell_o \equiv 10.\ \text{ft.}\ (3.048\ \text{m}),$$

$$\ell_f \equiv 10010.\ \text{ft.}\ (3051.054\ \text{m}),$$

$$\dot{\varphi} \equiv 10^{-3}\ \text{rad/sec.}$$

In comparison to the previous example this one will be different in that the remaining inputs, for the computer program, are taken directly from the analytical solution. In this regard the output, here, will serve to show the adequacy of the mathematical results to serve as prediction values.

A second part of this sample study uses the program TETHER and its iterator to solve the same problem. It should be remembered that the iterator is employed to obtain a useable set of initial values (for $\dot{\ell}_o$ and $(F/\tilde{m})_o$). In this procedure the iterator used the analytical results as an initial set of values which were subsequently modified and these new values employed as inputs.

The two separate solutions (obtained) are illustrated and compared below, with selected results plotted on Figs. III.23 and III.24. Figure III.23 shows ℓ and $\dot{\ell}$ (for both cases) graphed as functions of time. On the second figure one will find a time history of θ for the two cases. Some comments regarding these figures follow:

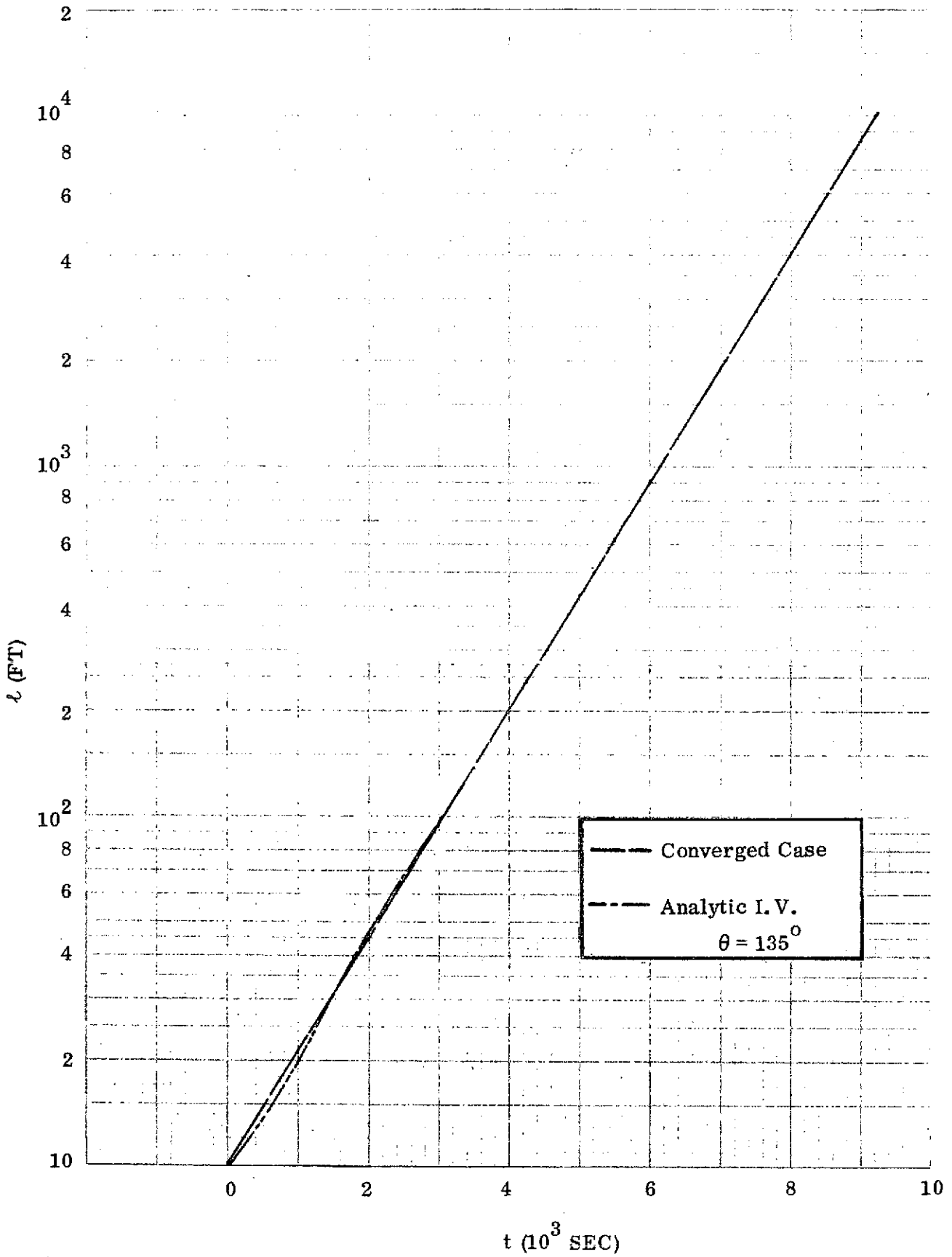

Fig. III.23(a). Comparison of a Mode C Operation, Using Analytic and Iterator Determined (converged case) Initial Values, for a Reel-Out Case.

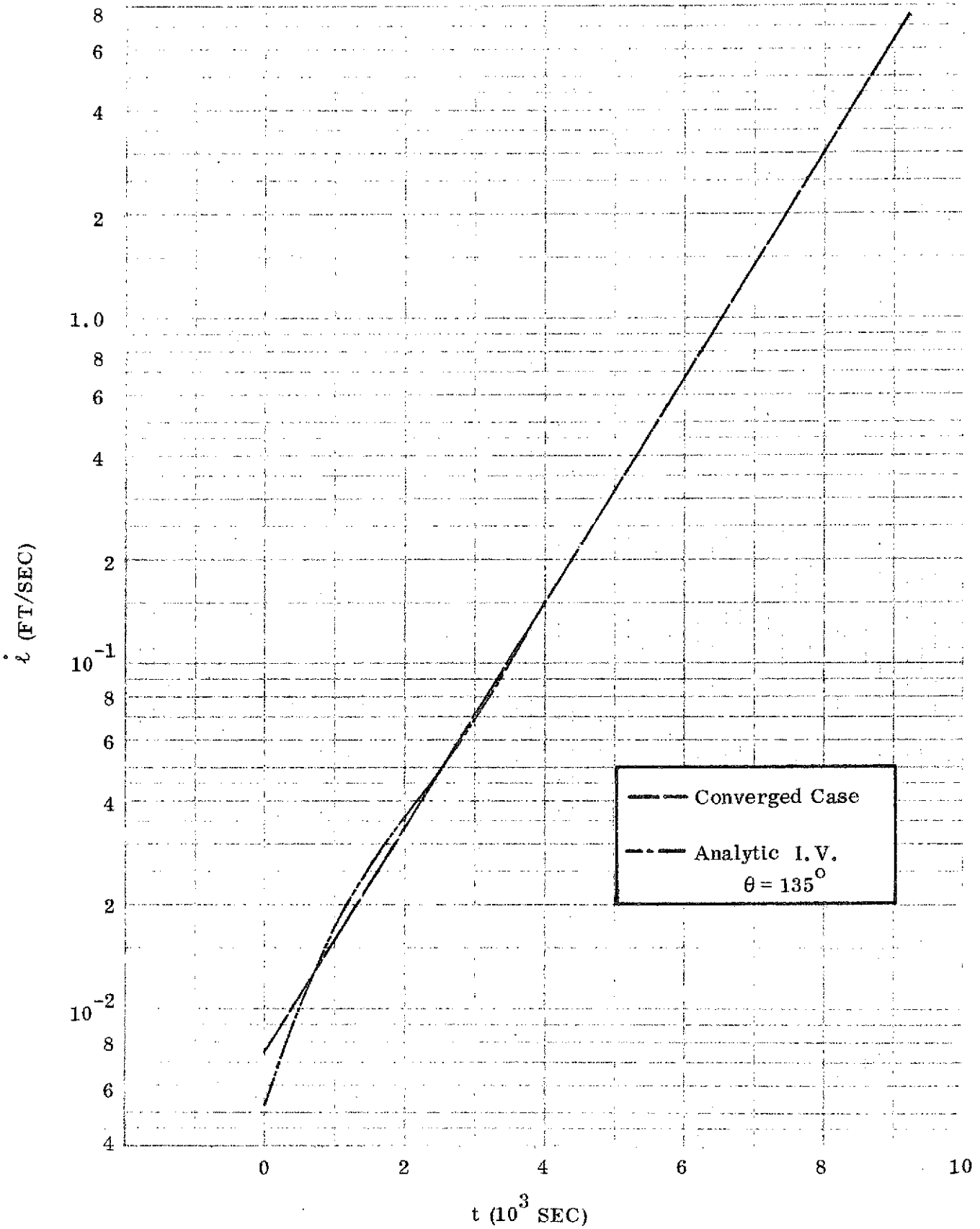

Fig. III.23(b). Comparison of a Mode C Operation, Using Analytic and Iterator Determined (converged case) Initial Values, for a Reel-Out Case.

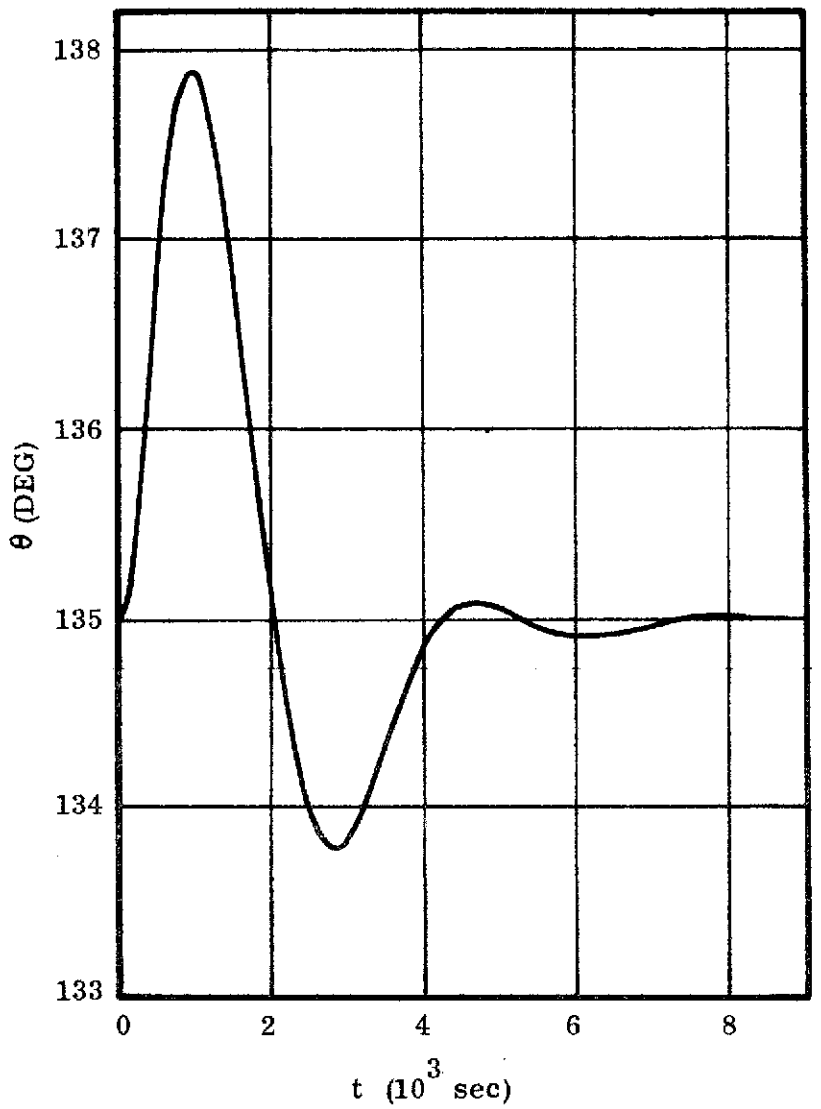

Fig. III.24. Variation in θ, During a Mode C ($\theta \cong 135^{\circ}$) Extension for Iteration Determined (converged case) Initial Values.

On Fig. III.23 it is seen that the "iterated" solution does not have the linearity which the other case exhibits. After inspecting the input parameters it is noted that the iterator has found a set of initial values ($\dot{\ell}_o$ and $(F/\tilde{m})_o$) which are different from the analytical ones. As a consequence the two solutions do not agree except near the terminal state (as they must). It is apparent that the iterator has not found the same solution as the analytical one; or, for that matter, the same one as would be acquired from the procedure in the first example. It is noted, however, that during the latter stages of this maneuver, these two solutions <u>are</u> essentially the same; and they do have essentially the same terminal conditions.

The second graph (Fig. III.24) shows that θ does not remain fixed in value for the iterator solution. During the initial phases of this maneuver θ is seen to vary; but, it does tend to a fixed value as the system approaches the terminus. Interestingly, the solution developed from the analytically defined initial values <u>does</u> retain θ as a fixed quantity; also, those inputs do allow the computed solution to reach a proper terminal state.

In addition to the two graphs just described there is a tabulation of selected data, below. These provide a more precise comparison of inputs and outputs from the numerical analysis, etc. In the tabulation initial and terminal parameters are indicated by (I.C.) and (T.C.), respectively.

	Numerical Results: using		Results from:
Quantity	Iterator Defined Inputs*	Analytically Defined Inputs	Mathematical Expressions
$\dot{\ell}_o$ (I.C.), (f/s)	$(5.267)10^{-3}$	$(7.5)10^{-3}$	$(7.5)10^{-3}$
$\dot{\ell}_f$ (T.C.), (f/s)	7.508	7.509	7.508
t, (sec)	9209.	9211.04	9211.67
$(F/\tilde{m})_o$ (f/s^2)	$(8.276)10^{-6}$	$(9.375)10^{-6}$	$(9.375)10^{-6}$
δ_1, δ_2	$0.9375\,(10^{-6})$, 0	$0.9375\,(10^{-6})$, 0	
θ_o (I.C.)(deg)	135	135	135
θ_f (T.C.)(deg)	135	135	135

*$\dot{\ell}_o$ and $(F/\tilde{m})_o$ values are determined by the iterator (where applicable).

Studying this tabulation it appears that the program TETHER can generate a solution which is close to that one acquired from the mathematically determined tension law. However, indications are that these two analyses may differ slightly as to how the terminal state is reached. It is not clear that the deviations seen here are typical; unfortunately there have not been sufficient numbers of cases studied to reach a more definitive conclusion.

One can conclude, however, that the iterator may achieve more than one solution (type) for a given problem. This is apparent when it is recognized that solutions, for both Mode A and Mode C operations, may exist with identical terminal states. (This is not surprising since the two modes differ primarily in the structure of the tension laws used). In addition, the time required for each mode type solution to reach the prescribed end conditions is markedly different. To a large extent, then, these solutions typify "fast" and "slow" tether extensions, respectively.

The case studies described above have all considered tether extensions exclusively; none of the examples represented a "reeling-in" maneuver. This is not to be construed as an indication that "wind-up" operations are not apparent, or important. One should remember that the two situations differ only slightly, in formulation. As was noted in discussing the analytical solution, a reel-in operation can be described just as readily as can the reel-out case. The primary difference between them can be explained in terms of the θ-quadrants which accomodate each, plus the obvious physical differences.

By all indications, any of these maneuvering situations can be handled by the computer program; and, certainly the analytical aspects of this problem present no difficulties at all, generally speaking.

One aspect of all these situations which remain unanswered, still, is the question of sensitivity. It can only be guessed as how the solutions might behave with regard to any and all input state conditions which may be applied. In

particular, it appears that simulations close to the region of $\theta = k(\pi/2)$ may present some difficulties with regard to sensitivity. However, it will be necessary to examine those situations carefully before explicit statements are made.

The next topic to be discussed is concerned with a means of representing the several tether operations in a universal format. The advantage of such a scheme is obvious in that all operational solutions, of a given type, can be represented by (say) a single set of parameters. Incidentally, the universal description of the results will be by derived graphs - the methodology for this is to be described below.

III.3.10 A Universal Representation for Tether Operations.

In this subsection it is shown that a single curve can represent a full family of solutions for either the Mode A or Mode B operations*. With this information one can immediately predict the behavior of tethered operations for a large variety of possible terminal and initial conditions. Also, as a natural consequence of this scheme, operational limits for each modal family of solutions are defined.

For the situations which will be shown and discussed below the problem types have been limited to those having in-plane motions; and, for extendible tethers. There is no reason to expect that examples having small normal displacements, and/or "wind-up" tethers could not be represented by a same idea.

(a) Dimensionless Quantities.

In representing each mode type there will be a set of defined, dimensionless quantities used. These numbers are typical to each operation; but they represent an entire class of simulations, simultaneously.

*Mode C operations are not included here since in the discussion of analytic solutions, a universal representation was found. That representation can be shown to be equivalent to the present one, in general.

The principal parameters used to describe the characteristics of a given system are obtained from the analysis carried out in section F.8, Appendix F. There the formulation provided the three quantities* (see eq. (F.17)):

$$N_v \equiv \frac{\dot{\ell}_f}{\dot{\ell}_o} ,$$

$$N_\ell \equiv \frac{\ell_f \dot{\varphi}}{\dot{\ell}_o} ,$$

and

$$N_f \equiv \frac{(F/\tilde{m})\,\ell_f}{\dot{\ell}_o^{\,2}} . \qquad \text{(III.19)}$$

These parameters (N_j) are dimensionless quantities describing, (1) the tether pay-out rates (N_v); (2) tether length (N_ℓ); and, (3) specific tension (N_f). In addition to the above, it is possible to define a dimensionless time parameter:

$$R_t \equiv \frac{\ell_f \dot{\varphi}}{\varphi \dot{\ell}_o} = \frac{N_\ell}{\varphi} . \qquad \text{(III.20)}$$

This ratio quantity has a different notational character because it was <u>not</u> mathematically derived; instead it is a physically defined parameter.

It is recalled that the Mode B systems are distinctive in that they contain a fixed-length, pendulous-motion not typical to Mode A operations. In order to represent these actions, by a dimensionless parameter, one can "borrow" from the definition (N_ℓ) and, consequently, define a new ratio parameter,

$$R_{sw} \equiv \frac{\ell_{swing} \dot{\varphi}}{\dot{\ell}_o} . \qquad \text{(III.21)}$$

Herein "ℓ_{swing}" refers to the tether length for the pendulous motion, per se; the remaining quantities have been defined earlier.

*A similar representation is found in reference [17]. In the reference it appears that some discrepancy exists in one of the parameters defined there. This gives rise to a question regarding the universality of that scheme. The parameters defined here do fit the concept of a generalized representation.

(b). Graphs for the Universal Representation.

Figures describing the variations in the dimensionless numbers (N_j) and ratios (R_j) have been plotted. Each graph is for a particular operational type (Mode A or Mode B) and for an applicable range of orientation angles, θ. For precise identification and discussion, each of these will be noted separately in the next few paragraphs.

(1). Figure III.25 represents operations of the Mode A (xxx/180) type. On that graph the dimensionless quantities describing that system are plotted as functions of θ_o (the initial orientation angle for the tether). For reference purposes, the applicable range shown by the abscissa is, $150^o \leq \theta_o \leq 281^o$. Consequently, for θ_o values outside of this range the tether system "fails" in agreement with some one or more of the criteria set down in section III.3.4.

The curves shown here were plotted using data obtained from computer runs of the program TETHER. Some of those same cases are represented by the plots discussed in section III.3.5.

The first figure describes all extensible tether operations which would lead to a final state (ℓ_f, $\theta_f = 180^o$; $\dot{\ell}_f$, $\dot{\theta}_f = 0$). Since this is for a Mode A operation, the tether does not have the "snubber" installed. Consequently, the line is free to unwind (and rewind) as it extends and "lowers" the suspended mass. (Recall that ℓ_f, θ_f, $\dot{\theta}_f$ are assigned state values, but that $\dot{\ell}_f$ is obtained from the operation itself).

(2). Figure III.26 is analogous to what is depicted on Fig. III.25 except that it is for a Mode B (xxx/180) operation. Here, the system has the "snubber" incorporated to disallow any intermediate "wind-up" of the line during the extension maneuver.

An inspection of the figure shows that the operational range, subject to the fail criteria described for these systems, is $155^o \leq \theta_o \leq 247^o$. (As before,

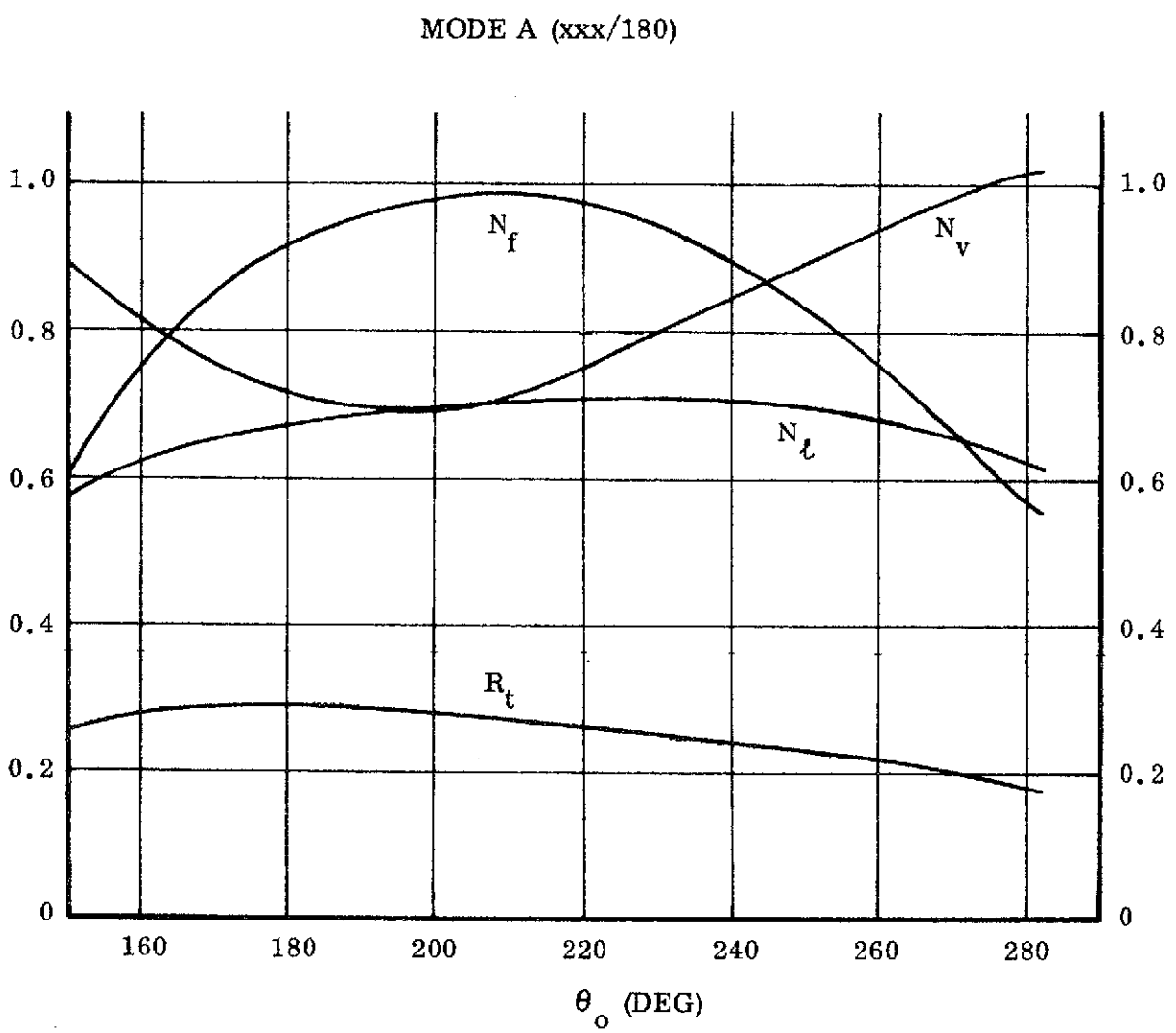

Fig. III.25. Mapping of Universal Parameters for Mode A Tether Extension Operations, with $\theta_f = 180^o$.

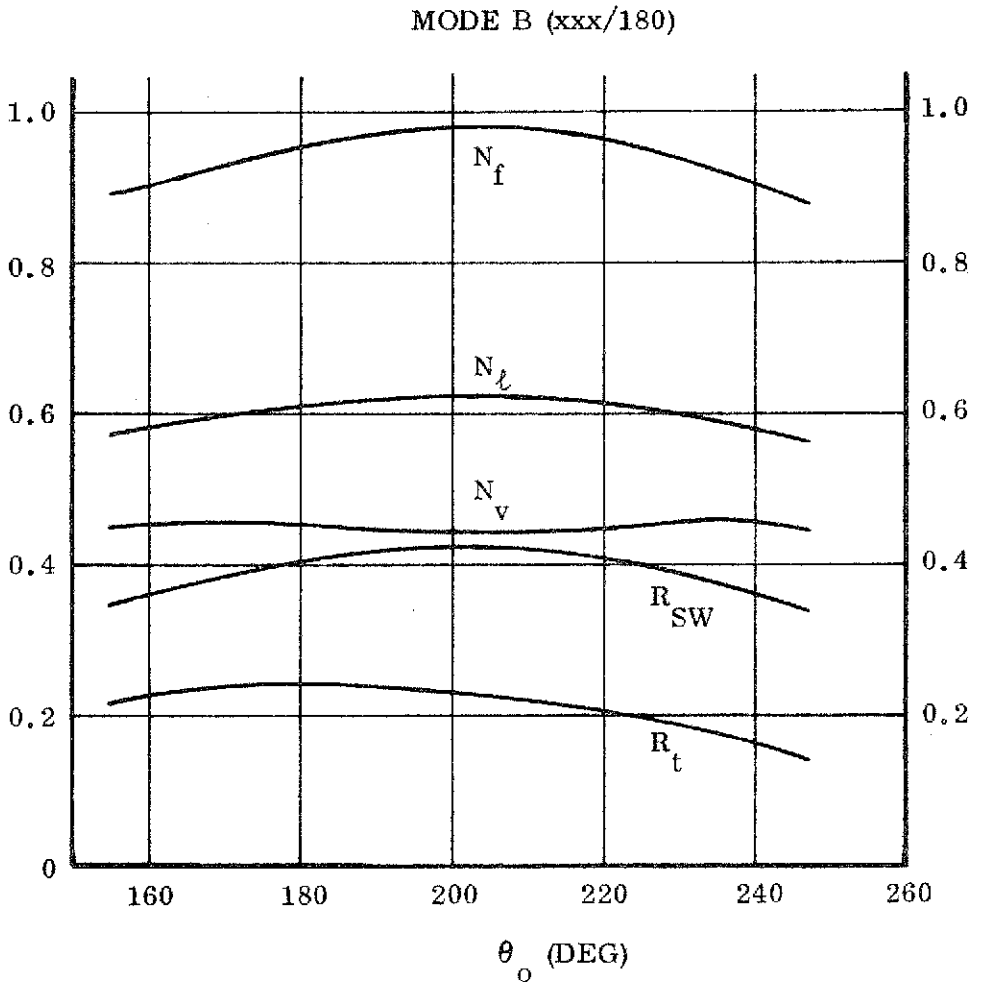

Fig. III.26. Mapping of Universal Parameters for Mode B Tether Extension Operations, with $\theta_f = 180^o$.

all operations are to terminate at a specified ℓ_f, with $\theta_f = 180^o$ and $\dot{\theta}_f = 0$; the value of $\dot{\ell}_f$ is not a prescribed quantity). This graph has, in addition to the curves shown on Fig. III.25, one for the parameters R_{sw} (see eq. III.21). How this figure, and the one above, may be used to predict operational characteristics will be explained subsequently.

(3). On Fig. III.27, parameters describing the Mode A (155/xxx) operations are shown as functions of the terminal orientation angle, θ_f. This graph is akin to that one on Fig. III.25; the principal exception being that here the initial value of θ is fixed. (The one set of values consistent to both plots is that representing the operation, Mode A (155/180)). It is interesting to see that these curves are skewed toward the lower end of the θ_f range. On the companion figure (III.25) the curves were generally symmetric about a median point on the plot. Also, on Fig. III.27, the curves show a small reversal trend at this lower end of the (abscissa) scale. (Note that these maneuvers occur for, $141.25^o \leq \theta_f \leq 205.90$, without "failure").

(4). The operation types depicted as "Mode B(210/xxx)" are found on Fig. III.28. This graph is akin to that one shown on Fig. III.26, except that the terminal angle θ_f is the variable, now. It is seen that maneuvers of this class can be accomodated, without failing, over the range $126^o \leq \theta_f \leq 195.5^o$; a "failure" here, as before, is defined by the same criteria as noted in the subsection above.

Earlier, when discussing the figures showing the geometry of these operations it was mentioned that for some cases Modes A and B were not distinguishable. In particular, the "snubber" is not activated for <u>all</u> Mode B maneuvers. Here this situation is graphically portrayed by a termination of the curve for the parameter R_{sw}. Looking at this figure one sees the snubber operating only in the range, $160.5^o \leq \theta_f \leq 195.5^o$; hence for $\theta_f \leq 160.5^o$ the two modal families are identical (when $\theta_o \equiv 210^o$). The disappearance of a pure

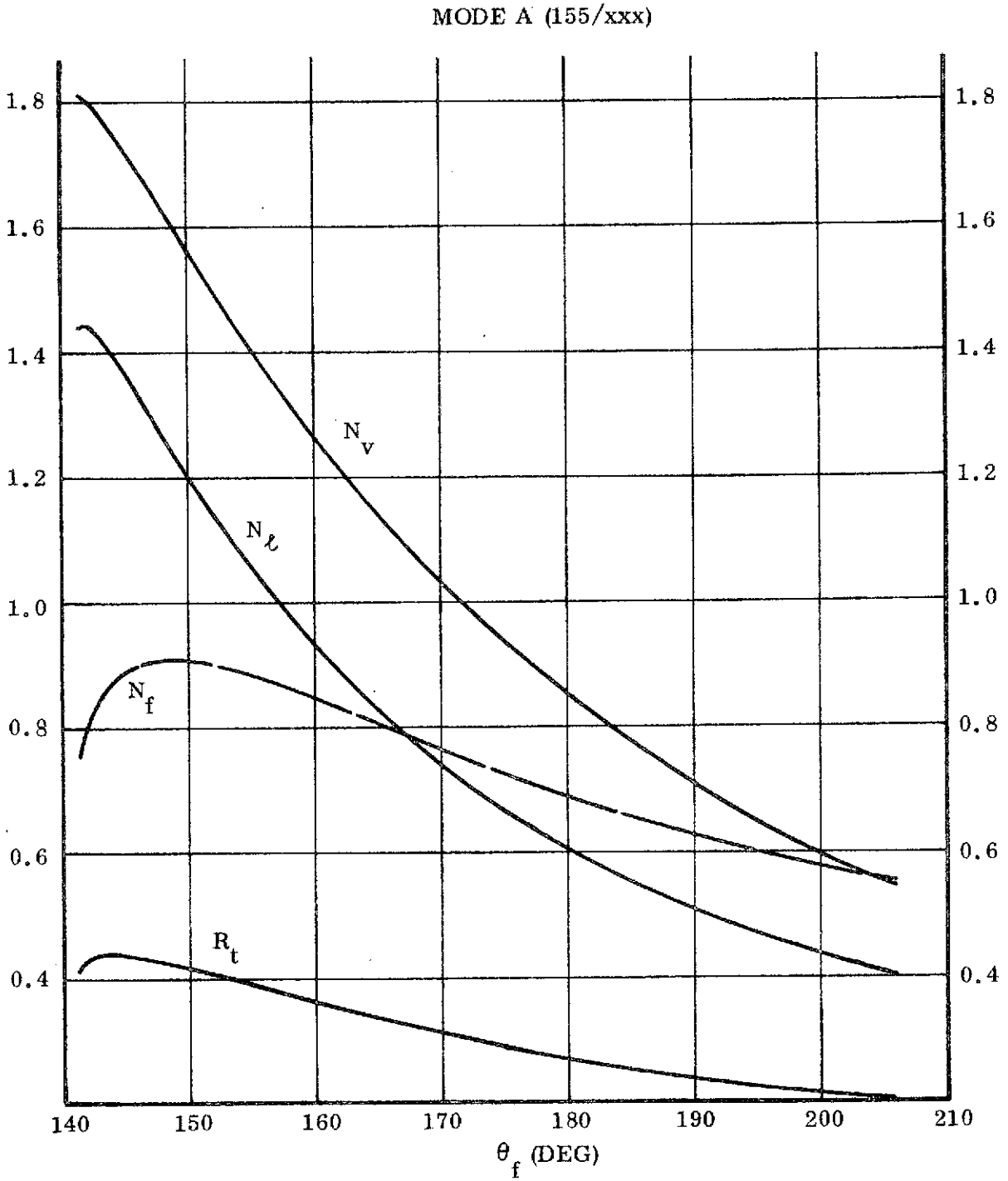

Fig. III.27. Mapping of Universal Parameters for Mode A Extension Operations, with $\theta_o = 155^o$.

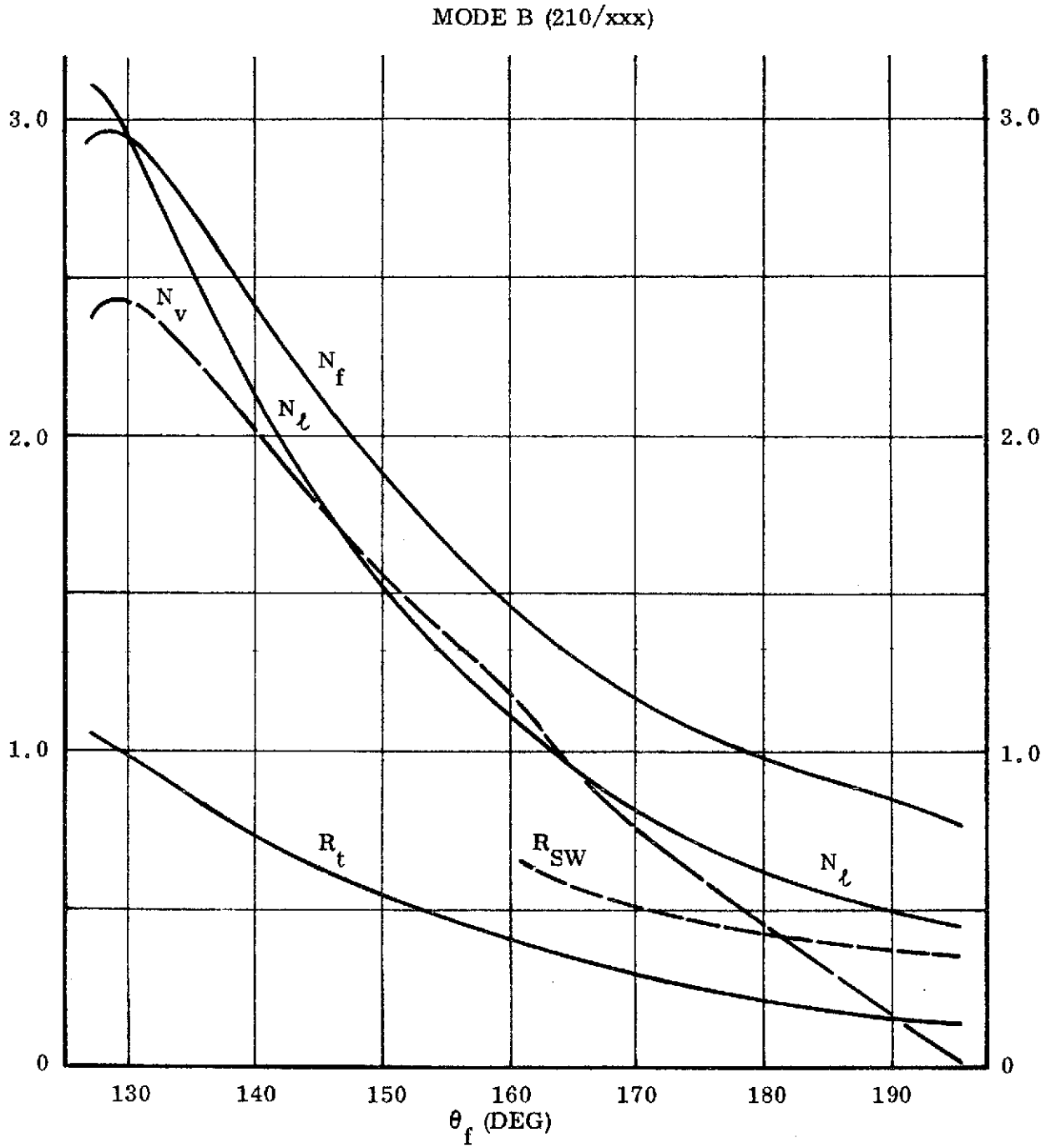

Fig. III.28. Mapping of Universal Parameters for Mode B Extension Operations, with $\theta_o = 210^o$.

pendulous action is also evident (to a lesser degree) on the curve for N_v; there, a marked change in curvature is seen to occur at $\theta \cong 160.5^{o}$. To correlate the data shown on this graph with that on Fig. III.26 one should look at values for the Mode B (210/180) situation.

Here, as on Fig. III.27, the curves are skewed toward the lower end of the θ_f range, with reversals indicated on a part of the data curves there. It is important to recognize that for these present types of operations there is a wider variation in the operating characteristics for these systems, compared to the earlier ones.

(c). Using the Universal Parameter Plots.

Previously it was mentioned that the universal parameter figures could be used to predict characteristics for an extensible tether operation. A procedure to do this will be outlined next. Since all operating situations are in principle, the same, only one example will be discussed.

For the sample case suppose that a Mode B (210/170) operation is to be performed. In this maneuver a tether supported mass (m_2) is to be lowered from a spacecraft (m_1), which is traveling along a circular orbit (r_1). Particle m_2 is let down to a final tether length (ℓ_f) "below" the main vehicle. In this operation the action commences with m_2 leaving m_1 along a line oriented at ($\theta =$) 210^{o}. The final position for m_2 is described by $\theta = 170^{o}$ (θ is measured from the local vertical).

Suppose that the circular orbit (r_1) is at an altitude where $\dot{\varphi} = (0.5)10^{-3}$ r/s. If the tether line is to extend to $\ell_f = (1.0)10^{4}$ m.; and the terminal conditions are such that $\dot{\theta}_f = 0$, when $\theta_f = 170^{o}$, then calculations may be carried out in the following sequence:

(1). From Fig. III.28, read:

$$N_{\ell} = 0.8068; \qquad N_{v} = 0.7542;$$

$$N_{f} = 1.163; \qquad R_{t} = 0.2945;$$

and $R_{sw} = 0.5087.$

(2). Determine $\dot{\ell}_{o}$ from N_{ℓ}; i.e.,

$$\dot{\ell}_{o} \equiv \frac{\ell_{f}\dot{\varphi}}{N_{\ell}} = \frac{[(1.0)10^{4}][(0.5)10^{-3}]}{0.8068} ,$$

or $\dot{\ell}_{o} = 6.1973$ m/s.

(3). Next, describe $F/\tilde{m}$ (a constant) from N_{f}; that is,

$$F/\tilde{m} \equiv \frac{N_{f}\dot{\ell}_{o}^{2}}{\ell_{f}} = \frac{1.163\ (6.1973)^{2}}{10^{4}} ,$$

or $F/\tilde{m}\ (\cong F/m_{2}) = 0.00447\ m/s^{2}.$

These calculations provide sufficient information to initiate the desired maneuver. In order to ascertain how long the operation will take; and to find out how the pendulous motion proceeds - as well as determining ℓ_{f} -- the procedure continues as shown below.

(4). To describe $\dot{\ell}_{f}$, use the definition of N_{v}; hence,

$$\dot{\ell}_{f} \equiv N_{v}\dot{\ell}_{o} = 0.7542\ (6.1973),$$

so $\dot{\ell}_{f} = 4.674$ m/s.

(5). The time needed to complete the tether extension is acquired from R_{t}, as:

$$t \equiv \frac{\varphi}{\dot{\varphi}} = \frac{N_{\ell}}{R_{t}\dot{\varphi}} = \left(\frac{0.8068}{0.2945}\right) 2.0\ (10^{3}) = 5479.12 \text{ sec.}$$

(6). The tether length, at the onset of the pendulous action, is;

$$\ell_{swing} \equiv \frac{\dot{\ell}_o R_{sw}}{\dot{\varphi}} = \frac{R_{sw}}{N_\ell}\ell_f = \left(\frac{0.5087}{0.8068}\right)10^4 = 6305.16 \text{ m.}$$

From the time computation it is seen that the main particle (m_1) travels roughly 0.436 orbits during the period when the tether is extending; hence, $\varphi_1 \cong 156.96^\circ$. Also, here, it is seen that at snubber activation the tether's fixed length is, $\ell_{sw} \cong 6305.$ m. Finally, at the terminal state ($\theta_f = 170^\circ$, $\dot{\theta}_f = 0$) the tether's extension rate is ($\dot{\ell}_f$) $\cong 4.67$ meter/sec.

(d). Correlation of Modal Type Maneuvers.

The example above is typical of one use which the engineering designer, and/or operations planner, could find for these universal plots. However, the curves have other uses which may be of significant value in preliminary planning stages. In particular, one application would be in the correlating of mode maneuvers and their characteristics. From this one could ascertain, quickly, the effects of (say) base orbit altitude (or, $\dot{\varphi}$) and tether length (ℓ_f) on a given operation.

As an illustration suppose that it is desired to find the influence of ($\dot{\varphi}$, ℓ_f) on a prescribed situation study. Here, then, Mode type is not of immediate concern, nor is the (θ_o/θ_f) characteristic, at this time. What is essential, and is inferred, is that the mode and operation must be consistent in the comparisons (to follow).

To correlate operations*, consider two hypothetical situations, designated as $(\sim)_a$, $(\sim)_b$. Now, by forming typical ratios (a to b, say) one can ascertain the parametric influence which is sought.

(1). For instance, using the number N_ℓ the initial payout rates may be related to one another by:

*For these correlations, the parameters (N_j, R_j) are assumed identical for the systems compared.

$$\frac{(\dot{\ell}_o)_b}{(\dot{\ell}_o)_a} = \frac{(\ell_f\dot{\varphi})_b}{(\ell_f\dot{\varphi})_a} \quad . \tag{III.22a}$$

(2). Using the dimensionless quantity N_v the terminal payout rates are correlated as:

$$\frac{(\dot{\ell}_f)_b}{(\ell_f)_a} = \frac{(\dot{\ell}_o)_b}{(\dot{\ell}_o)_a} \equiv \frac{(\ell_f\dot{\varphi})_b}{(\ell_f\dot{\varphi})_a} \quad . \tag{III.22b}$$

(3). Making use of N_f it is shown that the (constant) specific tensions are related by:

$$\frac{(F/\tilde{m})_b}{(F/\tilde{m})_a} = \frac{(\ell_f\dot{\varphi}^2)_b}{(\ell_f\dot{\varphi}^2)_a} \quad . \tag{III.22c}$$

(4). As an indicator of the time requirements, for the maneuvers, it is found that this correlation can be given as:

$$\frac{t_b}{t_a} = \frac{\dot{\varphi}_a}{\dot{\varphi}_b} \quad . \tag{III.22d}$$

(5). Lastly, if the maneuver would be one having a fixed-length pendulous motion, which developed during the maneuver, the line lengths for this would be related by:

$$\frac{(\ell_{swing})_b}{(\ell_{swing})_a} = \frac{(\ell_f)_b}{(\ell_f)_a} \quad , \tag{III.22e}$$

(obviously).

From an inspection of eqs. (III.22) it is evident that when a particular operation is to be conducted (from a given orbit ($\dot{\varphi}$ = constant)) then the various maneuvering characteristics are correlated accordingly. Specifically, the extension rates ($\dot{\ell}_o$, $\dot{\ell}_f$), the specific tensions and the pendulous swinging motions

are all related (directly) to the length ratio, $(\ell_f)_b/(\ell_f)_a$, for this situation.

Conversely, when the operations are considered for different altitudes (i.e., for varying $\dot{\varphi}$), but for a same tether length (ℓ_f), the correlations are differently described. Here, the extension rates ($\dot{\ell}_o$, $\dot{\ell}_f$), and the operating times (t), are proportional to the ratio $(\dot{\varphi})_b/(\dot{\varphi})_a$. The tension requirements, however, depend on the square of the $(\dot{\varphi})$ ratio, while the ℓ_{swing} parameters are unaffected.

According to the word descriptions in the paragraph above, the various maneuver characteristics are in a same ratio as the $\dot{\varphi}$ and ℓ_f ratios, respectively. In this regard, for instance, a doubling of tether length (for $\dot{\varphi}$ fixed) would lead to a doubling of the pull back force and the extension rates. Likewise, changing altitudes (varying the base orbits) would similarily alter the maneuver time and extension rates (directly); but, the line tensions are affected as the square of the orbital turning rate $(\dot{\varphi})$ ratio.

Finally, if one would correlate operations for simultaneous changes in both parameters ($\dot{\varphi}$, ℓ_f) it is evident that the operational characteristics are all differently affected (and to the degree indicated in the appropriate equations above).

One reminder here: These correlations have all been described under the supposition that they represent only those maneuvers for a given (specified) Mode type (A, or B) and for a prescribed (θ_o/θ_f) operation. This, one recognizes, is essential to the results above since the correlations are developed using an assumed constancy for the parameters (N_j, R_j).

III.3.11 Remarks.

In agreement with the information presented throughout section III.3, the reader should have a much better understanding of extensible tethered body operating modes; the control of these systems, and their handling requirements.

Generally, from the studies reported here it is evident, now, that a properly designed system can be usefully employed for a variety of space related applications. It has been demonstrated that the control of tethers can be accomplished; and, it is easy to surmise that the "costs" involved for many of these tasks would be quite moderate, in terms of tether weight.

The three operational schemes described and examined in this section, Modes (A, B and C), are sufficiently general to take care of most local transfer situations, which could involve men and/or materials. Having the ability to maintain control and to manipulate tethers it is possible to use these systems for all sorts of extra vehicular tasks where safety and/or transport lines would be needed.

Also, with the ability to represent families of solutions, by means of the universal dimensionless parameters, the task of designing these systems is immensely easier than if one attempted to evaluate each case individually. Of course the results (shown) are by no means complete. In order to describe a complete parametric representation, for these several types of tethered body maneuvers, one would need to produce carpet plots similar to those found herein. In accomplishing these tasks the basic ideas have been set down and the procedures are well enough known now for this work to continue.

One last, but important, remark concerning the universal parametric representations should be made:

As a test on the validity of these concepts and ideas, various spot checks were made, on the systems types, to ascertain whether or not the universality of these data was indeed true. For this the computer program (TETHER) was exercised using, as inputs, information developed from the plots, Figures III.25 through III.28. In some cases the $\dot{\varphi}$ values (orbit altitudes) were varied; in others the tether lengths (ℓ_f) were changed; and, for some few cases both parameters were altered simultaneously. Most of the parameter variations introduced

in this sampling were "moderate"; i.e., their magnitudes were realistic in terms of earth orbiting spacecraft, space stations, etc.

For all of these cases examined it was found that data developed from the program (TETHER), using inputs determined from the dimensionless parameters (N_j, R_j), agreed* to within less than one-half of one percent (as a maximum). In most instances, the characteristics of these systems were found to differ by less than one-quarter of one percent. These checks have given confidence and credence to the method and to its ability to predict behavior for tether applications.

It is apparent that these systems would be very "flexible" insofar as their useage is concerned. In addition, they are more adaptable than "rigid-arm" devices; and, the ability to rewind and reuse the tethers should place them in a most favorable position compared with "reaction devices" used to (say) transfer orbiting masses.

Aside from the fact that extensible tethers are versatile in their application and use, it can be demonstrated that these systems represent only a modest weight penalty. That is, the weight of tether per unit of mass handled by these systems is quite small. For instance, it is known that for low altitude operations a twenty mile tether would only weigh about six percent as much as the mass (weight) it could handle. (In all likelyhood this is a conservative estimate). For most applications, such extensive tether length would not be used, hence the weight requirement for the tether would be almost negligible. In view of the comparative simplicity which tethered body systems possess, it is evident that they represent a concept which should be given very serious consideration in future space operations.

*"Agreement" is for comparisons between iterator developed (TETHER) results, and those determined from the figures.

SOME APPLICATIONS FOR TETHERED BODY SYSTEMS

IV.1 General.

In this section some specific examples, utilizing tethers, will be described and discussed. The applications to be considered here are, first, associated with a gravity gradient stabilized configuration; and, second, those which will make special use of a rotating tethered body system.

For all of these applications the bodies are presumed to be connected by ideal tethers; i.e., lines without mass and with negligible elastic properties. In addition, the entire system is gravitationally attracted by an ideal central mass particle, (μ). Consequently, in the gravity gradient stabilized mode of motion the bodies are radially aligned; and, the two suspended particles are held in position by the tension in the tether.

When the system above is stabilized, the configuration represents a convenient "platform" from which to initiate a transfer maneuver. Also, a particle in this same configuration could be manipulated so it experiences the various "g" levels associated with several different space applications. These are the problem types to be examined in the following paragraphs.

The rotating tether system, mentioned above, suggests a second scheme which can be used to initiate a transfer maneuver. This concept will be compared with the stabilized system (above) to ascertain what advantage, if any, can be gained by introducing a velocity component arising from the tether's rotation.

The sketch, Fig. IV.1, is presented to clarify the notation and geometry pertaining to these examples.

Since the stabilized mode represents an "in-plane" orientation, the to-be-compared "rotating system" will have a like orientation. This is done for both convenience and reality; and follows from the assumptions set down above.

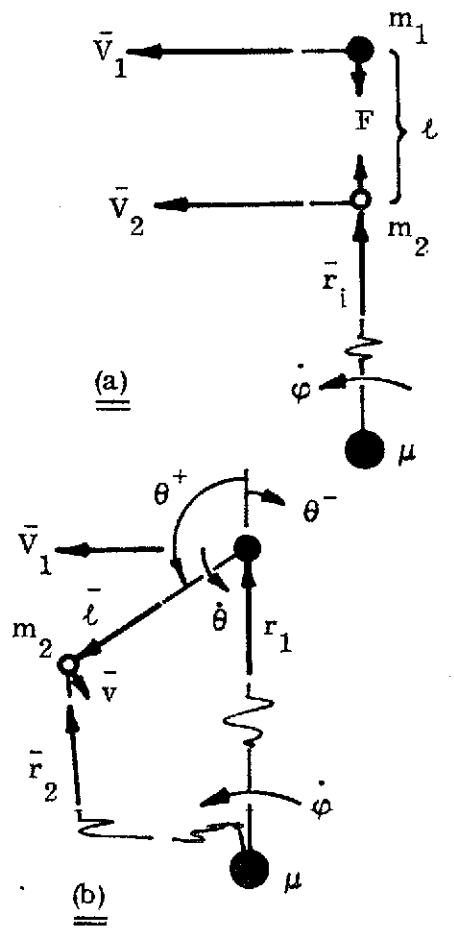

Fig. IV.1. Sketch Describing (a) Stabilized and (b) Rotating Tether Systems.

IV.2 Gee Force Developed in a Stabilized Tether System.

The system shown in Fig. IV.1(a) has been examined to ascertain what levels of force might be produced on the bodies making up that configuration. Since the system is assumed to be stabilized, then both mass particles move at a same rate ($\dot{\varphi}$) about the central mass particle (μ). Also, in this configuration, m_1 and m_2 are radially aligned; hence, there is no pendulous motion to be considered for the tether.

Again, for convenience, it is assumed that $m_1 \gg m_2$, hence the c.g. of the system is located at m_1. Consequently, the c.g. is, now, considered to circulate about μ at the rate $\dot{\varphi} \equiv \dot{\varphi}_1$. In addition, the orbit for m_1 is allowed to be circular; hence, $\dot{\varphi}_1$ and r_1 are a priori, chosen constants for these examples.

The mathematics which is used in describing this example's results is found in Appendix C. The formulation developed there includes the various assumptions noted above, and is specialized for the idea of a stabilized configuration. That is, the position parameters (ℓ, θ) are fixed in value, with $\theta \equiv \pi$.

As an aid in generalizing the results obtained here, the equations have been written in a dimensionless format. In part, the specific tension parameter, $\tau \left(\equiv \dfrac{F/\tilde{m}}{r_1 \dot{\varphi}^2} \right)$, is expressed in terms of the dimensionless tether length,

λ ($\equiv \ell/r_1$). That is, (see eq. (C.10b)) $\tau = \tau(\lambda)$; or,

$$\tau = \frac{\lambda}{1-\lambda}\left[3 + \lambda\left(\frac{\lambda}{1-\lambda}\right)\right] . \tag{IV.1}$$

In this equation the quantity $\lambda/(1-\lambda)$ defines a second length parameter for the problem; namely,

$$\frac{\lambda}{1-\lambda} = \frac{\ell}{r_2} . \tag{IV.2}$$

Equation (IV.1) does not describe the "tether tension" in a form expressing the "gee-level" developed at the suspended particle (m_2). In order to recast τ so that it can be expressed as some multiple of a reference "gee", the expression (above) is modified to become the "specific force" parameter,

$$\tilde{F}_g \equiv \frac{F/m_2}{g_o} . \tag{IV.3}$$

This quantity ($\tilde{F}_g$) is recognized as the specific tension (F/m_2) expressed in ratio to the reference "gee" value (g_o). Since this reference value is related to the radial displacement, r_o, then it can be shown that (see section C.5, Appendix C),

$$\tilde{F}_g \equiv \tau\left(\frac{r_o}{r_1}\right)^2 ;$$

or, making use of eq. (IV.1),

$$\tilde{F}_g = \frac{\lambda}{1-\lambda}\left[3+\lambda\left(\frac{\lambda}{1-\lambda}\right)\right]\left(\frac{r_o}{r_1}\right)^2 . \tag{IV.4}$$

As an example for eq. (IV.4), suppose that r_o is selected to be the average geoid radius for earth, then $\tilde{F}_g$ would represent F/m expressed in "earth gees". (It should be evident that this expression remains a dimensionless quantity; and that it has retained its universal character).

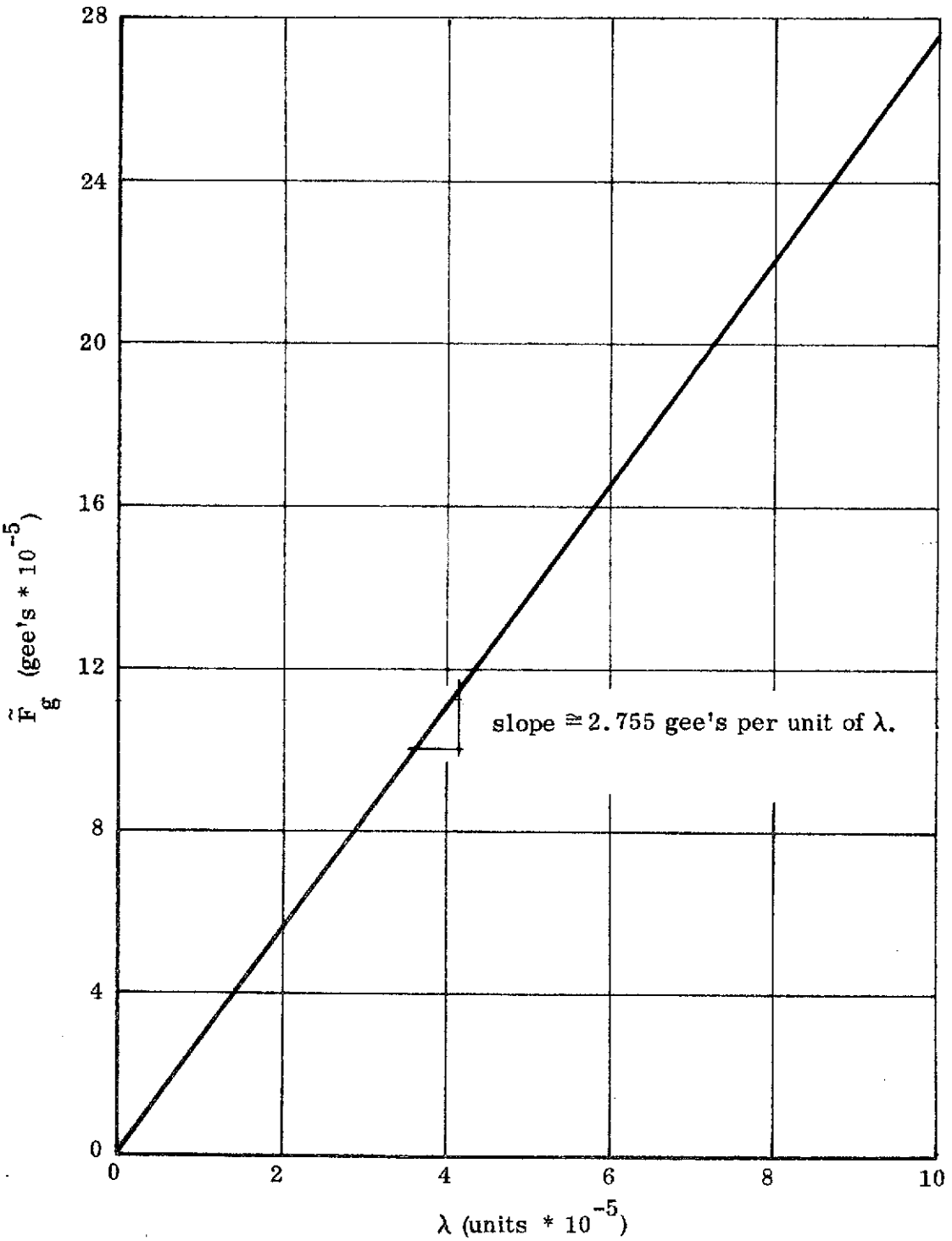

Fig. IV.2. Specific Force (in gee's) Developed on a Tether Suspended Mass, as a Function of Tether Length ($\lambda \equiv \ell/r_1$). Reference Circular Orbit at 150 n.m. Altitude.

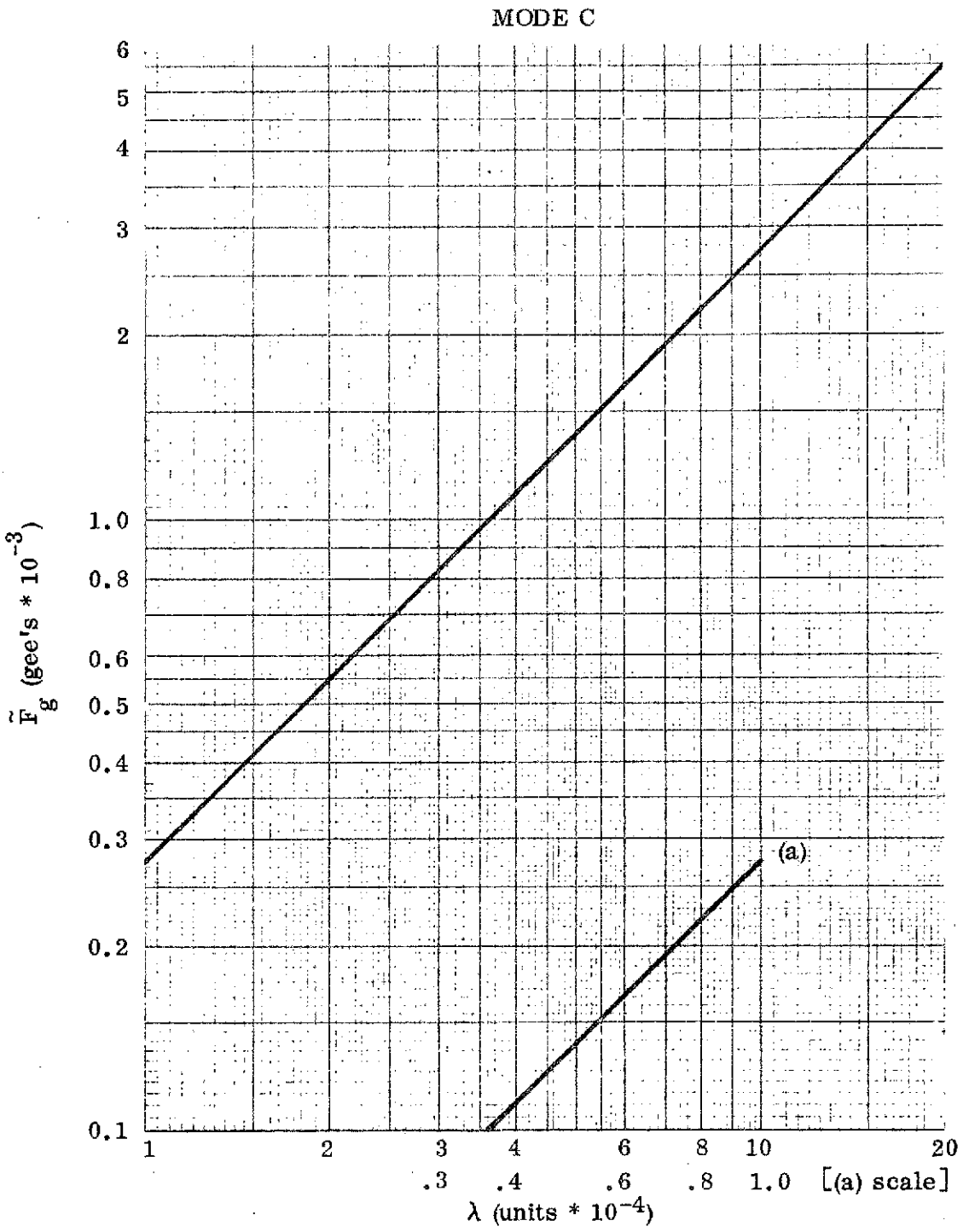

Fig. IV.3. Specific Force (in gee's) Developed on a Mass Suspended by a Stabilized Tether System. Reference orbit at 150 n.m. Altitude.

The above expression for $(\tilde{F}_g)$ is found plotted as a function of λ ($\equiv \ell/r_1$) on Figs. (IV.2, IV.3) below. Note that Fig. (IV.3) is actually an extension of Fig. (IV.2); it encompasses the range $10^{-4} \leq \lambda \leq 2(10^{-3})$. (For purposes of definition a value of "ℓ", the tether length, corresponding to $\lambda = 10^{-4}$ is: $\ell = 2183.664$ ft., when r_1 corresponds to a 150 n.m. orbit altitude. Also, it is seen, from Fig. IV.2, that a tether of this length would allow m_2 to experience a specific force $(\tilde{F}_g)$ of (approximately) 27.55 (10^{-5}) gee's. This level of force is recognized to be a consequence of the "unbalance" provided by the stabilized system; it represents the net difference in centrifugal force and gravitational attraction experienced by m_2 in its stabilized configuration).

Fig. IV.3 extends the $\tilde{F}_g$ (λ) range, shown on the previous graph; also, it overlaps a portion of that graph. (Note the curve (a), on Fig. IV.3, and its corresponding scale).

As an example of these data: From the figure it is seen that a specific force of 10^{-3} gees is developed on a tethered mass having a connecting line ($\lambda \cong .364$) 1.3 n.m. long (this corresponds to a length of approximately 2420. meters).

It should be obvious that these stabilized systems have a potential to develop large variations in the "gee force", acting on a suspended mass for various scientific and other purposes. In the stable configuration small line lengths are associated with very low-gee levels while long lines would simulate more moderate values.

In addition, experiments which require controlled levels of gee, over a range of intensity (but within a realistic variation) could be accomodated by these same tether suspended mass systems. These schemes are conceptually more desirable than others which have been proposed - especially those which have been envisioned to operate in conjunction with rotating space stations.

There, a desired level of "gee" might possibly be no larger than the force variation which would be experienced as a consequence of the rotation itself. Also, it should be mentioned that (now) many operational problems, associated with the locating and stabilizing of such systems, can be overcome if one would take advantage of the control and handling concepts described in the foregoing sections.

IV.3 Transfer From a Stabilized System.

Aside from the applications just discussed, the tether suspended mass system is also ideally situated to initiate a transfer maneuver. In its stabilized configuration the suspended particle is positioned where it could undertake a transfer simply by having the tether "cut", thus detaching the suspended mass.

When this particle is released, it immediately commences the transfer maneuver from (say) an "apocenter", moving toward a new "pericenter". Necessarily this statement supposes that m_2 is released from a position between m_1 and μ.

A mathematical analysis, which is set down in (a part of) Appendix D, considers this same problem and develops the formulae for the characteristics of these transfers. There the developments are directed toward obtaining those equations which describe the transfer parameters, but does so in terms of λ ($\equiv \ell/r_1$).

Of particular interest, here, are the expressions which define the state conditions at pericenter. Recognizing that a converse maneuver (pericenter-to-apocenter transfer, with m_2 released from "outside" of the m_1 orbit) may be of interest, both sets of equations are tabulated in Appendix D.

Table D.I lists several of the orbit parameters for these transfer modes, each given in terms of the dimensionless length (λ). To illustrate these quantities several are noted below (for transfer to a pericenter):

(a). As a description of the "launch" conditions:

$$\left(\frac{r_2}{r_1}\right)_o = \left(\frac{V_2}{V_1}\right)_o = 1 - \lambda, \tag{IV.4}$$

where (r_2, V_2) define the state for m_2, stabilized.

(b). As characteristics of the "transfer path",

(1). The specific momentum, and eccentricity are:

$$\frac{h_2}{h_1} \equiv (1-\lambda)^2, \text{ and } \epsilon_2 = \lambda\,[3\,(1-\lambda) + \lambda^2]. \tag{IV.5}$$

(2). Orbit "size" and transfer time;

$$\frac{a_2}{r_1} = \frac{1-\lambda}{2-(1-\lambda)^3}, \text{ and } \frac{t}{P_1} = \frac{1}{2}\left[\frac{1-\lambda}{1-(1-\lambda)^3}\right]^{3/2}. \tag{IV.6}$$

wherein, P_1 is the period of the reference orbit.

(c). Radius and speed, at the pericenter:

$$\frac{r_{p_2}}{r_1} = \frac{(1-\lambda)^4}{2-(1-\lambda)^3}, \text{ and } \frac{V_{p_2}}{V_1} = \frac{2-(1-\lambda)^3}{(1-\lambda)^2}. \tag{IV.7}$$

(d) The specific tension, in the tether, just prior to release, is determined from:

$$\frac{T}{m_2}\left(\frac{r_1}{V_1^2}\right) = \frac{\lambda}{1-\lambda}\left[3 + \lambda\left(\frac{\lambda}{1-\lambda}\right)\right]. \tag{IV.8}$$

(Note, this last expression is identical, in form, to eq. (IV.1). In all of the above equations $(\sim)_1$ and $(\sim)_2$ refer to particles m_1 and m_2 at their appropriate positions).

In order to show how these quantities vary, with λ, each has been plotted. These data are found on Fig. (IV.4, IV.5), below. On each graph the abscissa (λ)

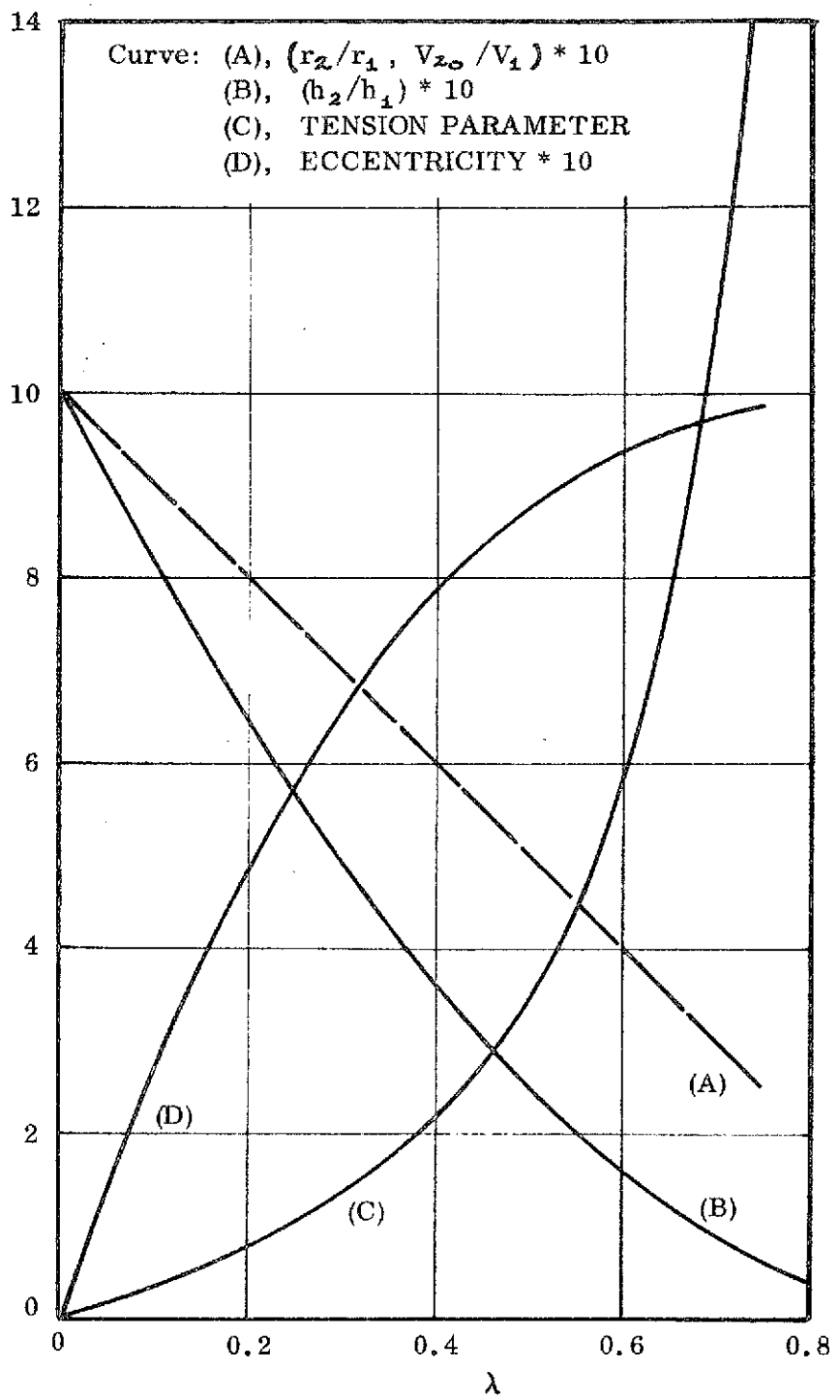

Fig. IV.4. Expected Variations for Parameters Describing a Tether Initiated Transfer. Here the Tension Parameter $\equiv (T/m_2)(r_1/v_1^2)$ with λ ($\equiv \ell/r_1$) the Dimensionless Line Length.

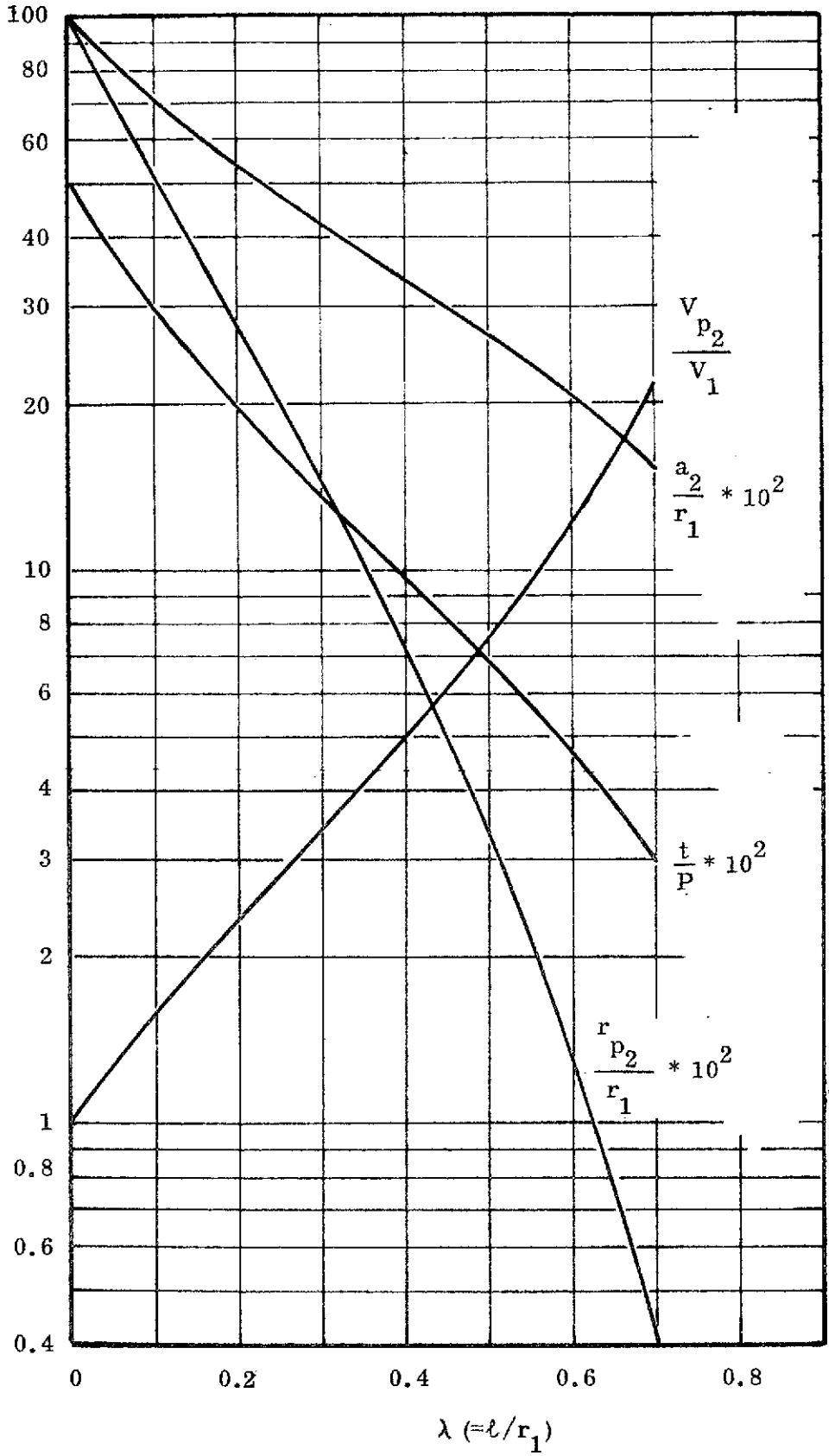

Fig. IV.5. Transfer Parameters for a Mass Released from a Gravity Gradient Stabilized Tether, as a Function of Length (λ).

extends over the range $0 \leq \lambda \leq 0.8$; this is rather extensive in view of the definition ($\lambda \equiv \ell/r_1$). Of course, these graphs are not restricted to any particular altitude range; however, the equations were developed from two-body considerations and have an implied constraint.

The purpose in preparing these figures was to indicate the general behavior of these quantities, and to note any pecularities which they might exhibit. Conversely, the most "applicable region" for these two graphs, insofar as realistic operations are concerned, would be that region adjacent to $\lambda = 0$. There one sees how the plotted parameters might be influenced by "actual" tether lengths. From studying these figures one can determine the relative degree in change, which should be expected for an "extended tether line", in a stabilized tandem configuration. (The reader is cautioned to view each graph rather carefully and to ascertain whether or not a multiplier is implied for each of the curves).

It would seem redundant at this point to undertake any extensive discussions on these curves. Certainly the information shown there is readily understood without additional comment.

IV.3.1 A Comparison Transfer.

The transfer operation, above, will be compared to an equivalent Hohmann maneuver. This particular comparison was selected because the Hohmann transfer is well known, and because its description has a simplicity of representation. The mathematical description of this maneuver is found in section (D.8), Appendix D. For quick reference, the pertinent expressions may be found listed in Table D.II, Appendix D.

A graphic comparison and description of these two transfers operations is found on Figs. (IV.6) and (IV.7). There, one will find, as an example, a transfer, to a 70 n.m. (pericenter) altitude, from circular orbits ranging up to 500 n.m. altitude.

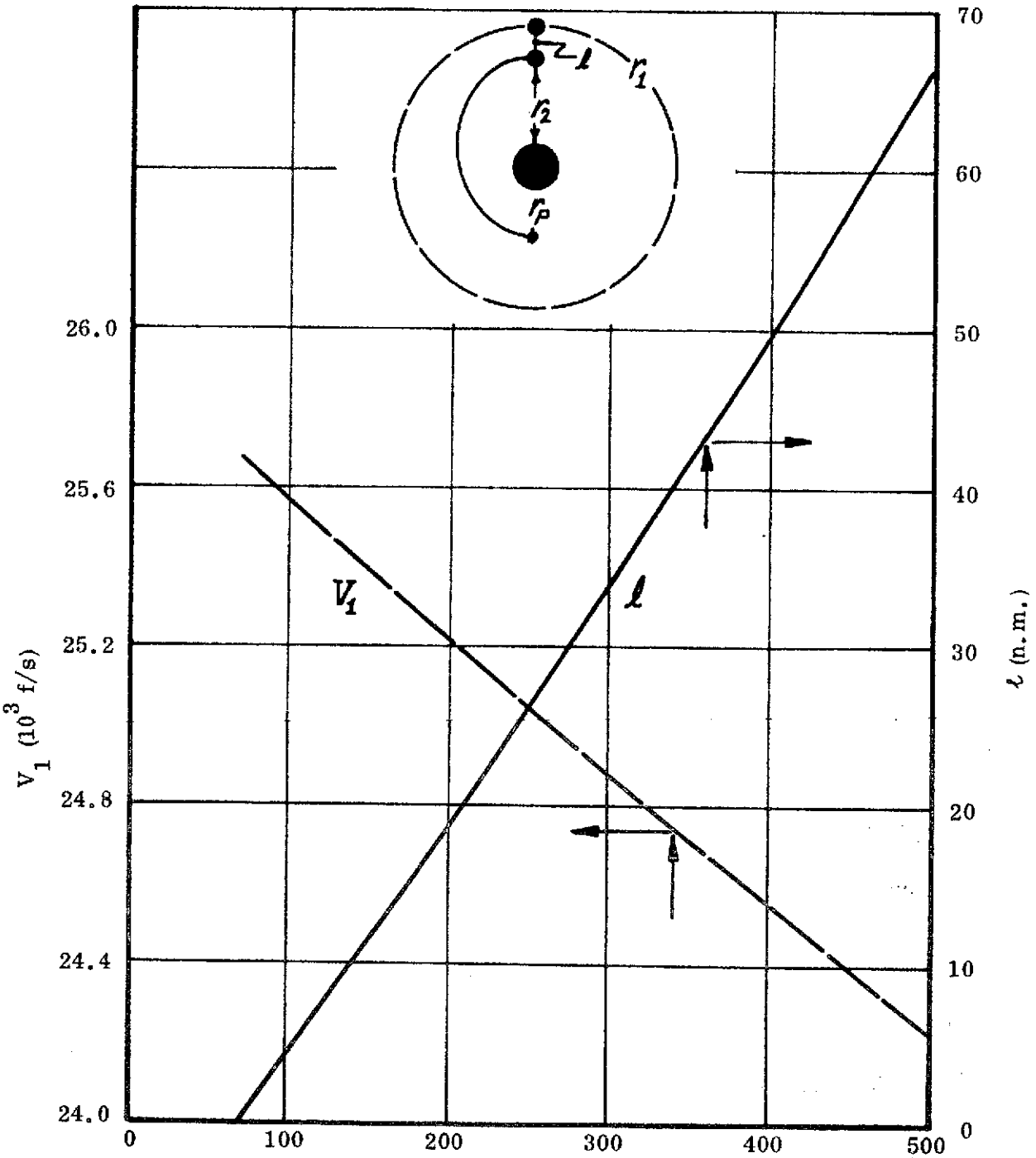

Fig. IV.6. Description of Tether Length (ℓ) Required to Provide Transfers to a 70 n.m. Peri-Center Altitude as a Function of Reference Orbit Altitude, H (n.m.). Also shown is Reference Orbit Speed (V_1, fps) with Altitude (H).

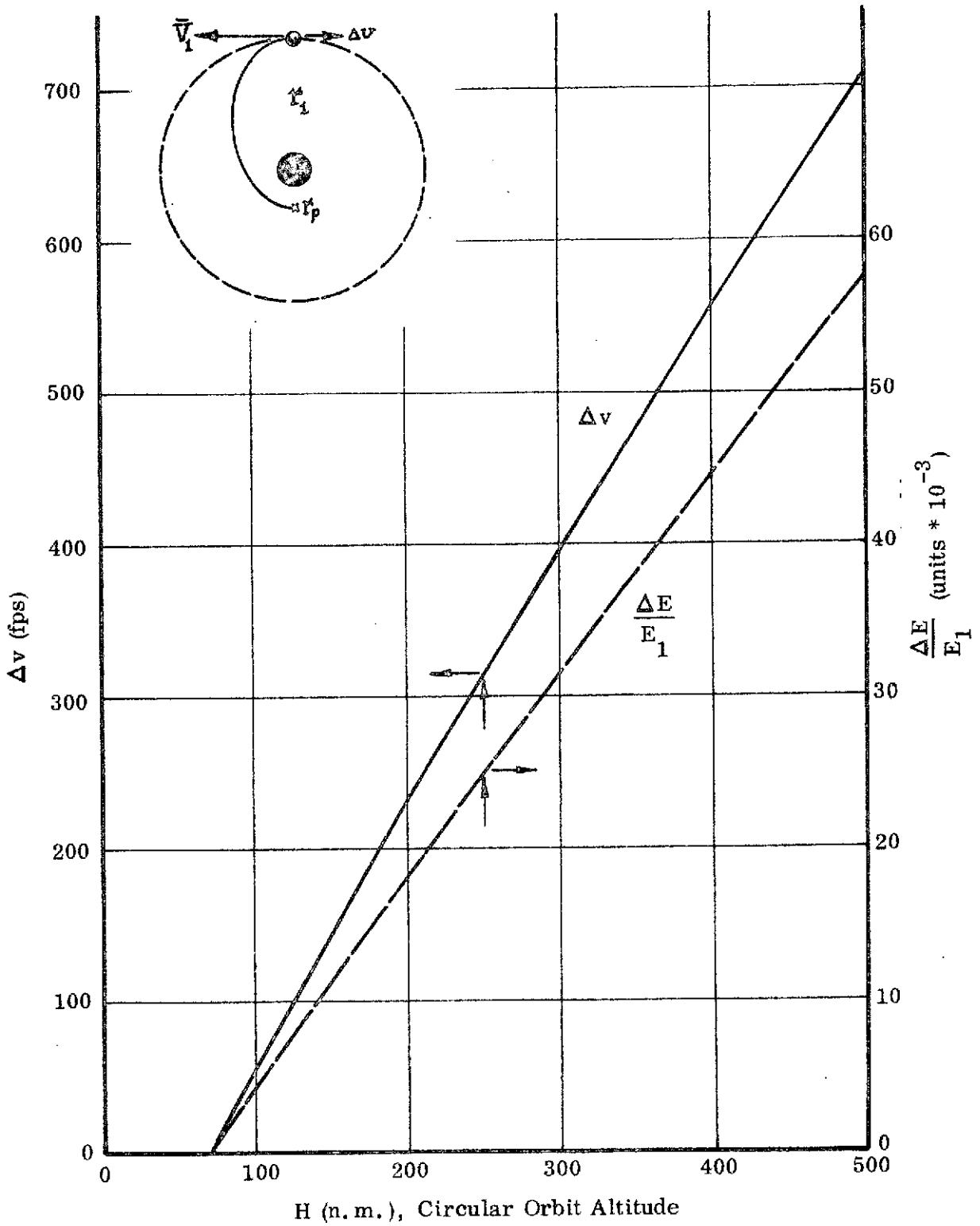

Fig. IV.7. Description of Δv Requirement, and Energy Change (ΔE), for Hohmann Transfers to a 70 n.m. Pericenter Altitude as a Function of Reference Orbit Altitude (H, n.m.).

On Fig. (IV.6) the tether length (ℓ), needed to initiate these transfers, is plotted against the circular orbit altitude (H). Also, on the same figure, the circular orbit speed (V_1, in f/s) is plotted versus the same altitude scale.

To aid in clarifying the information found on this figure consider the following example:

Suppose a particle is suspended from an orbiting spacecraft which is orbiting earth at a 300 n.m. altitude. If the particle is to be transfered to a position 70 n.m. above earth, using a free (ballistic) arc, it would need a tether $\ell \cong 34.1$ n.m. long. In other words, the particle would be released from a gravity-gradient stabilized position 34.1 n.m. "below" the spacecraft; hence its "release altitude" would be (approximately) 265.9 n.m.

Because of its "suspended" position, the particle, at release, would have an "orbiting" speed V_2 ($=(1-\lambda)\, V_1$, see eq. (IV.4)) of 24647. f/s. (Note that from the figure, $V_1 \cong 24873$ f/s; and, by definition, $\lambda \equiv \ell/r_1 \cong .9909$).

From the information plotted on Fig. IV.7, the corresponding Hohmann transfer (from a 300 n.m. circular orbit to the 70 n.m. pericenter) would require a $\Delta v \cong 395.$ f/s. This means that the particle would be "ejected" from the spacecraft, <u>against</u> the orbital motion, at a relative speed of 395. f/s.

Also, as an added bit of information, the specific energy changed (ΔE) needed for this transfer maneuver can be determined from Fig. (IV.7). For this example, one can read, $\Delta E/E_1 \cong 0.032$; and since $E_1 \equiv - V_1^2/2$, with V_1 corresponding to the 300 n.m. (circular orbit) altitude, then it is easy to show that $\Delta E = - 9.898\ (10^6)\ f^2/s^2$.

IV.3.2 <u>Influence of Launch Speed on the Transfer.</u>

The transfer operation just described was initiated from a gravity-gradient stabilized configuration; with ℓ, θ fixed in value, and $\dot{\ell} = \dot{\theta} = 0$. Now, according to the investigations described in section III it is also possible to locate a particle

at a given ℓ, θ position with $\dot{\theta} = 0$, but $\dot{\ell} > 0$! In this case a transfer maneuvers may not necessarily be initiated at the same physical state conditions.

To account for this difference (in $\dot{\ell}$, primarily) the analysis in Appendix D was modified to show the influence of $\dot{\ell}$ on these transfer operations. In that analysis, $\dot{\ell}$ would replace the speed $|\dot{\bar{x}}|$, (this corresponds to a radially directed velocity component). Subsequently, the influence of the parameter on the transfer is demonstrated there. (It should be recognized that these modified maneuvers do not initiate at (say) apocenter, per se, but begins at a location beyond that position (for $\dot{x} < 0$). Correspondingly, the subsequent pericenter's altitude is altered). As an easy reference, illustrating the influence on this "residual velocity", $\dot{\bar{x}}$, a tabulation for several of the transfer quantities is given in Table D.III, Appendix D. The parameters listed in the table are derived in section D.16 of the appendix.

In section D.12 (Appendix D) an equivalent length-of-tether problem is described; and a method of solution is outlined. There, the influence of $\dot{\bar{x}}$, on the transfer maneuver, is converted into an added length of tether. For this representation, the problem is solved to yield that length of line (ℓ_{eq}) which should be provided in order to attain a same pericenter radius, from a (purely) stabilized configuration. Necessarily both of these situations are presumed to be referenced to a same base orbit (i.e., all maneuvers are referred to the same circular, reference orbit, r_1).

To illustrate this equivalence situation, a sample case is outlined below. For this example the reference orbit is assumed to be at an altitude of 300 n.m. From a stabilized tether the test particle (m_2) is released, and should attain a pericenter altitude of about 70 n.m.

Now, in illustrating the influence of $\dot{x}$, several values of λ'_o ($\equiv \dot{x}/V_1$) are assumed; and, the equivalent length of tether (ℓ_{eq}) is determined for each using the scheme described in section D.12, Appendix D.

For this example the base orbit (r_1) is circular; its altitude is 300 n.m.; and, the vehicle (m_1) moves at a speed, V_1 = 24873.06 f/s. The static (stabilized) tether length is chosen as (ℓ_o =) 34.076 n.m. When m_2 is released from this location it reaches a pericenter which has an altitude of (approximately) 70.454 n.m. For several assumed values of $\dot{\ell}$ ($\equiv -\dot{x}$), nondimensionally defined as λ'_o, the added length (of tether, $\Delta\ell$) to reach the same pericenter altitude is calculated. These results are tabulated below:

$\lambda'_o \equiv (\dot{\ell}/V_1)$	Pericenter Alt., H_p (n.m.)	Increment in Tether Length $\Delta\ell$ (ft)
0* (0.0 f/s)	70.454*	0.0*
0.001 (24.87 f/s)	70.38	68.71 (20.94m)
0.002 (49.75 f/s)	70.202	228.01 (69.50m)
0.005 (124.4 f/s)	68.932	1594.23 (485.92m)
0.01 (248.8 f/s)	64.544	5692.22 (1734.99m)
0.02 (497.5 f/s)	48.758	20491.49 (6245.82m)
0.05 (1243.7 f/s)	-26.084**	93349.43 (28452.96m)

* This is the static stabilized tether situation ($\dot{\ell} = 0$).
**A pericenter below earth's surface.

From the table one can see that there is only a small effect on the pericenter (and only a small change in tether length) so long as the "terminal pay-out" rate ($\dot{\ell} \equiv |\dot{\bar{x}}|$) is below, approximately, one percent of orbit speed (V_1). However, corresponding to this added speed, the increment in tether length (to be added to ℓ_o, accounting for the effect of $\dot{\ell}$ in redefining the pericenter) would amount to roughly 2.5 percent of the initial length.

It is equally apparent that the effect of $|\dot{\bar{x}}|$ is not linearly related to $\Delta\ell$ (the added tether length); the tabulated information most vividly exhibits this fact. E.g.; increasing the speed $|\dot{\bar{x}}|$ by a factor of 5 is equivalent to more than a

16 fold increase in added tether length. On the basis of these findings, here, it would seem that an advantage may be had by not nulling the residual speed(s) for many of the extendible tether operations, if a transfer maneuver follows.

IV.4 Transfer from a Rotating Tether System.

Having seen the advantage to be gained by adding a velocity increment to an otherwise stabilized tether system, it is logical to extend this idea, and to consider transfers originating from rotating tethered mass systems. The concept which is to be examined, next, will employ the tether as a device used to induce the velocity increment. Here the tether connected mass (m_2) will be assumed to rotate about the main orbiting particle (m_1) at some prescribed rate ($\dot{\theta}$).

In order not to complicate the analysis it will be assumed that during rotation the tether remains inelastic and has a fixed length. In this regard the transfer can be accomodated from any θ-position by simply "cutting" the line and allowing m_2 to (immediately) proceed with the transfer maneuver along a ballistic arc. Quite naturally, one of the main purposes in this simulation is to determine what altitudes might be reached, by the particle (m_2), corresponding to these acquired pericenters.

As an aid in this investigation the calculations were carried out by means of a specially developed computer program. This is described, mathematically, in Appendix G; there all of the general and particular expressions needed to solve for this situation are developed.

In the operation of this program the fixed-length tether's rotation is constrained to the plane of motion for the main vehicle (m_1). The main variable of influence (here) is the relative velocity which is developed as a consequence of the rate, $\dot{\theta}$. (Of course, the gravitation attraction on the tethered body (m_2) is accounted for in these expressions. Also, the program accepts rotations which are "with" and "against" the main body orbital rotation).

At each step in the calculation procedure the output lists a pericenter radius and speed; the angle of transfer to pericenter; and its relative position and speed; also, the line tension. As a consequence the investigator may monitor (and trace) the history of the relative motion - as well as the developed pericenter values - throughout the entire computational procedure. A perusal of Appendix G is recommended for those readers who are interested in the formulation and the possible output quantities from this program.

In order to illustrate the effect of a rotating tether system on this transfer operation a study case has been examined, using several $\dot{\theta}$ rates, for a given base orbit. This will be described and discussed below.

IV.4.1 Example.

For this sample case a circular reference orbit at an altitude of 300 n.m. is assumed. The rotating tether system will be considered to operate at rates of: 1, 2, 3, and 6 deg/sec.; and, to use a 5000 ft. (1524.m) line. As before, it is assumed that $m_2 \ll m_1$; hence, the rotating mass is not presumed to perturb the base orbit.

For these operations the tether is assumed to have reached its "steady-state" of rotation; consequently, any "transients" which occur are a consequence of the dynamics in the formulation. Also, the analysis will be set to begin at $\theta \equiv 0^{\circ}$; this selection is arbitrarily made, it has no influence on the output results, per se. A schematic of this problem is shown below (Fig. IV.8).

From this sketch it is seen that $\bar{v}$ is the relative velocity for m_2; it is due to the rotation ($\dot{\theta}$). Now, as a consequence, the "inertial velocity" $\bar{V}_2$ is;

$$\bar{V}_2 \equiv \bar{V}_1 + \bar{v},$$

where $\bar{v} \equiv (\bar{\ell} \times \bar{e}_z)\ \dot{\theta}$. As shown on the figure, this system is rotating at $+\dot{\theta}$.

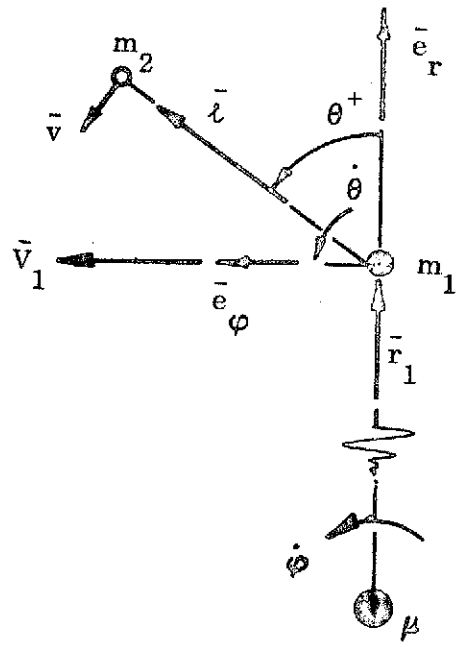

Fig. IV.8. Schematic of the rotating tether system.

Here r_1, $\dot{\varphi}_1$ are fixed values; $\bar{v} \equiv$ relative velocity of m_2 ($\bar{v} = \bar{\ell} \times \dot{\theta}\, \bar{e}_z$, where $\bar{e}_z \equiv \bar{e}_r \times \bar{e}_\varphi$).

Incidentally, this direction will be used for the data presented below since "negative rates" leads to larger pericenter radii.

(a). Results.

Selected data from these example situations are presented, and discussed, below.

(1). Using the values of $\dot{\theta}$ noted above, several curves, each showing a trace of the pericenter altitudes which could be developed from these rotating systems, are depicted on Fig. IV.9.

The left ordinate scale describes pericenter altitude (in n.m.), corresponding to each $\dot{\theta}$, and for a release at the θ value noted on the abscissa. (Incidentally, due to the symmetry of these results, data are plotted only for $0 \leq \theta \leq 180^\circ$; for the second half of the θ-rotation this curve is repeated, but from 180° to 0°!)

The right hand ordinate indicates the change in pericenter altitude (ΔH) which occurs for a transfer originating at each of the θ-values noted on the abscissa.

From this figure it should be noted that, at $\theta = 0$, the initial altitude (H) > 300 n.m. (and, correspondingly, $\Delta H < 0$). This is indicative of the initial position caused by the tether length ($\ell = 5000$ ft) in this problem.

As would be expected, a largest change in (pericenter) altitude is acquired by the system with the largest $\dot{\theta}$-rate; and, for a "release" at the $\theta = 180^\circ$ position.

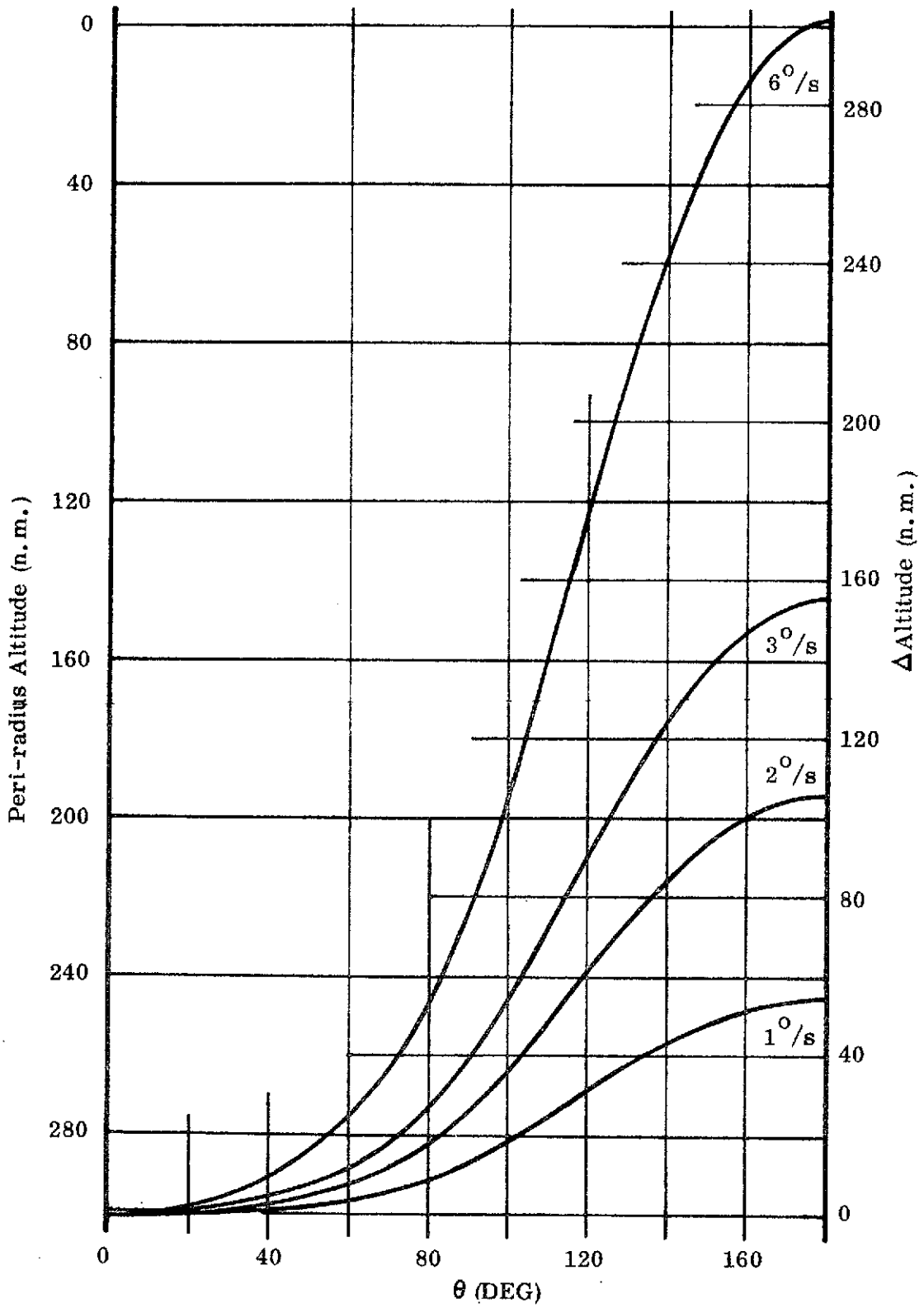

Fig. IV.9. Description of Pericenter Altitudes Acquired from a Rotating Tether System. Altitudes are Described in Terms of θ (position) and for Selected + $\dot{\theta}$ Rates.

At this position the particle (m_2) is moving counter to the orbit's motion, hence it produces the largest change in "launch" speed. Also, here, the position (r_2) of m_2 is smallest; so, the combined effects couple and lead to a largest change in specific energy.

Studying Fig. IV.9 one can see that for a rotational rate of 6 deg/sec the system can lead to a ballistically attained pericenter which is <u>below</u> the geoid's surface. However, at a rotation of 3 deg/sec the best that can be done (here) is to reach a pericenter at approximately half the circular orbit altitude. It appears that if this system is to produce a pericenter, at 70 n.m. altitude, it would need a rotation ($\dot{\theta}$) of roughly 4.5 deg/sec. Of course, this same altitude <u>could</u> be reached from a release at (say) $\theta \cong 136^{\circ}$ using the 6 deg/sec rotational rate. Thus, with a large enough rotation (such as the 6 deg/sec) this system may reach <u>almost</u> any desired (lower pericenter) altitude by means of a properly controlled release position (θ). Conversely (though not shown here), if the rotation would be reversed this system would allow the suspended particle to ascend to higher* altitudes, also.

(2). Figure IV.10 is included to illustrate the transfer angle ($\Delta\varphi_2$), which m_2 must pass over, in going from its release position (θ) to the acquired pericenter. Thus, this figure is a companion to the previous one (Fig. IV.9).

What is most interesting here is that for these rotation rates (1°/sec through 6°/sec) there does not seem to be much change (or influence) produced on the transfer angle. That is, except for the region around $\theta \cong 90^{\circ}$ there is very little change (if any) noted in $\Delta\varphi$. In particular, for a release <u>beyond</u> $\theta \cong 120^{\circ}$ (through $\theta = 180^{\circ}$) the same transfer angle is needed for all of these $\dot{\theta}$-rates.

Incidentally, this figure has an abscissa scale extending over $0 \leq \theta \leq 180^{\circ}$ only. This is (also) due to the symmetry found in the results. Thus, the curve from $180^{\circ} \leq \theta \leq 360$ can be read by imaging the present curve into the $\theta = \pi$ line. Of course, for $\theta \geq 180^{\circ}$ the particle must move over an arc ($\Delta\varphi$) > 180° to reach the acquired pericenter.

*Systems of this type are not considered at this time, though the program is capable of these simulations.

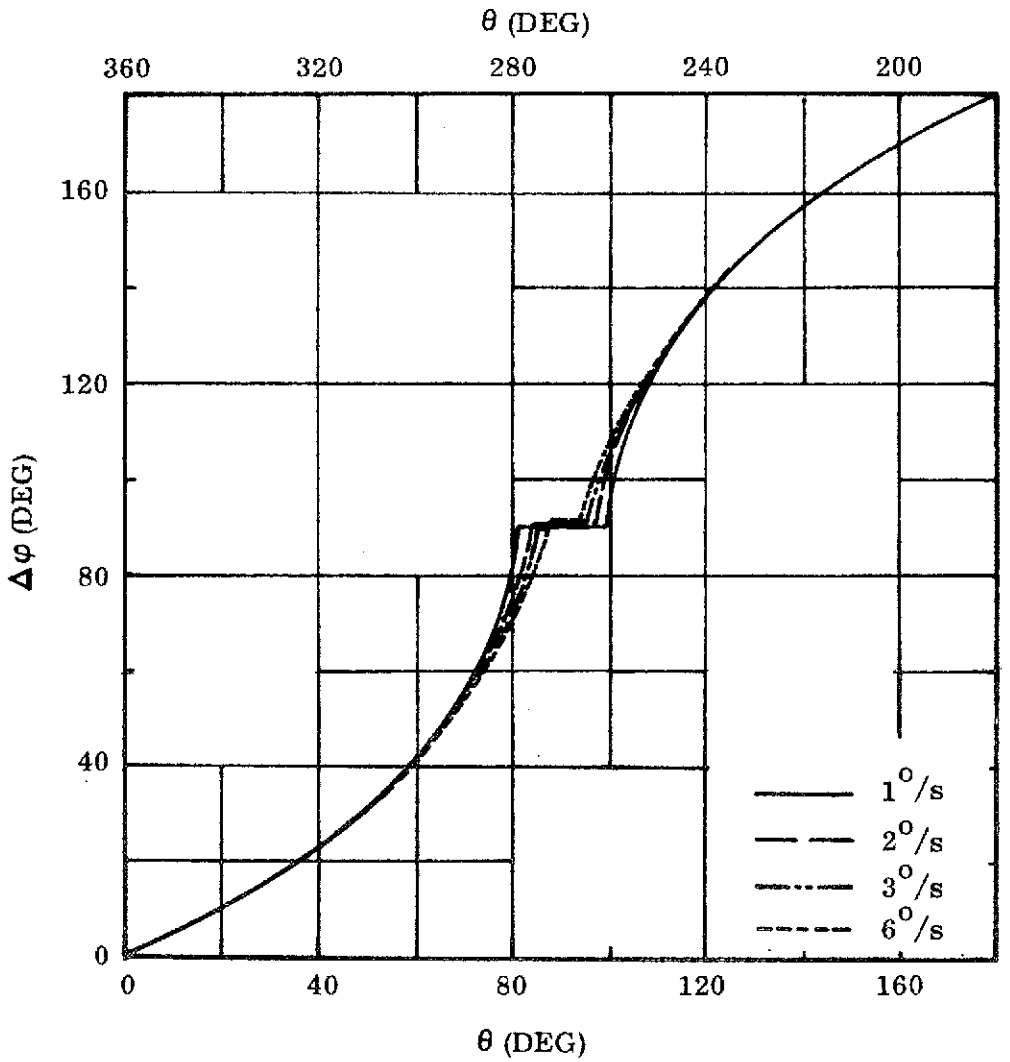

Fig. IV.10. Transfer Angles ($\Delta\varphi$), Required to Reach Pericenter, for a Rotating Tether Suspended Mass Particle.

(3). The information provided on Fig. IV.11 notes the specific force (F/m_2) developed in the tether line (as a tensile force) for each rotational rate used here. This quantity (in f/s^2) is referenced to the θ-position (in degrees) for each rate. (Note that the scales are incremented differently for each of these rotations).

(It would be informative to compare these figures with some of the (rotational) curves presented on Figs. I.4(b) and I.5(b) (section I). The similarity in geometry is very marked (as it should be)).

Here, again, the abscissa scale extends over only half of the intended range. Once more, this has been done in view of the symmetry which is apparent for these curves.

A cursory look at this last figure will indicate that the specific force (F/m_2) decreases slightly, as the system approaches the $\theta = \pi/2$ position(s), and increments again as the $\theta = \pi$ position is approached. This variation is repeated as the system continues to rotate to the $3\pi/2$ and 2π locations, respectively. The apparent change in force (or the amplitude of these curves) is relatively unaffected by these rates of rotation. It is evident, now, that for moderate rates (up to 6 deg/sec) the primary force to be overcome, by the tethers, in these systems is that due to centrifugal action.

In connection with this mentioning of force levels, it is worth noting the rather large change in "gee" levels which the specific tensions imply; and, the variations in these due to each rotation ($\dot{\theta}$). A tabulation is shown below to illustrate this point:

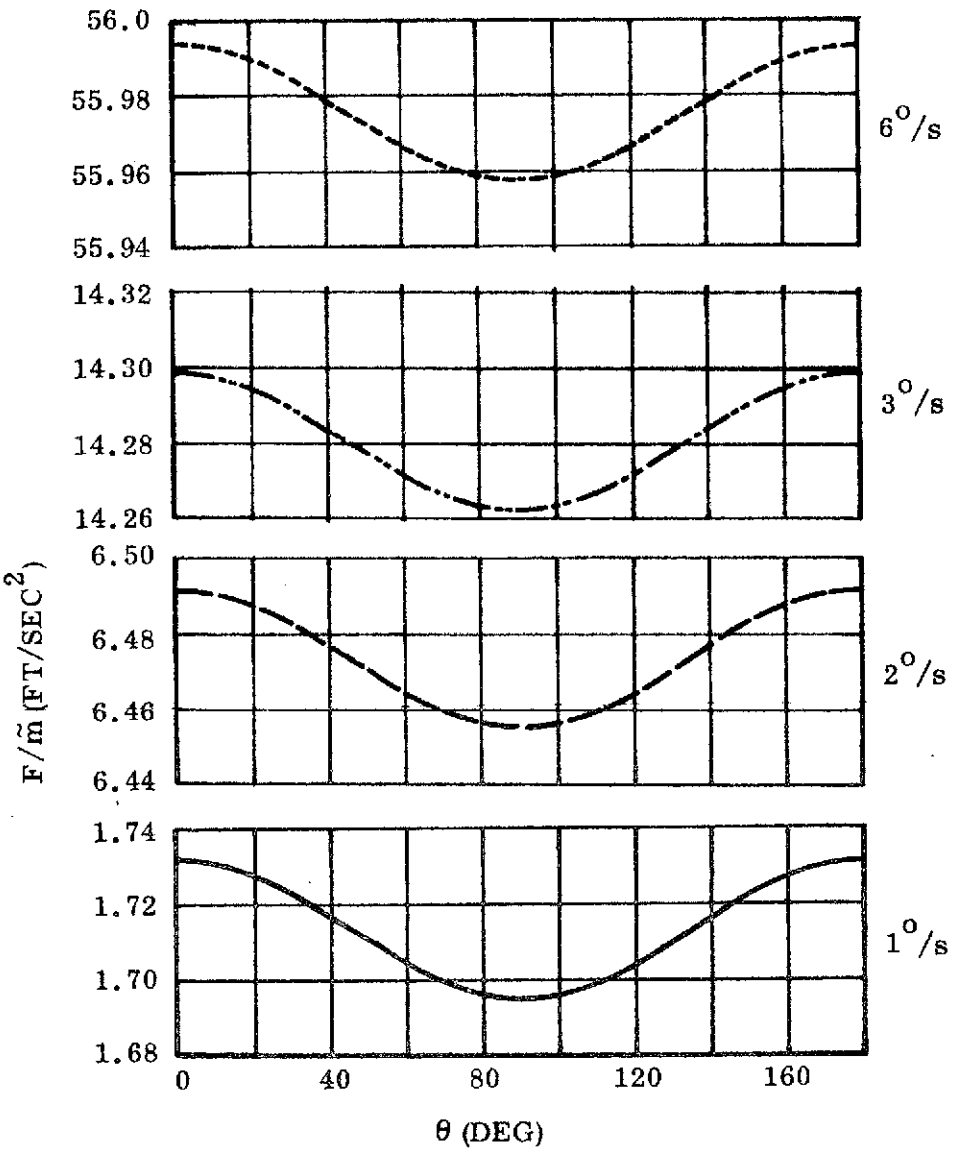

Fig. IV.11. Specific Force Developed in Tethers due to System Rotation(s). Note Different Scales, for each Rotational Rate.

Rotation Rate	Maximum F/m_2 (earth's gee's)	Variation; $\Delta F/m_2$ (decrement)
1^o/s (1/6 rpm)	0.0537	2.0%
2^o/s (1/3 rpm)	0.2015	0.75%
3^o/s (1/2 rpm)	0.443	0.45%
6^o/s (1 rpm)	1.738	0.115%

IV.5 Discussion.

The studies described in this section of the report have considered several tether system applications which could be used for purposes other than those discussed in sections II and III. In particular the systems have been employed as the means to develop (various) gee-field levels, and for the initiation of transfer maneuvers. To a large extent these schemes require the establishment of a stabilized suspended body configuration. In this regard some of the previous handling and maneuvering capability studies would be directly applicable to providing for such configurations. (Of course, other approaches would be equally applicable for some of the same purposes).

Experimenters, planning to make use of space stations and other non-maneuvering vehicles, would quickly recognize the advantage of tethers as depicted here. Once a stable tether configuration is achieved, a connected experiment package is essentially at a constant gee level, and would remain so (within the limits of the natural gravitational variations). Also, the very wide variation* in gee-level which is available under this concept makes the idea amenable to a large number of applications -- from those needing near zero acceleration to (say) those in the vicinity of one-to two-tenths gee. Recalling that there are cyclic changes in the gee levels, produced by rotating tethered systems, and especially at the lower gee ranges, then the stabilized configurations are much more attractive for precision work.

*Experiments in manufacturing processes, bio-medical and engineering, artificial gravity, etc. could fit within these ranges. Also, these same ideas could have operational engineering applications for the vehicle itself.

In the analysis pertaining to orbit transfers the philosophy there was to describe systems which could serve to achieve "initial values" leading to a priori defined pericenter radii. For these purposes several variations of the basic idea were pursued. In each some added capability was introduced, with a subsequent result of enhancing the system's ability to better achieve this common goal. That is, the ideas here have evolved from a basic stabilized system, through the addition of a "vertical" velocity component, to a system which was described as a pure rotating tethered body concept.

It is to be expected that many other uses of these same systems (and concepts) will be brought to light by those persons who are planning to make use of "space" as a future experimental laboratory environment. Hopefully, these data will find their way to such prospective investigators; and that they, in turn, will see their needs described here.

A SATELLITE TO SATELLITE ORBIT DETERMINATION AND ERROR ANALYSIS PROGRAM

Analytical Description

V.1 Introduction.

Many programs exist for the determination of orbits based on ground observations. If such programs are adapted to describe the relative displacements for two orbiting satellites, moving in close proximity to one another, the errors in each individual satellite's position, while possibly acceptable for itself, will project into completely unacceptable errors in their relative position.

In order to avoid this difficulty an orbit determination schedule, based on the relative equations of motion, has been developed and is presented here.

V.2 General Discussion of Features for Various Orbit Determination and Error Analysis Schedule.

The component parts of any orbit determination scheme are numerous; each may be introduced in a variety of ways, thus producing a large variety of different possible approaches. In the following paragraphs there is to be found a description of one such approach, its various parts, and a brief justification for the methods selected.

(a). State Vector.

The simplest and most satisfactory description of a relative motion is one which is comprised of the cartesian components of the relative displacement and velocity vectors; incidentally, this description is not subject to the singularities which arise from the use of the Keplerian elements. Other quantities which are to be determined in the problem are adjoined to the state vector; it is planned here to include, among these quantities, the central mass parameter, μ.

In our case the state vector will consist of:

ΔR the relative displacement vector.

$\Delta \dot{R}$ the relative velocity vector.

It will be augmented by:

(1). Dynamic biases in:

(a). μ, gravitational constant; and

(b). possibly other quantities.

(2). Observational biases, due to:

(a). Platform alignment errors; and

(b). Platform drift rates.

(3). Errors in the position and velocity of the reference satellite.

(b). Equations of Motion.

The state vector is propagated, in time, by numerical integration of the equations of motion.

In our case, these expressions contain the familiar equations of motion for the "mother" satellite; and could include a similar set to be written for the second, or "daughter", satellite. However, when the two bodies are in close proximity, large errors may arise from the simple subtraction of components; therefore, a set of relative equations of motion has been chosen for use here. Unfortunately, a set of linearized expressions is not adequate in all cases, since during the motion large relative displacements may occur. For this reason Lancaster's equations* of motion have been selected for use in this formulation.

Generally speaking, the equations are written in a modified Encke form. The procedure requires that one numerically integrates the "deviations" from a Kepler orbit. This method, for a single satellite, is well known and is described in reference [1].

*See reference [2].

The equations of relative motion are expressed in Lancaster's form, (see reference [2]); these are given below for reference purposes:

The equations for a Kepler orbit are written as follows:

$$T = C + A\,(1-\cos C) - B \sin C, \tag{V.1}$$

$$\bar{r} = [1-H\,(1-\cos C)]\,\bar{r}_0 + [D\,(1-\cos C) + N \sin C]\,\bar{v}_0, \tag{V.2}$$

$$\bar{v} = -(P \sin C)\,\bar{r}_0 + [1-S\,(1-\cos C)]\,\bar{v}_0, \tag{V.3}$$

where

$\bar{r}$ = position vector at time t, $r = |\bar{r}|$,

$\bar{v}$ = velocity vector at time t, $v = |\bar{v}|$,

E = eccentric anomaly at time t,

a = semimajor axis, $b = 1/a$, $c = a^{1/2}$,

k^2 = μ = gravitational constant,

$\bar{r} \cdot \bar{v}$ = scalar product of $\bar{r}$ and $\bar{v}$,

$A = \bar{r}_0 \cdot \bar{v}_0/(kc)$, $B = 1-r_0 b$, $T = ktb/c$,

$H = a/r_0$, $D = a(\bar{r}_0 \cdot \bar{v}_0)/\mu$, $N = r_0 c/k$,

$P = kc/(rr_0)$, $S = a/r$, $C = E - E_0$,

and a zero subscript indicates the value at time 0.

Let subscript 1 on a symbol designate the value of that symbol for particle 1, on orbit 1, and subscript 2 the value for particle 2 on orbit 2.

Next, define:

$$\gamma = C_2 - C_1, \quad \epsilon = \bar{r}_2 - \bar{r}_1, \quad \lambda = \bar{v}_2 - \bar{v}_1, \quad \tau = T_2 - T_1,$$

and

$$\alpha = A_2 - A_1.$$

Also, let;

$$\beta = B_2 - B_1,\ \eta = H_2 - H_1,\ \delta = D_2 - D_1,\ \nu = N_2 - N_1,$$

$$\rho = P_2 - P_1,\ \sigma = S_2 - S_1.$$

If a subscript 1 is placed on all symbols in eqs. (V.1, V.2 and V.3); and if the resulting equations are subtracted from the set with subscripts 2 on all symbols, one obtains:

$$T' = \gamma + A'(1-\cos\gamma) - B' \sin\gamma, \tag{V.4}$$

$$\epsilon = (1-H_1F)\,\epsilon_0 + (D_1F + N_1G)\,\lambda_0 - (H_2Q + \eta F)\,\bar{r}_{20} + (D_2Q + \delta F + N_2R + \nu G)\,\bar{v}_{20}, \tag{V.5}$$

$$\lambda = -P_1G\,\epsilon_0 + (1-S_1F)\,\lambda_0 - (P_2R + \rho G)\,\bar{r}_{20} - (S_2Q + \sigma F)\,\bar{v}_{20}; \tag{V.6}$$

wherein

$$F = 1 - \cos C_1,\ G = \sin C_1, \tag{V.7}$$

$$T' = \tau + \beta G - \alpha F, \tag{V.8}$$

$$A' = A_2 \cos C_1 + B_2 \sin C_1, \tag{V.9}$$

$$B' = B_2 \cos C_1 - A_2 \sin C_1, \tag{V.10}$$

$$Q = \cos C_1 (1-\cos\gamma) + \sin C_1 \sin\gamma, \tag{V.11}$$

$$R = \cos C_1 \sin\gamma - \sin C_1 (1-\cos\gamma). \tag{V.12}$$

To obtain equations for α, β, τ, η, δ, ν, ρ and σ which do not suffer a loss of significant digits due to the subtraction of nearly equal numbers, one may proceed as follows:

$$kcA = \bar{r}_0 \cdot \bar{v}_0,$$

$$k(c_2A_2 - c_1A_1) = \bar{r}_{20} \cdot \bar{v}_{20} - \bar{r}_{10} \cdot \bar{v}_{10},$$

$$k[c_2 (A_2-A_1) + A_1 (c_2-c_1)] = \bar{r}_{20} \cdot \bar{v}_{20} - \bar{r}_{10} \cdot \bar{v}_{10}.$$

In order to avoid the loss of accuracy which occurs from the subtraction of nearly equal numbers the differences are written as follows:

$$kc_2\alpha = \bar{r}_{20} \cdot \bar{v}_{20} - \bar{r}_{10} \cdot \bar{v}_{10} - kA_1 (c_2-c_1), \tag{V.13}$$

$$\beta = r_{10} (b_1-b_2) - b_2 (r_{20} - r_{10}), \tag{V.14}$$

$$c_2\tau = - kt (b_1-b_2) - T_1 (c_2-c_1), \tag{V.15}$$

$$r_{10}\eta = a_2-a_1-H_2 (r_{20}-r_{10}), \tag{V.16}$$

$$\mu\delta = a_2 (\bar{r}_{20} \cdot \bar{v}_{20} - \bar{r}_{10} \cdot \bar{v}_{10}) + (a_2-a_1) \bar{r}_{10} \cdot \bar{v}_{10}, \tag{V.17}$$

$$k\nu = c_2 (r_{20} - r_{10}) + r_{10} (c_2-c_1), \tag{V.18}$$

$$r_{10}r_1\rho = k (c_2-c_1) - P_2 [r_2 (r_{20}-r_{10}) + r_{10} (r_2-r_1)], \tag{V.19}$$

$$r_1\sigma = a_2-a_1-S_2 (r_2-r_1), \tag{V.20}$$

$$\bar{r}_{20} \cdot \bar{v}_{20} - \bar{r}_{10} \cdot \bar{v}_{10} = \lambda_0 \cdot \bar{r}_{10} + \epsilon_0 \cdot \bar{v}_{20}, \tag{V.21}$$

$$r_{20}-r_{10} = \epsilon_0 \cdot (\bar{r}_{10} + \bar{r}_{20})/(r_{10} + r_{20}), \tag{V.22}$$

$$r_2-r_1 = \epsilon \cdot (\bar{r}_1 + \bar{r}_2)/(r_1 + r_2), \tag{V.23}$$

$$c_2-c_1 = (a_2-a_1)/(c_1 + c_2), \tag{V.24}$$

$$a_2-a_1 = a_1a_2 (b_1-b_2), \tag{V.25}$$

$$b_1-b_2 = 2(r_{20} - r_{10})/r_{10}r_{20} + \lambda_0 \cdot (\bar{v}_{10} + \bar{v}_{20})/\mu. \tag{V.26}$$

In the derivation of eq. (V.26) use was made of the expression:

$$b = 2/r - v^2/\mu. \tag{V.27}$$

(c). Covariance Matrix.

The error ellipsoid about a state estimate (see paragraph (b)) is given by:

Covariance Matrix

$$P_{AUG} = E\left\{ \begin{pmatrix} \Delta\Delta R \\ \Delta\Delta\dot{R} \\ \Delta b_s \\ \Delta b_u \end{pmatrix} \qquad (\Delta\Delta R^T \;\; \Delta\Delta\dot{R}^T \;\; \Delta b_s \;\; \Delta b_u) \right\}$$

where: Δb_s = biases to be solved for,

and Δb_u = biases whose effects are considered, but which are not to be determined.

Here E is the expected value; and, the superscript T is used to denote the transpose of a vector.

For economy of storage, and economy of computation, the covariance matrix is partitioned as indicated below:

$$P_{AUG} = \begin{pmatrix} P & C \\ C^T & B \end{pmatrix}$$

wherein

$$P \equiv E \left\{ \begin{pmatrix} \Delta\Delta R \\ \Delta\Delta\dot{R} \\ \Delta b_s \end{pmatrix} \begin{pmatrix} \Delta\Delta R^T & \Delta\Delta\dot{R}^T & \Delta b_s{}^T \end{pmatrix} \right\}$$

$$C \equiv E \left\{ \begin{pmatrix} \Delta\Delta R \\ \Delta\Delta\dot{R} \\ \Delta b_s \end{pmatrix} \begin{pmatrix} \Delta b_u{}^T \end{pmatrix} \right\}$$

and

$$B \equiv E \left\{ \begin{pmatrix} \Delta b_u & \Delta b_u{}^T \end{pmatrix} \right\} .$$

The biases, Δb_s, included in P, are those biases which may be corrected by the differential correction process; however, the biases Δb_u are not expected to be estimated.

(d). Propagation of the Covariance Matrix Between Observations.

While it is essential to update the state vector between observations, and to do so with extreme precision, the requirements for propagating the covariance matrix are not as rigorous. Formally, the propagation is accomplished by:

$$P(t) = \phi\,(t, t_o)\; P(t_o)\; \phi^T\,(t, t_o),$$

wherein,

$$\phi\,(t, t_o) = \frac{\partial S(t)}{\partial S(t_o)} \quad , \tag{V.28}$$

with S being the state vector:

$$S \equiv \begin{pmatrix} \Delta R \\ \Delta\dot{R} \\ \Delta b_s \end{pmatrix} .$$

The partial derivatives in equation (V.28) may be evaluated by either integrating the variational equations, or by the "secant" method. Each method requires the integration of a large number of differential equations, making the attendant computer program costly to run. Fortunately experience with single satellite orbit determination programs has shown that for arcs which are not too long the partial derivatives obtained from a Kepler orbit are of adequate accuracy. However, longer arcs may be accomodated by piecing together several short arc matrices, along changing reference orbits, as indicated below:

$$\phi\,(t,\ t_o) = \phi\,(t,\ t_{R_N})\,\phi\,(t_{R_N},\ t_{R_{N-1}})\ldots$$

$$\ldots\ \phi\,(t_{R_1},\ t_o).$$

Here t_{R_N}, $t_{R_{N-1}}$ etc. are "rectification" times, i.e., times at which the reference Kepler orbit is changed. (The necessary partial derivatives, from Lancaster's relative equations of motion, are derived in Appendix A).

(e). Observation Processing.

The modified Kalman scheme, for observation processing, is well known. Its equations are summarized below:

$$\begin{pmatrix} \Delta R \\ \Delta \dot{R} \\ \Delta b_s \end{pmatrix} (t_{OBS} + 0) = \begin{pmatrix} \Delta R \\ \Delta \dot{R} \\ \Delta b_s \end{pmatrix} (t_{OBS} - 0) + \Delta S, \tag{V.29}$$

$$P(t_{OBS} + 0) = P(t_{OBS} - 0) + \Delta P, \tag{V.30}$$

$$C(t_{OBS} + 0) = C(t_{OBS} - 0) + \Delta C, \tag{V.31}$$

$$B(t_{OBS} + 0) = B(t_{OBS} - 0); \tag{V.32}$$

where

$$\Delta S = K\Delta y,$$

$$\Delta P = -K(HP + FC^T),$$

$$\Delta C = -K(HC + FB), \qquad (V.33)$$

$$K = (PH^T + CF^T)\, Y^{-1},$$

$$Y = HPH^T + HCF^T + FC^T H^T + FBF^T + \epsilon^2.$$

Quantities may be transferred from the Δb_s to the Δb_u category by zeroing the corresponding component of K.

The new symbols in equations (V.29 - V.33) are defined as follows:

Δy $\equiv$ observation residual,

H $\equiv$ $\frac{\partial y}{\partial S}$, derivative of the observation with respect to the state,

F $\equiv$ $\frac{\partial y}{\partial b_u}$, derivative of the observation with respect to the bias,

ϵ^2 $\equiv$ noise in the observation.

The H matrix, for relative range and range-rate, is described in Appendix A.4, eqs. (H.1) and (H.2).

V.3 Summary and Conclusion.

(1). The equations and flow logic for an orbit determination and error analysis method, based on relative equations of motion, has been obtained.

(2). This scheme (or a similar one) is necessary when an accurate determination of the relative position and velocity, for neighboring satellites, is needed.

(3). The scheme may be used to detect the onset of dangerous instabilities in (say) reel-in, reel-out operations, for tethered vehicle.

CONCLUDING REMARKS

VI.1 General.

The information provided in this report is the consequence of an investigation directly related to orbiting tethered bodies, and to the description of a relative motion, orbit determination procedure. It is expected that these results will aid materially in the design and planning for future space operations.

From the very nature of these tether studies, it would be useful to give consideration to this information whenever there is a need for local transport capabilities, in space; or, when extra vehicular activities are contemplated.

The analytical and numerical work reported on here clearly indicates that tethers may provide for controlled handling of cargo, materials, experimental packages and for rescue operations in space. The ability to transport mass particles to and from orbiting spacecraft, using light weight lines, and to do so by simple manipulative means, suggests a marked advantage over other methods. The fact that these connectors can be reused, time and time again, and for a variety of purposes, makes them even more attractive. Add to this the capability to provide transport over a large range of distances - up to tens of kilometers - it would be difficult to visualize the use of other systems for most of these same operational situations.

From a perusal of the foregoing findings one can easily conclude that tethers have not been given the consideration warranted as useful work and safety devices. Most likely this past neglect has been largely a consequence of not knowing how to manipulate them so that adequate control could be maintained. Knowing, as we do now, how easily these systems can be made to behave, as desired, it seems reasonable to conclude that they will be more favorably considered in the future.

In one of the latter sections of this report it was shown (mathematically) that by means of a "stabilized" tether a mass particle could be properly located so that at release it would move, immediately, onto a free transfer arc. This scheme affords a way to initiate transfers by a system which can be used over and over again. That is, if the tethers are rewound, after each transfer, the lines obviously have an almost limitless life-time. Of course these same lines could be employed for many other operational uses as well.

For instance, the same gravity gradient, stabilized, static tether offers an ideal way to achieve a rather wide range of "gee's". (Necessarily the range afforded by this scheme has practical limits due to the length(s) of line which can be utilized). The advantage provided by this operation is that whatever the gee-load developed, it would have very little variation once the system is stabilized. The only variance which should be experienced, by such a suspended mass, would be that due to inhomogeneities of mass within the attracting primary (e.g., masscons). It goes almost without saying that the static line would allow for a gee-range from practically zero to whatever upper limit could be provided by a (practical) length of connecting line. This method suggests the means to conduct a variety of experiments, each of which could depend on a different level of "gee". Similarily, the same suspension concept fits well into the needs for some proposed space manufacturing methods, and for engineering requirements of the spacecraft itself (e.g., liquids transfer).

In the paragraphs above there was mention made of transfers from "stable" static lines. It is worth noting that transfers may be initiated by other means, or by modifications to the static system. Two illustrations of these operating schemes were described and examined in the report. Those variations considered were, first, the influence of a velocity component added to the stable (static) tether; and, second, a whirling (or rotating) tethered mass system.

These examples, illustrated in the report, were aimed at the establishment of a low altitude pericenter -- allowing for a subsequent reentry maneuver. However, it should be apparent that these same ideas can be gainfully used to accomodate other transfer operations; and, possibly, for other uses all together different from the above.

In the first part of the investigation undertaken here, studies were made to examine the consequences of the system's mechanical properties coupled with its gravitational attraction. In a similar manner the influence of orbit eccentricity was examined, also. This last parameter appears as an added factor in studies of the suspended body's motion state.

Prior to the introduction of eccentricity the aim was to determine how the several parameters (mechanical and otherwise), singly and coupled, affected the system's behavior. In these evaluations the state variables were non-dimensionalized, and the expressions simplified so that the main influences were the ones brought out. The information sought for here was mainly descriptive in nature rather than explicit definitions of the motions. (A review of the summarization (see section II.3) will be more definitive of the implications in these statements).

Following from these first studies a look at the force(s) generated by rotating and/or oscillating systems was made. The definitions found here are in evidence over and over again throughout the report (either directly or indirectly), as other phases of the investigation are examined.

With the background which is available, on the use and application of tethered body systems, it is to be expected that their utility will be more in evidence, in the future. It should not be concluded, however, that follow-on tasks are not to be undertaken - relevant to the design and implementation of these schemes - this would be an erronous supposition.

There are obvious extensions of the work (reported here) which should be completed. And, there will always be inovations and modifications which need to be examined. Some of the more interesting tasks, worthy of attention, are those which would consider the influence of tether mass, per se; and the sensitivity studies associated with the control and handling of these systems. The natural extensions of this reported work, and the additional information on the method studied (herein) are tasks important to a fuller understanding of tethered operations. Hopefully interested and inquisitive investigators will be motivated (sufficiently) to continue the work. In the opinion of the present investigator this is an interesting and challenging problem area, one which is worth the effort of further study. Also, it seems that the applications of this concept represent a versatility which has somehow been overlooked or passed by in previous situations.

The orbit determination scheme, described here, is an inovation of previously defined methods, and represents a concept which easily could be modified and applied to tether operations. An examination of the mathematical developments will verify that the scheme is composed from a particular set of relative motion expressions and the familiar Kalman filtering technique. The basic difference between this and other orbit determination methods is that the present one is referenced to a moving base point -- the main vehicle.

It should be noted that the mathematics of this method are complete, as reported. Consequently, the scheme could be implemented as a working program without difficulty. This program would most likely be cast into an Encke scheme; and, for this, a good bit of the formulation has already been worked out (though it is not outlined here).

The implementation of this method to the tethered bodies problem is envisioned as a scheme to warn of the onset of undesired motions. Possibly, the addition of a means to monitor tether tension and orientations, within the

program, could provide the indicators needed for these warnings. Regardless, with the information available now - concerning the motions for (say) controlled tether motions - the orbit determination program could be keyed to this system. Such a concept would provide for a needed link in tether "design", insofar as safety and versatility are concerned.

Final Report

TETHERED BODY PROBLEMS AND RELATIVE MOTION ORBIT DETERMINATION

(CONTINUED)

PART II

J.B. Eades, Jr.
Henry Wolf

Contract NAS5-21453
Report No. 72-35
August 1972

ANALYTICAL MECHANICS ASSOCIATES, INC.
10210 GREENBELT ROAD
SEABROOK, MARYLAND 20801

APPENDIX A

MATHEMATICAL DEVELOPMENTS*

A.1 Introduction

A recent paper by Lancaster [2] outlines a procedure for calculating of the position vector, ϵ, and velocity vector, λ, of one space vehicle (denoted by subscript 2) relative to a reference vehicle (denoted by subscript 1). Both vehicles are assumed to be in Keplerian motion about earth, whose gravitational constant $\mu \equiv GM$. The procedure described there is exact (no approximations are introduced) and is designed to avoid the loss of significance, due to subtraction, for the case when the two vehicles remain close together for a long time.

In this appendix expressions will be obtained for the partial derivatives of the vectors (ϵ and λ) with respect to their initial values (ϵ_o and λ_o), and with respect to μ. Also, expressions will be developed for the range and range-rate of the second vehicle, relative to the first (or, reference vehicle), as well as derivatives of the range and range-rate with respect to ϵ, λ and μ.

For the most part Lancaster's notation will be used. It is assumed that the two body motion has been previously calculated according to his procedure. Any reference to equations appearing in Lancaster's paper will have a prefix L attached to the equation number(s). The following modifications are made in Lancaster's notation:

R_1, R_2 will be the position vectors of the two bodies relative to the earth (these were denoted by boldface r_1, r_2 in reference [2]).

R_{10}, R_{20}, $\dot{R}_{10}$, $\dot{R}_{20}$ describe the initial position and velocity vectors, relative to earth; these were noted by boldface r_{10}, r_{20}, v_{10}, v_{20} in Lancaster's paper.

$F_1 \equiv 1-\cos C_1$, was noted as F (reference [2]);

$G_1 \equiv \sin C_1$, was the quantity G (reference [2].

*Mathematical developments in Appendix A due to Dr. Mary Payne of AMA, Inc.

We will introduce many new parameters, including

$\dot{R}_1$, $\dot{R}_2$ ≡ the velocity vectors for the two bodies, relative to earth;

$$F_2 = F_1 + Q \text{ (i.e. } F_2 = 1-\cos C_2);$$

$$G_2 = G_1 + R \text{ (i.e. } G_2 = \sin C_2);$$

$$f_1 = F_1 - 1;$$

$$f_2 = F_2 - 1;$$

$$\Delta a = a_2 - a_1, \text{ (computed from L25);}$$

and $$\Delta b = b_2 - b_1, \text{ (computed from L26).} \qquad \text{(A.2)}$$

It is easy to show (see section A.5) that

$$r_i = |R_i| = a_i (1 + A_i G_i + B_i f_i), \text{ for } i = 1,2;$$

(this is Lancaster's italic r_i). (A.3)

Also, let

$$\Delta r \equiv \frac{\Delta a}{a_1} r_1 + a_2 (A_2 R + B_2 Q + \alpha G_1 + \beta f_1); \qquad \text{(A.4)}$$

this will replace Lancaster's calculation of $r_2 - r_1$ in equation L23.

The relative position and velocity vectors, ϵ and λ, are defined as follows:

$$R_2 = R_1 + \epsilon, \qquad \dot{R}_2 = \dot{R}_1 + \lambda,$$

$$R_{20} = R_{10} + \epsilon_o, \text{ and } \dot{R}_{20} = \dot{R}_{10} + \lambda_o. \qquad \text{(A.5)}$$

The partial derivative matrix, which is to be constructed, is the 7x7 matrix:

$$\phi \equiv \begin{bmatrix} \frac{\partial \epsilon}{\partial \epsilon_o} & \frac{\partial \epsilon}{\partial \lambda_o} & \frac{\partial \epsilon}{\partial \mu} \\ \frac{\partial \lambda}{\partial \epsilon_o} & \frac{\partial \lambda}{\partial \lambda_o} & \frac{\partial \lambda}{\partial \mu} \\ 0 & 0 & 1 \end{bmatrix} \tag{A.6}$$

wherein

$$\frac{\partial \epsilon}{\partial \epsilon_o} = \left(\frac{\partial \epsilon_i}{\partial \epsilon_{o_j}} \right), \text{ with } \begin{cases} i = \text{row number} \\ j = \text{column number;} \end{cases} \tag{A.7}$$

and, similarly for $\partial \epsilon / \partial \lambda_o$, $\partial \lambda / \partial \epsilon_o$, $\partial \lambda / \partial \lambda_o$. The quantities $\partial \epsilon / \partial \mu$ and $\partial \lambda / \partial \mu$ are 3 component column vectors, while the two zeros represent 3 component null row vectors. Using the defining equations for ϵ and ϵ_o, it is seen that

$$\frac{\partial \epsilon}{\partial \epsilon_o} = \frac{\partial (R_2 - R_1)}{\partial \epsilon_2} = \frac{\partial R_2}{\partial \epsilon_o} = \frac{\partial R_2}{\partial R_{20}} \frac{\partial R_{20}}{\partial \epsilon_o} + \frac{\partial R_2}{\partial \dot{R}_{20}} \frac{\partial \dot{R}_{20}}{\partial \epsilon_o} = \frac{\partial R_2}{\partial R_{20}} \frac{\partial (R_{10} + \epsilon_o)}{\partial \epsilon_o}$$

$$+ \frac{\partial R_2}{\partial \dot{R}_{20}} \frac{\partial (\dot{R}_{10} + \lambda_o)}{\partial \epsilon_o} = \frac{\partial R_2}{\partial R_{20}} , \tag{A.8}$$

since R_{10}, $\dot{R}_{10}$ (and hence R_1 and $\dot{R}_1$) and λ_o are independent of ϵ_o; and,

$$\frac{\partial \epsilon_o}{\partial \epsilon_o} = I = \frac{\partial R_{20}}{\partial \epsilon_o} . \tag{A.9}$$

Similarly;

$$\frac{\partial \epsilon}{\partial \lambda_o} = \frac{\partial R_2}{\partial \dot{R}_{20}} ,$$

$$\frac{\partial \lambda}{\partial \epsilon_o} = \frac{\partial \dot{R}_2}{\partial R_{20}} ,$$

$$\frac{\partial \lambda}{\partial \lambda_o} = \frac{\partial \dot{R}_2}{\partial \dot{R}_{20}} ,$$

$$\frac{\partial \epsilon_o}{\partial \lambda_o} = \frac{\partial \lambda_o}{\partial \epsilon_o} = 0 = \frac{\partial R_{20}}{\partial \lambda_o} = \frac{\partial \dot{R}_{20}}{\partial \epsilon_o} ,$$

and

$$\frac{\partial \lambda_o}{\partial \lambda_o} = I = \frac{\partial \dot{R}_{20}}{\partial \lambda_o} . \qquad \text{(A.10)}$$

Thus all derivatives with respect to ϵ_o and λ_o may be replaced by derivatives with respect to R_{20} and $\dot{R}_{20}$, respectively. In addition all derivatives of the parameters pertaining to the reference body, with respect to ϵ_o, λ_o (or R_{20}, $\dot{R}_{20}$), are set to zero.

Lancaster's equations L5 and L6, for <u>computing</u> ϵ and λ, have the form:

$$\varphi = x_1 \epsilon_o + x_2 \lambda_o + x_3 R_{20} + x_4 \dot{R}_{20} ; \qquad \text{(A.11)}$$

where x_1 and x_2 depend on R_{10} and $\dot{R}_{10}$ only. Hence,

$$\frac{\partial \varphi}{\partial \epsilon_o} = (x_1 + x_3) I + R_{20} \operatorname{grad}_{R_{20}} x_3 + \dot{R}_{20} \operatorname{grad}_{R_{20}} x_4 ,$$

$$\frac{\partial \varphi}{\partial \lambda_o} = (x_2 + x_4) I + R_{20} \operatorname{grad}_{\dot{R}_{20}} x_3 + \dot{R}_{20} \operatorname{grad}_{\dot{R}_{20}} x_4 , \qquad \text{(A.12)}$$

where, as shown in section A.5, the gradients are to be interpreted as row vectors; consequently these terms will yield 3x3 matrices. The coefficients x_3 and x_4 are (small) differences of a function in R_{10}, $\dot{R}_{10}$ and the same function in R_{20}, $\dot{R}_{20}$. As discussed in Section A.5, their gradients can be written as linear combinations of R_{20}^T and $\dot{R}_{20}^T$.

Next, the following notation is introduced: for any scalar parameter z, let

$$\text{grad}_{R_{20}} z \equiv z_{11} R_{20}^T + z_{12} \dot{R}_{20}^T,$$

and

$$\text{grad}_{\dot{R}_{20}} z \equiv z_{21} R_{20}^T + z_{22} \dot{R}_{20}^T . \tag{A.13}$$

In many instances such a parameter will already have a subscript (e.g., A_1, A_2, B_1, B_2, etc.) but since only parameters with subscript 2 will have non-vanishing gradients with respect to R_{20} and $\dot{R}_{20}$, no ambiguity will result from dropping this subscript and introducing a double subscript notation when writing the gradients. Gradients with respect to R_{20} and $\dot{R}_{20}$ will not involve small differences, consequently no special care is required in their calculation.

Many of the derivatives with respect to μ do involve small differences; thus, the formulas given are designed to avoid loss of significance.

The derivative of a scalar z with respect to μ will be denoted by an asterisk: for instance,

$$\frac{\partial z}{\partial \mu} \equiv z^* . \tag{A.14}$$

In section A.2 there is a listing of the derivatives, for most of Lancaster's parameters, with respect to μ, R_{20} and $\dot{R}_{20}$, using the notation defined in eqs. (A.13) and (A.14). It should be mentioned that additional parameters are introduced as necessary.

In the third section is found the 7x7 partial derivative matrix (ϕ) expressed in terms of the results given in section A.2. Finally, in section A.4, one finds the expressions for range and range-rate, and the derivatives with respect to μ, ϵ and λ. Lastly, section A.5 contains a few proofs. It is hoped that with this organization of the material the construction of a computer program, for these derivatives, will be expedited.

A.2 Partial Derivatives of Lancaster's Parameters

Most of the following derivatives are readily verified from the definitions given in reference [2]. The one exception is $\gamma^* \equiv \partial\lambda/\partial\mu$; this is derived in the section A.5. In order to illustrate the notation used here, an example exercise is shown which applies it to the semimajor axes (a_1, a_2) and their difference, $\Delta a = a_2 - a_1$. Now,

$$a_i^* \equiv \frac{\partial a_i}{\partial \mu} \quad (\text{for } i = 1, 2),$$

and

$$\Delta a^* \equiv \frac{\partial \Delta a}{\partial \mu} \ ;$$

also

$$\text{grad}_{R_{20}} a_2 = a_{11} R_{20}^T + a_{12} \dot{R}_{20}^T \ (=\text{grad}_{R_{20}} \Delta a),$$

and

$$\text{grad}_{\dot{R}_{20}} a_2 = a_{21} R_{20}^T + a_{22} \dot{R}_{20}^T \ (= \text{grad}_{\dot{R}_{20}} \Delta a).$$

The starred parameters will be obtained for most of Lancaster's symbols. Gradients, with respect to R_{20} and $\dot{R}_{20}$, of those symbols with subscript 1, vanish; hence gradients of differences, such as Δa, are identical to those for the corresponding parameter with a subscript 2.

a, Δa

$$a_i^* = \frac{a_i}{\mu}\,(1-2H_i), \qquad (i = 1,2),$$

$$\Delta a^* = \frac{(1-2H_1)\,\Delta a}{\mu} - \frac{2\eta a_2}{\mu},$$

$$a_{11} = 2H_2^{\,2}/r_{20},$$

$$a_{12} = a_{21} = 0,$$

$$a_{22} = \frac{2a_2^{\,2}}{\mu}.$$

A, α

$$A_i^* = -\frac{A_i}{\mu}\,(1-H_i), \qquad (i = 1,2),$$

$$\alpha^* = \frac{1}{\mu}\left[\eta A_2 - \alpha\,(1-H_1)\right],$$

$$A_{11} = -A_2H_2/r_{20}^{\,2},$$

$$A_{12} = A_{21} = \frac{1}{\sqrt{\mu a_2}},$$

$$A_{22} = -\frac{A_2a_2}{\mu}.$$

B, β

$$B_i^* = -\frac{1+B_i}{\mu}, \qquad (i = 1,2),$$

$$\beta^* = -\beta/\mu,$$

$$B_{11} = \frac{1+B_2}{r_{20}^{\,2}},$$

$$B_{12} = B_{21} = 0,$$

$$B_{22} = 2r_{20}/\mu.$$

T, τ

$$T_i^* = -T_i (1-3 H_i)/\mu , \qquad (i = 1,2),$$

$$\tau^* = \frac{1}{\mu} [\tau (3 H_2 - 1) + 3\eta T_1] ,$$

$$T_{11} = -\frac{3 H_2 T_2}{r_{20}^2} ,$$

$$T_{12} = T_{21} = 0 ,$$

$$T_{22} = -\frac{3a_2}{\mu} T_2 .$$

H, η

$$H_i^* = \frac{H_i}{\mu} (1-2 H_i), \qquad (i = 1,2),$$

$$\eta^* = \frac{\eta}{\mu} [1-2 (H_1 + H_2)] ,$$

$$H_{11} = \frac{H_2 (2H_2 - 1)}{r_{20}^2} ,$$

$$H_{12} = H_{21} = 0 ,$$

$$H_{22} = \frac{2r_{20}}{\mu} \cdot H_2^2 .$$

D, δ

$$D_i^* = -\frac{2 H_i D_i}{\mu} , \qquad (i = 1,2),$$

$$\delta^* = -\frac{2}{\mu} [\eta D_1 + H_2 \delta] ,$$

$$D_{11} = 2 D_2 H_2 / r_{20}^2 ,$$

D, δ (cont)

$$D_{12} = D_{21} = a_2/\mu ,$$

$$D_{22} = 2\, a_2\, D_2/\mu ,$$

N, ν

$$N_i^* = -\frac{H_i N_i}{\mu} . \qquad (i = 1,2),$$

$$\nu^* = -\frac{1}{\mu}\left[\nu H_2 + \eta N_1\right],$$

$$N_{11} = \frac{N_2 (1 + H_2)}{r_{20}^2},$$

$$N_{12} = N_{21} = 0 ,$$

$$N_{22} = a_2 N_2/\mu .$$

C

$$C_i^* = \frac{a_i}{r_i}\left[T_i^* - F_i A_i^* + G_i B_i^*\right], \quad (i = 1, 2),$$

$$C_{ij} = \frac{a_2}{r_2}\left[T_{ij} - F_2 A_{ij} + G_2 B_{ij}\right], \quad \begin{matrix}(i = 1,2)\\ (j = 1,2).\end{matrix}$$

T', γ

$$T'^* = \tau^* - (\alpha G_1 + \beta f_1)\, C_1^* - F_1 \alpha^* + G_1 \beta^*,$$

$$\gamma^* = \frac{a_2}{r_2}\left\{T'^* - (A_2 R + B_2 Q)\, C_1^* + \frac{A_2 Q(1-H_2}{\mu}\right.$$

$$\left. - \frac{(1+B_2)R}{\mu}\right\}.$$

See section A.5 for a derivation of these formulas.

F, G

$$F_1^* = G_1 C_1^*,$$

$$G_1^* = - f_1 C_1^*,$$

$$F_{ij} = G_2 C_{ij}, \qquad (i = 1, 2) \quad (j = 1, 2),$$

$$G_{ij} = - f_2 C_{ij}.$$

Q, R

$$Q^* = R C_1^* + (R + G_1) \gamma^*,$$

$$R^* = - Q C_1^* = (f_1 + Q) \gamma^*.$$

r, Δr

$$\xi_i = G_i A_i^* + f_i B_i^* - (A_i f_i - B_i G_i) C_i^*, \qquad (i = 1, 2),$$

$$r_i^* = \frac{r_i}{a_i} a_i^* + a_i \xi_i, \quad (i = 1, 2),$$

$$\xi_3 = A_2 R + B_2 Q + \alpha G_1 + \beta f_1,$$

$$\xi_4 = A_2^* R + B_2^* Q + \alpha^* G_1 + \beta^* f_1,$$

$$\xi_5 = A_2 R^* + B_2 Q^* + \alpha G_1^* + \beta F_1^*,$$

$$\Delta r^* = \frac{r_1}{a_1} \Delta a^* + \Delta a \, \xi_1 + a_2^* \xi_3 + a_2 (\xi_4 + \xi_5),$$

$$r_{ij} = \frac{r_2}{a_2} a_{ij} + a_2 (A_2 G_{ij} + A_{ij} G_2 + B_2 F_{ij} + f_2 B_{ij}), \quad (i = 1, 2) \quad (j = 1, 2).$$

P, ρ

$$P_i^* = P_i \left(\frac{a_i^*}{2a_i} - \frac{r_i^*}{r_i} + \frac{1}{2\mu} \right), \qquad (i = 1, 2),$$

$$\zeta_1 = \frac{\Delta r}{r_1 r_2} r_1^* - \frac{1}{r_2} \Delta r^*,$$

$$\zeta_2 = \frac{1}{2} \Delta b \, a_2^* + \frac{1}{2a_1} \Delta a^*,$$

$$\rho^* = \rho \left[\frac{a_2^*}{2a_2} - \frac{r_2^*}{r_2} + \frac{1}{2\mu} \right] + P_1 (\zeta_1 + \zeta_2),$$

$$P_{ij} = P_2 \left[\frac{a_{ij}}{2a_2} - \frac{r_{ij}}{r_2} - \frac{1}{r_{20}^2} \delta_{1i} \cdot \delta_{1j} \right], \qquad \begin{matrix} (i = 1, 2) \\ (j = 1, 2). \end{matrix}$$

S, σ

$$S_i^* = \frac{1}{r_i} (a_i^* - S_i r_i^*), \qquad (i = 1, 2),$$

$$\sigma^* = -\frac{\Delta r}{r_1 r_2} a_2^* + \frac{1}{r_1} \Delta a^* - \frac{\sigma}{r_2} r_2^* + S_1 \zeta_1,$$

$$S_{ij} = \frac{1}{r_2} \left[a_{ij} - S_2 r_{ij} \right], \qquad \begin{matrix} (i = 1, 2) \\ (j = 1, 2). \end{matrix}$$

This completes the set of derivatives for Lancaster's parameters. Note that in all instances, a parameter with subscript "12" is identical with that whose subscrip is "21".

A.3 The ϕ Matrix

To obtain the elements of the ϕ matrix let:

$$X_1 = 1 - H_1 F_1,$$

$$X_2 = D_1 F_1 + N_1 G_1,$$

$$X_3 = -(H_2 Q + \eta F_1)(= H_1 F_1 - H_2 F_2),$$

$$X_4 = D_2 Q + \delta F_1 + N_2 R + \nu G_1 \ (= D_2 F_2 + N_2 G_2 - D_1 F_1 - N_1 G_1),$$

$$Y_1 = -P_1 G_1,$$

$$Y_2 = 1 - S_1 F_1,$$

$$Y_3 = -(P_2 R + \rho G_1)(= P_1 G_1 - P_2 G_2),$$

$$Y_4 = -(S_2 Q + \sigma F_1)(= S_1 F_1 - S_2 F_2);$$

so that

$$\epsilon = X_1 \epsilon_o + X_2 \lambda_o + X_3 R_{20} + X_4 \dot{R}_{20},$$

$$\lambda = Y_1 \epsilon_o + Y_2 \lambda_o + Y_3 R_{20} + Y_4 \dot{R}_{20}.$$

Then, again using the asterisks to denote derivatives with respect to μ:

$$X_1^* = -(H_1 F_1^* + H_1^* F_1),$$

$$X_2^* = D_1 F_1^* + D_1^* F_1 + N_1 G_1^* + N_1^* G_1,$$

$$X_3^* = -[H_2 Q^* + H_2^* Q + \eta F_1^* + \eta^* F_1],$$

$$X_4^* = D_2 Q^* + D_2^* Q + \delta F_1^* + \delta^* F_1 + N_2 R^* + N^*_2 R + \nu G_1^* + \nu^* G_1,$$

$$Y_1^* = -[P_1^* G_1 + P_1 G_1^*],$$

$$Y_2^* = -\left[S_1 F_1^* + S_1^* F_1\right],$$

$$Y_3^* = -\left[P_2 R^* + P_2^* R + \rho G_1^* + \rho^* G_1\right],$$

$$Y_4^* = -\left[S_2 Q^* + S_2^* Q + \sigma F_1^* + \sigma^* F_1\right].$$

The subscripts on the X's and Y's cannot be dropped without ambiguity; consequently the double subscript notation is dropped and the gradients are written as row vectors, U_i^T and V_i^T:

$$\operatorname{grad}_{R_{20}} X_i = \operatorname{grad}_{\dot{R}_{20}} X_i = \operatorname{grad}_{R_{20}} Y_i = \operatorname{grad}_{\dot{R}_{20}} Y_i = 0, \quad (i = 1, 2),$$

$$\psi_1 = H_2 F_{12},$$

$$\psi_2 = D_2 F_{12} + D_{12} F_2 + N_2 G_{12},$$

$$\psi_3 = P_2 G_{12} + P_{12} G_2,$$

$$\psi_4 = S_2 F_{12} + S_{12} F_2,$$

$$U_1^T = \operatorname{grad}_{R_{20}} X_3 = -\left\{(H_2 F_{11} + H_{11} F_2) R_{20}^T + \psi_1 \dot{R}_{20}^T\right\},$$

$$U_2^T = \operatorname{grad}_{\dot{R}_{20}} X_3 = -\left\{\psi_1 R_{20}^T + (H_2 F_{22} + H_{22} F_2) \dot{R}_{20}^T\right\},$$

$$U_3^T = \operatorname{grad}_{R_{20}} X_4 = \left\{(D_2 F_{11} + D_{11} F_2 + N_2 G_{11} + N_{11} G_2) R_{20}^T + \psi_2 \dot{R}_{20}^T\right\},$$

$$U_4^T = \operatorname{grad}_{\dot{R}_{20}} X_4 = \left\{\psi_2 \dot{R}_{20}^T + (D_2 F_{22} + D_{22} F_2 + N_2 G_{22} + N_{22} G_2) \dot{R}_{20}^T\right\},$$

$$V_1^T = \text{grad}_{R_{20}} Y_3 = -\{(P_2 G_{11} + P_{11} G_2) R_{20}^T + \psi_3 \dot{R}_{20}^T\},$$

$$V_2^T = \text{grad}_{\dot{R}_{20}} Y_3 = -\{\psi_3 R_{20}^T + (P_2 G_{22} + P_{22} G_2) \dot{R}_{20}^T\},$$

$$V_3^T = \text{grad}_{R_{20}} Y_4 = -\{(S_2 F_{11} + S_{11} F_2) R_{20}^T + \psi_4 \dot{R}_{20}^T\},$$

$$V_4^T = \text{grad}_{\dot{R}_{20}} Y_4 = -\{\psi_4 R_{20}^T + (S_2 F_{22} + S_{22} F_2) \dot{R}_{20}^T\}.$$

The elements of the ϕ matrix can now be written as:

$$\frac{\partial \epsilon}{\partial \epsilon_o} = (X_1 + X_3) I + R_{20} U_1^T + \dot{R}_{20} U_3^T,$$

$$\frac{\partial \epsilon}{\partial \lambda_o} = (X_2 + X_4) I + R_{20} U_2^T + \dot{R}_{20} U_4^T,$$

$$\frac{\partial \epsilon}{\partial \mu} = X_1 * \epsilon_o + X_2 * \lambda_o + X_3 * R_{20} + X_4 * \dot{R}_{20},$$

$$\frac{\partial \lambda}{\partial \epsilon_o} = (Y_1 + Y_3) I + R_{20} V_1^T + \dot{R}_{20} V_3^T,$$

$$\frac{\partial \lambda}{\partial \lambda_o} = (Y_2 + Y_4) I + R_{20} V_2^T + \dot{R}_{20} V_4^T,$$

$$\frac{\partial \lambda}{\partial \mu} = Y_1 * \epsilon_o + Y_2 * \lambda_o + Y_3 * R_{20} + Y_4 * \dot{R}_{20}.$$

A.4 Range and Range-Rate Derivatives

The range of the second vehicle, measured from the reference vehicle, is defined by:

$$\bar{\rho} \equiv |R_2 - R_1| \equiv |\epsilon| .$$

Correspondingly, the range-rate is:

$$\dot{\bar{\rho}} = \frac{d}{dt} |\epsilon| = \frac{\epsilon \cdot \dot{\epsilon}}{|\epsilon|} = \frac{\epsilon \cdot \lambda}{|\epsilon|} .$$

Now, it can be shown that

$$\text{grad}_{\epsilon} \bar{\rho} = \frac{\partial \bar{\rho}}{\partial \epsilon} = \frac{\epsilon^T}{|\epsilon|} ,$$

$$\text{grad}_{\lambda} \bar{\rho} = \frac{\partial \bar{\rho}}{\partial \lambda} = 0,$$

$$\frac{\partial \bar{\rho}}{\partial \mu} = \frac{1}{|\epsilon|} \epsilon \cdot \frac{\partial \epsilon}{\partial \mu} , \qquad \text{(H.1)}$$

$$\text{grad}_{\epsilon} \dot{\bar{\rho}} = \frac{\partial \dot{\bar{\rho}}}{\partial \epsilon} = \frac{\lambda^T}{|\epsilon|} - \frac{\epsilon \cdot \lambda}{|\epsilon|^3} \epsilon^T = \frac{[\epsilon \times (\lambda \times \epsilon)]}{|\epsilon|^3} ,$$

$$\text{grad}_{\lambda} \dot{\bar{\rho}} = \frac{\partial \dot{\bar{\rho}}}{\partial \lambda} = \epsilon^T / |\epsilon| ,$$

and

$$\frac{\partial \dot{\bar{\rho}}}{\partial \mu} = \frac{\epsilon \cdot \frac{\partial \lambda}{\partial \mu}}{|\epsilon|} + \frac{\lambda \cdot \frac{\partial \epsilon}{\partial \mu}}{|\epsilon|} - \frac{\epsilon \cdot \lambda}{|\epsilon|^3} \left(\epsilon \cdot \frac{\partial \epsilon}{\partial \mu}\right)$$

$$= \frac{\epsilon \cdot \frac{\partial \lambda}{\partial \mu}}{|\epsilon|} + \frac{1}{|\epsilon|^3} \left(\epsilon \cdot \left[\frac{\partial \epsilon}{\partial \mu} \times (\epsilon \times \lambda)\right]\right) . \qquad \text{(H.2)}$$

These derivatives are to be evaluated, using expressions found in Ref. [2] for ϵ and λ, and the expressions given in the preceding section for $\partial \epsilon / \partial \mu$ and $\partial \lambda / \partial \mu$. Either of the expressions for $\frac{\partial \dot{\bar{\rho}}}{\partial \epsilon}$ and $\frac{\partial \dot{\bar{\rho}}}{\partial \mu}$ may be used.

A.5 Derivations

In this section is a derivation for the expressions given in eq. (A.3), for r_1 and r_2; a justification for the interpretation of the gradients in eq. (A.12) as row vectors; and, a derivation of the expression given for γ^* in section A.2.

1. From reference [2] we have

$$\sqrt{\frac{\mu}{a^3}}\, T = C + A\,(1-\cos C) - B \sin C, \quad (L.1), \tag{A.1}$$

with $C = E - E_o$; as a consequence $\dot{C} = \dot{E}$. (A.2)

In addition, for two body orbits,

$$\sqrt{\frac{\mu}{a^3}}\, T = E - e \sin E, \tag{A.3}$$

and

$$r = a\,(1-e \cos E). \tag{A.4}$$

Differentiating eqs. (A.1) and (A.3), with respect to T, and making use of eqs. (A.2) and (A.4), it is found that,

$$(1 + A \sin C - B \cos C)\,\dot{C} = (1-e \cos E)\,\dot{E}\ ; \tag{A.5}$$

or

$$\frac{r}{a} = 1 + A \sin C - B \cos C = 1 + GA + fB. \tag{A.6}$$

2. Consider the two column vectors,

$$Y = \begin{pmatrix} y_1 \\ y_2 \\ y_3 \end{pmatrix}, \text{ and } \quad X = \begin{pmatrix} x_1 \\ x_2 \\ x_3 \end{pmatrix} . \tag{A.7}$$

These are related by: $Y = f(x_1, x_2, x_3)\, X$; wherein f is a scalar. (A.8)

Let the 3x3 partial derivative matrix be defined as:

$$\frac{\partial Y}{\partial X} \equiv \left(\frac{\partial y_i}{\partial x_j}\right), \quad \begin{cases} i = \text{row number} \\ j = \text{column number.} \end{cases} \tag{A.9}$$

Since eq. (A.8) can be written as

$$y_i = f(x_1, x_2, x_3)\, x_i, \tag{A.10}$$

then

$$\frac{\partial y_i}{\partial x_j} = f\,\delta_{ij} + x_i \frac{\partial f}{\partial x_j}. \tag{A.11}$$

If $\frac{\partial f}{\partial x_i}$ is defined as a row vector, then

$$\frac{\partial f}{\partial x} = \left(\frac{\partial f}{\partial x_1}, \frac{\partial f}{\partial x_2}, \frac{\partial f}{\partial x_3}\right) = \text{grad}_X f, \tag{A.12}$$

and consequently from eq. (A.9),

$$\frac{\partial Y}{\partial X} = f\,I + \left(x_i \frac{\partial f}{\partial x_j}\right) = f\,I + \begin{pmatrix} x_1 \\ x_2 \\ x_3 \end{pmatrix} \left(\frac{\partial f}{\partial x_1}, \frac{\partial f}{\partial x_2}, \frac{\partial f}{\partial x_3}\right)$$

$$= f\,I + X\,\text{grad}_X f. \tag{A.13}$$

For the problem considered here the dependence of f, on the components of X, is restricted: Setting $x = |X|$, f is a function of only the two scalars x and $X \cdot A$, where A is a vector independent of X: i.e.

$$f = f(x, X \cdot A), \tag{A.14}$$

hence

$$\frac{\partial f}{\partial X} = \frac{\partial f}{\partial x}\frac{X^T}{x} + \frac{\partial f}{\partial (X \cdot A)} A^T. \tag{A.15}$$

The vector X is either R_{20} (or $\dot{R}_{20}$) and the scalar product is $R_{20} \cdot \dot{R}_{20}$. Consequently A^T will be $\dot{R}_{20}^T$ or (R_{20}^T) according to whether the gradient is with respect to R_{20} or $\dot{R}_{20}$.

3. Derivation of γ^*:

From Reference [2]:

$$T' \equiv \tau + \beta G_1 - \alpha F_1 = \gamma + A' (1-\cos \gamma) - B' \sin \gamma, \text{ (see L4 and L8);} \quad (A.16)$$

hence

$$\gamma^* (1+A' \sin \gamma - B' \cos \gamma) = T'^* - A'^* (1-\cos \gamma) + B'^* \sin \gamma. \quad (A.17)$$

However,

$$A' = A_2 \cos C_1 + B_2 \sin C_1, \quad (L9)$$

$$B' = B_2 \cos C_1 - A_2 \sin C_1, \quad (L10)$$

and

$$\gamma = C_2 - C_1. \quad (A.18)$$

Now, the coefficient of γ^* is readily shown to be r_2/a_2. Furthermore, the differentiation of A' and B' with respect to μ yields

$$A'^* = B' C_1^* + A_2^* \cos C_1 + B_2^* \sin C_1,$$

$$B'^* = - A' C_1^* + B_2^* \cos C_1 - A_2^* \sin C_1 . \quad (A.19)$$

A substitution of these expressions into the A'*, B'* terms, in eq. (A.17), yields (after some trignometric manipulations) for these terms,

$$- \left[A_2 R + B_2 Q \right] C_1^* - A_2^* Q + B_2^* R, \quad (A.20)$$

consequently,

$$\gamma^* = \frac{a_2}{r_2} \left\{ T'^* - (A_2 R + B_2 Q)\, C_1^* - A_2^* Q + B_2^* R \right\} , \qquad (A.21)$$

where T'^* is obtained from the first expression given for T', in eq. (A.16);

$$T'^* = \tau^* + \beta^* G_1 + \beta G_1^* - \alpha^* F_1 - \alpha F_1^* . \qquad (A.22)$$

Now, the expressions given for T'^*_1 and γ^*, in section A.3, are obtained from eqs. (A.21) and (A.22), using the equation previously obtained for A_2^*, B_2^*, α^* β^*, F_1^* and G_1^*.

APPENDIX B

AN ANALYTICAL DESCRIPTION OF THE TETHERED (TWO) BODIES PROBLEM (INCLUDING AN ELASTIC TETHER)

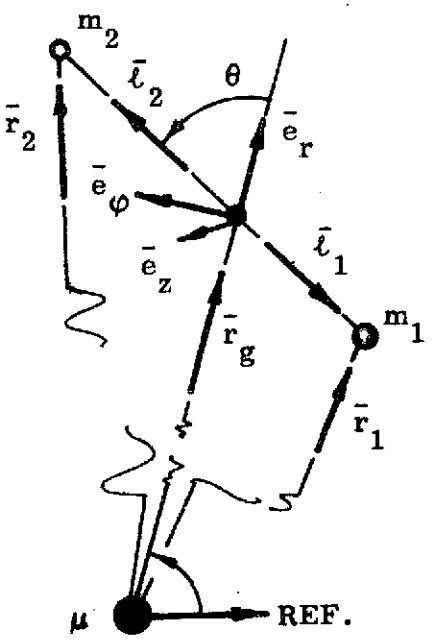

Fig. B.1. Tethered System Geometry. Note: $\ell + \ell = \ell$; $\bar{r}_i = \bar{r}_g + \ell_i$, (i = 1,2).

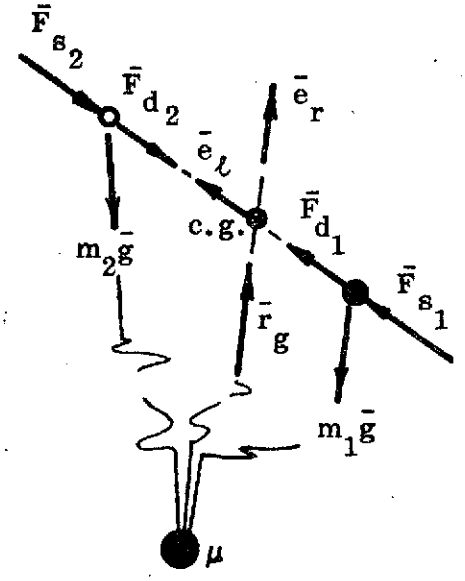

Fig. B.2. Forces assumed for Tethered Systems.

B.1 Introduction.

A two-body, tether connected, mass system is in orbital motion about the primary μ. The forces action on each body are those due to:

(1) the gravitational attraction of μ,

(2) the elasticity of the tether.

The physical properties of the tether are assumed to be such that the forces are; (1) proportional to the stretch (producing an elastic restoring force); and, (2) proportional to the rate of extension (leading to a damping force).

Assuming linear elasticity these force magnitudes are represented as:

$$F_s \sim k\,(\ell - \ell_o), \tag{B.1a}$$

for the spring force; and

$$F_d \sim c\,\dot{\ell}, \tag{B.1b}$$

for the damping force; wherein k, c are the constants of proportionality; ℓ_o is the unstretched length (of the tether); ℓ, $\dot{\ell}$ are the instantaneous length and rate-change of length.

B.2 Equations of Motion.

Writing the dynamical equations of motion to describe the tether action (i.e., body m_2 relative to m_1), then;

$$\ddot{\bar{\ell}} \equiv \ddot{\bar{\ell}}_2 - \ddot{\bar{\ell}}_1 = (\ddot{\bar{r}}_2 - \ddot{\bar{r}}_g) - (\ddot{\bar{r}}_1 - \ddot{\bar{r}}_g) \equiv \ddot{\bar{r}}_2 - \ddot{\bar{r}}_1 = -\mu\left(\frac{\bar{r}_2}{r_2^3} - \frac{\bar{r}_1}{r_1^3}\right) + \frac{\bar{F}_{s2}}{m_2} - \frac{\bar{F}_{s1}}{m_1}$$

$$+ \frac{\bar{F}_{d2}}{m_2} - \frac{\bar{F}_{d1}}{m_1}. \qquad \text{(B.2a)}$$

In these expressions $\bar{F}_{s_i} = F_s (-1)^{1+i} \bar{e}_\ell$, $\bar{F}_{d_i} = F_d (-1)^{1+i} \bar{e}_\ell$, consequently, after some manipulation, one finds

$$\ddot{\bar{\ell}} = -\mu\left(\frac{\bar{r}_2}{r_2^3} - \frac{\bar{r}_1}{r_1^3}\right) - \bar{\ell}\left[\frac{k}{m_2}\left(1 - \frac{\ell_o}{\ell}\right) + \frac{c}{m_2}\frac{\dot{\ell}}{\ell}\right]\left(\frac{M}{m_1}\right), \qquad \text{(B.2b)}$$

where $M \equiv \Sigma m_i$, and $\dot{\bar{\ell}}$ is presumed parallel to $\bar{\ell}$, generally. In addition it is assumed that $\ell \geq \ell_o$ throughout a specific motion.

For purposes of description (and for numerical work) the "unit operator", $\mathcal{K}$, is introduced into these expressions as a control quantity. It has been presumed that the elastic tether cannot accept compression, hence the operator is as shown below:

$$\text{if } \ell \geq \ell_o, \quad \mathcal{K} = 1;$$

or,

$$\text{if } \ell \leq \ell_o, \quad \mathcal{K} = 0. \qquad \text{(B.3)}$$

When the logic for $\mathcal{K}$ is included with the forces (F_s and F_d) then the tether does not enter into the dynamics of the problem when there is no stretch present.

B.3 Kinematics.

To complete the problem in consistant coordinates the acceleration $(\ddot{\bar{\ell}})$ will be described, kinematically. In this regard, since,

$$\bar{\ell} \equiv \ell\, \bar{e}_\ell$$

then

$$\dot{\bar{\ell}} \equiv \dot{\ell}\, \bar{e}_\ell + \ell\, \dot{\bar{e}}_\ell \equiv \dot{\ell}\, \bar{e}_\ell + (\bar{\omega}_\ell \times \bar{e}_\ell)\, \ell\,,$$

wherein $\bar{\omega}_\ell$ is the angular velocity of the triad (of which $\bar{e}_\ell$ is a member) relative to inertial space. Here $\bar{\omega}_\ell \equiv (\dot{\theta} + \dot{\varphi}_g)\, \bar{e}_z$, hence

$$\dot{\bar{\ell}} = \dot{\ell}\, \bar{e}_\ell + \ell\, (\dot{\theta} + \dot{\varphi}_g)\, \bar{e}_n,$$

since $\bar{e}_n \equiv \bar{e}_z \times \bar{e}_\ell$. Correspondingly, it can be shown that the acceleration is:

$$\ddot{\bar{\ell}} = \left[\ddot{\ell} - \ell\, (\dot{\theta} + \dot{\varphi}_g)^2\right] \bar{e}_\ell + \left[2\dot{\ell}\, (\dot{\theta} + \dot{\varphi}_g) + \ell\, (\ddot{\theta} + \ddot{\varphi}_g)\right] \bar{e}_n\,. \tag{B.4}$$

Eq. (B.4) is used in place of the acceleration in (say) eqs.(B.2).

B.4 The Gravity Force.

Before eq. (B.2) can be represented in a consistent format it is necessary to express the gravity terms compatible with the other quantities present. In this regard write the position vectors $(\bar{r}_i)$ as

$$\bar{r}_i \equiv \bar{r}_g + \bar{\ell}_i = r_g\, \bar{e}_r + (-1)^i \ell_i\, \bar{e}_\ell\,. \tag{B.5}$$

As a consequence of this,

$$\bar{r}_i^{\,2} = r_g^{\,2} + 2\bar{r}_g \cdot \bar{e}_\ell\, (-1)^i\, \ell_i + \ell_i^{\,2};$$

or,

$$\frac{r_i}{r_g} = \left[1 + 2\,(-1)^i\, \frac{\ell_i}{r_g} \cos\theta + \left(\frac{\ell_i}{r_g}\right)^2\right]^{1/2} \equiv \Delta_i\,, \tag{B.6}$$

for (i = 1, 2).

Also, for component projections, if each $\bar{r}_i$ is projected onto $\bar{e}_\ell$ and $\bar{e}_n$ (respectively), and in turn, then (see eq. (B.5)):

$$\bar{r}_i \cdot \bar{e}_\ell = r_g \cos\theta + (-1)^i \ell_i ,$$

and

$$\bar{r}_i \cdot \bar{e}_n = - r_g \sin\theta, \quad (i = 1, 2). \tag{B.7}$$

Making use of eqs. (B.6), (B.7), it is evident that the specific gravity force may be written as follows:

$$-\frac{\mu}{r_g^3}\left(\frac{\bar{r}_2}{\Delta_2^3} - \frac{\bar{r}_1}{\Delta_1^3}\right) = -\frac{\mu}{r_g^3}\left\{\left[r_g \cos\theta\left(\frac{1}{\Delta_2^3} - \frac{1}{\Delta_1^3}\right) + \frac{\ell_2}{\Delta_2^3} + \frac{\ell_1}{\Delta_1^3}\right]\bar{e}_\ell + \left[r_g \sin\theta\left(\frac{1}{\Delta_2^3} - \frac{1}{\Delta_1^3}\right)\right]\bar{e}_n\right\}, \tag{B.8}$$

wherein eqs. (B.5) have been employed for the description of $\bar{r}_i$.

B.5 Component Equations of Motion.

Having described the various quantities making up the dynamical equations of motion one can, now, obtain the components of these, parallel to ($\bar{e}_\ell$, $\bar{e}_n$), directly. Thus, after substitution and separation it is found that the scalar expressions are:

$$\ddot{\ell} - \ell(\dot{\theta} + \dot{\varphi}_g)^2 = -\frac{\mu}{r_g^3}\left[r_g \cos\theta\left(\frac{1}{\Delta_2^3} - \frac{1}{\Delta_1^3}\right) + \frac{\ell_1}{\Delta_1^3} + \frac{\ell_2}{\Delta_2^3}\right] - (\mathcal{K})\,\ell\left[\frac{k}{m_2}\left(1 - \frac{\ell_o}{\ell}\right) + \frac{c}{m_2}\frac{\dot{\ell}}{\ell}\right]\frac{M}{m_1},$$

and

$$2\dot{\ell}\,(\dot{\theta}+\dot{\varphi}_g)+\ell\,(\ddot{\theta}+\ddot{\varphi}_g)=\frac{\mu}{r_g^{\,3}}\left[r_g\sin\theta\left(\frac{1}{\Delta_2^{\,3}}-\frac{1}{\Delta_1^{\,3}}\right)\right], \qquad \text{(B.9)}$$

respectively.

Here $\mathcal{K}$ is the unit operator described in eqs. (B.3), $M \equiv \sum_1^2 m_i$; the remaining terms have been described previously.

For identification purposes, the terms on the left side of these expressions arise from the kinematic description of the acceleration while those on the right are due to the forces assumed to be present. The terms with "μ" as a multiplier are the associated gravitational quantities, while those multiplied by the operator ($\mathcal{K}$) are due to the elasticity of the system (the "external" forces). It is well to keep track of these various components so that one can identify the influence each plays in subsequent approximations.

B.6 Approximations to the Equations of Motion.

Due to the non-linearity, and coupling between the coordinates, in eqs. (B.9), it is a usual practice to introduce various approximations to reduce these equations.

(NOTE: In the work which follows, the operator "$\mathcal{K}$" is deleted, for convenience, with the tacit understanding that it can be recalled and inserted as desired).

(a) One of the first approximations to be introduced is that associated with the $\Delta_i^{\,3}$ quantities (see eq. (B.6) for this definition). Since $\ell_i \ll r_g$ then it is reasonable to replace these with the following ($1^{\underline{st}}$ order) expressions:

$$\Delta_i^{\,3} \equiv \left[1+2\,(-1)^i\frac{\ell_i}{r_g}\cos\theta+\frac{\ell_i^{\,2}}{r_g^{\,2}}\right]^{-3/2} \cong 1-3\,(-1)^i\frac{\ell_i}{r_g}\cos\theta+\text{H.O.T.}, \qquad \text{(B.10)}$$

for $(i = 1, 2)$.

As a consequence the component equations (B.9) may be recast into the forms:

$$\ddot{\ell} - \ell\,(\dot{\theta}+\dot{\varphi})^2 \cong \frac{\mu\ell}{2r_g^{\,3}}\left[1+3\cos 2\theta\right] - \left[\frac{k}{\tilde{m}}\,(\ell-\ell_o) + \frac{c}{\tilde{m}}\dot{\ell}\right],$$

and

$$\ell\,(\ddot{\theta}+\ddot{\varphi}) + 2\dot{\ell}\,(\dot{\theta}+\dot{\varphi}) \cong -\frac{3\mu\ell}{2r_g^{\,3}}\sin 2\theta\,; \tag{B.11}$$

wherein the $(\sim)_g$ has been dropped from φ_g (for concise notation) and $\tilde{m} \equiv \frac{m_1 m_2}{\Sigma m_i}$, $(i = 1,2)$ is the reduced mass of the system.

(b) The tether length (ℓ) has an unstretched (ℓ_o) and a stretch $(\varkappa)$ length; these bear the following relation to one another:

Letting $\quad \ell \equiv \ell_o + \varkappa$; then $\dot{\ell} = \dot{\varkappa}$ and $\ddot{\ell} = \ddot{\varkappa}$.

Now, if $\quad \sigma \equiv \frac{\varkappa}{\ell_o}$; then, $\dot{\sigma} \equiv \frac{\dot{\varkappa}}{\ell_o}$, and $\ddot{\sigma} \equiv \frac{\ddot{\varkappa}}{\ell_o}$.

Making appropriate substitutions into eqs. (B.11), it is easily demonstrated that those expressions reduce to:

$$\ddot{\sigma} + \frac{c}{\tilde{m}}\,\dot{\sigma} + \left\{\frac{k}{\tilde{m}} - (\dot{\theta}+\dot{\varphi})^2 - \frac{\mu}{2r_g^{\,3}}\,(1+3\cos 2\theta)\right\}\sigma \cong \frac{\mu}{2r_g^{\,3}}\,(1+3\cos 2\theta) + (\dot{\theta}+\dot{\varphi})^2,$$

and

$$\ddot{\theta} + \frac{2\dot{\sigma}}{1+\sigma}\,\dot{\theta} + \frac{3\mu}{2r_g^{\,3}}\sin 2\theta \cong -\left(\ddot{\varphi} + \frac{2\dot{\sigma}}{1+\sigma}\,\dot{\varphi}\right). \tag{B.12}$$

It is interesting to recognize that the last equation, here, can be recast into the form:

$$\frac{d}{dt}\left[(1+\sigma)^2\,(\dot{\theta}+\dot{\varphi})\right] \cong -\,(1+\sigma)^2\,\frac{3\mu}{2r_g^{\,3}}\sin 2\theta, \tag{B.12a}$$

which is indicative of variations in the relative moment of momentum for this situation.

In these expressions the origin of each component term is quite evident. Those with the μ-multipliers are gravitational components while those containing k, c are due to the (assumed) elasticity of the tether. All other elements in the equations are a consequence of the (defined) accelerations.

(c) The Small Displacement Approximation is introduced, next, to render the differential equations more amenable to mathematical manipulation. For this reduction it will be assumed that products and powers of the primary variants and their derivatives are of negligible order; and, that corresponding to this,

$$\sin\theta \cong \theta,\ \sin 2\theta \cong 2\theta,\ \cos 2\theta \cong 1.0.$$

If these constraints are introduced, and if the quantity $(1+\sigma)^{-1}$ is approximated by an appropriate series expansion, then it is found that eqs. (B.12) reduce to:

$$\ddot{\sigma} + \frac{c}{m}\dot{\sigma} + \left\{\frac{k}{m} - \left(\dot{\varphi}^2 + 2\frac{\mu}{r_g^3}\right)\right\}\sigma - (2\dot{\varphi})\,\dot{\theta} \cong \left(\frac{2\mu}{r_g^3} + \dot{\varphi}^2\right),$$

and

$$\ddot{\theta} + \frac{3\mu}{r_g^3}\theta + (2\dot{\varphi})\,\dot{\sigma} \cong -\ddot{\varphi}. \qquad \text{(B.13)}$$

Eqs. (B.13) should represent the essence of the problem, subject to the restrictions imposed on the motion. Though the non-linearity has been removed (except through the influence of the orbit, via the $\dot{\varphi}$, etc. terms) the expressions remain coupled, kinematically, through the Coriolis terms. This coupling suggests a difficulty in obtaining analytic solutions for the problem, in general.

The origin of the various terms in each of these equations remains clear. That is, the terms involving the parameter k, c are due to the elasticity of the tether (with the unit operator, $\mathcal{K}$, still implied); while those terms involving μ are due to gravitational effects. All other terms (involving σ, θ and their derivatives) arise from the definition of acceleration impressed onto the formulation.

These are a consequence of the frame of reference representation selected for the problem.

B.7 Description of Spring and Damping Constants.

The representation of k and c used here can be described by the following brief discussion:

Since the spring force is presumed to be proportional to the "stretch" $(\ell-\ell_o)$, then for a general situation (as depicted by the sketch below) the force-displacement diagram may appear as shown.

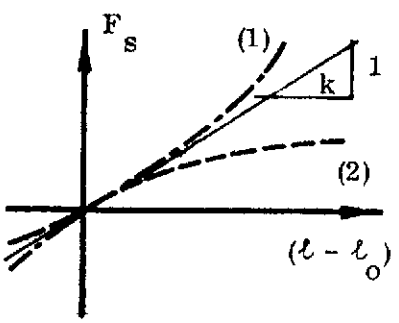

Fig. B.3. Description of Spring Force.

Here the springs [(1), (2)] are non-linear, with (1) representing a "hard" spring while (2) suggests a "soft" one. For either representation the "linear spring" is represented by the "constant" variation of force with displacement (see the vicinity of the origin). That is, the spring constant (k) will be described by the slope of the curve in its linear range. Hence,

$$k \equiv \frac{\Delta F_s}{\Delta(\ell-\ell_o)} \quad \text{(a constant).}$$

A representation for the "linear damping force" parallels the ideas set down above for the linear spring force. Here, the damping is (linearly) related to the rate of change of ℓ $(\dot{\ell})$; hence, a representation of this situation may be expressed , as noted below.

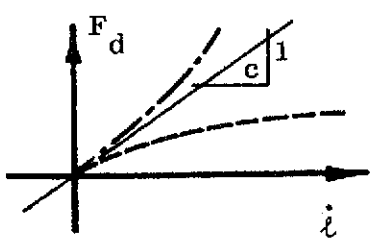

Fig. B.4. Damping Force.

As before, the law governing the change in force, with $\dot{\ell}$, away from the origin is not of concern. The presumption of linear elasticity considers only the region in which the constant of proportionality (c)

is apparent. Thus,

$$c \cong \frac{\Delta F_d}{\Delta \dot{\ell}} \quad \text{(a constant)}.$$

The ideas of linear elasticity are not unduly restrictive since the concept is, or may be adapted to, a rather realistic physical situation. If the linearity is not physically evident in the system, it might be mechanically reproduced to a significant degree.

B.8 Gravity Gradient.

To acquire an expression for the gradient of the gravitational effect, on these systems, it should be recognized that the point mass gravitational parameter μ can be equated to "g" by

$$\mu = - gr^2 ,$$

where g, r are "local" values. These quantities can be related, simply, to some reference level of g (say g_o) by means of

$$g = g_o \left(\frac{r_o}{r} \right)^2 .$$

Now, with $\mu = \mu(r)$ it is evident that the "gradient of g", is:

$$\frac{dg}{dr} = \frac{2\mu}{r^3} = - \frac{g}{r} , \qquad \text{(B.14)}$$

where g, r are (still) local valued quantities.

B.9 Special Cases.

(a) Circular Orbit

As a special case for the motion of a tethered body system, assume a reference (or base) orbit which is circular. In this regard, then, r_g and $\dot{\varphi}_g$ become constants. As a consequence the orbital speed is:

$$V_g \equiv \sqrt{\left(\frac{\mu}{r_g}\right)} = r_g \dot{\varphi}_g ,$$

hence,

$$\dot{\varphi}_g^{\,2} = \frac{\mu}{r_g^{\,3}} . \tag{B.15}$$

If this relationship is incorporated into the motion equations (B.13), one finds:

$$\ddot{\sigma} + \frac{c}{\tilde{m}} \dot{\sigma} + \left[\frac{k}{\tilde{m}} - 3\dot{\varphi}^2\right] \sigma \cong 2\dot{\varphi}\,\dot{\theta} + 3\dot{\varphi}^2 ,$$

and

$$\ddot{\theta} + 3\dot{\varphi}^2 \theta \cong -2\dot{\varphi}\,\dot{\theta} . \tag{B.16}$$

This set of reduced, specialized expressions may be examined to describe various aspects of the small displacement variations of the tethered system. A look at eqs. (B.15) will show that these remain coupled (through the Coriolis terms) and are not amenable to a simple analytic solution.

(b) Static State .

When the tethered system reaches its "static state" the physical motions cease and an equilibrium condition is attained. Examining eqs. (B.16) for this situation one notes that

$$\sigma_{st} = \frac{3\dot{\varphi}^2}{\frac{k}{\tilde{m}} - 3\dot{\varphi}^2} = \frac{1}{\frac{k/\tilde{m}}{3\dot{\varphi}^2} - 1}$$

or, defining $\Omega^2 \equiv \dfrac{k/\tilde{m}}{3\dot{\varphi}^2}$, then

$$\sigma_{st} = \frac{1}{\Omega^2 - 1} . \tag{B.17a}$$

From the second expression in eq. (B.16) it is immediately apparent that

$$\theta_{st} = 0. \tag{B.17b}$$

(c) Uncoupled, Independent Motions.

In order to describe the types of motion which the tethered system may acquire, consider the cases wherein the governing expressions (B.16) are uncoupled. In this regard it may be assumed that these occur independently - not necessarily as a physically realized situation, but as a vehicle of convenience here.

(1) Motion in σ alone ($\theta \Rightarrow \theta_{st}$)

From eq. (B.16), it is seen that this motion may be described by:

$$\ddot{\sigma} + \frac{c}{\tilde{m}}\dot{\sigma} + \left[\frac{k}{\tilde{m}} - 3\dot{\varphi}^2\right]\sigma = 3\dot{\varphi}^2,$$

or, using the definition of $\Omega^2 \left(\equiv \frac{k/\tilde{m}}{3\dot{\varphi}^2}\right)$, then

$$\ddot{\sigma} + \frac{c}{\tilde{m}}\dot{\sigma} + 3\dot{\varphi}^2\,[\Omega^2 - 1]\,\sigma \cong 3\dot{\varphi}^2 . \tag{B.18a}$$

Now, since there is a non-zero static displacement (σ_{st}) apparent to the system, let the motion be described about this as a datum, or

$$\sigma \equiv \sigma_{st} + \tilde{\sigma},$$

where $\tilde{\sigma}$ defines the displacement about (σ_{st}). Then eq. (B.18a) can be cast into the form

$$\ddot{\tilde{\sigma}} + \frac{c}{\tilde{m}}\dot{\tilde{\sigma}} + 3\dot{\varphi}^2\,[\Omega^2 - 1]\,(\sigma_{st} + \tilde{\sigma}) \cong 3\dot{\varphi}^2;$$

and, inserting eq. (B.16a), then

$$\ddot{\tilde{\sigma}} + \frac{c}{m}\dot{\tilde{\sigma}} + 3\dot{\varphi}^2 (\Omega^2 - 1)\,\tilde{\sigma} \cong 0 \ . \qquad \text{(B.18b)}$$

(2) Motion in θ alone ($\sigma \Rightarrow \sigma_{st}$)

From eqs. (B.15) it is evident that this case is represented by

$$\ddot{\theta} + 3\dot{\varphi}^2 \theta \cong 0 \ , \qquad \text{(B.19)}$$

which is indicative of a Simple Harmonic Motion (SHM) for this variable. What is implied (here) is that the system oscillates in the vicinity of θ_{st} ($\equiv 0$), and suggests a motion for the tethered system which would appear much like that of a pendulum.

B.10 A General Description of the Approximate Motions.

For the sake of completeness a brief discussion of the motion types depicted by eqs. (B.18, B.19) is presented here.

The general form of these equations can be expressed as,

$$\ddot{\xi} + \frac{c}{m}\dot{\xi} + \frac{k}{m}\xi = f(t) \ , \qquad \text{(B.20a)}$$

where the constants (k, c, m) have the same meaning as before, but $f(t)$ can be construed as some elementary driving function. The basic motion type, for $\xi(t)$, is acquired from the solution to the homogeneous equation above. The characteristics for that expression are immediately recognized to be

$$s_{1,2} = -\frac{c}{2m} \pm \sqrt{\left(\frac{c}{2m}\right)^2 - \frac{k}{m}} \ . \qquad \text{(B.20b)}$$

For simple harmonic motion (c=0), one recognizes that the "natural frequency" of this system is defined by

$$\omega_n \equiv \sqrt{\frac{k}{m}} \ , \qquad \text{(B.20c)}$$

while the "damped frequency, ($c \neq 0$), is described by,

$$\omega_d \equiv \omega_n \sqrt{\frac{c^2}{4mk} - 1} \quad . \tag{B.20d}$$

Recalling that the critical damping constant for such a system can be defined as

$$c_c = 2\sqrt{mk} \quad ; \tag{B.20e}$$

then, rewriting eq. (B.20b), as

$$s_{1,2} = \left[-\frac{c}{c_c} \pm i \sqrt{1 - \left(\frac{c}{c_c}\right)^2} \right] \omega_n \, , \tag{B.21a}$$

it should be evident that these characteristics are indicative of a damped sinusoidal motion so long as $(c/c_c) < 1.0$. Representing eq. (B.21a) symbolically as

$$s_{1,2} = a \pm i\, \omega_d \, , \tag{B.21b}$$

it should be evident that the Argand diagram for this root set can be represented as shown below, for a given set of constants (a, ω_d).

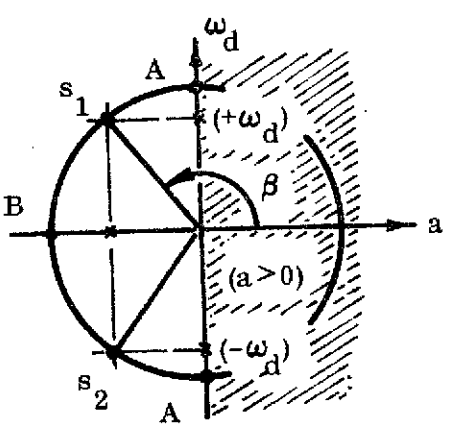

Fig. B.5. Argand Diagram for a "Roots" Representation.

The case depicted on this Argand diagram ($s_{1,2}$) is for a "damped oscillation", i.e., $a < 0$. When $a > 0$, the motion is one which is being fed energy through a "negative-damping parameter". The angle β (shown here) can be described as

$$\pm \beta = \tan^{-1}\left(\frac{\sqrt{1-(c/c_c)^2}}{-c/c_c} \right) . \tag{B.21c}$$

Also, points "A" are indicative of $c=0$ (hence

$\omega_d = \omega_n$); and point "B" represents $\omega_d = 0$ (hence $c = c_c$), a no oscillation case.

From eq. (B.21b) it should be evident that the period of any oscillatory motion is related to ω_d while the time constant for such motions will be related to the parameter "a". Recalling that the period of an oscillatory motion is described by

$$T = \frac{2\pi}{\omega} ,$$

then it is evident that the period of the damped motion is:

$$T_d = \frac{2\pi}{\omega_d} = \frac{T_n}{\sqrt{1-\left(\frac{c}{c_c}\right)^2}} , \qquad \text{(B.22a)}$$

where T_n describes the pure oscillatory case. As a consequence of this statement it is apparent that increased damping causes an increment in the timing of the motion.

With the time constant defined as that time interval required for the amplitude to reduce the amount (1/e); and, with the envelope for these damped motion described by

$$\xi_e \equiv \xi_o \exp (at),$$

where ξ_o is some (initial, or t=0) value of the amplitude (true or hypothetical), then the time to reach the desired displacement (say $\xi_e(t_c)$) can be determined from

$$\xi_e(t_c) \equiv \frac{\xi_o}{e} = \xi_o \exp (at_c).$$

As a consequence of this mathematical statement, the time constant (t_c) is:

$$t_c = \frac{1}{a} . \qquad \text{(B.22b)}$$

Making an appropriate substitution for "a", it follows that

$$t_c = -\frac{1}{\omega_n \frac{c}{c_c}} = -\frac{\sqrt{1-\left(\frac{c}{c_c}\right)^2}}{\omega_d \left(\frac{c}{c_c}\right)} \quad . \tag{B.22c}$$

It should be apparent, now, that eqs. (B.22) represent a method by which the damping, etc. for the system could be determined, experimentally.

APPENDIX C

NET FORCE DEVELOPED BY A STABILIZED, ORBITING TETHERED SYSTEM

C.1 Introduction.

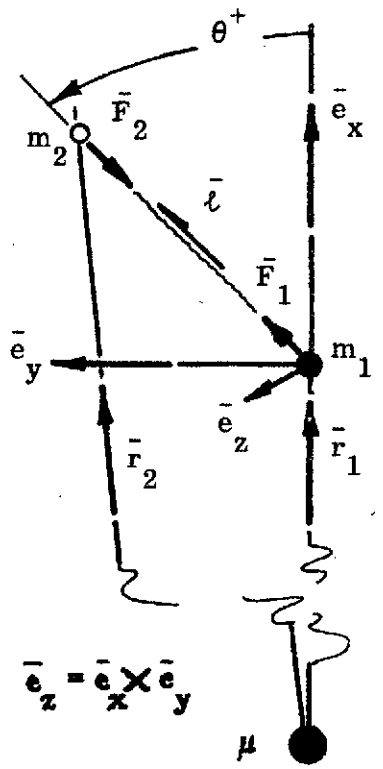

Fig. C.1. Sketch Describing the Tethered Bodies System.

The general system to be studied here consists of two mass particles (m_i) in motion about a central attracting mass particle (μ). The two orbiting particles are connected by a tether ($\bar{\ell}$), and the system is oriented, relative to the local vertical according to θ.

The entire system has a motion, ω, about μ; however, the state of m_2 is referred to the moving triad ($\bar{e}_x$, $\bar{e}_y$, $\bar{e}_z$) which has its origin at m_1. As a consequence, this is the relative state of motion for m_2.

For this example the tether is considered to be a non-elastic member; the line of action for the force in the tether is along the line joining the m_i; and there is no mutual attraction between the particles (m_i).

In order to achieve a desired degree of mathematical tractability it will be assumed that m_1 moves along a circular orbit (at the rate, $\dot{\varphi}$); also, the motion of m_2 will be confined to the (x, y)- or motion-plane.

C.2 Equations of Motion.

The two particles are presumed to have Keplerian motion (each) with the position vectors related by

$$\bar{r}_2 = \bar{r}_1 + \bar{\ell}, \tag{C.1}$$

as shown on Fig. C.1.

From classical mechanics the differential equations describing these motions are:

$$m_i \ddot{\bar{r}}_i = -\frac{\mu m_i}{r_i^3}\,\bar{r}_i + \bar{F}_i, \qquad (i = 1,2) \tag{C.2}$$

leading directly to the corresponding relative displacement equation,

$$\ddot{\bar{\ell}} = \frac{\mu}{r_1^3}\left[(1-\Delta^{-3})\,\bar{r}_1 - \Delta^{-3}\,\bar{\ell}\right] - (F/\tilde{m})\,\bar{e}_\ell\,; \tag{C.3}$$

wherein $\tilde{m} = \dfrac{m_1 m_2}{m_1 + m_2}$ (the reduced mass*); F is the force magnitude (in the tether), and Δ is defined as;

$$\Delta \equiv \frac{r_2}{r_1} = \left(1 + 2\frac{\ell}{r_1}\cos\theta + \frac{\ell^2}{r_1^2}\right)^{1/2};$$

here, $\bar{e}_\ell$ is the unit vector, $\bar{\ell}/\ell$.

C.2.1 Kinematic Definition of $\ddot{\bar{\ell}}$.

Since the relative displacement vector ($\bar{\ell}$) can be defined as

$$\bar{\ell} \equiv \ell\,\bar{e}_\ell = (x\bar{e}_x + y\,\bar{e}_y + z\,\bar{e}_z), \tag{C.4}$$

then replacing the triad ($\bar{e}_x$, $\bar{e}_y$, $\bar{e}_z$) by another, designated as ($\bar{e}_\ell$, $\bar{e}_n$, $\bar{e}_z$) one can differentiate (C.4) to acquire a description of the velocity, $\dot{\bar{\ell}}$. That is,

*It should be recognized that if $m_1 \gg m_2$, then $\tilde{m} \cong m_2$. The symbol $\tilde{m}$ is retained here for the more general inference.

$$\dot{\bar{\ell}} = \dot{\ell}\,\bar{e}_\ell \equiv \dot{\ell}\,\bar{e}_\ell + \ell\,(\bar{\omega} \times \bar{e}_\ell), \tag{C.5a}$$

with $\bar{\omega} \equiv \omega \bar{e}_z$. An alternate, and more familiar, expression for $\dot{\bar{\ell}}$ is,

$$\dot{\bar{\ell}} = \dot{\ell}\,\bar{e}_\ell + \ell\,\omega \bar{e}_n . \tag{C.5b}$$

Carrying the differentiation one step further, to provide for $\ddot{\bar{\ell}}$, it can be shown that

$$\ddot{\bar{\ell}} = (\ddot{\ell} - \ell\,\omega^2)\,\bar{e}_\ell + (2\,\dot{\ell}\,\omega + \ell\,\dot{\omega})\,\bar{e}_n$$

$$= (\ddot{\ell} - \ell\,\omega^2)\,\bar{e}_\ell + \frac{1}{\ell}\,\frac{d}{dt}\,(\ell^2 \omega). \tag{C.5c}$$

Here $\bar{\omega}$ is understood to be the angular velocity vector for the triad $(\bar{e}_\ell, \bar{e}_n, \bar{e}_z)$.

Next, separating $\bar{r}_1$ into proper components; that is,

$$\bar{r}_1 = r_1\,(\cos\theta \bar{e}_\ell - \sin\theta\,\bar{e}_n); \tag{C.6}$$

then eqs. (C.3) and (C.5c) may be joined, and written as the scalar set given by:

$$(\ddot{\ell} - \ell\,\omega^2) = \frac{\mu}{r_1^3}\left[(1 - \Delta^{-3})\cos\theta - \Delta^{-3}\,\frac{\ell}{r_1}\right] r_1 - F/\tilde{m}, \tag{C.7a}$$

and

$$(2\dot{\ell}\,\omega + \ell\,\dot{\omega}) = \frac{1}{\ell}\,\frac{d}{dt}\,(\ell^2 \omega) = \frac{\mu}{r_1^3}\,(1 - \Delta^{-3})\,r_1 \sin\theta . \tag{C.7b}$$

Equations (C.7) are a general set of governing differential equations which may be examined for the in-plane motion of the tethered system.

C.3 Special Case (Circular Orbit).

Here the reference orbit is selected (arbitrarily) to be circular. For this case those quantities which are affected are those noted below:

$$r_1 = \text{constant};\ \dot{\varphi}_1 = \text{constant};$$

$$\dot{r}_1 = \ddot{\varphi}_1 = 0;\ \text{and}\ \dot{\varphi}_1^{\,2} = \frac{\mu}{r_1^{\,3}}\ .$$

Introducing these conditions into eqs. (C.7) it is found that they may be recast as:

$$\frac{\ddot{\ell}}{r_1\dot{\varphi}_1^{\,2}} = \frac{\ell}{r_1} + \left[(1-\Delta^{-3})\cos\theta - \Delta^{-3}\,\frac{\ell}{r_1}\right] + \frac{F/\tilde{m}}{r_1\dot{\varphi}_1^{\,2}}\ , \tag{C.8a}$$

and

$$\frac{2\dot{\ell}\,(\dot{\varphi}_1+\dot{\theta})}{r_1\dot{\varphi}_1} + \frac{\ell\,\ddot{\theta}}{r_1\dot{\varphi}_1^{\,2}} = (1-\Delta^{-3})\sin\theta\ . \tag{C.8b}$$

Introducing the dimensionless variable $\lambda\ (\equiv \ell/r_1)$, and transforming the independent variable, t, to φ_1, via $\varphi_1 = \dot{\varphi}_1 t$, it follows that eqs. (C.8) may be reduced to:

$$\lambda'' = \lambda + (1-\Delta^{-3})\cos\theta - \lambda\Delta^{-3} - \tau\ , \tag{C.9a}$$

and

$$\lambda'\,(1+\theta') + \lambda\,\theta'' = (1-\Delta^{-3})\sin\theta\ ; \tag{C.9b}$$

wherein

$$\Delta \equiv \left[1 + 2\lambda\cos\theta + \lambda^2\right]^{1/2}\ ,$$

and

$$\tau \equiv \frac{F/\tilde{m}}{r_1\dot{\varphi}_1^{\,2}}\ .$$

Eqs. (C.9) describe the in-plane motion of a tethered system, in dimensionless variables, for the system influenced by a central field gravity-gradient and subjected to a tether force which constrains the movement of the suspended masses.

C.4 A Gravity-Gradient Stabilized System.

Suppose that this tethered system is "stabilized" in gravity-gradient. That is, the tether is "vertically aligned", and has no relative motion ($\dot{\ell} = \dot{\theta} = 0$). For this case the mass (m_2) is in "equilibrium" with the tether force counteracting the net force due to external influences.

The question to be answered here is, "how much force acts on m_2, due to external effects, in its stabilized configuration?"

For this situation let $\theta = \pi$ and $\dot{\theta} = \dot{\ell} = 0$; consequently eqs. (C.9) may be further reduced to yield:

$$\tau = (\lambda - 1)(1 - \Delta^{-3}) , \tag{C.10a}$$

wherein.

$$\Delta = (1 - 2\lambda + \lambda^2)^{1/2} = (1 - \lambda).$$

Clearing eq. (C.10a) one finds that $\tau \equiv \tau(\lambda)$ becomes

$$\tau = \left(\frac{\lambda}{1-\lambda}\right)\left(3 + \lambda\,\frac{\lambda}{1-\lambda}\right), \tag{C.10b}$$

expressing the net force in the system in terms of λ ($\equiv \ell/r_1$). This last expression may be interpreted as the resultant force acting on $\tilde{m}$ ($\cong m_2$). In effect this force represents the resultant of the actions produced from gravitational attraction and centrifugal force (this can be recognized from a study of the physical system, and as verified from (say) eqs. (C.8)). The quantity, $\lambda/(1-\lambda)$, has an interesting interpretation. Expanded

$$\frac{\lambda}{1-\lambda} = \frac{\ell}{r_1 - \ell} = \frac{r_1 - r_2}{r_2} ,$$

where the r_i ($i = 1, 2$) define the orbits traced out by the masses, m_i. Here, as before, r_1 is the reference (circular) orbit while r_2 describes the trajectory for m_2. (See Fig. C.1 for concurrence).

Equation (C.10b), being dimensionless, is a general form expression useful for any orbital altitude where one central point of mass attraction is a reasonable assumption. The force parameter (τ) relates the specific force ($F/\tilde{m} \cong F/m_2$) to the centrifugal force ($CF_1 = r_1\dot{\varphi}_1^2$); consequently, a graphing of $\tau(\lambda)$ should provide useful general information which is readily transformed into useful particular information, for this system.

C.5 The Specific Force in Gee's.

Rather than present the force (τ) in its present dimensionless units, suppose this parameter is to be given in (say) earth gee's. That is, let $\tau \equiv \tau(g_o)$, where g_o is the acceleration of gravity, at the geoid's surface (r_o), in whatever units one would desire.

Returning to eq. (C.10b) it is apparent that there

$$\tau \equiv \frac{F/\tilde{m}}{r_1\dot{\varphi}_1^2} \equiv G(\lambda) \cong \frac{F/m_2}{r_1\dot{\varphi}_1^2} \quad , \tag{C.11}$$

where $G(\lambda)$ represents the right-hand side of that expression. As a consequence, from eq. (C.11), the specific tether force,

$$F/m_2 = r_1\dot{\varphi}_1^2 \, [G(\lambda)] \, . \tag{C.12}$$

Since the gravitational acceleration (g_o) can be defined by μ/r_o^2, then with $r_1\dot{\varphi}_1^2 \equiv \mu/r_1^2$, eq. (C.12) can be written as,

$$\frac{F/m_2}{g_o} \equiv \tilde{F}_g = \frac{r_o^2}{r_1^2} \, [G(\lambda)] \, , \tag{C.13a}$$

relating the specific force to some g_o value. In this expression r_o is the earth's (average) radius while r_1 is the radius of the circular orbit for m_1. Here $\tilde{F}_g$ is dimensionless, as is $\lambda \equiv \ell/r_1$ (tether length in ratio to r_1).

In expanded form the result from above is given by,

$$\tilde{F}_g = \left(\frac{\lambda}{1-\lambda}\right)\left[3+\lambda\left(\frac{\lambda}{1-\lambda}\right)\right]\left(\frac{r_o}{r_1}\right)^2, \qquad \text{(C.13b)}$$

relating F/m_2 (for $m_1 \gg m_2$) to (say) the earth's gravitational acceleration at the average surface radius, r_o.

APPENDIX D

TRANSFER ORBIT PROPERTIES FOR A PARTICLE RELEASED FROM A STABILIZED TETHER SYSTEM

D.1 Introduction.

In this appendix the problem situation to be examined has to do with the orbits developed by a particle released from a stabilized gravity-gradient tethered system. The characteristics of these orbits will be defined, for different initial state conditions. For comparison purposes, a Hohmann type transfer will be described in order to determine the relative "costs" for each mode.

D.2 The Tether Initiated Orbit.

For this study the two particles (m_j) are assumed to be gravity-gradient stabilized (moving at given ω_1 ($\equiv \dot{\varphi}_1$) rate, with tether aligned in a radial direction).

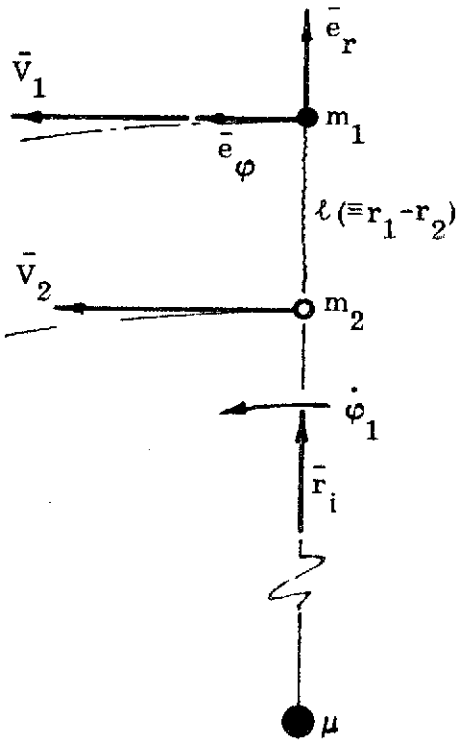

Fig. D.1(a). Geometry.

Particle m_1 (assuming $m_1 \gg m_2$) moves on a circular path (r_1), at a speed $V_1 \left(V_1 \equiv V_c \equiv \sqrt{\mu / r_1} \right)$ - thus, initial conditions for the two orbits are known (a priori).

Using an inelastic tether, and without other disturbances presumed, one can determine the orbit parameters which describe the subsequent motion for m_2, after release.

D.3 Kinematic Descriptions.

According to the assumptions outlined above, the initial orbital speeds are:

$$V_1 \left(\equiv V_{1_o} \right) = r_1 \omega_1 = \sqrt{\mu / r_1} , \qquad \text{(D.1a)}$$

and

$$V_{2_o} = r_2 \, \omega_1 \, . \tag{D.1b}$$

As a general definition of orbital speed, recall that:

$$V^2 = \left(\frac{\mu}{h}\right)^2 \left[1 + \epsilon^2 + 2\epsilon \cos \varphi \right], \tag{D.2}$$

where, in general,

$h \equiv$ specific angular momentum,

$$= \left|\bar{r} \times \bar{V}\right| = rV_{\varphi} = r^2 \dot{\varphi} \; ; \tag{D.3}$$

wherein,

$\varphi \equiv$ position angle (measured from pericenter).

$\dot{\varphi} \equiv$ local angular rate for an orbiting mass particle.

D.4 Orbit Conditions.

In order to ascertain where on a given free orbit the released particle might be, the following conditions are noted:

(a) If $V < V_c$ (local) the motion is for a particle above its orbital minor axis (for closed paths); or, it is moving on the apocentric portion of its ellipse.

(b) If $V > V_c$ (local) the motion on an ellipse is below (on the pericentric side) of the minor axis (assuming closed figures).

(c) If $V = V_c$ (local), the particle is at the minor axis position (where $r \equiv a$); or, the motion may be circular.

D.5 Initial (Release) Conditions.

Suppose that m_2 is released from its tether at some initial time without any relative motion. Consequently, the subsequent path for m_2 would be on an ellipse, with the following local (initial) conditions (see Fig. D.1):

$$@\ t = t_o; \qquad r_{2_o} = r_1 - \ell, \qquad V_{2_o} (\equiv V_2) = r_{2_o}\,\omega_1,$$

$$\text{or} \qquad V_{2_o} = (r_1 - \ell)\,\omega_1 = V_1 - \ell\,\omega_1.$$

Expressed in terms of the dimensionless parameter (λ),

$$V_{2_o} = V_1\,(1 - \ell/r_1) \equiv V_1\,(1 - \lambda), \tag{D.4}$$

where $\lambda \equiv \ell/r_1$.

The corresponding specific angular momentum (h_2) for this situation is:

$$h_{2_o} = r_2 V_2 = (r_1 - \ell)\left(1 - \frac{\ell}{r_1}\right) V_1 = r_1 V_1 \left(1 - \frac{\ell}{r_1}\right)^2,$$

or

$$h_{2_o} = h_1\,(1 - \lambda)^2. \tag{D.5}$$

D.5.1 Tether Tension.

When the system is stabilized m_2 must be "supported" by a tension in the tether. Considering the nature of the stabilized system, then the equations of motion for m_2 (see eqs. (C.2), Appendix C) may be written as:

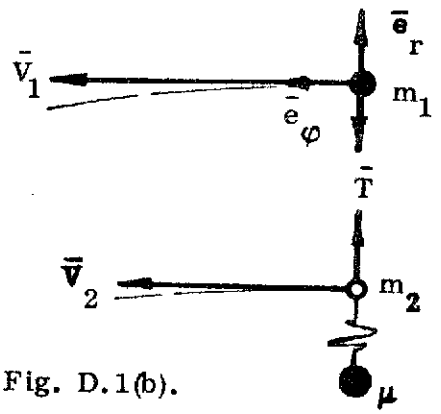

Fig. D.1(b).

$$\cancel{\ddot{r}_2}^{\,0} - r_2\,\omega_1^{\,2} = -\frac{\mu}{r_2^{\,2}} + \frac{T}{m_2}, \qquad (r_2 \equiv \text{constant})$$

or, after rearranging and making substitutions from above,

$$\frac{T}{m_2} = \frac{V_1^{\,2}}{r_1}\left[\left(\frac{r_1}{r_2}\right)^2 - \frac{r_2}{r_1}\right]. \tag{D.6a}$$

Here T is the line tension, other terms are defined previously. Now, since $r_2 = r_1 - \ell = r_1\,(1 - \lambda)$, for the stabilized system, then after substitution eq. (D.6a) is:

$$\frac{T}{m_2} = \frac{V_1^2}{r_1}\,\lambda\left[\frac{3}{1-\lambda} + \left(\frac{\lambda}{1-\lambda}\right)^2\right]. \qquad \text{(D.6b)}$$

D.6 Orbit Parameters.

The analysis here is concerned with determining the parameters which describe the "free orbit" produced by simply 'cutting' the tether - releasing m_2 from its stabilized tethered state.

D.6.1 Eccentricity.

Knowing the initial (t_o^-) state for m_2, then at release (t_o^+), the free orbit's eccentricity can be determined from eq. (D.4), written as,

$$V_{2_o}^2 = \left(\frac{\mu}{h_{2_o}}\right)^2\left[1 + \epsilon_2^2 + 2\epsilon_2 \cos\varphi_{2_o}\right], \qquad \text{(D.7)}$$

wherein φ_{2_o} will describe the apocenter of the free orbit, (i.e. $V_{2_o} < V_c$ (local), see section D.4).

Now, from eq. (D.7),

$$V_{2_o} = \frac{\mu}{h_2}(1 - \epsilon_2);$$

or, using eqs. (D.4, D.5),

$$V_1(1-\lambda) = \frac{\mu(1-\epsilon_2)}{h_1(1-\lambda)^2},$$

wherein $V_1 \equiv \sqrt{\mu/r_1}$ and, $h_1 = r_1 V_1$. After some manipulation, it is found that

$$\epsilon_2 = \lambda\left[3(1-\lambda) + \lambda^2\right]. \qquad \text{(D.8)}$$

D.6.2 Semi-major Axis.

To describe the "size" of the orbit for m_2, consider the specific energy (E_2) expression:

$$E_2 = \frac{V_2^2}{2} - \frac{\mu}{r_2} = -\frac{\mu}{2a_2} \quad , \tag{D.9}$$

which can be evaluated at any convenient location on the m_2-orbit. Thus, with the known initial conditions,

$$V_{2_o} = V_1 (1-\lambda), \quad r_{2_o} = r_1 (1-\lambda),$$

substituted into eq. (D.9) it is found that,

$$\frac{a_2}{r_1} = \frac{1-\lambda}{1+3\lambda(1-\lambda)+\lambda^3} = \frac{1-\lambda}{2-(1-\lambda)^3} \quad . \tag{D.10}$$

D.6.3 Peri-Radius.

To determine the peri-radius for the m_2-orbit, after release from the tether, recall that from the polar conic expression this radius is described by:

$$r_p = a\,(1-\epsilon). \tag{D.11a}$$

Consequently, it follows that $\frac{r_p}{r_1} = \frac{a}{r_1}(1-\epsilon)$, for this problem; and, using eq. (D.10),

$$\frac{r_{p_2}}{r_1} = \frac{(1-\lambda)^4}{1+3\lambda(1-\lambda)+\lambda^3} = \frac{(1-\lambda)^4}{2-(1-\lambda)^3} \quad . \tag{D.11b}$$

D.6.4 Time to Reach Peri-Radius.

With the conditions of the problem such that the initial point is at apo-center, then the time required to reach the (new) pericenter in half-a-period.

Now, to describe the time for this operation, note that

$$t = \pi \sqrt{\frac{a_2^3}{\mu}} = \frac{\text{Period}_1}{2} \sqrt{\frac{a_2^3}{r_1^3}} \quad ,$$

or,

$$\frac{t}{\text{Period}_1} = \frac{1}{2} \left[\frac{(1-\lambda)}{1+3\lambda\,(1-\lambda)+\lambda^3} \right]^{3/2} = \frac{1}{2} \left[\frac{1-\lambda}{2-(1-\lambda)^3} \right]^{3/2} . \tag{D.12}$$

D.6.5 Speed at Peri-Radius.

The speed of m_2 when it reaches its new peri-center may be found from the statement for conservation of specific moment of momentum. For example, on the m_2 orbit ,

$$(rV)_{peri} = (rV)_{apo} ;$$

hence, symbolically,

$$V_{p_2} = \frac{r_{a_2}}{r_1} \frac{r_1}{r_{p_2}} V_{a_2} .$$

Now, if eq. (D.11b), and the initial values are introduced, then

$$\frac{V_{p_2}}{V_1} = \frac{1+3\lambda\,(1-\lambda)+\lambda^3}{(1-\lambda)^2} = \frac{2-(1-\lambda)^3}{(1-\lambda)^2} . \tag{D.13}$$

D.7 Summary.

The various parameter, conditions, etc. examined above were for the case of a gravity-gradient stabilized system hanging in a vertical direction toward the attracting primary (μ). In this regard the free orbit transfer was initiated from an apocenter.

For the converse situation of a stabilized system hanging away from the primary the initial point becomes a pericenter, and the "free" orbit has a subsequent motion toward apocenter. To account for the differences in these two modes of operation the following table has been prepared. There the corresponding parameters, etc. are listed (as equations) for reference purposes.

TABLE D.I

ORBIT TRANSFERS FROM A STABILIZED ORBIT

Init. Point (description)	Initial State		Specific Moment of Momentum	Free Orbit Conditions and Parameters
	$r_{2_o}/r_1 =$	$V_{2_o}/V_1 =$	h_{2_o}/h_1	Specific Tension T/m_2
Apo-center[(a)]	$1-\lambda$	$1-\lambda$	$(1-\lambda)^2$	$\frac{V_1^2}{r_1}\lambda\left[\frac{3}{1-\lambda}+\left(\frac{\lambda}{1-\lambda}\right)^2\right]$
Peri-center	$1+\lambda$	$1+\lambda$	$(1+\lambda)^2$	$\frac{V_1^2}{r_1}\lambda\left[\frac{3}{1+\lambda}+\left(\frac{\lambda}{1+\lambda}\right)^2\right]$

(a) System described in the development

Init. Point (description)	Free Orbit Conditions and Parameters			
	Eccentricity ϵ_2	Semi-Major axis, a_2/r_1	Peri-Radius r_{p_2}/r_1	Apo-Radius r_{a_2}/r_1
Apo-center	$\lambda\left[3(1-\lambda)+\lambda^2\right]$	$\frac{1-\lambda}{2-(1-\lambda)^3}$	$\frac{(1-\lambda)^4}{2-(1-\lambda)^3}$	$1-\lambda$
Peri-center	$\lambda\left[3(1+\lambda)+\lambda^2\right]$	$\frac{1+\lambda}{2-(1+\lambda)^3}$	$1+\lambda$	$\frac{(1+\lambda)^4}{2-(1+\lambda)^3}$

(table continued on next page)

TABLE D.I (cont)

ORBIT TRANSFERS FROM A STABILIZED ORBIT

Init. Point (description)	Free Orbit Conditions and Parameters		
	Time[(b)] to Complete Transfer, t/Period$_1$	Pericenter Speed V_{p_2}/V_1	Apocenter Speed V_{a_2}/V_1
Apo-center	$\frac{1}{2}\left[\frac{1-\lambda}{2-(1-\lambda)^3}\right]^{\frac{3}{2}}$	$\frac{2-(1-\lambda)^3}{(1-\lambda)^2}$	$1-\lambda$
Peri-center	$\frac{1}{2}\left[\frac{1+\lambda}{2-(1+\lambda)^3}\right]^{\frac{3}{2}}$	$1+\lambda$	$\frac{2-(1+\lambda)^3}{(1+\lambda)^2}$

(b) Hohmann type transfers are used; $(\text{Period})_1 \equiv 2\pi/\dot{\varphi}_1$.

D.8 A Hohmann Transfer.

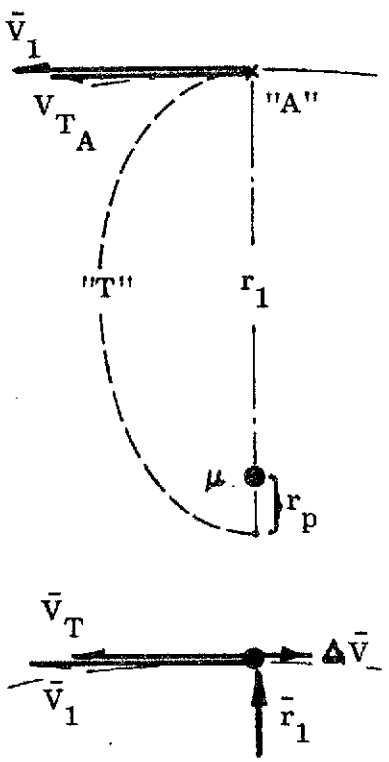

Fig. D.2. The Hohmann Transfer.

The purpose here is to describe the Δv (impulse) requirement needed to achieve a "transfer" from the initial (r_1) orbit to a peri-center (r_p) of known dimension. Since the initial point "A" (see Fig. D.2) lies on a circular orbit then the transfer is obviously a Hohmann transfer; thus, the energy change is to be a minimum.

The motivation for this computation is to determine the $\Delta\bar{v}$ "cost", and to use this as a measure of comparison with other transfer modes.

To initiate the transfer, the velocity on path r_1 ($\bar{V}_1$) has added to it an impulse ($\Delta\bar{v}$); this should produce a "proper, initial

velocity $(\bar{V}_T)$" for the transfer ellipse. Thus, for the transfer orbit,

$$\bar{V}_{T_A} \equiv \bar{V}_1 + \Delta\bar{v} \,. \tag{D.14}$$

On the transfer path the specific energy (E_T) can be expressed by;

$$E_T = \frac{V_{T_A}^2}{2} - \frac{\mu}{r_1} = -\frac{\mu}{2a_T} \quad ; \tag{D.15a}$$

which refers to the initial point "A".

The specific energy for a particle on path (r_1) is recognized to be

$$E_1 = \frac{V_1^2}{2} - \frac{\mu}{r_1} = -\frac{\mu}{2a_1} \,,$$

but $a_1 \equiv r_1$, so

$$E_1 = \frac{V_1^2}{2} - V_c^2 \equiv \frac{-V_1^2}{2} \,. \tag{D.15b}$$

For the evaluation of eq. (D.15a), recognize that

$$2a_T \equiv r_1 + r_p = r_1 \left(1 + \frac{r_p}{r_1}\right); \tag{D.16}$$

while the speed term, appearing there, is

$$V_{T_A} = \left| \bar{V}_1 + \Delta\bar{v} \right| . \tag{D.17}$$

With r_p given, a priori, then eq. (D.15a) can be used - in conjunction with eqs. (D.16, D.17) - to calculate (or correlate) (r_p) with the speed component, Δv. That is, making appropriate substitutions, and solving the resulting quadratic, it is found that the required increment in speed (Δv) is defined by

$$\Delta v = V_1 \left\{ 1 \pm \sqrt{\frac{2r_p/r_1}{1+(r_p/r_1)}} \right\}, \tag{D.18a}$$

wherein $1 \geq \frac{r_p}{r_1} > 0$. Now by necessity the negative sign is selected; consequently,

$$\Delta v = V_1 \left\{ 1 - \sqrt{\frac{2r_p/r_1}{1+(r_p/r_1)}} \right\} ; \tag{D.18b}$$

and, accordingly,

$$V_{T_A} = V_1 - \Delta v. \tag{D.18c}$$

Equations (D.18) have shown that the size of the impulse, to be applied at a selected point on the circular trajectory, is directly related to the size of the pericenter (r_p) which is to be produced.

D.8.1 The Change in Energy.

The change in specific energy (ΔE) necessary to get onto the transfer path from the circular orbit (r_1) is readily determined. That is, if one defines this change in specific energy as

$$\Delta E \equiv E_T - E_1 , \tag{D.19}$$

where E_T and E_1 are expressed in eqs. (D.15a, D.15b); then it is easy to show that

$$\Delta E = \frac{-\mu}{2r_1} \left(\frac{1-(r_p/r_1)}{1+(r_p/r_1)} \right) \tag{D.20a}$$

or, in ratio to E_1, (see eq. (D.15b)),

$$\frac{\Delta E}{E_1} = \frac{1-r_p/r_1}{1+r_p/r_1} . \tag{D.20b}$$

D.8.2 The Specific Energy Describing the Transfer Path.

With the result given in eqs. (D.20), eq. (D.19) can be recast as follows:

Since,

$$\frac{E_T}{E_1} \equiv 1 + \frac{\Delta E}{E_1} ,$$

then, when eq. (D.20b) is employed here, one finds

$$\frac{E_T}{E_1} = \frac{2}{1+(r_p/r_1)} . \tag{D.21}$$

Equation (D.21) defines the ratio of specific energy (on the transfer path to that on the initial, circular orbit) and does so in terms of the desired pericenter radius ratio (r_p/r_1).

D.9 The Effect of Tether Length (ℓ) on an Orbit Transfer.

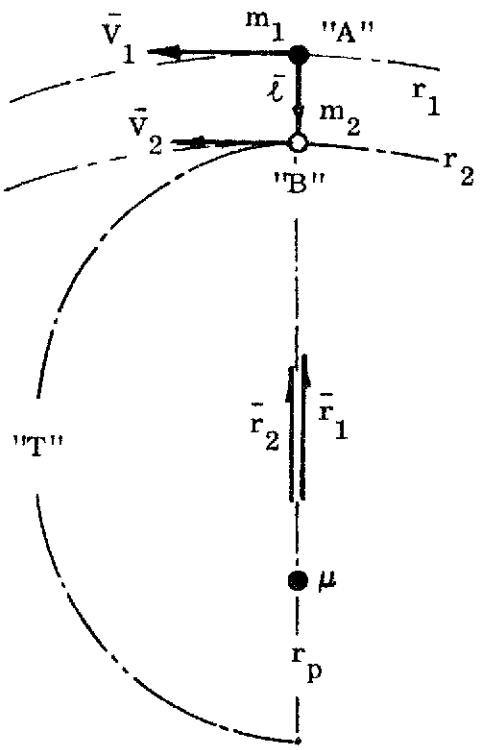

Fig. D.3. Transfer from a Stable Tether Configuration.

The concept applied here differs, to some small extent, from that examined in the foregoing section in that the initial point (now) is not on the circle (r_1) but on the concentric path (r_2). See Fig. D.3.

For this problem situation it is presumed that the particle (m_2) is moving along the path (r_2) at a speed

$$V_2 \equiv r_2 \dot{\varphi}_1 . \tag{D.22}$$

Here $\dot{\varphi}_1$ is the angular speed of particle m_1 moving along the circle, r_1. The two particles are connected by the tether and m_2 is stabilized in gravity gradient. Since the two mass particles are radially aligned (by assumption) then they must move at a same angular rate, $\dot{\varphi}_1$.

When relating the two particles (m_i), with respect to specific energy levels, it is apparent that:

(1) The specific energy for path r_1 is given by eq. (D.15b) above.

(2) The energy level for m_2, at "B", but on the transfer path ("T"), is defined by;

$$E_2 = \frac{V_B^2}{2} - \frac{\mu}{r_2} = -\frac{\mu}{2a_T} \quad , \tag{D.23}$$

where $V_B = V_2 \equiv r_2\dot{\varphi}_1$ (see eq. (D.22)), $r_2 = r_1 - \ell$ and $2a_T \equiv r_2 + r_p$.

After making appropriate substitutions (recognizing that $\frac{r_2}{r_1} = 1 - \frac{\ell}{r_1} \equiv 1-\lambda$) then it can be shown that eq. (D.23) reduces to the following "equivalent" statement:

$$\frac{r_p}{r_1} = \frac{(1-\lambda)^4}{2-(1-\lambda)^3} \quad . \tag{D.24}$$

(Note that this statement matches that given by eq. (D.11b)).

Equation (D.24) defines the size of the peri-radius produced by a particle released from a stabilized gravity-gradient orbit, having been suspended from m_1 by a tether of length ℓ. A comparison of eqs. (D.24) and (D.18a) would relate the tether length (ℓ) to a required Δv (impulse) producing a same pericenter radius in the presence of a central point attraction (μ).

In order to relate the two (equivalent) transfers (that due to the impulse, producing the Hohmann transfer to r_p, and that produced from a suspended mass (m_2)), the specific energy ratio for the present scheme is needed. For this, the energy ratio (E_2/E_1) is described from eqs. (D.15b) and (D.23); or,

$$\frac{E_2}{E_1} = -\frac{V_B^2}{V_1^2} + 2\,\frac{r_1}{r_2} = -\frac{(r_2\dot{\varphi}_1)^2}{(r_1\dot{\varphi}_1)^2} + 2\,\frac{r_1}{r_2} \quad , \tag{D.25a}$$

since $V_B \equiv r_2\dot{\varphi}_1$ and $V_1^2 = \mu/r_1$. Recalling that $r_2/r_1 = 1 - \ell/r_1$ ($\equiv 1-\lambda$), then eq. (D.25a) becomes,

$$\frac{E_2}{E_1} = \frac{2-(1-\lambda)^3}{(1-\lambda)} \equiv \frac{E_T}{E_1} . \qquad \text{(D.25b)}$$

From here, eq. (D.25b) is to be compared with eq. (D.21) to ascertain the energy levels describing the impulsive (Δv) and the tethered mass transfer modes.

In order to complete the comparison between these systems one last ratio is needed, that for specific energy change. In this regard define the energy change (from the orbit of m_1 to that of m_2 during transfer) as

$$\Delta E = E_2 - E_1 ;$$

and the energy ratio as,

$$\frac{\Delta E}{E_1} = \frac{E_2}{E_1} - 1 = \frac{\lambda\,(4-3\lambda+\lambda^2)}{1-\lambda} . \qquad \text{(D.26)}$$

Equations (D.26) and (D.20b) describe like energy ratios, for the tethered and impulsive transfer schemes, respectively. When these results are compared, for a same pericenter radius, one finds the energy change brought about by the "extended tether" system transfer, and that by a particle undertaking a Hohmann transfer.

D.10 Summary.

The expressions developed in section (D.9) were for a transfer situation whereby the initial position was an assumed apocenter. In order to illustrate the converse case, of a transfer from a pericenter to an apocenter, the table below was constructed to display the appropriate expressions. There one will find these two situations described, in equation format.

TABLE D. II.

ORBIT TRANSFER COMPARISONS

Initial Position description (Apo-Peri-center)	Hohmann Transfer		
	$\Delta\bar{V}$ described[a]	$\frac{\Delta v}{V_1}$ (Impulse Magnitude)[b]	Energy Change $\Delta E/E_1$
Apo-center ($r_a = r_1$)	$\lvert\bar{V}_T\rvert = V_1 - \Delta v$	$\frac{\Delta v}{V_1} = 1 - \sqrt{\frac{2(r_p/r_1)}{1+(r_p/r_1)}}$	$\frac{1-(r_p/r_1)}{1+(r_p/r_1)}$
Peri-center ($r_p = r_1$)	$\lvert\bar{V}_T\rvert = V_1 + \Delta v$	$\frac{\Delta v}{V_1} = -1 + \sqrt{\frac{2(r_a/r_1)}{1+(r_a/r_1)}}$	$\frac{1-(r_a/r_1)}{1+(r_a/r_1)}$

(a) $\pm$ sgn infers with (+), against (-) $\bar{V}_1$;

(b) r_p, r_a define peri- apo-radii, resp; r_1 is the initial (circular) radius.

Initial Position description (Apo-Peri-center)	Hohmann Transfer	Transfer from a Stable Gravity-Gradient Position		
	Orbit Energy Ratio E_T/E_1	Terminal Position[c]	Energy Change $\Delta E/E_1$	Orbit Energy Ratio E_T/E_1
Apo-center ($r_a = r_1$)	$\frac{2}{1+(r_p/r_1)}$	$\frac{r_p}{r_1} = \frac{(1-\lambda)^4}{2-(1-\lambda)^3}$	$\frac{\lambda(4-3\lambda+\lambda^2}{1-\lambda}$	$\frac{2-(1-\lambda)^3}{1-\lambda}$
Peri-center ($r_p = r_1$)	$\frac{2}{1+(r_a/r_1)}$	$\frac{r_a}{r_1} = \frac{(1+\lambda)^4}{2-(1+\lambda)^3}$	$\frac{-\lambda(4+3\lambda+\lambda^2}{1+\lambda}$	$\frac{2-(1+\lambda)^3}{1+\lambda}$

(c) defined in terms of the tether length ($\ell = \lambda r_1$);

(d) $\Delta E \equiv E_T - E_1$, ($E_T \equiv$ energy on transfer orbit).

D.11 Effect of Initial Speed on Tethered Transfers.

Since the orbital transfer, from a tethered position, could be initiated from a radial position, with a radial speed, the next development will describe this influence on the maneuver.

In addition to the system "hanging vertically", now it will have a speed component ($\pm \dot{x}$), along the aligned tether. Consequently, the resultant speed (V'_2) is different from the stabilized position speed (V_2). (See Fig. D.4).

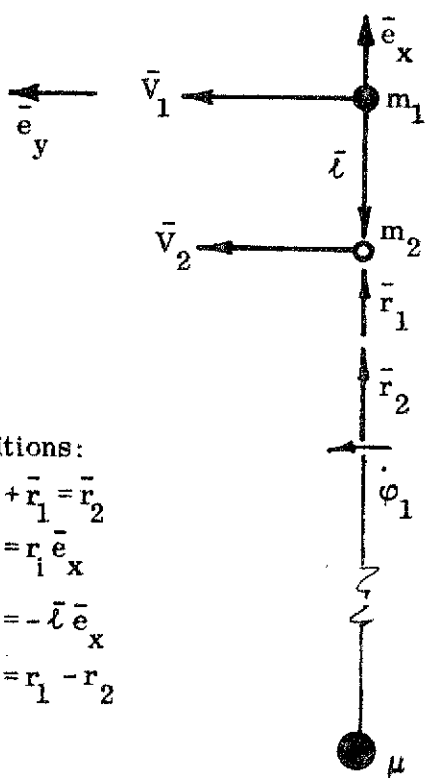

Definitions:

$\bar{\ell} + \bar{r}_1 = \bar{r}_2$

$\bar{r}_i = r_i \bar{e}_x$

$\bar{\ell} = -\ell \bar{e}_x$

$\ell = r_1 - r_2$

Fig. D.4. Geometry for Transfer, with $\dot{\bar{x}}$.

The system, stabilized in gravity gradient, moves at the angular speed ω_1 ($\equiv \dot{\varphi}_1$), hence

$$V_1 = r_1 \dot{\varphi}_1,$$

$$V_2 \equiv r_2 \dot{\varphi}_1,$$

$$\therefore \quad \frac{r_2}{r_1} = \frac{V_2}{V_1}.$$

Assuming that m_2 is suspended from m_1 and located between* m_1 and μ, then

$$r_1 \equiv |\bar{r}_1| = r_2 + \ell,$$

or

$$\left(\frac{r_2}{r_1}\right)_o = 1 - \frac{\ell_o}{r_1} \equiv 1 - \lambda_o, \qquad \text{(D.27)}$$

where $(\sim)_o$ implies an initial value.

Now, if m_2 is to have an added velocity component $\dot{\bar{x}}_o$ ($\equiv \pm \dot{x}_o \bar{e}_x$), then the initial velocity vector ($\bar{V}'_{2_o}$) is defined by,

*An analysis for $\overline{m_1}$ located between m_2 and μ would be described in analogous fashion.

$$\bar{V}'_{2_o} \equiv \bar{V}_{2_o} + \dot{\bar{x}}_o \,. \tag{D.28}$$

Now, in view of eq. (D.28), it follows that the speed V'_2 is

$$V'_{2_o} = \left(V_2^{\,2} + \dot{x}^2 + 2\bar{V}_2 \cdot \dot{\bar{x}} \right)_o^{1/2} ,$$

where, by definition $\bar{V}_{2_o} \cdot \dot{\bar{x}}_o \equiv 0$ (orthogonal vectors, here), hence

$$V'_{2_o} = \left(V_2^{\,2} + \dot{x}^2 \right)_o^{1/2} \,. \tag{D.29a}$$

In ratio to $|\bar{V}_1|$, one has

$$\left(\frac{V'_2}{V_1} \right)_o = \left(\frac{V_2^{\,2}}{V_1^{\,2}} + \frac{\dot{x}^2}{V_1^{\,2}} \right)_o^{1/2} = \left[(1-\lambda)^2 + \left(\frac{\pm \dot{x}}{V_1} \right)^2 \right]_o^{1/2} ,$$

so,

$$\left(\frac{V'_2}{V_1} \right)_o \equiv \left[(1-\lambda)^2 + (\lambda')^2 \right]_o^{1/2} , \quad \text{where } \lambda'_o \equiv \frac{|\dot{\bar{x}}_o|}{V_1} \,. \tag{D.29b}$$

(Note that $(V_2/V_1)^2 \equiv (1-\lambda)^2$ infers the transfer mode with m_2 located according to eq. (D.27)).

D.11.1 Elevation Angle (γ_o).

Since the velocity component $\dot{\bar{x}}_o$ has been introduced, the system (if released) does not initiate a "free orbit" at apocenter; but is at some neighboring position "close to" apocenter. Thus, there is an elevation angle (γ_2); not zero (as at apocenter) but which has some non-zero (±) value.

Recognizing that

$$\bar{V}_2 \equiv V_2 \bar{e}_y \,, \tag{D.30}$$

then it follows that

$$\bar{V}_2 \cdot \bar{V}'_2 \equiv V_2 V'_2 \cos \gamma_2,$$

or

$$\cos \gamma_2 = \frac{\bar{V}_2 \cdot \bar{V}'_2}{V_2 V'_2} \quad .$$

Examining eqs. (D.30) and (D.28), one can see that

$$\bar{V}_2 \cdot \bar{V}'_2 = V_2^2 \ ,$$

hence

$$\cos \gamma_{2_o} = \left(\frac{V_2}{V'_2}\right)_o = \frac{1-\lambda_o}{\left[(1-\lambda_o)^2 + (\lambda'_o)^2\right]^{\frac{1}{2}}} = \frac{1}{\left[1 + \left(\frac{\lambda'_o}{1-\lambda_o}\right)^2\right]^{\frac{1}{2}}} \ . \tag{D.31}$$

D.11.2 Energy (E_2), for the Transfer Orbit.

By definition the specific energy for the "free orbit" can be defined by,

$$E_2 = \frac{V'^2_2}{2} - \frac{\mu}{r_{2_o}} = -\frac{\mu}{2a_2} \ , \tag{D.32a}$$

while the energy for m_1 is described by

$$E_1 = -\frac{V_1^2}{2} \ . \tag{D.32b}$$

Writing the energy ratio, then;

$$\frac{E_2}{E_1} = -\left(\frac{V'_2}{V_1}\right)^2_o + 2\,\frac{r_1}{r_{2_o}} = \frac{r_1}{a_2} \ ,$$

or

$$\frac{E_2}{E_1} = -\left[(1-\lambda)^2 + (\lambda')^2\right]_o + \left(\frac{2}{1-\lambda}\right)_o = \frac{r_1}{a_2} \ ;$$

so

$$\frac{E_2}{E_1} = \left[\frac{(1+\lambda^3) + (1-\lambda)(3\lambda - \lambda'^2)}{(1-\lambda)}\right]_o = \frac{r_1}{a_2} \quad . \tag{D.33}$$

D.11.3 Moment of Momentum (h_2).

By definition the specific moment of momentum, for the "free orbit" of m_2, can be described generally as

$$h_2 = r_2 V'_2 \cos \gamma_2, \tag{D.34a}$$

or, in ratio to h_1 ($\equiv r_1 V_1$),

$$\frac{h_2}{h_1} = \frac{r_2}{r_1} \frac{V'_2}{V_1} \cos \gamma_2.$$

Evaluating for the initial state, specified earlier, it is found that,

$$\frac{h_2}{h_1} = (1-\lambda_o)^2. \tag{D.34b}$$

D.11.4 Eccentricity (ϵ_2).

The path eccentricity (ϵ_2), for the "free orbit" is expressed as

$$\epsilon_2 = \left[1 + \frac{h_2^2}{\mu^2}(2E_2)\right]^{1/2}; \tag{D.35a}$$

or, in terms of the ratio parameters,

$$\epsilon_2^2 = 1 + (1-\lambda)_o^3 \left\{\left[(1-\lambda)_o^2 + (\lambda')_o^2\right](1-\lambda)_o - 2\right\},$$

and

$$\epsilon_2 = \sqrt{\epsilon_2^2} \quad . \tag{D.35b}$$

D.11.5 Radius to Pericenter (r_{p_2}).

The pericenter radius, for the free orbit, is described from the conic equation as

$$r_{p_2} = a_2 (1-\epsilon_2). \tag{D.36a}$$

Expressed in ratio to r_1, the radius of the circular orbit, one finds that

$$\frac{r_{p_2}}{r_1} = \frac{a_2}{r_1} (1-\epsilon_2), \tag{D.36b}$$

where a_2/r_1 and ϵ_2 are defined in eqs. (D.35b) and (D.33), respectively. Due to the complexity of these expressions (in λ, λ') they are not written here! However, for reference purposes the ratio a_2/r_1, is noted to be:

$$\frac{a_2}{r_1} = \frac{(1-\lambda)_o}{2 - (1-\lambda)_o^3 - (\lambda')_o^2 (1-\lambda)_o} = \frac{(1-\lambda)_o}{(1+\lambda^3)_o + (3\lambda - \lambda'^2)_o (1-\lambda)_o} \tag{D.37}$$

(See eq. (D.33)).

D.11.6 Speed at Pericenter (V_{p_2}).

When the particle (m_2) reaches pericenter its speed differs from the value at the initial point (V'_2), but can be related to that speed through the momentum expression. That is, writing,

$$h_2 \equiv r_{p_2} V_{p_2},$$

then

$$V_{p_2} = \frac{h_2}{r_{p_2}} = \left(\frac{h_2}{h_1} \frac{r_1}{r_{p_2}}\right)\left(\frac{h_1}{r_1}\right); \tag{D.38a}$$

or, in ratio form,

$$\frac{V_{p_2}}{V_1} = \left(\frac{h_2}{h_1}\frac{r_1}{r_{p_2}}\right) . \qquad \text{(D.38b)}$$

Inserting values for the ratios on the right, then it is found that

$$\frac{V_{p_2}}{V_1} = (1-\lambda)_o^2 \frac{r_1}{a_2(1-\epsilon_2)} ,$$

or

$$\frac{V_{p_2}}{V_1} = \frac{(1-\lambda)_o}{1-\epsilon_2}\left\{2 - (1-\lambda)\left[(1-\lambda)^2 + (\lambda')^2\right]\right\}_o . \qquad \text{(D.38c)}$$

D.11.7 Transfer Angle to Pericenter ($\Delta\varphi_2$) .

Since the initial point on the orbit is not at apocenter, then the angle from that position to pericenter is not known, a priori, but is of interest to this study.

An inspection of the problem's geometry will show that the elevation angle (γ_2) is positive if sgn $\dot{x} > 0$, and vice versa; correspondingly, if $\gamma_2 > 0$ the transfer is larger than π, while if $\gamma_2 < 0$ the transfer angle is less than π.

From the definition of γ_2 it is easy to show that a solution for the transfer angle ($\Delta\varphi_2$) is obtained from,

$$\cos\varphi_2 = -\frac{\sin^2\gamma_2}{\epsilon_2} \pm \sqrt{\cos^2\gamma_2\left(1-\frac{\sin^2\gamma_2}{\epsilon_2^2}\right)} , \qquad \text{(D.39)}$$

subject to the following conditions:

If $\gamma_2 > 0$, $\Delta\varphi_2 = 2\pi - \varphi_2$.

If $\gamma_2 < 0$, $\Delta\varphi_2 = \varphi_2$;

and, if $(r_2/a_2) > 1.0$ the radical is negative while if $(r_2/a_2) < 1.0$, the radical is positive.

D.12 An Equivalence Problem

The conditional problem examined here has considered a "free orbit" established by releasing (in-plane) a mass m_2 which has some radial velocity $(\dot{\bar{x}})$. This particle is released from a position located on the "local vertical" axis.

In the previous investigation a gravity gradient, stabilized system was studied, but that one had no initial speed component, $|\dot{\bar{x}}|$. It is proposed now to look at these two systems and to ascertain what advantage or penalty might be had by including a velocity component $(\bar{x})$. In this regard the criterion for comparison (here) will be selected as the pericenter radius which is achieved by these systems.

To establish a comparison index, an "equivalent length of tether" is to be determined; this is the tether length equivalent, corresponding to a velocity component $\dot{\bar{x}}$. This length will necessarily be the added length of tether needed to produce a same pericenter radius as for a system which does not have the speed, $\pm\dot{x}$.

Assuming a same peri-radius, and the same basic orbit (r_1), then one sets the two radii equal to one another and determines an effective (equivalent) tether length for the system with $\dot{x} = 0$.

In order to determine the equivalent length, one can describe a peri-radius ratio in terms of λ_e $(\equiv \frac{\ell_{eq}}{r_1})$; that is, write (from eqs. (D.11a), (D.10)),

$$\frac{r_{p_2}}{r_1} = \frac{(1-\lambda_e)(1-\epsilon_e)}{2-(1-\lambda_e)^3} \quad , \tag{D.40}$$

wherein $\epsilon_e \equiv \sqrt{1+(1-\lambda_e)^3[(1-\lambda_e)^3 - 2]}$. Now, the left side of the equation is obtained from

$$\frac{r_{p_2}}{r_1} = \frac{(1-\lambda)_o(1-\epsilon_2)}{2-(1-\lambda)_o^3 - (\lambda')_o^2(1-\lambda)_o} , \tag{D.41a}$$

with

$$\epsilon_2 = \sqrt{1+(1-\lambda)_o^3\{[(1-\lambda)_o^2 + (\lambda')_o^2](1-\lambda)_o - 2\}} . \tag{D.41b}$$

In utilizing this scheme one may proceed as follows:

(a) For a given set of parameters (λ, λ'), use eqs. (D.41) to define ϵ_2 and r_{p_2}/r_1.

(b) Knowing r_{p_2}/r_1, use eqs. (D.40) to ascertain a value for λ_e.

(c) This value, λ_e, describes the equivalent length of tether (needed) to produce the peri-radius (r_{p_2}) when $\dot{x} = 0$!

D.13 Summary.

The operational methodology developed above was concerned with a tethered mass system suspended so that the transferring particle (m_2) was "released" from a radial position between m_1 and μ. In this regard the transfer, for m_2, was from a "near" apocenter position to a pericenter location.

Of necessity, there is a converse situation, possible, wherein the release point is near to the pericenter, and the transfer is to an apocenter radius. In order to show a comparison between these two like (but unlike) cases the pertinent parameters are tabulated below.

TABLE D. III.

ORBIT PARAMETERS FOR TRANSFERS

INCLUDING $\dot{\bar{x}}$ (VELOCITY INCREMENT)

Initial Point* description: Near to,	Initial Position $(\lambda_o)^{(a)}$	Initial Speed Ratio $(V'_2/V_1)_o$ (b)	Initial Elevation Angle (γ_{2_o})
Apo-center	$\left(\frac{r_2}{r_1}\right)_o = 1-\lambda_o$	$\left[(1-\lambda)_o^2+\lambda'^2_o\right]^{\frac{1}{2}}$	$\cos^{-1}\left(\left[1+\left(\frac{\lambda'_o}{1-\lambda_o}\right)^2\right]^{\frac{1}{2}}\right)$
Peri-center	$\left(\frac{r_2}{r_1}\right)_o = 1+\lambda_o$	$\left[(1+\lambda)_o^2+\lambda'^2_o\right]^{\frac{1}{2}}$	$\cos^{-1}\left(\left[1+\left(\frac{\lambda'_o}{1+\lambda_o}\right)^2\right]^{\frac{1}{2}}\right)$

(a) $\lambda_o \equiv \frac{\ell_o}{r_1}$; (b) $\lambda'_o \equiv |\dot{\bar{x}}|/V_1$.

Initial Point description: Near to,	Transfer Energy Ratio (E_2/E_1)	Sp. Momentum Ratio $\left(\frac{h_2}{h_1}\right)_o$	Path Eccentricity ϵ_2
Apo-center	$\frac{(1+\lambda_o^3)+(1-\lambda_o)(3\lambda_o-\lambda'^2_o)}{1-\lambda_o}$	$(1-\lambda_o)^2$	$1+(1-\lambda)_o^3\{[(1-\lambda)_o^2+\lambda'^2_o](1-\lambda)_o^{-2}\}$
Peri-center	$\frac{(1-\lambda_o^3)-(3\lambda_o+\lambda'^2_o)(1+\lambda_o)}{1+\lambda_o}$	$(1+\lambda_o)^2$	$1-(1+\lambda_o)^3\{(1-\lambda_o^3)-(3\lambda_o+\lambda'^2_o)(1+\lambda_o)\}$

(table continued on next page)

*Initial Point descriptions refer to situations wherein $\dot{x}$ is $+\dot{x}$ and $-\dot{x}$, respectively. When $\dot{\bar{x}}$ is in the direction of $\bar{e}_x$ then $\gamma_o > 0$, and the operation begins in the vicinity of the pericenter. Hence the notation used here.

TABLE D. III. (cont)

ORBIT PARAMETERS FOR TRANSFERS

INCLUDING $\bar{x}$ (VELOCITY INCREMENT)

Initial Position description	Semi-major axis (ratio) a_2/r_1	Speed at Terminal Position
Apo-center	$\dfrac{(1-\lambda)_o}{(1+\lambda^3)_o+(3\lambda-\lambda'^2)_o(1-\lambda)_o}$	$\dfrac{V_{p_2}}{V_1}=\dfrac{(1-\lambda)_o}{1-\epsilon_2}\{2-(1-\lambda)_o[(1-\lambda)_o^2+(\lambda')_o^2]\}$
Peri-center	$\dfrac{1+\lambda_o}{(1-\lambda_o^3)-(3\lambda_o+\lambda'^2_o)(1+\lambda_o)}$	$\dfrac{V_{a_2}}{V_1}=\dfrac{(1+\lambda)_o}{(1+\epsilon_2)}\{(1-\lambda_o^3)-(3\lambda_o^3+\lambda'^2_o)(1+\lambda_o)\}$

Initial Position description: Near to,	Terminal Radius description
Apo-center	$\dfrac{r_{p_2}}{r_1}=\dfrac{a_2}{r_1}(1-\epsilon_2)$
Peri-center	$\dfrac{r_{a_2}}{r_1}=\dfrac{a_2}{r_1}(1+\epsilon_2)$

APPENDIX E

DEVELOPMENT OF EQUATIONS FOR TETHERED BODY SYSTEMS

E.1 Introduction.

In this appendix a general development of the dynamical equations is described. Here two mass particles, connected by a tether, move about a single primary particle (μ). The geometry for this system is shown on Fig. E.1.

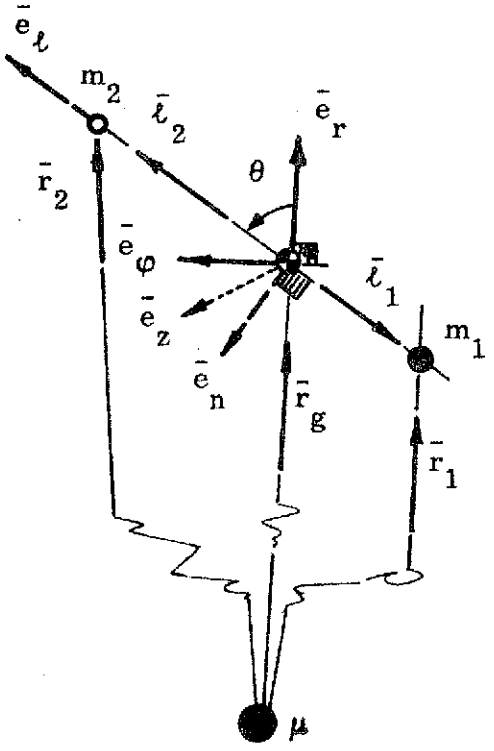

Fig. E.1. Geometric Description.

E.2 Position Geometry.

From the sketch it is evident that the masses are located, relative to μ, by

$$\bar{r}_i = \bar{r}_g + \bar{\ell}_i, \quad (i = 1, 2). \tag{E.1}$$

Also, as a definition let

$$\bar{\ell} \equiv \bar{\ell}_2 - \bar{\ell}_1 , \tag{E.2}$$

wherein $\bar{\ell} \equiv \ell\,(\bar{e}_\ell)$, $\bar{\ell}_i = \ell_i\,(-1)^i\,\bar{e}_\ell$; with $\bar{e}_\ell$ a unit vector of the triad $(\bar{e}_\ell, \bar{e}_n, \bar{e}_z)$ centered at m_1. (Note, also that a reference triad $(\bar{e}_r, \bar{e}_\varphi, \bar{e}_z)$, is centered at the c.g., which is located, from μ, by $\bar{r}_g$). Now, for in-plane motions, the angle θ positions the vector $\bar{e}_\ell$ relative to $\bar{e}_r$; as a consequence of θ, the two triads are connected by the transformation matrix:

$$\begin{pmatrix} \bar{e}_\ell \\ \bar{e}_n \\ \bar{e}_z \end{pmatrix} = \begin{pmatrix} \cos\theta & \sin\theta & 0 \\ -\sin\theta & \cos\theta & 0 \\ 0 & 0 & 1 \end{pmatrix} \begin{pmatrix} \bar{e}_r \\ \bar{e}_\varphi \\ \bar{e}_z \end{pmatrix} , \tag{E.3}$$

or

$$\bar{e}_j = \left[T_{jk} \right] \bar{e}_k \ , \quad (j = \ell, \ n, \ z; \ k = r, \ \varphi, \ z).$$

Making use of eq. (E.3) in (E.1) it is found that,

$$\bar{r}_i = \left[r_g \cos \theta + (-1)^i \ell_i \right] \bar{e}_\ell - (r_g \sin \theta) \bar{e}_n,$$

and

$$r_i = r_g \left[1 + \left(\frac{\ell_i}{r_g} \right)^2 + 2 (-1)^i \frac{\ell_i}{r_g} \cos \theta \right]^{\frac{1}{2}}, \tag{E.4}$$

with (i = 1, 2).

E.3 An Euler Sequence of Rotations.

To account for the out-of-plane geometry another position angle (ψ) must be designated; this will account for the $z^{\underline{th}}$ coordinate which arises in a general, three-dimensional representation.

When the two-positional Euler angle sequence is used it is essential to have three triads designated; the intermediate one to accomodate the mid-position orientation - between the desired beginning-and-ending-frames of reference.

For the situation visualized here the "beginning" triad will be designated as ($\bar{e}_r$, $\bar{e}_\varphi$, $\bar{e}_z$) - centered at the c.g. The terminal, or "ending", triad will be like the one denoted above but called the ($\bar{e}_\ell$, $\bar{e}_n$, $\bar{e}_{z'}$) triad; and the intermediate one will be designated as the ($\bar{e}_{\ell'}$, $\bar{e}_{n'}$, $\bar{e}_{z'}$) triad.

The operational sequence for applying the rotations is as follows: To locate the ($\bar{e}_{\ell'}$, $\bar{e}_{n'}$, $\bar{e}_{z'}$) triad, a rotation (ψ) will be applied about $\bar{e}_r$. This would be analogous to a yawing action, about the local vertical. The second rotation (θ) will occur about $\bar{e}_{z'}$, and will position the final triad ($\bar{e}_\ell$, $\bar{e}_n$, $\bar{e}_{z'}$).

This sequence of rotations leads to the following transformation matrices, and to the relations noted below:

(1) The rotation, ψ, impressed on the triad $(\bar{e}_r, \bar{e}_\varphi, \bar{e}_z)$, to locate the intermediate one $(\bar{e}_{\ell'}, \bar{e}_{n'}, \bar{e}_{z'})$, is expressed by:

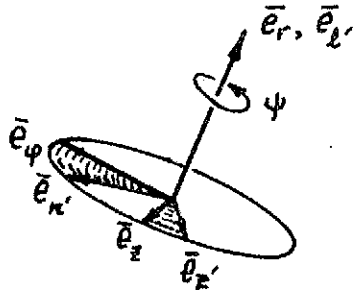

$$\begin{pmatrix} \bar{e}_{\ell'} \\ \bar{e}_{n'} \\ \bar{e}_{z'} \end{pmatrix} = \begin{pmatrix} 1 & 0 & 0 \\ 0 & \cos\psi & \sin\psi \\ 0 & -\sin\psi & \cos\psi \end{pmatrix} \begin{pmatrix} \bar{e}_r \\ \bar{e}_\varphi \\ \bar{e}_z \end{pmatrix}, \qquad \text{(E.5a)}$$

or $\quad \bar{e}_j = \left[T_{jk}\right] \bar{e}_k$, for $(j = \ell', n', z'; k = r, \varphi, z)$.

(2) The rotation, θ, is applied about $\bar{e}_{z'}$ to locate the triad $(\bar{e}_\ell, \bar{e}_n, \bar{e}_{z'})$; the transform for this is:

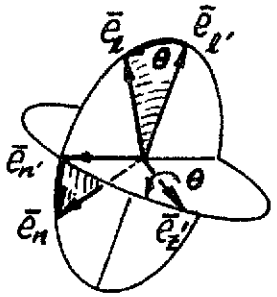

$$\begin{pmatrix} \bar{e}_\ell \\ \bar{e}_n \\ \bar{e}_{z'} \end{pmatrix} = \begin{pmatrix} \cos\theta & \sin\theta & 0 \\ -\sin\theta & \cos\theta & 0 \\ 0 & 0 & 1 \end{pmatrix} \begin{pmatrix} \bar{e}_{\ell'} \\ \bar{e}_{n'} \\ \bar{e}_{z'} \end{pmatrix}, \qquad \text{(E.5b)}$$

or $\quad \bar{e}_\ell = \left[T_{\ell k}\right] \bar{e}_j$, for $(\ell = \ell, n, z'; j = \ell', n', z')$.

Fig. E.2. Euler Angles.

If these (two) matrices are combined, then the transform, relating the "final-" to the "initial-" triad, is:

$$\begin{pmatrix} \bar{e}_\ell \\ \bar{e}_n \\ \bar{e}_{z'} \end{pmatrix} = \begin{pmatrix} \cos\theta & \sin\theta\cos\psi & \sin\theta\sin\psi \\ -\sin\theta & \cos\theta\cos\psi & \cos\theta\sin\psi \\ 0 & -\sin\psi & \cos\psi \end{pmatrix} \begin{pmatrix} \bar{e}_r \\ \bar{e}_\varphi \\ \bar{e}_z \end{pmatrix}. \qquad \text{(E.5c)}$$

It should be apparent that the transform which describes $(\bar{e}_r, \bar{e}_\varphi, \bar{e}_z)$ in terms of $(\bar{e}_\ell, \bar{e}_n, \bar{e}_{z'})$ is simply the transpose of the matrix immediately above.

In general, and in the developments which follow here, to keep the problem simple (in arithmetic) only one positional angle will be used, (θ). In this regard the motions of the two mass particles are constrained to a single plane of action - this plane can be described, at any instant, by the "state-vectors" for both (or either) of the bodies.

Consequently, the formulations which follow will have $\psi = 0$; and, therefore, the positional transformation matrix to be used is the one given in eq. (E.3a).

E.4 External Forces.

The investigation being conducted here considers, as forces acting on the two mass particles, only those arising from the central mass attraction (gravitational effect), and the tether force ($\bar{F}_i$). No other forces (of consequence) will be assumed herein.

Without designating the physical nature of the tether force; but in order to define it geometrically, let it be designated as follows:

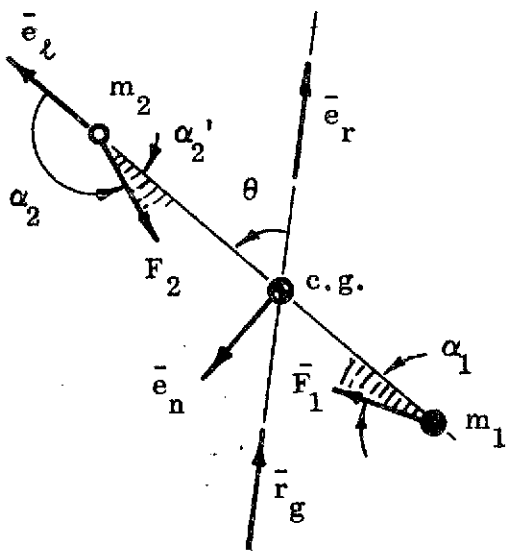

Fig. E.3. Forces and Orientation.

From the sketch one sees that the orientation angles, for the vectors of force ($\bar{F}_i$), relative to $\bar{e}_\ell$, are noted to be, α_i. Consequently,

$$\frac{\bar{F}_i \cdot \bar{e}_\ell}{|\bar{F}_i|} = \cos \alpha_i, \quad (i = 1,2); \tag{E.6a}$$

and/or, alternately,

$$\alpha_i' \equiv (i+1)\,\pi - \alpha_i, \quad (i = 1,2). \tag{E.6b}$$

Without considering any other external forces (in-or out-of-plane), the above representation will suffice.

E.5 Dynamical Equations for the Motion.

A formulation of the dynamical equations follows directly from Newton's laws of motion. The (two) descriptive expressions are written below, for reference purposes; and reduced to the specific form, directly.

Considering only the forces noted above, then one can write

$$(m_i \dot{\bar{r}}_i)^{\cdot} = - m_i \frac{\mu}{r_i^3} \bar{r}_i + \bar{F}_i, \quad (i = 1,2);$$

or,

$$\ddot{\bar{r}}_i = - \frac{\mu}{r_i^3} \bar{r}_i + \frac{\bar{F}_i}{m_i} - \frac{\dot{m}_i \dot{\bar{r}}_i}{m_i}, \quad (i = 1,2). \tag{E.7a}$$

To complete the formulation of this problem, it is necessary to (kinematically) relate the "acceleration" to the problem's geometry; this is undertaken next.

In eq. (E.7a) the term involving $\dot{m}_i$ would be interpreted as the "loss of mass", from the bodies (m_i), as a consequence of paying-out the tether. In general, here, the tether is considered to be a massless member so that the term(s) involving $(\dot{m})$ would be neglected.

E.6 Kinematic Equations.

In this section of the development the vector velocity and acceleration are described, kinematically. For convenience these quantities are described in the two triads of reference $(\bar{e}_\ell, \bar{e}_n, \bar{e}_z)$ and $(\bar{e}_r, \bar{e}_\varphi, \bar{e}_z)$; however, it should be recalled that both of these reference frames are in motion relative to inertial space. Also, one should note that these reference triads do not have a same rotational velocity vector associated with them - this will cause some differences in the kinematic statements for the two frames.

Since (see eq. (E.1)

$$\bar{r}_i \equiv r_g \bar{e}_r + \ell_i (-1)^i \bar{e}_\ell , \quad (i = 1, 2) ,$$

then

$$\dot{\bar{r}}_i = \dot{r}_g \bar{e}_r + r_g \dot{\bar{e}}_r + \dot{\ell}_i (-1)^i \bar{e}_\ell + \ell_i (-1)^i \dot{\bar{e}}_\ell , \tag{E.8}$$

wherein

$$\dot{\bar{e}}_r = \bar{\omega}_g \times \bar{e}_r , \ (\omega_g \equiv \dot{\varphi}_g); \text{ or } \dot{\bar{e}}_r = \dot{\varphi}_g \bar{e}_\varphi ,$$

and

$$\dot{\bar{e}}_\ell = \bar{\omega}_\ell \times \bar{e}_\ell , \ (\omega_\ell \equiv \dot{\theta} + \dot{\varphi}_g); \text{ or } \dot{\bar{e}}_\ell = (\dot{\theta} + \dot{\varphi}_g) \bar{e}_n . \tag{E.9}$$

If the transformation matrices (for $\psi = 0$) are also introduced, then it can be shown that the velocity vector ($\dot{\bar{r}}_i$) is given by:

$$\dot{\bar{r}}_i = \left[\dot{r}_g \cos\theta + r_g \dot{\varphi}_g \sin\theta + (-1)^i \dot{\ell}_i\right] \bar{e}_\ell + \left[r_g \dot{\varphi}_g \cos\theta - \dot{r}_g \sin\theta + (-1)^i \ell_i (\dot{\theta} + \dot{\varphi}_g)\right] \bar{e}_n ;$$

for $(i = 1, 2)$. (E.10)

Next, when the $\dot{\bar{r}}_i$ expression is differentiated, one finds that the (final) kinematic equation for the acceleration is:

$$\ddot{\bar{r}}_i = \left\{\left(\ddot{r}_g - r_g \dot{\varphi}_g^{\,2}\right) \cos\theta + \left(2\dot{r}_g \dot{\varphi}_g + r_g \ddot{\varphi}_g\right) \sin\theta + (-1)^i \left[\ddot{\ell}_i - \ell_i (\dot{\theta} + \dot{\varphi}_g)^2\right]\right\} \bar{e}_\ell$$

$$+ \left\{- (\ddot{r}_g - r_g \dot{\varphi}_g^{\,2}) \sin\theta + (2\dot{r}_g \dot{\varphi}_g + r_g \ddot{\varphi}_g) \cos\theta + (-1)^i \left[2\dot{\ell}_i (\dot{\theta} + \dot{\varphi}_g)\right.\right.$$

$$\left.\left. + \ell_i (\ddot{\theta} + \ddot{\varphi}_g)\right]\right\} \bar{e}_n , \quad \text{when } (i = 1, 2). \tag{E.11a}$$

Additionally, since $\bar{e}_\ell = \bar{e}_r \cos\theta + \bar{e}_\varphi \sin\theta$, and $\bar{e}_n = -\bar{e}_r \sin\theta + \bar{e}_\varphi \cos\theta$; then,

$$\ddot{\bar{r}}_i = \left\{(\ddot{r}_g - r_g \dot{\varphi}_g^{\,2}) + (-1)^i \left[\ddot{\ell}_i - \ell_i (\dot{\theta} + \dot{\varphi}_g)^2\right] \cos\theta - (-1)^i \left[2\dot{\ell}_i (\dot{\theta} + \dot{\varphi}_g)\right.\right.$$

$$\left.\left. + \ell_i (\ddot{\theta} + \ddot{\varphi}_g)\right] \sin\theta\right\} \bar{e}_r + \left\{(2\dot{r}_g \dot{\varphi}_g + r_g \ddot{\varphi}_g) + (-1)^i \left[\ddot{\ell}_i - \ell_i (\dot{\theta} + \dot{\varphi}_g)^2\right] \sin\theta\right.$$

(equation continued on next page)

$$+ (-1)^i \left[2\dot{\ell}_i \, (\dot{\theta} + \dot{\varphi}_g) + \ell_i \, (\ddot{\theta} + \ddot{\varphi}_g) \right] \cos\theta \Big\} \bar{e}_\varphi \, ; \qquad \text{(E.11b)}$$

and $(i = 1, 2)$.

Equations (E.11) are the expressions which may be incorporated into the dynamical equations of motion to describe the problem in terms of its geometry and its physical parameters. The resulting expressions are those which (in principle) must be integrated to define a time history of the state of motion.

E.7 A Specialization. Circular Orbit for r_g.

Let it be assumed, now, that the c.g. of the system moves along a circular path (hence r_g = constant, $\dot{\varphi}_g$ = constant).

Now, for this constraint note that the appropriate equation of motion is:

$$(m_1 + m_2) \, \ddot{\bar{r}}_g = - \frac{\mu (m_1 + m_2)}{r_g^{\,3}} \, \bar{r}_g \, , \qquad \text{(E.12a)}$$

wherein, kinematically,

$$\ddot{\bar{r}}_g \equiv (\ddot{r}_g - r_g \dot{\varphi}_g^{\,2}) \, \bar{e}_r + (2\dot{r}_g \dot{\varphi}_g + r_g \ddot{\varphi}_g) \, \bar{e}_\varphi \, ; \qquad \text{(E.12b)}$$

which reduces (here) to,

$$\ddot{\bar{r}}_g = - r_g \dot{\varphi}_g^{\,2} \, \bar{e}_r \, .$$

Consequently, eq. (E.12a) becomes,

$$r_g \dot{\varphi}_g^{\,2} = \frac{\mu}{r_g^{\,2}} \, , \quad (\text{since } \bar{r}_g \equiv r_g \, \bar{e}_r),$$

or

$$\dot{\varphi}_g^{\,2} = \frac{\mu}{r_g^{\,3}} \, . \qquad \text{(E.13)}$$

This relation is quite useful in subsequent reductions to the equations of motion.

Carrying this specialization into the kinematic expression, developed above, it is evident that the appropriate velocity $(\dot{\bar{r}}_i)$ and acceleration $(\ddot{\bar{r}}_i)$ equations are:

$$\dot{\bar{r}}_i = \left[r_g \dot{\varphi}_g \sin\theta + (-1)^i \dot{\ell}_i\right]\bar{e}_\ell + \left[r_g \dot{\varphi}_g \cos\theta + (-1)^i \ell_i (\dot{\theta} + \dot{\varphi}_g)\right]\bar{e}_n \; ; \tag{E.14a}$$

and

$$\ddot{\bar{r}}_i = \left\{-r_g \dot{\varphi}_g^{\,2} \cos\theta + (-1)^i \left[\ddot{\ell}_i - \ell_i (\dot{\theta} + \dot{\varphi}_g)^2\right]\right\}\bar{e}_\ell + \left\{r_g \dot{\varphi}_g^2 \sin\theta + (-1)^i \left[2\dot{\ell}_i (\dot{\theta} + \dot{\varphi}_g) + \ell_i \ddot{\theta}\right]\right\}\bar{e}_n \; ; \text{ for } (i = 1,2); \tag{E.14b}$$

(the reduction of the $\ddot{\bar{r}}_i$ equation, referred to the $(\bar{e}_r, \bar{e}_\varphi, \bar{e}_z)$-triad, is:

$$\ddot{\bar{r}}_i = \left\{-r_g \dot{\varphi}_g^{\,2} + (-1)^i \left[\ddot{\ell}_i - \ell_i (\dot{\theta} + \dot{\varphi}_g)^2\right]\cos\theta - (-1)^i \left[2\dot{\ell}_i (\dot{\theta} + \dot{\varphi}_g) + \ell_i \ddot{\theta}\right]\sin\theta\right\}\bar{e}_r$$

$$+ \left\{(-1)^i \left[\ddot{\ell}_i - \ell_i (\dot{\theta} + \dot{\varphi}_g)^2\right]\sin\theta + (-1)^i \left[2\dot{\ell}_i (\dot{\theta} + \dot{\varphi}_g) + \ell_i \ddot{\theta}\right]\cos\theta\right\}\bar{e}_\varphi \; , \tag{E.14c}$$

with $(j = 1,2)$).

Next, when these reduced kinematic definitions are used in the dynamical equations, the following expression is obtained:

$$\left\{-r_g \dot{\varphi}_g^{\,2} \cos\theta + (-1)^i \left[\ddot{\ell}_i - \ell_i (\dot{\theta} + \dot{\varphi}_g)^2\right]\right\}\bar{e}_\ell + \left\{r_g \dot{\varphi}_g^{\,2} \sin\theta + (-1)^i \left[2\dot{\ell}_i (\dot{\theta} + \dot{\varphi}_g) + \ell_i \ddot{\theta}\right]\right\}\bar{e}_n = -\frac{\mu}{r_i^3}\left\{\left[r_g \cos\theta + (-1)^i \ell_i\right]\bar{e}_\ell - r_g \sin\theta\, \bar{e}_n\right\} + \frac{F_i}{m_i}\left[\cos\alpha_i\, \bar{e}_\ell + \sin\alpha_i\, \bar{e}_n\right]; \tag{E.15}$$

wherein

$$r_i^{-3} = r_g^{-3}\left[1 + \left(\frac{\ell_i}{r_g}\right)^2 + 2\,(-1)^i\,\frac{\ell_i}{r_g}\cos\theta\right]^{-3/2} \equiv r_g^{-3}\,\Delta^{-3}, \qquad \text{(E.16)*}$$

and $(i = 1, 2)$. As noted earlier the $\dot{m}_i$ have been deleted.

If eq. (E.15) is separated into its scalar components (referred to the $(\bar{e}_r, \bar{e}_\varphi, \bar{e}_z)$-triad, and constrained for $\psi = 0$) then it is easy to show that:

$$\underbrace{-r_g\dot{\varphi}_g^{\,2}\cos\theta + (-1)^i\left[\ddot{\ell}_i - \ell_i\,(\dot{\theta} + \dot{\varphi}_g)^2\right]}_{a} = \underbrace{-\frac{\mu}{r_g^{\,3}\Delta_i^{\,3}}\left[r_g\cos\theta + (-1)^i\ell_i\right]}_{g}$$

$$\underbrace{+\frac{F_i}{m_i}\cos\alpha_i}_{e}\,; \qquad \text{(E.17a)}$$

and

$$\underbrace{r_g\dot{\varphi}_g^{\,2}\sin\theta + (-1)^i\left[2\dot{\ell}_i\,(\dot{\theta} + \dot{\varphi}_g) + \ell_i\,\ddot{\theta}\right]}_{a} = \underbrace{\frac{\mu}{r_g^{\,3}\Delta_i^{\,3}}\left[r_g\sin\theta\right]}_{g}$$

$$\underbrace{+\frac{F_i}{m_i}\sin\alpha_i}_{e}\,. \qquad \text{(E.17b)}$$

Here, as before, $(i = 1, 2)$.

In the above expressions the terms were marked by "a", "g", and "e" - this has been done to identify the source (or origin) of each term in the equations. These designations indicate that the appropriate quantities arise from,

a ≡ acceleration component (consequence of selecting a moving triad of reference, in part);

g ≡ gravitational terms;

*Note that the expression for r_i^{-3} has a simple approximation (based on $\ell_i \ll r_g$): That is, since $r_i^{-3} \equiv r_g^{-3}\,\Delta_i^{-3}$, then $\Delta_i^{-3} \cong 1 - 3\,(-1)^i\,\frac{\ell_i}{r_g}\cos\theta + O\left(\frac{\ell_i}{r_g}\right)^2$.

e ≡ external (specific) force quantities.

If the terms making up eq. (E.17) are regrouped, and if eq. (E.13) is introduced, one can show that:

$$\underbrace{(-1)^i\left[\ddot{\ell}_i - \ell_i\,(\dot{\theta}+\dot{\varphi}_g)^2 + \ell_i\dot{\varphi}_g^{\,2}\,\Delta_i^{-3}\right]}_{a} = \underbrace{r_g\dot{\varphi}_g^{\,2}\cos\theta\,(1-\Delta_i^{-3})}_{a\quad g} + \underbrace{\frac{F_i}{m_i}\cos\alpha_i}_{e}\;; \qquad \text{(E.18a)}$$

and

$$\underbrace{(-1)^i\left[2\dot{\ell}_i\,(\dot{\theta}+\dot{\varphi}_g) + \ell_i\ddot{\theta}\right]}_{a} = -\underbrace{r_g\dot{\varphi}_g^{\,2}\sin\theta(1-\Delta_i^{-3})}_{a\quad g} + \underbrace{\frac{F_i}{m_i}\sin\alpha_i}_{e};\ \text{for } (i=1,2). \qquad \text{(E.18b)}$$

E.8 Dimensionless Variables.

The equations described above are written in terms of dimensional, physical quantities. Even though these are descriptive of the problem, its geometry, etc., it is felt that a more compact (dimensionless) notation is desirable. In this regard the following quantities are introduced:

Let $\lambda_i \equiv \dfrac{\ell_i}{r_g}$, $\tau_i \equiv \dfrac{F_i/m_i}{r_g\dot{\varphi}_g^{\,2}}$; and, change the independent variable from t to φ by means of:

$\dfrac{1}{\dot{\varphi}_g}\dfrac{d}{dt} \equiv \dfrac{d}{d\varphi}$; hence, ordered derivatives are noted to be:

$$\left[\frac{\dot{(\sim)}}{\dot{\varphi}_g}\right]^{(n)} \equiv \left[(\sim)'\right]^{(n)}, \qquad \text{(E.19)}$$

where "n" designates the order of the derivative.

Now, if eqs. (E.18) are divided through by $(r_g\dot{\varphi}_g^{\,2})$, and the transforms

(eq. (E.19)) are utilized, it follows that these differential equations may be recast as:

$$(-1)^i\left[\lambda''_i - \lambda_i (1+\theta')^2 + \lambda_i \Delta_i^{-3}\right] = \cos\theta\left[1-\Delta_i^{-3}\right] + \tau_i \cos\alpha_i ,$$

and

$$(-1)^i\left[2\lambda'_i (1+\theta') + \lambda_i \theta''\right] = -\sin\theta\,(1-\Delta_i^{-3}) + \tau_i \sin\alpha_i , \qquad \text{(E.20)}$$

wherein

$$\Delta_i \equiv \left[1+2\,(-1)^i \lambda_i \cos\theta + \lambda_i^2\right]^{1/2} , \quad (i = 1, 2).$$

Equations (E.20) are the same differential equations, describing the motion, as before, except that the variables are now non-dimensional, and the time dependence has been replaced by a position dependence.

E.9 Conversion from ℓ_i to ℓ.

So far the equations, as developed, describe a motion for the two (i^{th}) bodies - somewhat independently - with respect to c.g. In order to examine the full tethered motion it is best to convert to a full tethered separation; that is, to rewrite the expressions in terms of (say) ℓ rather than ℓ_i. This is accomplished by the following means:

Since $\ell \equiv |\bar{\ell}_1| + |\bar{\ell}_2|$; and, from the sketch (E.1), $\bar{r}_i = \bar{r}_g + (-1)^i \ell_i \bar{e}_\ell$, with $\bar{\ell} + \bar{\ell}_1 = \bar{\ell}_2$, then it is evident that

$$\bar{\ell} = \bar{\ell}_2 - \bar{\ell}_1 = (\ell_1 + \ell_2)\,\bar{e}_\ell \equiv \ell\,\bar{e}_\ell ;$$

with the understanding that,

$$\ell_1 = \frac{m_2 \ell}{\Sigma m_i} , \quad \ell_2 = \frac{m_1 \ell}{\Sigma m_i} , \qquad (i = 1, 2),$$

(which proves out as

$$\ell \equiv \ell_1 + \ell_2 = \frac{(m_2 + m_1)\,\ell}{\Sigma m_i} \equiv \ell_{\underline{\text{QED.}}} \quad). \tag{E.21}$$

Now, in order to convert eqs. (E.20) from (say) λ_i to λ ($\equiv \ell / r_g$), write (E.20) for each i^{th} body and add according to the idea set down in eq. (E.21). When this has been done and terms are collected, it can be shown that the resulting expressions are:

$$\lambda'' - \lambda\,(1+\theta')^2 + \left(\frac{\lambda_1}{\Delta_1^{\,3}} + \frac{\lambda_2}{\Delta_2^{\,3}}\right) = \cos\theta\left(\frac{1}{\Delta_1^{\,3}} - \frac{1}{\Delta_2^{\,3}}\right) + \tau_2 \cos\alpha_2 - \tau_1 \cos\alpha_1,$$

and

$$\lambda\theta'' + 2\lambda\,(1+\theta') = \sin\theta\left(\frac{1}{\Delta_2^{\,3}} - \frac{1}{\Delta_1^{\,3}}\right) + \tau_2 \sin\alpha_2 - \tau_1 \sin\alpha_1. \tag{E.22}$$

In these last expressions:

$$\lambda \equiv \left(\frac{\ell_1 + \ell_2}{r_g}\right) \text{ or } \lambda = \Sigma\lambda_i;\ (\sim)' \equiv \frac{1}{\dot\varphi_g}\,\dot{(\sim)};\ \Delta_i \equiv \left[1 + 2\,(-1)^i \lambda_i \cos\theta + \lambda_i^{\,2}\right]^{1/2};$$

$$\tau_i \equiv \frac{F_i/m_i}{r_g \dot\varphi_g^{\,2}}\ ; \qquad \text{for } (i = 1, 2).$$

E.10 A Special Situation.

In the following specialization it will be assumed that m_1 is the "main" (or more massive) body for the tethered system while m_2 is a much smaller mass. Consequently in defining the motion of m_2, consider eq. (E.18a) written for this body. That is,

$$\ddot\ell_2 - \ell_2\,(\dot\theta + \dot\varphi_g)^2 + \ell_2 \dot\varphi_g^{\,2} \Delta_2^{\,-3} = r_g \dot\varphi_g^{\,2} \cos\theta\left[1 - \Delta_2^{\,-3}\right] + \frac{F_2}{m_2}\cos\alpha_2\,,$$

and likewise, from eq. (E.18b),

$$2\dot{\ell}_2 \left(\dot{\theta}+\dot{\varphi}_g\right)^2 + \ell_2 \ddot{\theta} = - r_g \dot{\varphi}_g^{\,2} \sin\theta \left(1-\Delta_2^{-3}\right) + \frac{F_2}{m_2} \sin\alpha_2 \,. \tag{E.23}$$

Now, since $\ell_2 \equiv \frac{m_1 \ell}{M}$ $(M \equiv \Sigma m_i)$, then (E.23) can be rewritten as,

$$\frac{\ddot{\ell}\, m_1}{M} - \frac{\ell m_1}{M}\left(\dot{\theta}+\dot{\varphi}_g\right)^2 + \frac{m_1 \ell}{M} \dot{\varphi}_g^{\,2} \Delta_2^{-3} = r_g \dot{\varphi}_g^{\,2} \cos\theta \left(1-\Delta_2^{-3}\right)$$

$$+ \frac{F_2}{m_2} \cos\alpha_2 \,,$$

and

$$\frac{2\dot{\ell} m_1}{M}\left(\dot{\theta}+\dot{\varphi}_g\right) + \frac{\ell m_1}{M}\ddot{\theta} = - r_g \dot{\varphi}_g^{\,2} \sin\theta \left(1-\Delta_2^{-3}\right) + \frac{F_2}{m_2} \sin\alpha_2 \,.$$

Next, converting the above equations to dimensionless variables one finds that:

$$\lambda'' - \lambda \left(1+\theta'\right)^2 + \lambda \Delta_2^{-3} = \frac{M}{m_1} \cos\theta \left(1-\Delta_2^{-3}\right) + \frac{F_2}{\tilde{m}} \frac{\cos\alpha_2}{r_g \dot{\varphi}_g^{\,2}} \,,$$

and

$$2\lambda' \left(1+\theta'\right) + \lambda \theta'' = - \sin\theta \frac{M}{m_1} \left(1-\Delta_2^{-3}\right) + \frac{F_2}{\tilde{m}} \frac{\sin\alpha_2}{r_g \dot{\varphi}_g^{\,2}} \,, \tag{E.24}$$

wherein

$$\lambda \equiv \frac{\ell}{r_g} \;;\; (\sim)' = \frac{(\dot{\sim})}{\dot{\varphi}_g} \;;\; M \equiv \Sigma m_i \;;\; \Delta_2 \equiv \left[1+2\lambda_2 \cos\theta + \lambda_2^{\,2}\right]^{1/2} .$$

To make the expressions above, eqs. (E.24), more amenable to solution the following (added) restrictions are made:

(a) Let $m_1 \gg m_2$ (i.e., $M \cong m_1$).

(b) Let $\ell \ll r_g$; thence, $\Delta_2^{-3} \equiv \left[1+2\lambda \frac{m_1}{M} \cos\theta + \lambda^2 \frac{m_2}{M^2}\right]^{-3/2}$

$$\cong \left[1+2\lambda \cos\theta + \lambda^2\right]^{-3/2}$$

$$\cong 1 - 3\lambda \cos\theta + \text{H.O.T.}$$

As a consequence of the reductions, eqs. (E.24) reduce to:

$$\lambda'' - \lambda (1+\theta')^2 + \lambda (1-3\lambda \cos\theta) \cong \cos\theta (3\lambda \cos\theta) + \tau_2 \cos\alpha_2 ,$$

and

$$\lambda\theta'' + 2\lambda'(1+\theta') \cong -\sin\theta (3\lambda \cos\theta) + \tau_2 \sin\alpha_2 ;$$

or, retaining only first order terms in λ and λ' then:

$$\lambda'' - \lambda\theta' (2+\theta') - \frac{3\lambda}{2} (1+\cos 2\theta) \cong \tau_2 \cos\alpha_2 ,$$

and

$$\lambda\theta'' + 2\lambda' (1+\theta') + \frac{3\lambda}{2} \sin 2\theta \cong \tau_2 \sin\alpha_2 .$$

The parameter λ, used to represent the tether length is not necessarily a best representation in all instances. A (sometimes) more convenient normalizing quantity is the extreme length of the tether ($\equiv \ell_m$), for a given situation.

Defining $\lambda_m \equiv \frac{\ell_m}{r_g}$, and introducing a <u>new nondimensional length</u> (σ), where

$$\sigma \equiv \frac{\ell}{\ell_m} = \frac{\lambda}{\lambda_m} ,$$

(recognizing that λ_m is a fixed parameter for a given problem situation), then eqs. (E.25) can be rewritten, immediately, as:

$$\sigma'' - \sigma\theta' (2+\theta') - \frac{3}{2}\sigma(1+\cos 2\theta) \cong \frac{\tau_2 r_g}{\ell_m} \cos\alpha_2,$$

and

$$\sigma\theta'' + 2\sigma'(1+\theta') + \frac{3}{2}\sigma \sin 2\theta \cong \frac{\tau_2 r_g}{\ell_m} \sin\alpha_2 .$$

To describe a more appropriate form for τ_2, let

$$\frac{\tau_2 r_g}{\ell_m} \equiv \tau_m = \frac{F_2/\tilde{m}}{\ell_m \dot{\phi}_g^2},$$

hence the present non-dimensional, reduced differential equations for the motion are:

$$\sigma'' - \sigma\theta' (2+\theta') - \frac{3}{2}\sigma(1+\cos 2\theta) \cong \tau_m \cos\alpha_2,$$

and

$$\sigma\theta'' + 2\sigma'(1+\theta') + \frac{3}{2}\sigma \sin 2\theta \cong \tau_m \sin\alpha_2. \qquad \text{(E.25)}$$

This last set of expressions describe (to a reasonably, expected degree of approximation) the in-plane motion for a tethered system constrained as noted in the development. Basically, the tether is massless; it may have some freedom for motion itself (through α); and, the system experiences only gravity forces in addition to the tether force. Also, the base (reference) orbit for this situation is circular.

The set of equations (above, and given as eqs. (E.25)) describe the action of m_2 relative to m_1, since m_1 is on the circular path about μ. One should note that these expressions are (as yet) coupled and non-linear, hence a simple analytical solution is not apparent (without added conditions being imposed).

APPENDIX F

AN ANALYSIS FOR THE EXTENDIBLE TETHER SYSTEM

F.1 Introduction.

The system is assumed to be composed of two point masses (m_i) connected by a hard-line tether subjected to a tension force. The hardline has an instantaneous length, ℓ, and is located by the angle, θ, measured from the local vertical ($\bar{e}_r$); with sgn $\theta = \pm 1$ according to direction of motion.

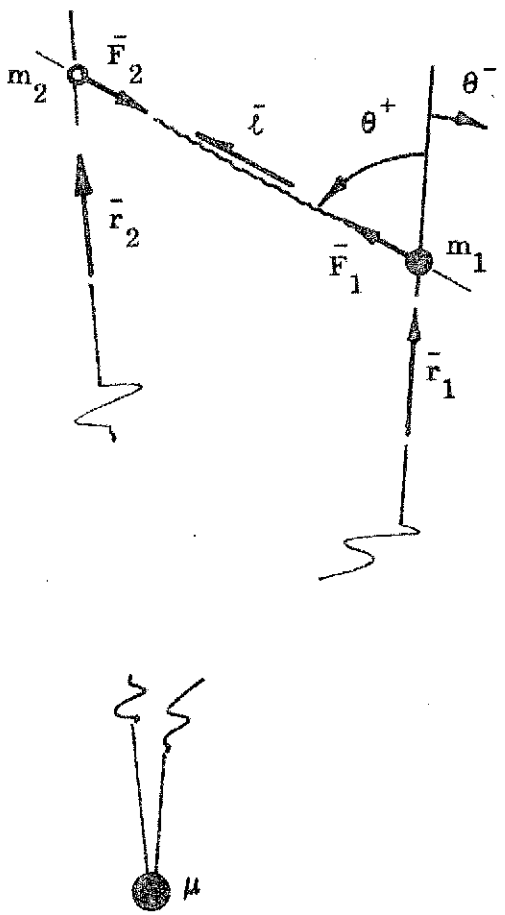

Fig. F.1. Geometric Description.

Forces other than tension and gravity are neglected. The particles would describe independent, two-body orbits if the tether force would vanish.

F.2 Equations of Motion.

In agreement with Fig. F.1, the differential equations of motion* may be written as:

$$\ddot{\bar{r}}_1 = -\frac{\mu}{r_1^3}\bar{r}_1 + \frac{F}{m_1}\frac{\bar{\ell}}{\ell},$$

$$\ddot{\bar{r}}_2 = -\frac{\mu}{r_2^3}\bar{r}_2 - \frac{F}{m_2}\frac{\bar{\ell}}{\ell}; \qquad \text{(F.1)}$$

where $F \equiv |\bar{F}_1|, |\bar{F}_2|$.

Since $\bar{\ell} = \bar{r}_2 - \bar{r}_1$, and $\ddot{\bar{\ell}} = \ddot{\bar{r}}_2 - \ddot{\bar{r}}_1$, then from eq. (F.1),

*The analysis here is similar to that in Appendix E, but sufficiently different to warrant being included as a separate development.

$$\ddot{\bar{\ell}} = -\frac{\mu}{r_1^3}\left[\left(\frac{r_1}{r_2}\right)^3(\bar{r}_1+\bar{\ell}) - \bar{r}_1\right] - \frac{F}{\tilde{m}}\frac{\bar{\ell}}{\ell}\ , \tag{F.2}$$

wherein $\tilde{m} \equiv \dfrac{m_1 m_2}{m_1+m_2}$ (reduced mass for the system).

Defining the length ratio (r_2/r_1),

$$\Delta \equiv \left(\frac{r_2}{r_1}\right) = \left[\frac{r_1^2 + 2\bar{r}_1\cdot\bar{\ell} + \bar{\ell}\cdot\bar{\ell}}{r_1^2}\right]^{1/2},$$

then,

$$\Delta^{-3} = \left[1 + 2\frac{\ell}{r_1}\cos\theta + \frac{\ell^2}{r_1^2}\right]^{-3/2}. \tag{F.3}$$

Now, the dynamical equation for the tether can be expressed as,

$$\ddot{\bar{\ell}} = \frac{\mu}{r_1^3}\left[(1-\Delta^{-3})\,\bar{r}_1 - \Delta^{-3}\,\bar{\ell}\right] - \frac{F}{\tilde{m}}\frac{\bar{\ell}}{\ell}\ . \tag{F.4}$$

Next, a kinematical statement for $\ddot{\bar{\ell}}$ must be written; then these two expressions are joined, and the scalar motion expressions are extracted.

F.3 Kinematic Definition for $\ddot{\bar{\ell}}$.

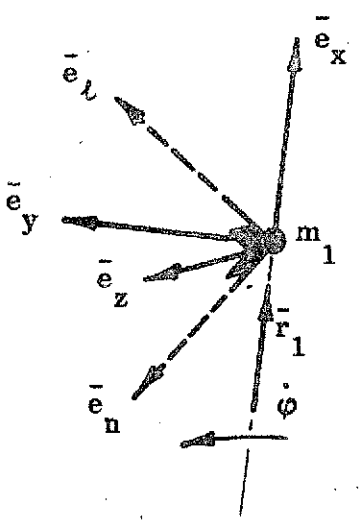

Fig. F.2. Reference Triads.

At m_1 two triads may be defined. One, $(\bar{e}_x, \bar{e}_y, \bar{e}_z)$, an orthogonal cartesian system with $\bar{e}_x$ in the radial direction; $\bar{e}_y$, in the (local) transverse direction; and $\bar{e}_z$ normal to the plane of motion. The second, denoted as $(\bar{e}_\ell, \bar{e}_n, \bar{e}_z)$, has $\bar{e}_\ell$ in the direction of $\bar{\ell}$; $\bar{e}_n$ is the "normal" vector; and, $\bar{e}_z$ is as before.

The two triads have a motion about μ so that they may retain their described

orientations. The "motion" of the triad $(\bar{e}_\ell, \bar{e}_n, \bar{e}_z)$ is described by $\bar{\omega}_\ell \equiv (\dot{\theta}+\dot{\varphi}_1)\,\bar{e}_z$, where $\dot{\varphi}$ is the angular rate for m_1 as it moves on its orbit. The $\bar{\omega}$ for the other triad is simply $\bar{\omega} = \dot{\varphi}_1\,\bar{e}_z$.

Since $\bar{\ell} \equiv \ell\,\bar{e}_\ell$, then the kinematical manipulations here are markedly similar to those shown in section B.3, Appendix B. Consequently the description of the acceleration vector is

$$\ddot{\bar{\ell}} = (\ddot{\ell} - \ell\,\omega_\ell^2)\,\bar{e}_\ell + (2\dot{\ell}\,\omega_\ell + \ell\,\dot{\omega}_\ell)\,\bar{e}_n, \tag{F.5}$$

wherein $\omega_\ell \equiv |\bar{\omega}_\ell| = \dot{\theta} + \dot{\varphi}_1$. (The subscript $(\sim)_g$, in Appendix B, is dropped in agreement with the definition of $\dot{\varphi}_1$).

To write the scalar equations of motion, combine eqs. (F.3) and (F.5) noting that,

$$\bar{r}_1 = r_1 \cos\theta\,\bar{e}_\ell - r_1 \sin\theta\,\bar{e}_n,$$

and obtain as a result,

$$\ddot{\ell} = \ell\,\omega_\ell^2 + \frac{\mu}{r_1^3}\left[(1-\Delta^{-3})\,r_1\cos\theta - \ell\,\Delta^{-3}\right] - \frac{F}{\tilde{m}},$$

and

$$\ell\,\dot{\omega}_\ell = -2\,\dot{\ell}\,\omega_\ell - \frac{\mu}{r_1^3}\left[(1-\Delta^{-3})\,r_1\sin\theta\right]. \tag{F.6}$$

These two expressions are analogous to the equations described in section B.5, Appendix B.

The terms involving Δ^{-3} here are a consequence of gravity gradient; those involving ω_ℓ are the (so-called) fictitious acceleration, or kinematic,quantities; while $F/\tilde{m}$ is the "applied" force acting on the system. Here this force is the tether tension.

F.4 Specialization for the Tether Problem.

To affect this specialization assume that $m_1 \gg m_2$; hence assume that m_1 moves along a circular orbit. Then following the corresponding reductions in section E.7, Appendix E, it is evident that eq. (F.4) can be recast as

$$\ddot{\bar{\ell}} = \dot{\varphi}^2 \left[(1-\Delta^{-3})\, \bar{r}_1 - \Delta^{-3}\, \bar{\ell} \right] - \frac{F}{\tilde{m}}\, \frac{\bar{\ell}}{\ell} \,. \tag{F.7}$$

Also, it is easy to show that the scalar equations (F.6) reduce to the following set:

$$\ddot{\ell} = \ell \dot{\varphi}_1^{\,2} \left(1 + \frac{\dot{\theta}}{\dot{\varphi}_1}\right)^2 + r_1 \dot{\varphi}_1^{\,2} \left[(1-\Delta^{-3}) \cos\theta - \frac{\ell}{r_1}\, \Delta^{-3} \right] - \frac{F}{\tilde{m}} \,,$$

and

$$\ell \ddot{\theta} = -2\dot{\ell}\dot{\varphi}_1 \left(1 + \frac{\dot{\theta}}{\dot{\varphi}_1}\right) - r_1 \dot{\varphi}_1^{\,2} \left[(1-\Delta^{-3}) \sin\theta \right]; \tag{F.8}$$

wherein

$$\Delta^{-3} \equiv \left(1 + 2\,\frac{\ell}{r_1}\cos\theta + \frac{\ell^2}{r_1^{\,2}}\right)^{-3/2} .$$

F.5 Dimensionless Variables.

Eqs. (F.8) indicate a natural non-dimensionalization of the governing differential equations. This, fortunately, parallels the scheme used in section (E.8), Appendix E. Therefore, following that pattern it is easy to show the set of equations (F.8) become:

$$\lambda'' = \lambda (1+\theta')^2 + (1-\Delta^{-3}) \cos\theta - \lambda \Delta^{-3} - \tau \,,$$

$$\lambda \theta'' = -2\lambda' (1+\theta') - (1-\Delta^{-3}) \sin\theta \,; \tag{F.9}$$

wherein

$$\Delta^{-3} \equiv (1 + 2\lambda\cos\theta + \lambda^2)^{-3/2}, \text{ and } \tau \equiv \frac{F/\tilde{m}}{r_1 \dot{\varphi}_1^{\,2}}$$ (the ratio of specific force to specific centrifugal force).

Eqs. (F.9) are the same "undiluted" set as (F.7); hence, they cannot be made to yield a closed form solution.

One can see that the θ-equation is not directly influenced by "F", though it is influenced, implicitly, through ℓ, $\dot{\ell}$ (or λ, λ').

The general regimes of motion to be considered here are in the second and third quadrants (where $|\theta|$ normally lies between $\pi/2$ and π). In this regard one can see, for instance, that θ'' is negative when $\lambda' > 0$ and $\theta' \gtrless 0$. This verifies the condition that $\dot{\theta}$ will usually go to zero along the arc of motion for m_2.

F.6 Linearization and Reduction of the Governing Expressions.

The term Δ^{-3} can be approximated as:

$$\Delta^{-3} \equiv (1 + 2\lambda \cos\theta + \lambda^2)^{-3/2} \cong 1 - 3\lambda \cos\theta + \text{H.O.T.} \; ; \tag{F.10}$$

and, as a consequence eqs. (F.9) reduce to:

$$\lambda'' = 2\lambda\theta' + \lambda\theta'^2 + 3\lambda\cos^2\theta + 3\lambda^2\cos\theta - \tau \; ,$$

$$\lambda\theta'' = -2\lambda'(1+\theta') - \frac{3}{2}\lambda\sin 2\theta. \tag{F.11}$$

This reduction has not produced a set of expressions which can be conveniently handled for a closed form solution. Further reductions are necessary; some of these will be described subsequently.

F.7 An Equilibrium Condition.

Suppose that the system is "quiet" ($\dot{\ell} = \ddot{\ell} = \dot{\theta} = \ddot{\theta} = 0$); then from eqs. (F.8) one finds:

$$\ell\dot{\varphi}_1^{\,2} + r_1\dot{\varphi}_1^{\,2}\left[(1-\Delta^{-3})\cos\theta - \frac{\ell}{r_1}\,\Delta^{-3}\right] = \frac{F}{\tilde{m}}\ ,$$

and

$$r_1\dot{\varphi}_1^{\,2}\left[(1-\Delta^{-3})\sin\theta\right] = 0, \tag{F.12}$$

with

$$\Delta^{-3} \equiv \left(1 + 2\,\frac{\ell}{r_1}\cos\theta + \frac{\ell^2}{r_1^{\,2}}\right)^{-3/2}\ .$$

F.7.1 Conditions for Equilibrium.

A first condition noted is that, either:

$$\text{(a)} \qquad \Delta^{-3} = 1 \ \text{(i.e., } \ell = 0),$$

or

$$\text{(b)} \qquad \sin\theta = 0 \ (\theta = n\pi). \tag{F.13}$$

These are natural consequences for the system.

Suppose, for the moment, that $\ell \neq 0$, and $\theta = \pi$; then eq. (F.12) reduces to:

$$\frac{\ell}{r_1} - (1 - \Delta_1^{-3}) - \frac{\ell}{r_1}\,\Delta_1^{-3} = \frac{F}{\tilde{m}\, r_1\dot{\varphi}_1^{\,2}}\ ,$$

and

$$\Delta_1^{-3} = (1 - \frac{\ell}{r_1})^{-3} \cong 1 + 3\,\frac{\ell}{r_1}\ ;$$

or, using the dimensionless variables introduced in section (F.5),

$$\tau(\theta) = \tau(\pi) \cong 3\lambda\,(1-\lambda), \tag{F.14a}$$

as an approximate equilibrium tension definition.

If the system would be oriented so that $\theta = 0$, then from eq. (F.12),

$$\frac{\ell}{r_1} + (1 - \Delta^{-3}) - \frac{\ell}{r_1}\,\Delta^{-3} = \tau,$$

with

$$\Delta^{-3} = \left(1 + \frac{\ell}{r_1}\right)^{-3} \cong 1 - 3\,\frac{\ell}{r_1}\ ;$$

or, since $\lambda \equiv \dfrac{\ell}{r_1}$,

$$\tau(\theta) = \tau(0) \cong 3\lambda\,(1+\lambda), \tag{F.14b}$$

as the approximate level of tension for equilibrium, here.

F.8 A Simplified Energy Analysis.

To this point in the study, no concern has been given to the energy of the system, though it is of interest for several reasons.

In the following development a simplified analysis is undertaken for the purpose of determining how terms may be grouped in this problem. Such grouping have definite advantages; one reason is that this leads to an intrinsic form of nondimensionalizing for the various parameters defining the system and its motion.

Returning to eq. (F.2), the dynamical equation for the system; i.e.,

$$\ddot{\bar{\ell}} = \frac{\mu}{r_1^3}\left[(1 - \Delta^{-3})\,\bar{r}_1 - \bar{\ell}\,\Delta^{-3}\right] - \frac{\bar{F}}{\tilde{m}}\,\bar{e}_\ell, \tag{F.15a}$$

wherein

$$\Delta^{-3} \equiv \left[1 + 2\,\frac{\bar{\ell}\cdot r_1}{r_1^2} + \frac{\ell^2}{r_1^2}\right]^{-3/2}, \text{ and } \bar{e}_\ell \equiv \frac{\bar{\ell}}{|\ell|}\ .$$

Since $\ell \ll r_1$, for most situations of interest, then

$$\Delta^{-3} \to 1.0 \text{ for these many cases.}$$

Now, to the degree of approximation inferred here, eq. (F.15a) reduces to:

$$\ddot{\bar{\ell}} \cong \frac{\mu}{r_1^3}\,(-\bar{\ell}) - \frac{F}{\tilde{m}}\,\bar{e}_\ell\,; \tag{F.15b}$$

which is descriptive of the system insofar as $\bar{\ell}$ is concerned.

Now, scalar multiplication, using $\dot{\bar{\ell}}$, gives:

$$\dot{\bar{\ell}} \cdot \ddot{\bar{\ell}} \cong \frac{\mu}{r_1^3}\,(-\bar{\ell} \cdot \dot{\bar{\ell}}) - \frac{F}{\tilde{m}}\,\bar{e}_\ell \cdot \dot{\bar{\ell}}\,,$$

or, in terms of equivalents,

$$\frac{d}{dt}\left(\frac{\dot{\bar{\ell}} \cdot \dot{\bar{\ell}}}{2}\right) \cong -\dot{\varphi}_1^{\,2}\,\frac{d}{dt}\left(\frac{\bar{\ell} \cdot \bar{\ell}}{2}\right) - \frac{F}{\tilde{m}}\left(\frac{d\ell}{dt}\right),$$

wherein $\dot{\varphi}_1^{\,2} = \dfrac{\mu}{r_1^3}$ (for circular orbits). Now, a first integral from the above is:

$$\frac{\dot{\ell}^2}{\ell} + \frac{\ell^2 \dot{\varphi}_1^{\,2}}{2} + \frac{F}{\tilde{m}}\,\ell = \mathcal{C}, \tag{F.16a}$$

where $\mathcal{C}$ is a constant of integration.

Assuming that $\ell_o = 0$ and $\dot{\ell}_o$ = finite value, then $\mathcal{C} = \dfrac{\dot{\ell}_o^{\,2}}{2}$ and, consequently, for the final state,

$$\frac{\dot{\ell}_f^{\,2}}{2} + \frac{\ell_f^2 \dot{\varphi}_1^{\,2}}{2} + \frac{F}{\tilde{m}}\,\ell_f = \frac{\dot{\ell}_o^{\,2}}{2}\,; \tag{F.16b}$$

or, after rearranging,

$$\frac{\dot{\ell}_f^{\,2}}{\dot{\ell}_o^{\,2}} + \frac{\ell_f^2 \dot{\varphi}_1^{\,2}}{\dot{\ell}_o^{\,2}} + \frac{2(F/\tilde{m})\,\ell_f}{\dot{\ell}_o^{\,2}} = 1. \tag{F.16c}$$

This grouping of terms suggests combinations which describe the operating characteristics of the system. Logically, then, this system can be described by means of the parameters:

$$\frac{\dot{\ell}_f}{\dot{\ell}_o}, \quad \frac{\ell_f \dot{\varphi}_1}{\dot{\ell}_o}, \text{ and } \frac{(F/\tilde{m})\,\ell_f}{\dot{\ell}_o^{\,2}}. \tag{F.17}$$

These "numbers" may be evaluated for (say) one system and its operation; then, all other compatible operations for this system are described accordingly.

This allows one to describe all similar tether systems, of a same operational type, in terms of these same intrinsic quantities.

F.9 Extensible Tether with Variable Tension.

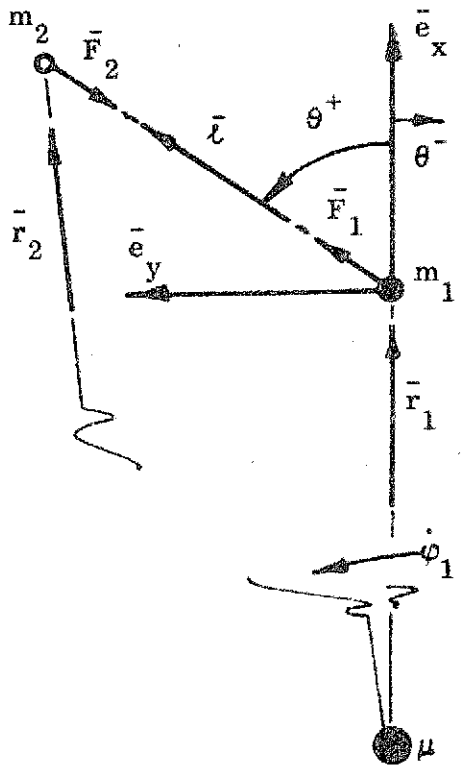

Fig. F.3. Description of Problem.

The development carried out here is for a tethered body system operating at a fixed position angle (θ), with variable tension. This tether is a flexible, massless connector capable of supporting an in-line force (tension) but no other forces.

The entire system moves about at a fixed rate ($\dot{\varphi}_1$). The positioning of m_2 is described by $\bar{r}_2$ measured from μ; and by $\bar{\ell}$ measured from m_1.

From the sketch it is apparent that the "inertial" position vector for m_2 is expressed as:

$$\bar{r}_2 = \bar{r}_1 + \bar{\ell}.$$

The scalar (in-plane) governing equations for the "tethered motion" are given

as eqs. (F.6). When the specialization of a circular orbit (r_1) is introduced, and the transformation of variables is included, the differential equations are those noted as eqs. (F.9). These are repeated here for convenience:

$$\lambda'' = \lambda\,(1+\theta')^2 + (1-\Delta^{-3})\cos\,\theta - \lambda\Delta^{-3} - \tau,$$

and

$$\lambda\,\theta'' = -2\lambda'\,(1+\theta') - (1-\Delta^{-3})\sin\theta\,; \tag{F.18}$$

wherein

$$\Delta \equiv (1+2\lambda\cos\theta+\lambda^2)^{1/2},$$

and

$$\tau \equiv \frac{F/\tilde{m}}{r_1\dot{\varphi}_1^{\,2}}\,.$$

If the restriction of constant θ is introduced, then eqs. (F.18) reduce to:

$$\lambda'' = (\lambda+\cos\theta)(1-\Delta^{-3}) - \tau,$$

and

$$\lambda' = -(1-\Delta^{-3})\,\frac{\sin\theta}{2}\,. \tag{F.19}$$

A simplification can be afforded by differentiating the second expression and incorporating it into the first equation. Thus, the differentiation produces,

$$\lambda'' = -\frac{3\lambda'}{2\Delta^5}\,(\lambda+\cos\theta)\sin\theta\,;$$

and, after incorporating the second of eqs. (F.19),

$$\lambda'' = \frac{3\sin^2\theta}{4\Delta^5}\,(1-\Delta^{-3})(\lambda+\cos\theta). \tag{F.20}$$

Now, in place of the first expression in eq. (F.19) write:

$$\tau = (1 - \Delta^{-3})(\lambda + \cos\theta)\left[1 - \frac{3\sin^2\theta}{4\Delta^5}\right]. \qquad \text{(F.21)}$$

Equations (F.19) and (F.21) give sufficient information to proceed with a solution to this problem. Herein, λ (hence Δ) can be specified - for a given situation - then the required speed (λ') and tension force (τ) are determined from these governing equations. These are the values which will assure the manipulation of a tethered body system at a fixed angle (θ).

On the premise that the quantity $(1 - \Delta^{-3}) \leq 0$, then it is evident that $\lambda' \geq 0$ so long as sgn $(\sin\theta) \geq 0$; and conversely $\lambda' \leq 0$ if the converse of the situations exists. What is implied, then, is that a "roll-out" system can be established in the first two θ-quadrants; and a "roll-in" system can be put into operation in the remaining quadrants.

It is apparent that $\lambda' \neq 0$ when $(1 - \Delta^{-3}) \neq 0$ and $\theta \neq 0, \pi$. This suggests a non-vanishing tether "extension" for <u>other than</u> local vertical actions; and for the positioning of m_2 <u>away from</u> m_1.

As a general evaluation, note that $0(\lambda) = 10^{-3}$; $0(1 - \Delta^{-3}) = -3\text{x}10^{-3}$, etc. Consequently, $0(\tau) \cong 10^{-3}$, and the system behaves as expected. As the antithesis of this, note that as $\lambda \to 0$, $(1 - \Delta^{-3}) \to 0$, hence λ' and τ become vanishingly small quantities. Or, the system ceases to be operable as a dynamic entity.

APPENDIX G

A ROTATING, TETHERED BODY SYSTEM

G.1 Introduction.

The subject of this appendix is the mathematical description of a tethered system which operates at a continuous rotation. Various expressions describing such a state of motion are to be developed; and, a subsequent "free orbit" determination is to be made. The "free orbit" description could be the consequence of releasing a tethered particle (m_2) at some arbitrary θ-position during the rotation.

The purpose in this immediate effort was to obtain equations for a computer program to evaluate such an operational maneuver.

G.2 Equations of Motion.

The basic differential equations describing this problem may be found in Appendix F, as eqs. (F.8), and eqs. (F.9). Since this latter set is simpler in format (dimensionless expressions), the descriptions below will result from a manipulation of these. Thus, the equation of interest are:

$$\lambda'' - \lambda\,(1+\theta')^2 = (1-\Delta^{-3})\cos\theta - \lambda\Delta^{-3} - \tau,$$

$$2\lambda'\,(1+\theta') + \lambda\,\theta'' = \frac{1}{\lambda}\,\frac{d}{d\varphi_1}\,[\lambda^2\,(1+\theta')] = -\,(1-\Delta^{-3})\sin\theta\,, \qquad \text{(G.1)}$$

wherein

$$\lambda \equiv \frac{\ell}{r_1}\,,\quad \tau \equiv \frac{F/\tilde{m}}{r_1\dot{\varphi}_1^{\,2}}\,,\quad (\sim)' = \frac{1}{\dot{\varphi}_1}\,(\dot{\sim}),\quad \text{and}$$

$$\Delta \equiv \left[1 + 2\lambda\cos\theta + \lambda^2\right]^{1/2}.$$

G.2.1 Special Case.

Suppose that the rotation of m_2, about m_1, occurs at λ = constant (ℓ fixed). Accordingly, eqs. (G.1) are modified to:

$$\tau = \lambda\left[(1+\theta')^2 - \Delta^{-3}\right] + (1-\Delta^{-3})\cos\theta,$$

and

$$\lambda\theta'' + (1-\Delta^{-3})\sin\theta = 0. \tag{G.2}$$

This last expression (for θ'') can be simplified by the following operations: A multiplication by θ', and the recognition of several equivalent differential forms, leading directly to:

$$\frac{d}{d\varphi_1}\left[\frac{\theta'^2}{2} - \frac{\cos\theta}{\lambda} - \frac{1}{\lambda^2\Delta}\right] = 0. \tag{G.3a}$$

As a consequence of this result, it is apparent that

$$\frac{(\lambda\theta')^2}{2} - \lambda\cos\theta - \frac{1}{\Delta} = \text{constant}. \tag{G.3b}$$

These expressions, ((G.3b), and the first of (G.2)), may be employed to determine a time history of $\dot{\theta}$ and τ during the rotational mode.

G.3 The Free Orbit, from a Rotating State.

This section will describe the free orbit which results from m_2 being released during the rotary motion about m_1. The case examined here considers in-plane motion only.

G.3.1 Position of Velocity Coordinates.

With m_2 "whirling" about m_1 (at $\pm\dot{\theta}$), then at any instant, m_2 is located relative to m_1 by

$$\bar{\ell} = \ell\,\bar{e}_\ell,$$

where $\bar{e}_\ell$ is a unit vector in the triad ($\bar{e}_\ell$, $\bar{e}_n$, $\bar{e}_z$), and is dependent on θ. Similarly, the relative velocity for m_2, due to the rotation ($\dot{\theta}$) is:

$$\bar{v}_2 = (\ell\,|\dot{\theta}|\,\bar{e}_n)\,\text{sgn}\,(\dot{\theta}), \tag{G.4}$$

wherein sgn $(\dot{\theta}) \equiv \pm 1$, depending on the rotational direction.

The inertial velocity for m_2 is recognized to be,

$$\bar{V}_2 = \bar{V}_1 + \bar{v}_2 , \tag{G.5a}$$

with

$$\bar{V}_1 \equiv r_1 \dot{\varphi}_1 \bar{e}_y . \tag{G.5b}$$

(See Fig. G.1) below.

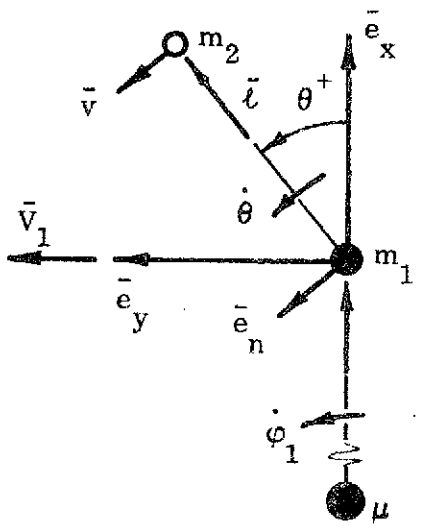

Fig. G.1. Description of Rotating Tether Systems.

From the figure it should be evident that the two relative positioning triads are related according to the transformation:

$$\begin{pmatrix} \bar{e}_\ell \\ \bar{e}_n \\ \bar{e}_z \end{pmatrix} = \begin{pmatrix} \cos\theta & \sin\theta & 0 \\ -\sin\theta & \cos\theta & 0 \\ 0 & 0 & 1 \end{pmatrix} \begin{pmatrix} \bar{e}_x \\ \bar{e}_y \\ \bar{e}_z \end{pmatrix} \tag{G.6}$$

As a consequence of eq. (G.6) the relative state equations may be recast as:

$$\bar{\ell} = \ell\,(\cos\theta\,\bar{e}_x + \sin\theta\,\bar{e}_y),$$

and $$\bar{v}_2 = \ell\,|\dot{\theta}|\,(-\sin\theta\,\bar{e}_\ell + \cos\theta\,\bar{e}_n)\,\mathrm{sgn}\,\dot{\theta}. \tag{G.7}$$

Carrying this operation into eq. (G.5a), it is found that:

$$\bar{V}_2 = \left[r_1\dot{\varphi}_1 + (\ell\,|\dot{\theta}|\cos\theta)\,\mathrm{sgn}\,\dot{\theta}\right]\bar{e}_y - \left[(\ell\,|\dot{\theta}|\sin\theta)\,\mathrm{sgn}\,\dot{\theta}\right]\bar{e}_x . \tag{G.8}$$

Herein, sgn $\theta = \pm 1$, and $\theta \equiv \theta_o + \dot{\theta} t$.

Making use of eq. (G.7) it is apparent that m_2 is located relative to μ by:

$$\bar{r}_2 = \bar{r}_1 + \bar{\ell} = (r_1 + \ell \cos\theta)\,\bar{e}_x + (\ell \sin\theta)\,\bar{e}_y . \qquad \text{(G.9)}$$

Next, making use of eqs. [(G.8), (G.9)] the corresponding speed and position ratios are readily obtained as:

(1) Speed Ratio:

$$\frac{V_2}{V_1} = \left[1 + \left(\frac{2\,|\bar{v}_2|}{V_1}\cos\theta\right)\operatorname{sgn}\dot{\theta} + \frac{v_2^{\,2}}{V_1^{\,2}}\right]^{1/2}. \qquad \text{(G.10a)}$$

(2) Position Ratio:

$$\frac{r_2}{r_1} = \left[1 + 2\frac{\ell}{r_1}\cos\theta + \left(\frac{\ell}{r_1}\right)^2\right]^{1/2} \equiv \Delta. \qquad \text{(G.10b)}$$

G.3.2 Momentum and Energy Equations.

For the free orbit, developed here as an operational maneuver:

(1) Momentum Expressions:

With $\bar{h} \equiv \bar{r} \times \bar{V}$, relative to μ; it follows that,

$$\bar{h}_1 = \bar{r}_1 \times V_1 = r_1^{\,2}\dot{\varphi}_1\,\bar{e}_z . \qquad \text{(G.11a)}$$

Similarly,

$\bar{h}_2 = \bar{r}_2 \times \bar{V}_2$, with $\bar{r}_2$, $\bar{V}_2$ defined in eqs. [(G.8), (G.9)].

After carrying out the indicated multiplications, one finds:

$$\bar{h}_2 = \bar{h}_1 + \left[(\ell\,|\dot{\theta}|)\operatorname{sgn}\dot{\theta} + r_1\ell\cos\theta\,(\dot{\varphi}_1 + |\dot{\theta}|\operatorname{sgn}\dot{\theta})\right]\bar{e}_z , \qquad \text{(G.11b)}$$

with $\bar{h}_1$ defined immediately above.

Expressing eq. (G.11b) as a ratio, then

$$\frac{h_2}{h_1} = 1 + \frac{\ell}{r_1}\left[\left(1 + \frac{|\dot\theta|}{\dot\varphi}\ \mathrm{sgn}\ \dot\theta\right)\cos\theta + \frac{\ell\,|\dot\theta|}{r_1\dot\varphi_1}\ \mathrm{sgn}\ \dot\theta\right]. \tag{G.11c}$$

(2) The specific energy expression for the m_2-orbit is defined as:

$$E_2 = \frac{V_2^2}{2} - \frac{\mu}{r_2} = -\ \frac{\mu}{2a_2}\ , \tag{G.12a}$$

or, with m_1 moving on a circular orbit (by assumption),

$$\frac{2E_2}{V_1^2} = \left(\frac{V_2}{V_1}\right)^2 - \frac{2}{r_2/r_1} = -\ \frac{1}{a_2/r_1}\ ,$$

which, after recognizing that $E_1 = -\ V_1^2/2$, leads directly to the result:

$$\frac{E_2}{E_1} = -\left(\frac{V_2}{V_1}\right)^2 + \frac{2}{r_2/r_1} = \frac{1}{a_2/r_1}\ . \tag{G.12b}$$

From this resultant one can obtain a description of

$$\frac{a_2}{r_1} = \frac{E_1}{E_2} \equiv \frac{1}{E_2/E_1}\ . \tag{G.12c}$$

with the ratios, (V_2/V_1) and (r_2/r_1) determined from eqs. (G.10).

G.3.3 Orbit Eccentricity.

The eccentricity for the free orbit of m_2 is determined from the expression:

$$\epsilon_2 = \left[1 + \frac{h_2^2}{\mu^2}\ (2E_2)\right]^{1/2}. \tag{G.13a}$$

In terms of the ratios defined above, this can be recast into the form:

$$\epsilon_2 = \left[1 - \left(\frac{h_2}{h_1}\right)^2\ \frac{E_2}{E_1}\right]^{1/2}, \tag{G.13b}$$

wherein the ratios are obtained from eqs. (G.11c) and (G.12b), respectively.

G.3.4 Angle Descriptions.

The elevation angle (γ_2), for the velocity vector $\bar{V}_2$, and the position angle (φ_2) on the free orbit, where m_2 is released from its tether, are to be described next.

(a) Since all motions are restricted to a single plane, and since $\bar{V}_1 \equiv V_1 \bar{e}_y$, then symbolically,

$$\cos \gamma_2 = \frac{\bar{V}_2 \cdot \bar{V}_1}{V_1 V_2} .$$

This can be reduced to,

$$\cos \gamma_2 = \frac{1 + \left(\frac{|\bar{v}_2|}{V_1} \cos \theta \right) \operatorname{sgn} \dot{\theta}}{V_2/V_1} , \qquad \text{(G.14)}$$

wherein $\frac{|\bar{v}_2|}{V_1} = \frac{\ell |\dot{\theta}|}{r_1 \dot{\varphi}_1}$; and, $\theta \equiv \theta_o + (|\dot{\theta}| t) \operatorname{sgn} \dot{\theta}$.

Due to the symmetry which is apparent for closed orbits, there is a concern regarding the sgn (γ_2). To overcome the ambiguity evident in eq. (G.14) the following test is suggested:

Define the x^{th} component of $\bar{v}_2$ by:

$$v_{2_x} \equiv \bar{v}_2 \cdot \bar{e}_x = - (\ell |\dot{\theta}| \sin \theta) \operatorname{sgn} \dot{\theta} . \qquad \text{(G.15a)}$$

As a consequence of eq. (G.15a), the test is:

$$\text{If: } v_{2_x} < 0, \text{ then } \gamma_2 < 0;$$

$$v_{2_x} > 0, \text{ then } \gamma_2 > 0. \qquad \text{(G.15b)}$$

Also, with $\sin \gamma_2 \equiv \pm \sqrt{1 - \cos^2 \gamma_2}$, then:

$$\text{If: } v_{2_x} < 0, \ \sin \gamma_2 < 0;$$
$$v_{2_x} > 0, \ \sin \gamma_2 > 0. \tag{G.15c}$$

(b) The position angle (φ_2), locating the "release point" for the free orbit, can be ascertained from a description of the elevation angle (γ_2). That is, with

$$\tan \gamma_2 = \frac{\epsilon_2 \sin \varphi_2}{1 + \epsilon_2 \cos \varphi_2} \equiv \frac{\sin \gamma_2}{\cos \gamma_2} ; \tag{G.16}$$

a quadratic expression in $\cos \gamma_2$ (say) can be obtained. This quadratic has a solution in the form:

$$\cos \varphi_2 = - \frac{\sin^2 \gamma_2}{\epsilon_2} \pm \sqrt{\cos^2 \gamma_2 \frac{\sin^2 \gamma_2}{\epsilon_2^2}} \quad . \tag{G.17}$$

The apparent ambiguity in sign, on the radical, can be rectified by examining the radius (at release) in comparison to the length a_2. (For a more complete discussion on the reasoning for this, see section H.4.3, Appendix H).

The conditions governing the choice of sign for the radical, in eq. (G.17) are as follows:

(1) If $r_2/a_2 > 1.0$, then sgn $(\sqrt{\sim}) = -1$.

(2) If $r_2/a_2 < 1.0$, then sgn $(\sqrt{\sim}) = +1$.

(Note: The quantity r_2/a_2 is described in eq. (G.12c)).

G.3.5 Pericenter Radius and Speed.

The magnitude of the state parameters at a pericenter (for the free orbit) are of interest here. These parameters are a set of terminal conditions to be described from the free orbit's characteristics.

With these characteristics as known quantities, now, then the desired descriptions are acquired immediately.

Hence, with the radius to pericenter defined as,

$$r_{p_2} = a_2 (1-\epsilon_2); \tag{G.18a}$$

its ratioed form is,

$$\frac{r_{p_2}}{r_1} = \frac{a_2}{r_1} (1-\epsilon_2), \tag{G.18b}$$

wherein a_2/r_1 and ϵ_2 are obtained from eqs. (G.12c) and (G.13).

The speed at pericenter is most simply defined from

$$V_{p_2} = \frac{h_2}{r_{p_2}} \equiv \frac{(h_2/h_1)}{(r_{p_2}/r_1)} \frac{h_1}{r_1} ,$$

or

$$\frac{V_{p_2}}{V_1} = \frac{(h_2/h_1)}{(r_{p_2}/r_1)} , \tag{G.18c}$$

with the ratios used here determined in eqs. (G.18b) and (G.11c), respectively.

G.4 Summary.

The various expressions and methods described in this appendix have been used to develop a computer program called TETHROT. This program was exercised to acquire information on the establishment of free orbits from a rotating tethered system.

APPENDIX H

COMPUTATIONAL EQUATIONS

H.1 Introduction.

In this appendix the equations employed in the main computer program (TETHER) are developed. These expressions are primarily for an extensible tethered body system, not considering the connecting line as an elastic member; and with the mass particles having Keplerian motions. For consistency with the formulations developed and manipulated in other sections of this report this development will consider the one particle, m_1 ($\gg m_2$), to be on a circular path. Particle m_2, however, travels its orbit under the added influence of the tether action.

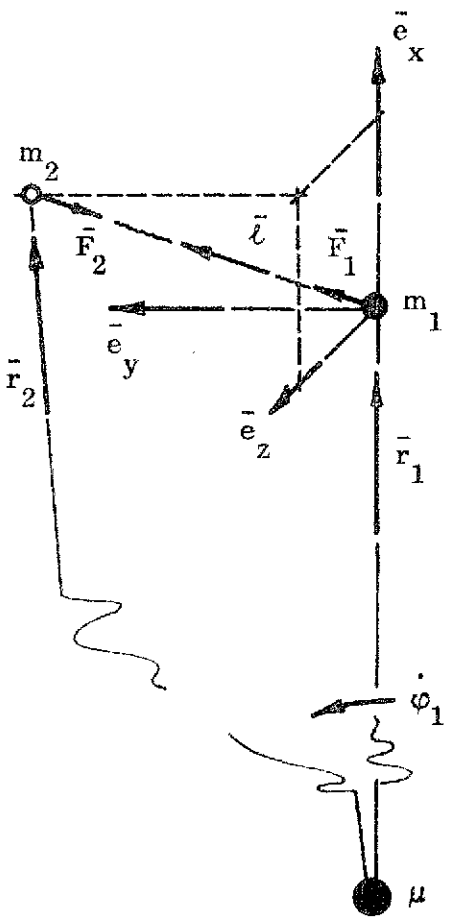

Fig. H.1. Geometry for the Computer Program.

H.2 Basic Formulation.

For compatibility with earlier programming efforts, the present development is primarily constructed in a cartesian representation. Also, the equations are cast into a dimensionless format, using the ideas set down in Appendix E. These equations are non-linear and coupled.

The motion for each body is treated as a two-body problem; the relative position vector $\bar{r}_r \equiv \bar{r}_r\,(x, y, z)$, with the triad ($\bar{e}_x$, $\bar{e}_y$, $\bar{e}_z$) attached to, and moving with m_1, thus $\bar{\omega} \equiv \dot{\varphi}_1\,\bar{e}_z$.

The tether ($\bar{\ell}$) is parallel to $\bar{r}_r$ and has a tension $|\bar{F}|$, thus:

$$\ddot{\bar{r}}_i = -\frac{\mu}{r_i^3}\,\bar{r}_i - \frac{(F/m_i)\,\bar{\ell}}{\ell} * \left[(-1)^i\right], \quad (i = 1,2). \tag{H.1}$$

From the geometry shown, $\bar{r}_2 = \bar{r}_1 + \bar{\ell}$, with

$$\bar{r}_2 \equiv (r_1 + x)\,\bar{e}_x + y\bar{e}_y + z\bar{e}_z \;;$$

hence

$$\left(\frac{r_2}{r_1}\right)^3 \equiv \Delta^3 = \left[\left(1 + \frac{x}{r_1}\right)^2 + \frac{y^2 + z^2}{r_1^2}\right]^{3/2}. \tag{H.2}$$

Since $\bar{\ell} = \bar{r}_2 - \bar{r}_1$, then $\ddot{\bar{\ell}} = \ddot{\bar{r}}_2 - \ddot{\bar{r}}_1$; and, from above,

$$\ddot{\bar{\ell}} = \ddot{\bar{r}}_2 - \ddot{\bar{r}}_1 = -\frac{\mu}{r_1^3}\left[\frac{r_1^3}{r_2^3}\,(\bar{\ell} + \bar{r}_1) - \bar{r}_1\right] - \frac{F\,\bar{\ell}}{\ell\tilde{m}} \;; \tag{H.3}$$

with

$$\tilde{m} \equiv \frac{m_1 m_2}{m_1 + m_2}.$$

H.2.1 Kinematics.

Defining the tether vector ($\bar{\ell}$) as,

$$\bar{\ell} = x\bar{e}_x + y\bar{e}_y + z\bar{e}_z \equiv x_i\bar{e}_i \;;$$

then:

$$\dot{\bar{\ell}} = \dot{x}_i\bar{e}_i + x_i\dot{\bar{e}}_i \;, \text{ etc.},$$

and, consequently, it is easy to show that:

$$\ddot{\bar{\ell}} = (\ddot{x} - 2\dot{y}\dot{\varphi}_1 - x\dot{\varphi}_1^2)\,\bar{e}_x + (\ddot{y} + 2\dot{x}\dot{\varphi}_1 - y\dot{\varphi}_1^2)\,\bar{e}_y + \ddot{z}\,\bar{e}_z. \tag{H.4}$$

H.2.2 Scalar Equations of Motion.

On combining the results above, and separating into scalar expressions, noting that $\dot{\varphi}_1^{\,2} = \mu/r_1^{\,3}$, it is found that:

$$\text{(a)*} \qquad \ddot{x} - 2\dot{y}\,\dot{\varphi}_1 - x\dot{\varphi}_1^{\,2} = -\,r_1\dot{\varphi}_1^{\,2}\left[\frac{1+(x/r_1)}{\Delta^3} - 1\right] - \frac{F_x}{\ell\tilde{m}}\,,$$

$$\text{(a)*} \qquad \ddot{y} + 2\dot{x}\,\dot{\varphi}_1 - y\dot{\varphi}_1^{\,2} = -\,r_1\dot{\varphi}_2\left[\frac{y/r_1}{\Delta^3}\right] - \frac{F_y}{\ell\tilde{m}}\,,$$

$$\ddot{z} = -\,r_1\dot{\varphi}_1^{\,2}\left[\frac{z/r_1}{\Delta^3}\right] - \frac{F_z}{\ell\tilde{m}}\,;$$

wherein

$$\Delta^3 = \left[\left(1+\frac{x}{r_1}\right)^2 + \frac{y^2+z^2}{r_1^{\,2}}\right]^{3/2}. \qquad \text{(H.5)}$$

Note: Eqs. (H.5) have been programmed to solve the tether problem for the conditions described, herein.

Since m_1 is assumed to move along a circular orbit, then there is a need to retain the inequality $m_2 \ll m_1$; however, there is no restriction on F (it may have any desired dependence); the coordinates (x, y, z) describe the relative displacements; and, the first time derivatives describe the relative speeds.

H.2.3 Dimensionless Variables.

Introduce as dimensionless variables the quantities defined by:

$$\xi \equiv \frac{x}{r_1}\,,\ \eta \equiv \frac{y}{r_1}\,,\ \zeta \equiv \frac{z}{r_1}\,;\ \xi' \equiv \frac{d(x/r_1)}{\dot{\varphi}_1\,dt} = \frac{d\xi}{d\varphi_1}\,,\ \text{etc.}\,;$$

and,

$$\tau \equiv \frac{(F/\tilde{m})}{\ell\dot{\varphi}_1^{\,2}} = \frac{(F/\tilde{m})}{\lambda r_1\dot{\varphi}_1^{\,2}}\,,\ \text{etc.,}\ \text{where}\ \lambda \equiv \ell/r_1\,. \qquad \text{(H.6)}$$

*(a), eqs. for the planar case.

Now, employing these in eqs. (H.5), one finds:

$$\xi'' - 2\eta' - \xi = \left[1 - \frac{1+\xi}{\Delta^3}\right] - \tau\xi\,,$$

$$\eta'' + 2\xi' - \eta = -\frac{\eta}{\Delta^3} - \tau\eta,$$

$$\zeta'' = -\frac{\zeta}{\Delta^3} - \tau\zeta\,; \qquad \text{(H.7)}^*$$

wherein

$$\Delta^3 \equiv \left[(1+\xi)^2 + \eta^2 + \zeta^2\right]^{3/2}.$$

H.2.4 The In-Plane Case.

The tether problem expressed in variables (ℓ, θ) describes the in-plane motion for m_2, relative to m_1. Since eqs. (H.1) express the problem, symbolically, then in place of eq. (H.2) one could write

$$\Delta^3 \equiv \left|\frac{\bar{r}_1 + \bar{\ell}}{r_1}\right|^3 = \left[\left(\frac{\ell}{r_1} + \cos\theta\right)^2 + \sin^2\theta\right]^{3/2}. \qquad \text{(H.8)}$$

Equation (H.3) is the dynamical expression for the system's "tether motion". The kinematic expression for $\ddot{\bar{\ell}}$ is that shown by eq. (F.5), Appendix F, wherein $\omega_\ell \equiv \dot{\theta} + \dot{\varphi}_1$. As a consequence of these definitions, etc. the scalar differential equations for this problem are those given as eqs. (F.6), Appendix F. Expanding the results given there, it is found that

$$\ddot{\ell} - \ell\,(\dot{\theta}+\dot{\varphi}_1)^2 = -\dot{\varphi}_1^{\,2}\left[\frac{\ell + r_1\cos\theta}{\Delta^3} - r_1\cos\theta\right] - \frac{F}{m}\,,$$

and

$$\ell\ddot{\theta} + 2\dot{\ell}\,(\dot{\theta}+\dot{\varphi}_1) = \dot{\varphi}_1^{\,2}\left[\frac{r_1\sin\theta}{\Delta^3} - r_1\sin\theta\right]. \qquad \text{(H.9)}$$

In dimensionless form these equations may be recast as:

* Actually, these are the equations programmed for solution in the program TETHER.

$$\lambda'' - \lambda\,(1+\theta')^2 = \cos\theta - \frac{\lambda+\cos\theta}{\Delta^3} - \tau_\ell\,,$$

$$\lambda\,\theta'' + 2\lambda'\,(1+\theta') = (\Delta^{-3} - 1)\sin\theta, \qquad \text{(H.10)}$$

wherein;

$$\lambda \equiv \frac{\ell}{r_1}\,,\quad \theta' = \frac{\dot\theta}{\dot\varphi_1}\,,\quad \Delta = [1+2\lambda\cos\theta + \lambda^2]^{1/2},$$

and,

$$\tau_\ell \equiv \frac{F/\tilde m}{r_1\dot\varphi_1^{\,2}}\,.$$

H.2.5 The Fixed Length, Pendulous Motion.

For computational purposes, eqs. (H.10) are useful in describing the pendulous motion for the tether problem, where ℓ is constant. These expressions are best to use in specializing for this mode of motion. This is,

for ℓ fixed; from eq. (H.9),

$$\frac{F}{\tilde m}\bigg|_{\ell=\mathcal{C}} = r_1\dot\varphi_1^{\,2}\left\{\left(\frac{\ell}{r_1}+\cos\theta\right)\left(1-\Delta^{-3}\right) + \frac{\ell}{r_1}\,\frac{\dot\theta}{\dot\varphi_1}\left(1+\frac{\dot\theta}{\dot\varphi_1}\right)\right\},$$

and,

$$\ddot\theta = -\,\frac{r_1}{\ell}\,\dot\varphi_1^{\,2}\,(1-\Delta^{-3})\sin\theta\,; \qquad \text{(H.11)}$$

with

$$\Delta^{-3} = \left(1 + 2\,\frac{\ell}{r_1}\cos\theta + \frac{\ell^2}{r_1^{\,2}}\right)^{-3/2}.$$

The second of eq. (H.11) can be manipulated as follows, for a solution:

(a) Multiply through the expression by $\dot\theta$; recognize that $\dfrac{\dot\theta\sin\theta}{\Delta^3} = \dfrac{d}{dt}\left(\dfrac{1}{\Delta}\right)$, etc; then obtain:

$$\frac{\dot\theta^2}{\dot\varphi_1^{\,2}} = 2\,\frac{r_1}{\ell}\left(\cos\theta + \frac{1}{\Delta}\right) + \mathcal{C}_1\,,$$

as a first integral. Here $\mathcal{C}_1$ is a constant of integration. Evaluating $\mathcal{C}_1$ for the condition; $\theta \to \theta_m$ as $\dot{\theta} \to 0$; then

$$\left(\frac{\dot{\theta}}{\dot{\varphi}_1}\right)^2 = 2\ \frac{r_1}{\ell}\left[\cos\theta - \cos\theta_m + \frac{1}{\Delta} - \frac{1}{\Delta_m}\right], \tag{H.12}$$

wherein

$$\Delta_m \equiv \left[1 + 2\frac{\ell}{r_1}\cos\theta_m + \frac{\ell^2}{r_1^2}\right]^{1/2}.$$

Unfortunately eq. (H.12) cannot be conveniently manipulated to determining θ_m without working through an iterative solution. This, of course, could be mechanized without much difficulty.

In order to describe the tether tension, at θ_m, the first of eqs. (H.11) can be made to yield:

$$\frac{F}{\tilde{m}}\bigg|_{\ell,\ \theta_m} = r_1\dot{\varphi}_1^2\left(\frac{\ell}{r_1} + \cos\theta_m\right)\left(1 - \Delta_m^{-3}\right), \tag{H.13}$$

wherein $\Delta_m \equiv \Delta(\theta_m)$, as shown above.

Rather than follow through with the mechanization hinted to above, for defining θ_m, etc., the simpler (linearized solution) should generally suffice. At least, these provide good estimates of where to look (first) in the iterative solution. Such a resultant has been obtained previously; it is:

$$\left(\frac{\dot{\theta}}{\dot{\varphi}_1}\right)^2 \cong \frac{3}{2}\left(\cos 2\theta - \cos 2\theta_m\right). \tag{H.14}$$

(Here one can find θ_m by "measuring" $\dot{\theta}$ at some θ, when ℓ is fixed, and acquire a <u>good</u> approximation for θ_m. This quantity is the angle amplitude for the pendulous mode).

Similarly, an estimate of $F/\tilde{m}$ is acquired from a modification of the first expression in eqs. (H.11). Letting $\Delta^{-3} \cong 1 - 3\cos\theta$, and accounting for

eq. (H.14), deleting the $(\ell/r_1)^2$ terms, then for the pendulous mode:

$$\left.\frac{F/\tilde{m}}{r_1\dot{\varphi}_1^{\,2}}\right|_{\ell} \cong 2\frac{\ell}{r_1}\left\{\frac{3}{4}(1-\cos 2\theta_m)+\frac{3}{2}\cos 2\theta+\frac{\dot{\theta}}{\dot{\varphi}_1}\right\}_{\ell = \text{fixed}},$$

or

$$\left[\frac{1}{2(\ell/r_1)}\right]\left[\left.\frac{F/\tilde{m}}{r_1\dot{\varphi}_1^{\,2}}\right|_{\ell}\right] \cong 3\left[\frac{1-\cos 2\theta_m}{4}+\frac{\cos 2\theta}{2}+\frac{1}{3}\frac{\dot{\theta}}{\dot{\varphi}_1}\right]. \qquad \text{(H.15)}$$

Eq. (H.15) will provide a time history of the tension, during the pendulous mode (ℓ fixed), as a function of θ.

In dimensionless variables eqs. (H.14) and (H.15) are described by:

$$\theta'^2 \cong \frac{3}{2}(\cos 2\theta - \cos 2\theta_m)$$

and

$$\frac{\tau}{2\lambda} \cong 3\left[\frac{1-\cos 2\theta_m}{4}+\frac{\cos 2\theta}{2}+\frac{\dot{\theta}}{3}\right]. \qquad \text{(H.16)}$$

H.3 Computational Procedures.

A Fixed Tension Mode, for Extensible Tethers.

This scheme uses eqs. (H.5), or its equivalent, in a program to determine the variations of state variables during this motion type.

The parameters for input are: characteristics of the circular orbit, for m_1; a level of tension (magnitude); and an initial relative state for m_2.

A Fixed Tension Mode, with the "Snubber" Included.

The basic difference in the operation here, from that above, is that the "snubber" is activated when $\dot{\ell} = 0$. There, θ_m is defined and the system operates in a "fixed length-pendulous mode" until the tension returns to the preset value.

When the preset tension is reached the snubber is removed (mathematically) and the operation reverts to that method used before it was engaged; i.e., a fixed tension mode, with $\dot{\ell} > 0$.

H.4 Description of a Free Orbit, from Tether Release.

The methodology described above is for extensible tether operations, where m_2 is constrained by the tensile force in the connecting line. On the supposition that the tether is "cut", and m_2 is allowed to move onto a "free" orbit; then the developments which follow will describe this situation. Herein the motion state is defined, the subsequent orbit is described, and certain desired "end conditions" are obtained.

H.4.1 The Initial State.

Assuming that the main body (m_1) motion is unaffected by the release of m_2 ($m_1 >> m_2$), then the state of m_2 with respect to m_1 is described as:

$$\bar{r}_r = \bar{r}_r\,(x, y, z); \text{ and, } \dot{\bar{r}}_r = \dot{\bar{r}}_r\,(\dot{x},\ \dot{y},\ \dot{z},\ \dot{\varphi}_1).$$

From the problem geometry (see Fig. H.1) the position of m_2 is

$$\bar{r}_2 = \bar{r}_1 + \bar{\ell} \equiv \bar{r}_1 + \bar{r}_r$$

$$= (r_1 + x)\,\bar{e}_x + y\,\bar{e}_y + z\,e_z, \tag{H.17a}$$

and the magnitude of r_2 is:

$$r_2 \equiv [(r_1 + x)^2 + y^2 + z^2]^{1/2}. \tag{H.17b}$$

Corresponding to this, it can be shown that the velocity is:

$$\dot{\bar{r}}_2 = (\dot{r}_1 + \dot{x} - y\dot{\varphi}_1)\,\bar{e}_x + [\dot{y} + (r_1 + x)\dot{\varphi}_1]\,\bar{e}_y + \dot{z}\,e_z. \tag{H.18a}$$

Defining $\bar{V}_2 \equiv V_{x_2} \bar{e}_x + V_{y_2} \bar{e}_y + V_{z_2} \bar{e}_z$, then from eq. (H.18a), note that:

$$V_{x_2} \equiv \dot{r}_1 + \dot{x} - y\dot{\varphi}_1 ,$$

$$V_{y_2} \equiv \dot{y} + (r_1 + x)\dot{\varphi}_1 ,$$

$$V_{z_2} \equiv \dot{z} ; \tag{H.18b}$$

and, also, that

$$V_2 = \left[V_{x_2}^{\ 2} + V_{y_2}^{\ 2} + V_{z_2}^{\ 2} \right]^{1/2} . \tag{H.18c}$$

H.4.2 Energy, Eccentricity, for m_2.-

The specific energy for the free orbit is defined by:

$$E_2 \equiv \frac{V_2^{\ 2}}{2} - \frac{\mu}{r_2} = -\frac{\mu}{2a_2} . \tag{H.19}$$

The quantities V_2, r_2 are known, hence the energy is readily determined. Also, by manipulation, the parameter a_2 is described, directly, by:

$$a_2 = -\frac{\mu}{2E_2} . \tag{H.20}$$

Since the orbital eccentricity is known to be:

$$\epsilon_2 = \left[1 + \frac{h_2^{\ 2}}{\mu^2} 2E_2 \right]^{1/2} , \tag{H.21}$$

then it is seen that ϵ_2 can be determined once an appropriate description for h_2 is found. The specific moment of momentum (magnitude) is evaluated in section (H.4.3), below.

H.4.3 Angle Relations.

The two principal angles to be determined here are the position and elevation angles, for m_2, at the release position. A method for this is outlined below.

(1) Specific Momentum (h_2) defined.

Since $\bar{h}_2 \equiv \bar{r}_2 \times \bar{V}_2 = h_{i_2} \bar{e}_{i_2}$, (i = x, y, z); with $\bar{r}_2$ and $\bar{V}_2$ described in section (H.4.1); it can be shown that:

$$h_{x_2} = y V_{z_2} - z V_{y_2},$$

$$h_{y_2} = z V_{x_2} - x V_{z_2},$$

$$h_{z_2} = (x + r_1) V_{y_2} - y V_{x_2}. \qquad \text{(H.22a)}$$

Corresponding to this the magnitude, h_2, is:

$$h_2 = [h_{i_2}^{\ 2}]^{1/2}. \qquad \text{(H.22b)}$$

(2) A unit normal vector ($\bar{n}_2$), which lies in the plane of motion, orthogonal to both $\bar{r}_2$, $\bar{h}_2$, is defined here as:

$$\bar{n}_2 = \frac{\bar{h}_2 \times \bar{r}_2}{h_2 r_2}. \qquad \text{(H.23)}$$

Note that r_2 is defined by eq. (H.17b).

(3) Having the vectors $\bar{V}_2$, $\bar{n}_2$, $\bar{r}_2$ (all in the plane of motion), then a means for determining γ_2 is as follows:

$$\frac{\bar{V}_2 \cdot \bar{n}_2}{V_2} \equiv \cos \gamma_2,$$

$$\frac{\bar{V}_2 \cdot \bar{r}_2}{v_2} \equiv \sin \gamma_2 ,$$

and

$$\gamma_2 \equiv \tan^{-1}\left(\frac{\bar{V}_2 \cdot \bar{r}_2}{\bar{V}_2 \cdot \bar{n}_2} \; \frac{1}{r_2} \right) \tag{H.24}$$

It is readily seen that γ_2 is the elevation angle of the velocity $\bar{V}_2$.

(4) Next, the position angle φ_2 is to be determined. Recall that,

$$\tan \gamma_2 = \frac{\epsilon_2 \sin \varphi_2}{1+\epsilon \cos \varphi_2} \equiv \frac{\sin \gamma_2}{\cos \gamma_2} \quad . \tag{H.25}$$

Nominally, for closed orbits $|\gamma_2| \leq \pi/2$, hence $\cos \gamma_2 \geq 0$, while $-1 \leq (\sin \gamma_2) \leq +1$. The sketch, below, indicates angle range and sign for the quadrants of that geometry.

Note that: $\gamma_2 \geq 0$ in Quadrants I, II,

$\gamma_2 \leq 0$ in Quadrants III, IV.

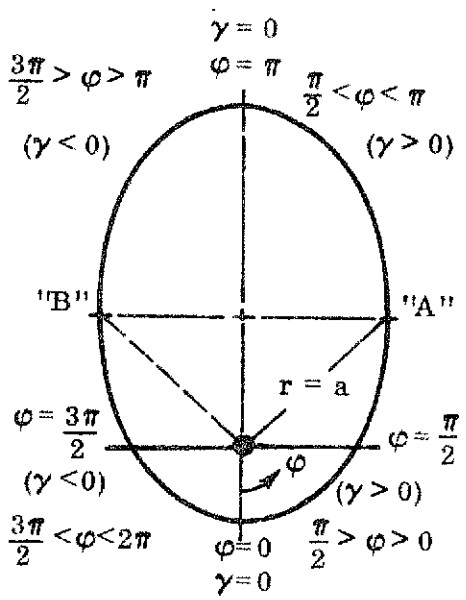

Fig. H.2. Angles; Descriptions.

The angle φ_2, locating m_2 on its free orbit, relative to the pericenter may be obtained as a solution to eq. (H.25). That is, after squaring that expression a solution to the quadratic is:

$$\cos \varphi_2 = -\frac{\sin^2 \gamma_2}{\epsilon_2} \pm \sqrt{\cos^2 \gamma_2 \left(1 - \frac{\sin^2 \gamma_2}{\epsilon_2^2}\right)} \tag{H.26a}$$

where the sign on the radical must be assigned in accord with the symmetry noted for the γ_2 angle. A methodology for assigning this sign is explained below:

It should be recognized that γ_2 is symmetric, in magnitude, about point "A" (see Fig. H.2), for the first half of orbit (I, II), and is positive; while it is symmetric about "B", for the second half (III, IV), but negative. Also, it is known that $(V=V_c)_{local}$ at A, B; but $(V \geq V_c)_{local}$ between $\varphi = 0$ and A, B. Conversely $(V \leq V_c)_{local}$ between A, B and $\varphi = \pm \pi$. In addition, one should recognize that $r_A = r_B = a_2$ at these positions.

With this information at hand it is noted that, at (A, B),

$$V_{A,B} \equiv \sqrt{\frac{\mu}{a_2}} = \sqrt{-2E_2} \ .$$

The test to be applied for determining the sign on the radical may be summarized as follows:

(1) If r_2 (local) $> a_2$, the sgn $(\sqrt{\sim}) = -1$.

(2) If r_2 (local) $< a_2$, the sgn $(\sqrt{\sim}) = +1$. (H.26b)

What is inferred here is that condition (1) describes positions in the apocentric region between "A" and "B", while condition (2) refers to the pericenter region (below the line A to B).

Suitable solutions to eq. (H.26a) may be obtained, now.

H.4.4 Pericenter Values.

The values to be determined here are the radius and speed at the pericenter position. Also of interest is the transfer angle, from the release point to the pericenter; however, this quantity is determined (implicitly) by φ_2.

The pericentric radius is described, from the conic equations, as

$$r_{p_2} = a_2 (1-\epsilon_2), \tag{H.27}$$

where a_2, ϵ_2 are given in eqs. (H.20), (H.21).

In a like manner the speed at pericenter can be described as

$$V_{p_2} = \frac{\mu}{h_2}(1+\epsilon_2) \tag{H.28a}$$

$$= \frac{h_2}{r_{p_2}} , \tag{H.28b}$$

with an expression for h_2 found in eq. (H.22b).

H.5 Summary.

The various descriptions set down in this appendix have been developed into a computer program (TETHER) which was exercised to provide various data needed in this study. A general outline of this program is the subject of Appendix I.

APPENDIX I

TETHER, A COMPUTER PROGRAM

I.1 Introduction.

TETHER is a computer program designed to solve for the relative motion of two bodies connected by a non-elastic tether and moving under the influence of a small initial displacement, a non-zero initial relative velocity and an initial tension. The main body is traveling on an undisturbed circular orbit, while the tethered body moves under the influence of gravity gradient, the initial velocity and the tether tension. The motion of this second body is described by a set of differential equations which are numerically integrated with respect to time, implicitly, and with respect to a position angle, explicitly.

In one of its selected modes of operation the program solves for the initial tension and initial velocity magnitude needed to have the tethered body reach a final tether length (L), at a prescribed positioning angle (θ), with the angular rate ($\dot{\theta}$) of zero.

The program operates under two main options. In one, the simple extensible tether problem, the tether pays out to the given length, satisfying the end conditions. In the other mode, the tether pays out until the rate of change of length goes to zero; then the system gyrates at a fixed length (until the tension builds up to the initial level) when the tether again pays out to the end length and end angle conditions.

I.2 Operating Modes.

In option "one" the differential equations are described symbolically as: $\ddot{R} = f(R, \dot{R}, T, t)$ where R, $\dot{R}$ are the position and velocity; T is the initial tension; and, t is the time for the program to run. The scalar equations describing this problem are:

$$x1 = x + 1 ,$$

$$W = (x1^2 + y^2 + z^2)^{3/2} ,$$

$$L = (x^2 + y^2 + z^2)^{1/2} ,$$ (dimensionless length of a tether; a positive number)

$$x'' = 2y' + x1 - \frac{x1}{W} - T \cdot \frac{x}{L} ,$$ (dimensionless)(T ≡ specific tension magnitude, a positive number)

$$y'' = -2x' + y - \frac{y}{W} - T \cdot \frac{y}{L} ,$$

$$z'' = -\frac{z}{W} - T \cdot \frac{z}{L} ,$$

$$L' = (x x' + y y' + z z')/L ,$$ (The dimensionless value for the tether "pay-out" rate).

(Primes denote angle derivatives: $d/d\varphi \equiv \frac{1}{\dot{\varphi}} \frac{d}{dt}$).

These equations are integrated until $L = R_f$, where R_f is an input quantity defining the final, desired tether length.

In option "two", the above equations are integrated until $\dot{L} = 0$. At this time the length of the tether, L, becomes fixed and the following equation is integrated (to determine the history of θ, with L = fixed value):

$$\theta'' = -\frac{1}{L}\left[(1-\Delta^{-3}) \sin \theta\right] ;$$

here $\Delta^{-3} \equiv [1 + 2L \cos \theta + L^2]^{-3/2}$. The starting conditions for this segment of the problem are:

$$\theta_o = \tan^{-1}\left(\frac{y}{x}\right) ,$$

and

$$\dot{\theta}_o = (x\dot{y} - y\dot{x})/(x^2 + y^2),$$

using the position and velocity at the instant when $\dot{L} = 0$.

The dynamic tether tension is computed as:

$$T_d = (L + \cos\theta)(1 - \Delta^{-3}) + L\,\theta'\,(2 + \theta').$$

Integration continues in this mode until the dynamic tension equals the initial tension ($T_d = T$). At this point, in the integration, the program reverts to the previous mode of operation.

The new position and velocity vectors are computed, to reinitiate the integration, and the program proceeds, again, under option one. Integration is terminated when $L = R_f$. The scalar, kinematic equations for R and V which initiate the option one mode again, are:

$$x = L\cos\theta \qquad \dot{x} = -L\,\dot{\theta}\sin\theta$$

$$y = L\sin\theta \qquad \dot{y} = +L\,\dot{\theta}\cos\theta$$

$$z = z \text{ (value at } \dot{L} = 0) \qquad \dot{z} = \dot{z} \text{ (value at } \dot{L} = 0).$$

Under either option the iterator routine, MINMX3, makes repeated calls to the integration package, using these trial trajectories to find a desired initial tension and velocity.

I.3 Inputs.

The inputs to the program are in dimensionless units; however, the program performs all calculations, and produces outputs in dimensionless units. The program is written in the FORTRAN IV language under the H compiler for the IBM 360 Operating System. A description of the inputs, program operations, and outputs follow below.

Inputs to TETHER are given through the namelist feature of the IBM Fortran IV programming language. The input namelist is called NML; every input required or used in the program is declared, by name, in the list. The general form for assigning an input value to a named quantity is, simply,

NAME = VALUE

Here NAME is the name assigned to the variable and included in the namelist. VALUE is a numerical or logical quantity consistent in form (i.e., logical, integer, or real) with NAME. Unless otherwise specified, all NML names commencing with the letters I-N represent integers; whereas all names commencing with the letters A-H or O-Z are double precision floating point numbers. Each namelist case must begin with the characters,

&NML

commencing in card column 2 and followed by at least one blank. Each namelist ends with the characters,

&END

preceded by at least one blank, if data is specified on the same line.

Card column 1 is ignored on all input cards. Multiple data assignments on a single card are permissible if separated by commas. Blanks in the variable field, VALUE, are taken as zeros. A comma following the last VALUE on a card is optional.

The order of the input data assignments is arbitrary; i.e., they need not be in the same order as listed in the namelist. In fact, there is no requirement that any specific input parameter be represented in the input data set. If no value is included in the inputs, for a particular parameter, the default value is used, if defined. (See Default Values).

For other details regarding the namelist feature, the reader is referred to the IBM System/360 Fortran IV Language manual. Namelist cases may be stacked in sequence. A single namelist error may wipe out the remaining namelist inputs.

I.4 Definition of Input Parameters.

NAME	DIMENSION	DESCRIPTION	DEFAULT
RIN	3	Initial input position vector, (nominally in feet).	
RDIN	3	Initial input velocity vector, (nominally in feet/sec.)(the magnitude of this quantity is an initial guess for the iterator).	
THRIN	3	Initial input specific tension magnitude, (nominally in feet/sec^2)(the magnitude of this quantity is an initial guess for the iterator).	
TO		Initial time in sec.	
TFIN		Final time in sec. (used as an upper limit, to terminate integration).	
EMU		Earth's gravitational constant ($feet^3/sec^2$).	1.4076468532785D16
RCNV		Conversion factor, to convert input position vector. (nominally into feet).	1.D0 5280.D0
VCNV		Conversion factor, to convert input velocity vector. (nominally into feet/sec.).	1.D0
R		Input circular orbital radius. (nominally in miles).	
HS		Integration step size.	0.1325D0

NAME	DIMENSION	DESCRIPTION	DEFAULT
LSRCH		Trigger to determine whether to use option 1 or option 2. (LSRCH = 0; option 1 - do not search for $\dot{L}$ =0). (LSRCH = 1; option 2 - search for $\dot{L}$ =0 and integrate $\dot{\theta}$ equation).	
ISOLVE		Trigger to determine whether to calculate a single trajectory or iterate for a solution. (ISOLVE=1, iterate), (ISOLVE=0, single trajectory).	
THETAF		Final value of θ to be iterated to.	
THETDF		Final value of $\dot{\theta}$ to be iterated to.	
RF		Length of tether to be integrated to. (Input in feet).	

The output for each case will be:

(1) The initial velocity magnitude.

(2) The initial tension magnitude.

(3) A time history of R, V, T (position, velocity, tension) L, $\dot{L}$, θ, $\dot{\theta}$, φ, $\dot{\varphi}$; and, if under option two, a time history of θ and T.

(4) A time history of the pericenter and the speed at pericenter, if the tether would be "cut" at <u>any time</u> during the integration.

(5) A time history of the position radius and speed, for the tethered mass, during the integration.

(6) A time history of the eccentricity, transfer angle to peri-radius, and the local elevation angle, for m_2.

All of the above outputs are tabulated during the normal operation of the program.

I.5 Sample Inputs.

Example Case: An in-plane simulation, wherein:

$$\theta_o = 150^o,\ \theta_f = 180^o,\ \dot{\theta}_f = 0^o/s,\ \ell_o = 1.0 \text{ ft},\ \ell_f = 10.000 \text{ ft},\ \dot{\ell}_o = 17.4 \text{ f/s},$$

also, set:

$$t_o = 0 \text{ sec},\ t_f = 4000 \text{ sec; estimate } F/m_2 \text{ (const)} \cong 0.00075 \text{ f/s}^2.$$

Let the operation be defined as type Mode A (reel-in, reel-out case, constant tension). For this case let the iterator be employed to determine a proper set of initial quantities (ISOLVE = 1).

Note: (1) For a Mode B operation, set LSRCH = 1.

(2) With ISOLVE = 1., the integration terminates when the end conditions (of state) are reached.

(3) For variable tension systems (Mode C), assign values to SOLPE, SLOPE2.

Inputs are:

```
&NML
 RIN = - 0.86603, + 0.50000, + 0.0000,
 RDIN = - 15.06892, + 8.100, + 0.0000,
 TO = 0.D0, TFIN = 4000.D0,
 EMU = 1.407646853278 5D16,
 RCNV = 1.0, VCNV = 1.0,
 R = 24145223.9527,
 HS = 0.15625D-1, LSRCH = 0., ISOLVE = 1.,
 THETAF = 180.0, THETDF = 0.0,
 RF = 1.D + 4,
 SOLVE = 0.D0, SOLVE2 = 0.D0
&END
```

I.6 The Iterator.

The iteratory used here is the software module (MINMX3) which drives the two-boundary value problem to a solution. The following discussion is taken from TOPCAT I*.

Correction scheme. - The iterator's underlying mathematical operation is formulated as follows. Let X denote the vector of independent variables and let Y denote the vector of dependent variables. The relationship between these two vectors is given by:

$$Y = F\ (X).$$

The vector function, F, is evaluated by integrating the trajectory; that is, given a complete set of control parameters and initial conditions, the corresponding values of the end conditions Y can be determined. Subroutine TRAJ maps X onto Y and is therefore the software package which corresponds to the function F. The problem is to find the vector X* which will result in specified values of the dependent variables Y*, that is to solve

$$Y^* = F\ (X^*)$$

where Y* is known. This is formulated as a minimization problem. The weighted sum of the residuals q_i is given by

$$q_i = \left[Y^* - F\ (X_i)\right]^T W_y \left[Y^* - F\ (X_i)\right],$$

where x_i is the current estimate of the independent variables and W_y is a diagonal, positive definite weighting matrix.

The problem is to choose a new value X_{i+1} to minimize q_{i+1}. If X_{i+1} is close to X_i, then

$$F\ (X_{i+1}) = F\ (X_i) + P\ \Delta X,$$

*Lion, P.M., Campbell, J.H., and Shulzycki, A.B., "TOPCAT I: Trajectory Optimization Program for Comparing Advanced Technologies", Aerospace Engineering Report No. 717s, Dept. of Aerospace and Mechanical Sciences, Princeton University, March 1966.

where $\Delta X = X_{i+1} - X_i$ and the partial derivative matrix, P, is given by

$$P = \frac{\partial Y}{\partial X} .$$

Evaluating q_{i+1} with the approximation leads to the expression

$$q_{i+1} = (\Delta Y - P\Delta X)^T W_y (\Delta Y - P\Delta X)$$

where ΔY, the residual vector, is given by

$$\Delta Y = Y^* - F(X_i) .$$

The problem is then to choose ΔX to minimize q.

Inhibitor control. - For nonlinear functions F, linear approximations work only if ΔX is small. Therefore, the following constraint is imposed:

$$\Delta X^T W_y \Delta X \leq \ell ,$$

where W_x is the input diagonal, positive definite weighting matrix associated with the independent parameters.

Attaching the constraint with a scalar inhibitor, λ, the vector to be minimized is given by:

$$Q = (\Delta Y - P\Delta X)^T W_y (\Delta Y - P\Delta X) + \lambda (\Delta X^T W_x \Delta X).$$

Finding the minimum of the vector function yields the solution:

$$\Delta X = (P^T W_y P + \lambda W_x)^{-1} P^T W_y \Delta Y.$$

It has been shown (see HILTOP reference) that as λ increases, ℓ decreases monotonically. Therefore, λ can always be chosen large enough to satisfy the above inequality. Moreover, if λ is sufficiently large, the correction is approximately:

$$\Delta X = \frac{1}{\lambda} W_x^{-1} (P^T W_y) \Delta Y.$$

For ΔX small enough, or λ large enough, we are guaranteed that,

$$q_{i+1} \leq q_i .$$

It is advantageous to take as large a step toward satisfying $Y^* = F(X^*)$ as possible. The procedure is initiated with a relatively small value of λ. The idea is to make a correction, determine if any improvement is made and, if not, cut back on the correction. The following iteration scheme is utilized. Given X_i, the trajectory is integrated again to produce Y_{i+1} starting with the values $X_{i+1} = X_i + \Delta X$, and q_{i+1} is calculated. q_{i+1} is then compared with q_i. If there is no improvement, λ is increased. ΔX is recalculated and a new trajectory integrated. This is repeated until an improvement results. When this happens, the trajectory is integrated again and the partial derivative matrix is computed. λ is reset to its original value. The iteration continues until q is less than the prescribed tolerance or no further improvement can be made or the maximum number of iterations is exceeded.

Constraints (dependent variables). - The constraints, Y, are divided into two types, parameters that are driven to a given value (point constraints), and parameters to be maximized or minimized (performance indices).

For a well-posed problem, there is only one performance index. For each dependent variable, y_i, two values must be specified. y_{min} and y_{max}. If a dependent variable is a point constraint, y_{min} and y_{max} are chosen close together

$$y_{min} = y^* - \delta ; y_{max} = y^* + \delta ,$$

where y^* is the desired value and δ is a tolerance utilized for weighting purposes. For the performance index, the interval is chosen so that it cannot possibly be attained if the other constraints are satisfied. For instance, if y

is to be minimized, y_{min} and y_{max} are taken smaller than attainable, conversely if y is to be maximized, y_{min} and y_{max} are taken larger than attainable. In this way the iteration procedure drives the variable to be optimized in the correct direction until no further improvement is possible or the input maximum number of iterations is exceeded.

Modes. - Two modes of solution are available, the indirect (select) mode and the direct (optimize) mode. In the indirect mode, a solution which satisfies the end conditions is attempted. Indirect optimization is performed in this mode. The direct mode computes a series of trajectories, each of which satisfies the specified end conditions while successively minimizing the performance index residual. The specified end conditions are first satisfied using the indirect mode while ignoring the performance index.

Weighting. - The scale matrices W_x and W_y are used to make elements of the vectors X and Y compatible for the iteration procedure. The relative importance of the variables is represented in this way. Differing magnitudes are compensated for through the weighting matrixes. W_x is input to the program, W_y is computed internally using the input tolerances and importance factors. For point constraint variables, the elements of W_y are given by the following relation:

$$W_y = \frac{2^{-38}}{\delta_y^2} ,$$

where δ_y is the corresponding tolerance.

The weighting factor for the performance index is computed from,

$$W_y = \frac{n}{r^2} \; 2^{-38} ,$$

when n is the number of dependent variables and r is the performance index residual. This balances the residual in the parameter being optimized against the weighted residuals in the other variables, to satisfy the constraints as the optimization proceeds.

REFERENCES

[1] Whitlock; Wolf, et. al., "Interplanetary Trajectory Encke Method Fortran Program Manual for the I.B.M. System/360," NASA X-643-70-330, GSFC, September 1970.

[2] Lancaster, E.R., "Relative Motion of Two Particles in Elliptic Orbits," AIAA Journal 8, pp. 1878-1879, (1970).

[3] Adams, Wm. M., Jr., "Dynamics of Two Slowly Rotating Point-Mass Vehicles Connected by a Massless Tether and in a Circular Orbit," NASA TN D-5599, January 1970.

[4] Bainum, P.M., et. al., "Attitude Stability and Damping of a Tethered Orbiting Interferometer Satellite System," JAS XIX, pp. 364-389, (1972).

[5] Chobotov, V., "Gravitational Excitation of an Extensible Dumbbell Satellite," AIAA Journal 4, pp. 1295-1300, (1967).

[6] Etkin, B., "Dynamics of Gravity-Oriented Orbiting Systems with Application to Passive Stabilization," AIAA Journal 2, pp. 1008-1014, (1964).

[7] Garg, S.C., "On the Use of Flexible Strings in Gravity-Gradient Stabilization", Inst. for Aerospace Studies, U. of Toronto, Canada, (1969).

[8] Meirovitch, L., et. al., "On the Effect of Aerodynamic and Gravitational Torques on the Attitude Stability of Satellites," AIAA Journal 4, pp. 2196-2202, (1966).

[9] Meirovitch, L., Methods of Analytical Dynamics, McGraw-Hill, (1970).

[10] McLachlan, N.W., Theory and Application of Mathieu Functions, Clarendon Press, Oxford, England, (1947).

[11] Newman, M., "The Motion of Tandem Orbiting Vehicles Linked by a Tether of Finite Mass," Report No. 70-5, AMA, February 1970.

[12] Newman, M., et. al., "Analytical Study of the Motion of Linked Tandem Orbiting Vehicles Including Rotational Degrees of Freedom," AMA Report No. 70-17, March 1970.

[13] Paul, B., "Planar Librations of an Extensible Dumbbell Satellite," AIAA Journal 1, pp. 411-418, (1963).

[14] Robe, T.R., "Stability of Two Tethered Unsymmetrical Earth-Pointing Bodies," AIAA Journal 6, pp. 2282-2288, (1968).

[15] Seto, Wm. W., Theory and Problems of Mechanical Vibrations, Schaum Publishing Co., New York, (1964).

[16] Swet, C.J., et. al., "Deployment of a Tethered Orbiting Interferometer," JAS XVII, pp. 44-59, (1969).

[17] Whisnant, J.M., et. al., "Orbital Deployment of Very Long Tethered Structures," APL Report TG 1102, The Johns Hopkins University, Applied Physics Lab., January 1970.